

**APPENDIX A**

**DELFT3D MODELING STUDY**

**INLET MANAGEMENT STUDY OF  
BLIND PASS AND ADJACENT BEACHES**

# DELFT3D MODELING STUDY

## INLET MANAGEMENT STUDY OF BLIND PASS AND ADJACENT BEACHES

### Table of Contents

1. MODELING OBJECTIVES.....	1
2. MODEL DATA .....	9
3. MODEL CONFIGURATION, CALIBRATION, AND PARAMETER SELECTION.....	22
4. PERFORMANCE OF INLET MANAGEMENT ALTERNATIVES .....	81
5. MODELING SUMMARY AND FINDINGS .....	126
6. REFERENCES .....	128

### List of Figures

Figure 1-1: Study area.....	3
Figure 1-2: Blind Pass 2009 Bathymetry – post-dredging condition (feet NAVD). .....	4
Figure 1-3: Blind Pass 2012 Pre-construction Bathymetry (feet NAVD). .....	6
Figure 1-4: Blind Pass bathymetry changes between 2009 and 2012 (feet). .....	6
Figure 1-5: Blind Pass 2016 before construction Bathymetry (feet NAVD). .....	7
Figure 1-6: Blind Pass bathymetry changes between 2009 and 2016 (feet). .....	7
Figure 2-1: Compiled mangrove and seagrass mapping. ....	12
Figure 2-2: Compiled mangrove and seagrass mapping – Blind Pass area. ....	13
Figure 2-3: NOAA/WW3 offshore wave data point. ....	14
Figure 2-4: Directional Wave Statistics at 26.51°N, 82.36°W. ....	15
Figure 2-5: Directional Wave Statistics at 26.51°N, 82.36°W. ....	16
Figure 2-6: Directional wind statistics. ....	18
Figure 2-7: Comparison of Measured wind data at COMPS C10 Station and Hindcast wind data at the selected NOAA/WW3 point (26°30'20.60"N, 82°21'40.82"W) – Dec 15, 2013 to Feb 15, 2014.....	19
Figure 2-8: Location of the wave, current and tide gauges.....	21
Figure 3-1: Modeling scheme. ....	23
Figure 3-2: Regional Wave Grid (white), Intermediate Wave Grid (yellow) and Local Wave Grid (red). .....	24
Figure 3-3: Regional Flow Grid (yellow) and Local Flow/Morphology Grid (blue). .....	25
Figure 3-4: Local Flow/Morphology Grid (blue) and Local Wave Grid (red). .....	26
Figure 3-5: Observed Waves during the Calibration Period. Offshore ADCP conditions were imposed along model offshore boundaries. ....	29
Figure 3-6: Winds during the Calibration Period – measured at COMPS Station C10.....	30
Figure 3-7: Water Levels during the Calibration Period. ....	31
Figure 3-8: Bathymetry over the Regional Wave Grid.....	32
Figure 3-9: Bathymetry over the Intermediate Wave Grid.....	33

Figure 3-10: Bathymetry over the Local Calibration Wave Grid through 2015. Color scale limits were changed relative to the maps in the previous pages to facilitate visualization.....	34
Figure 3-11: SWAN Model Results at the Nearshore ADCP. JONSWAP coefficients for bottom friction dissipation: 0.038 m <sup>2</sup> /s <sup>3</sup> . .....	37
Figure 3-12: SWAN Model Results at the Nearshore ADCP. JONSWAP coefficients for bottom friction dissipation: 0.067 m <sup>2</sup> /s <sup>3</sup> .....	38
Figure 3-13: SWAN Model Results at the Nearshore ADCP. JONSWAP coefficients for bottom friction dissipation: 0.096 m <sup>2</sup> /s <sup>3</sup> .....	39
Figure 3-14: Scatter Plot of SWAN Model Results at the Nearshore ADCP.....	40
Figure 3-15: Typical SWAN Results during the Calibration Period over the Regional Wave Grid. Black circle indicate the location of the Offshore and Nearshore ADCPs. ....	41
Figure 3-16: Typical SWAN Results during the Calibration Period over the Intermediate Wave Grid. Black circle indicate the location of the Nearshore ADCP. ....	42
Figure 3-17: Typical SWAN Results during the Calibration Period over the Local Wave Grid. ....	43
Figure 3-18: Bathymetry over the Regional Flow Grid.....	46
Figure 3-19: 2015 Bathymetry over the Local Flow (1992) Grid in feet NAVD.....	47
Figure 3-20: 2015 Bathymetry over the Local Flow Grid in feet NAVD (Close-up). ....	48
Figure 3-21: Variation of Chezy Friction Coefficient; mangrove = 8 m <sup>1/2</sup> /s; sea grass = 50 m <sup>1/2</sup> /s; other areas = 80 m <sup>1/2</sup> /s.....	50
Figure 3-22: Comparison between measured and simulated water levels and currents at the location of the Nearshore ADCP. Top: Water level; 2nd: U-velocity; 3rd: V-velocity; bottom: Velocity magnitude. ....	51
Figure 3-23: Comparison between measured and simulated water levels and currents at the location of the Redfish Pass ADCP. Top: Water level; 2nd: U-velocity; 3rd: V-velocity; bottom: Velocity magnitude. ....	52
Figure 3-24: Comparison between measured and simulated water levels and currents at the location of the Blind Pass Current Meter. Top: Water level; 2nd: U-velocity; 3rd: V-velocity; bottom: Velocity magnitude. ....	53
Figure 3-25: Comparison between measured and simulated water levels at the tide gauges deployed in the Pine Island Sound. Top: northern tide gauge; bottom: southern tide gauge. ....	54
Figure 3-26: Scatter Plot of Observed versus Simulated Water Levels and Currents – Nearshore ADCP.....	55
Figure 3-27: Scatter Plot of Observed versus Simulated Water Levels and Currents – Redfish Pass ADCP.....	56
Figure 3-28: Scatter Plot of Observed versus Simulated Water Levels and Currents – Blind Pass Current Meter.....	57
Figure 3-29: Scatter Plot of Observed versus Simulated Water Levels – Pine Island Sound North and South tidal gauges. ....	58
Figure 3-30: Comparison between measured and simulated (Local Flow model, horizontal eddy viscosity coefficient = 1 m <sup>2</sup> /s) water levels and currents at the Blind Pass Gauge location. Top: Water level; 2nd: East-West velocity; 3rd: North-South velocity; bottom: Velocity magnitude. ....	61
Figure 3-31: Scatter Plot of Observed versus Simulated (Local Flow model) water Levels and currents – Blind Pass Current Meter, horizontal eddy viscosity coefficient = 1 m <sup>2</sup> /s. ....	62
Figure 3-32: Local Flow model calibration results: ebb tide, mild waves/wind. ....	64
Figure 3-33: Local Flow model calibration results: flood tide, strong NW waves/wind. ....	65
Figure 3-34: Initial measured bathymetry for Morphology Calibration.....	67

Figure 3-35: Measured bathymetry and erosion(-)/sedimentation(+) by the end of the Morphology Calibration period (May 2012). .....	68
Figure 3-36: Wave climate schematization – Morphology calibration period. ....	71
Figure 3-37: Morphological tide schemes tested in the study. ....	74
Figure 3-38: Six Month Erosion (-feet) and Deposition (+feet) given the baseline simulation (full astronomical tides). .....	74
Figure 3-39: Six Month Erosion (-feet) and Deposition (+feet) given the tested Tide Schemes: #1 one diurnal component (top left); #2 one semidiurnal component (top right), #3 one semidiurnal component amplified 10% (bottom left); and #4 the so called M2C1 tide composed of both a diurnal and a semidiurnal component (bottom right) .....	75
Figure 3-40: Measured and modeled erosion/sedimentation map. ....	78
Figure 3-41: Measured and modeled volume changes for the morphology calibration period. Darker bars: Measured data; lighter bars: Delft3D model. ....	79
Figure 3-42: Net sediment transport map – Delft3D model, morphology calibration period. ....	80
Figure 4-1: 2016 Model bathymetry used as baseline in production runs - No Action. ....	81
Figure 4-2: Net bathymetry changes relative to No Action (difference between year 5 bathymetries). Dashed line represents dredge template boundary. ....	86
Figure 4-3: Observed changes in Wulfert Channel (images: Google Earth). Red line: Blind Pass dredge template; white line: reference contour. ....	87
Figure 4-4: Minimum Blind Pass channel cross-sectional area over the simulated period. ....	88
Figure 4-5: Simulated net beach volume changes relative to No Action, after 1 year. ....	90
Figure 4-6: Simulated net beach volume changes relative to No Action, after 5 years. ....	91
Figure 4-7: Simulated beach volume changes at profile R-111. ....	92
Figure 4-8: Minimum Blind Pass channel cross-sectional area over the simulated period – dredging alternatives. ....	93
Figure 4-9: Simulated beach volume changes after 1 year – dredging alternatives. ....	94
Figure 4-10: Simulated beach volume changes after 5 years – dredging alternatives. ....	95
Figure 4-11: Simulated beach volume changes at profile R-111 – dredging alternatives. ....	96
Figure 4-12: Minimum Blind Pass channel cross-sectional area over the simulated period – Blind Pass jetty alternatives. ....	97
Figure 4-13: Simulated beach volume changes after 1 year – Blind Pass jetty alternatives. ....	99
Figure 4-14: Simulated beach volume changes after 5 years – Blind Pass jetty alternatives. ....	100
Figure 4-15: Simulated beach volume changes at profile R-111 – Blind Pass jetty alternatives. ....	101
Figure 4-16: Minimum Blind Pass channel cross-sectional area over the simulated period – Beach Fill alternatives. ....	102
Figure 4-17: Simulated beach volume changes after 1 year – Beach Fill alternatives. ....	104
Figure 4-18: Simulated beach volume changes after 5 years – Beach Fill alternatives. ....	105
Figure 4-19: Simulated beach volume changes at profile R-111 – Beach Fill alternatives. ....	106
Figure 4-20: Minimum Blind Pass channel cross-sectional area over the simulated period – Sanibel Structure alternatives. ....	107
Figure 4-21: Simulated beach volume changes after 1 year – Sanibel Structure alternatives. ....	109
Figure 4-22: Simulated beach volume changes after 5 years – Sanibel Structure alternatives. .	110
Figure 4-23: Simulated beach volume changes at profile R-111 – Sanibel Structure alternatives. ....	111
Figure 4-24: Initial bathymetry for the Permitted Template. ....	115

Figure 4-25: Initial bathymetry given the Combined Scenario #1 (Dashed line represents dredge template boundary). .....	116
Figure 4-26: Initial bathymetry given the Combined Scenario #2 (Dashed line represents dredge template boundary). .....	116
Figure 4-27: Initial bathymetry given the Combined Scenario #3 (Dashed line represents dredge template boundary). .....	117
Figure 4-28: Net bathymetry changes relative to Permitted Template after 5.....	118
Figure 4-29: Minimum Blind Pass channel cross-sectional area over the simulated period – Combined Scenarios. ....	119
Figure 4-30: Simulated beach volume changes after 1 year – Combined Scenarios.....	121
Figure 4-31: Simulated beach volume changes after 5 years – Combined Scenarios. ....	122
Figure 4-32: Simulated beach volume changes at profile R-111 – Combined Scenarios. ....	123

### List of Tables

Table 2-1: Bathymetric and topographic surveys used in the Delft3D modeling of Blind Pass ..	10
Table 2-2: Location of the ADCP and tide gages measurements. ....	20
Table 3-1: Summary of grid properties.....	27
Table 3-2: SWAN calibration summary. ....	35
Table 3-3: Summary of the Delft3D-WAVE (SWAN) model parameters.....	36
Table 3-4: Regional flow calibration summary - Delft3D-FLOW model. ....	59
Table 3-5: Local flow calibration summary (Blind Pass gage) Delft3D-FLOW model.....	60
Table 3-6: Summary of the regional and local flow model definitions- Delft3D-FLOW Model. ....	63
Table 3-7: Simulated wave cases and their corresponding <i>morfac</i> values. ....	72
Table 3-8: Tested tide schemes.....	73
Table 3-9: Summary of Delft3D calibration parameters. ....	77
Table 4-1: Representative wave conditions used in the production runs.....	82
Table 4-2: Summary of the preliminary alternatives. ....	83
Table 4-3: Simulated alternatives - dredge and fill volumes. ....	84
Table 4-4: Design features considered in the Combined Scenarios. ....	113

### List of Sub-Appendices

Sub-Appendix A-1	Initial model bathymetry: Alternatives 0 to 9
Sub-Appendix A-2	Net bathymetry changes relative to Alternative 3a (Alternative 1b to 9, Year 5)
Sub-Appendix A-3	Additional Blind Pass Jetty Spur analysis
Sub-Appendix A-4	Net volume changes relative to “Permitted Template” over the 5 year simulation period
Sub-Appendix A-5	Storm simulations for Combined Alternatives

**DELFT3D MODELING STUDY**  
**INLET MANAGEMENT STUDY OF**  
**BLIND PASS AND ADJACENT BEACHES**

**1. MODELING OBJECTIVES**

**1.1. Objectives**

The overall objective of the modeling effort is to evaluate coastal processes at Blind Pass and analyze alternatives for their effect on the inlet, adjacent islands and coastal system. The selected model to achieve these objectives is the Delft3D model, specifically designed to simulate complex interactions of inlets, shoals and adjacent beaches.

The three-dimensional Delft3D model consists of several modules for the simulations of physical processes such as wave transformation, hydrodynamics, sediment transport, erosion, scour and deposition. After developing the model setup and calibrating the wave, flow and morphology modules using measured datasets, the numerical modeling tool was applied to evaluate sand bypassing, inlet processes and the performance of potential alternatives. These assessments encompass:

- The general erosion and sediment transport patterns near Blind Pass.
- Dredging options for the maintenance of the Blind Pass channel, along with the interior connections between Sunset Bay, Dinkins Bayou and Wulfert channel towards Pine Island Sound.
- Placement options for the dredged quantity.
- Structural alternatives for the Blind Pass jetty and the northern end of Sanibel Island.

Several management options were developed in coordination with the Technical Advisory Committee (TAC) and tested in the model. Model production runs were performed for average conditions (5 year simulations). Three final scenarios were also tested under two storm conditions (2016 Cold Front and 2004 Hurricane Charley). The results for each scenario were compared to baseline conditions (e.g. No Action and the Permitted Template) in order to compare different design components to support the alternatives analysis.

The results and opinions presented in this modeling appendix are of a purely technical nature as one component of analysis in the overall study. These findings should be viewed in conjunction with other coastal engineering assessments and prudent engineering judgment. The final conclusions and recommendations are presented with additional context in the main text of the report.

## **1.2. Summary of the Study Area's Coastal Environment**

Blind Pass is a relatively small connection between the Gulf of Mexico and Pine Island Sound. A long and shallow channel extends between the Pass and the Sound, named Wulfert Channel. In addition to Blind Pass, tides flow in/out of Pine Island Sound through considerably larger inlets: San Carlos Bay (to the south), Redfish Pass (north) and Captiva Pass and Boca Grande Pass (further north).

The sediment budget for Blind Pass and adjacent beaches is presented in the main report. The net alongshore sediment transport on the Gulf of Mexico beaches of Captiva and Sanibel Islands is from north to south. This is representative of the long-term average for the sediment budget analysis period (2009-2015), as the sediment drift intensity and direction varies on shorter timescales (i.e. storms, seasonal and inter-annual variations).

Blind Pass channel stability is dictated by the balance between wave and longshore transport processes closing the inlet, and tidal processes attempting to restore the opening. Over the last decade, the stability of the pass proved to be relatively poor, requiring multiple maintenance dredging projects to keep the channel open.

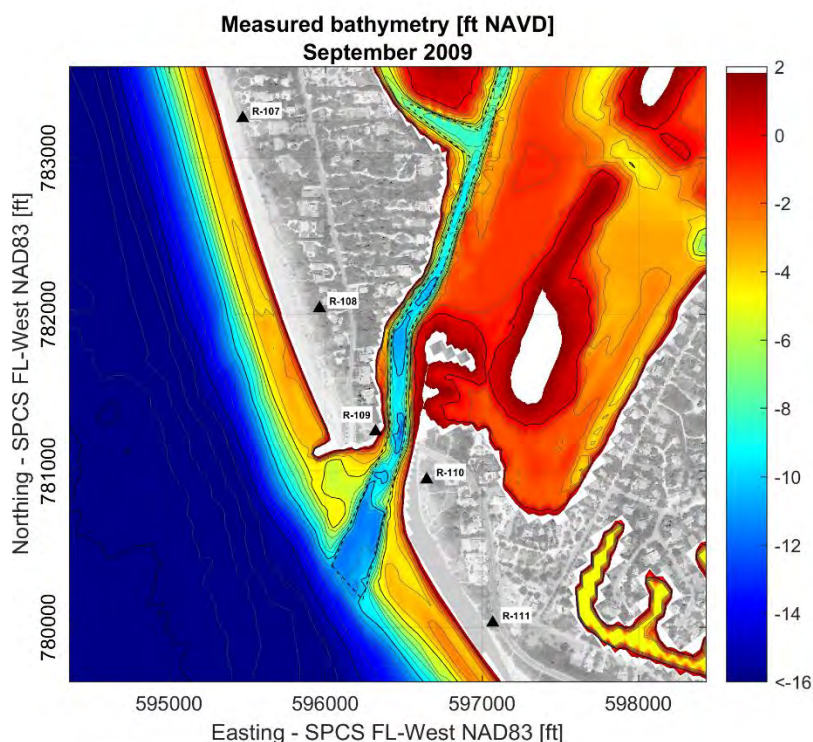
The opening of Redfish Pass in 1921 diminished the tidal flows through Blind Pass, reducing its size and stability. Blind Pass remained intermittently opened and experienced multiple natural closures and reopening by storm events. Blind Pass was mechanically opened for the first time in 2001, but closed again shortly thereafter. Beginning in 2008/09, Lee County implemented the Blind Pass Restoration Project with the objective of maintain Blind Pass in an open condition. Several maintenance dredging events have occurred since then. The dredging events and the inlet response based on monitoring reports is summarized in the main text in order to frame the context of the performance of the current management approach for Blind Pass, and the objectives of this study.



Figure 1-1: Study area.

### 1.2.1 Blind Pass Restoration Project

In 2008/2009, approximately 148,000 cubic yards of sediments were dredged from the Blind Pass channel by Lee County, re-establishing the connection to Pine Island Sound with the Blind Pass Restoration Project. The permitted dredging template was -10 ft NAVD seaward of bridge and along approximately half of the section landward of the bridge. Further inland, the template transitions to -9 ft and -8 ft NAVD at the connection with Roosevelt Channel and at the northern end of the template. The majority of the dredged sand in 2008 and 2009 was placed in Sanibel Island between R-112 and R-114+200. Approximately 11,100 cubic yards were hauled away by the City of Sanibel Public Works Department (CEC, 2010).



**Figure 1-2: Blind Pass 2009 Bathymetry – post-dredging condition (feet NAVD).**

Significant shoaling of Blind Pass occurred between August 2009 and January 2010. The amount of sand shoaled into the dredge template was approximately 40,100 cubic yards (CEC, 2010). Most of the shoaling occurred in the outer channel section as a shallow sandbar between Captiva and Sanibel Islands.

In response to the continued channel shoaling in the following years, Phase I of the first maintenance dredging of Blind Pass was started in 2012 and Phase II was completed in 2013 – approximately 3 years after the opening in 2009. The amount of sand excavated from the permitted borrow area totaled approximately 101,000 cubic yards (CEC, 2013). It is highlighted that approximately 40% of the infilled volume was measured only 5 months after construction – especially in the outer section of the channel (seaward of bridge).

The sand dredged in 2012 and 2013 was placed on Sanibel Island within the permitted fill limits: approximately 63,300 cubic yards between R-116 and R-118 (dredged from seaward of bridge); and approximately 37,600 cubic yards between R-112 and R-113.5 (dredged from landward of bridge).

Based on the June 2013 survey, the total volume within the Blind Pass dredge template was approximately 53,160 cubic yards (CEC, 2013), predominately in the sections seaward of bridge. This corresponds to approximately 53% of the total dredged volume completed in May 2013; and 84% of the volume dredged from the outer section of the channel (completed on September 2012 – 9 months before the referred survey).

Between June 2013 and July 2014, an additional 30,670 cubic yards of accretion was calculated within the dredging template, 33% seaward of bridge, 53% immediately landward of bridge and 13% further north (CEC, 2014). Based on the 2014 survey, the total volume within the Blind Pass dredge template was approximately 83,680 cubic yards.

The second maintenance dredging of Blind Pass was completed in June 2017. Approximately 89,700 cubic yards were excavated from the permitted dredge template, mostly from the outer channel seaward of bridge. Approximately 67,060 cubic yards were placed within the North Beach fill area between R-112 and R-114+200 and approximately 22,640 cubic yards were placed within the South Beach fill area between R-116 and R-118 (CEC, 2017).

The fast adjustment of the system after the dredging project suggests that the dredging template substantially exceeds the equilibrium channel cross-sectional area. This is especially the case in the outer section of the channel, seaward of the bridge. Consequently, tidal currents are not sufficient to maintain the dredged depths and the system bounces back to pre-dredging conditions.

The bathymetry maps from annual monitoring reports show that the northern sections of the channel are getting wider over time. This is due to the adjustment of the dredged slopes of the channel, resulting in deepening outside the template limits and accretion inside the channel limits, which is cleared in subsequent maintenance dredging projects. Theoretically, this process benefits the stability of the Pass, since it results in less restriction to water flow through the area and a (slight) increase of the tidal prism.

The outer section of the channel serves as a borrow area for beach nourishment projects in Sanibel Island. On the other hand, the dredged channel across the bypassing bar traps the sand transport within about a year following dredging projects, causing a deficit to adjacent areas. The sediment balance between the channel and adjacent beaches and the instability of Blind Pass channel, given by the predominance of the wave-induced alongshore drift over the tidal forces, are the primary challenge of maintaining Blind Pass.

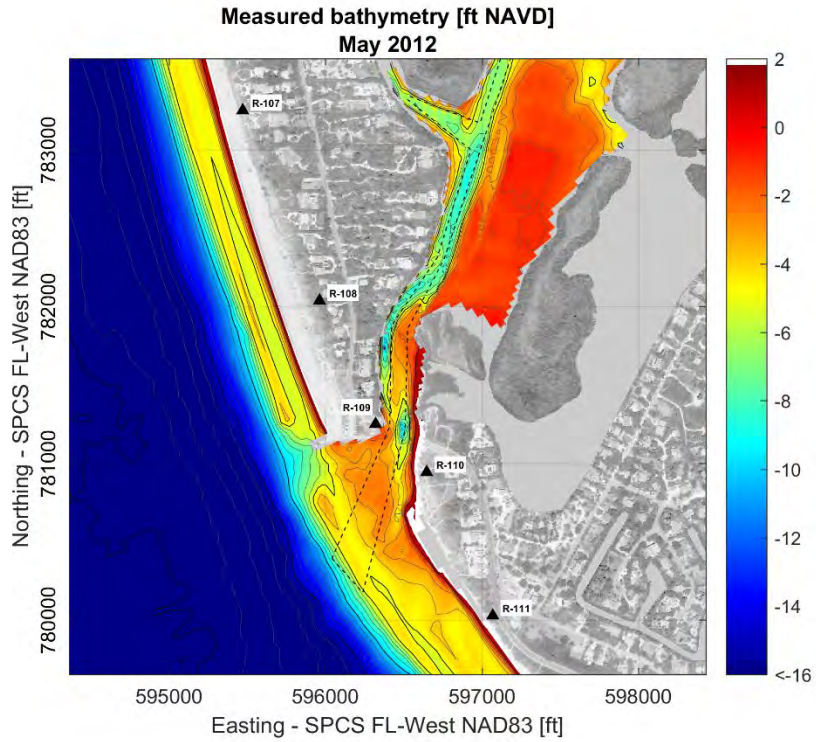


**Figure 1-3: Blind Pass 2012 Pre-construction Bathymetry (feet NAVD).**

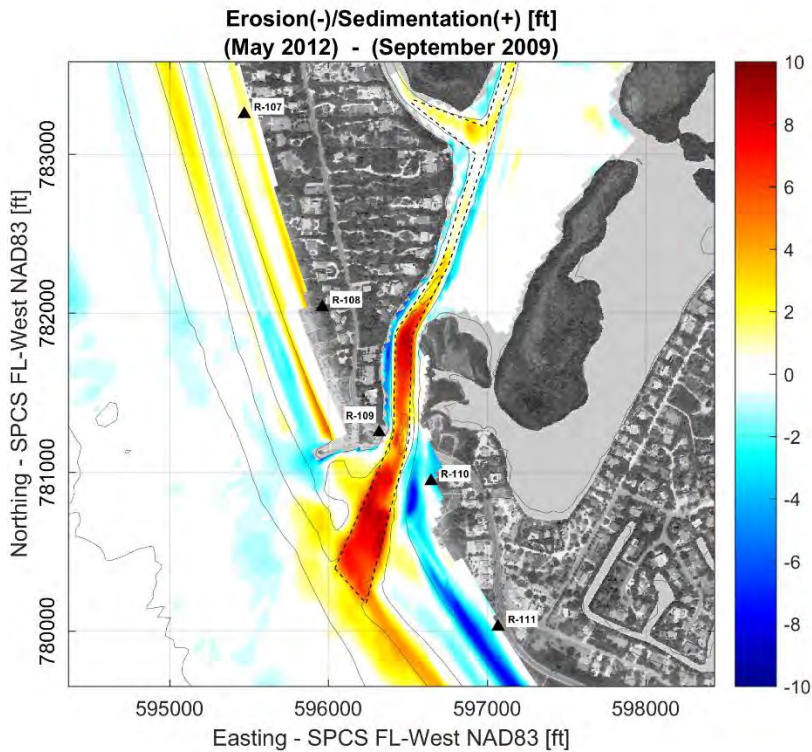


**Figure 1-4: Blind Pass bathymetry changes between 2009 and 2012 (feet).**

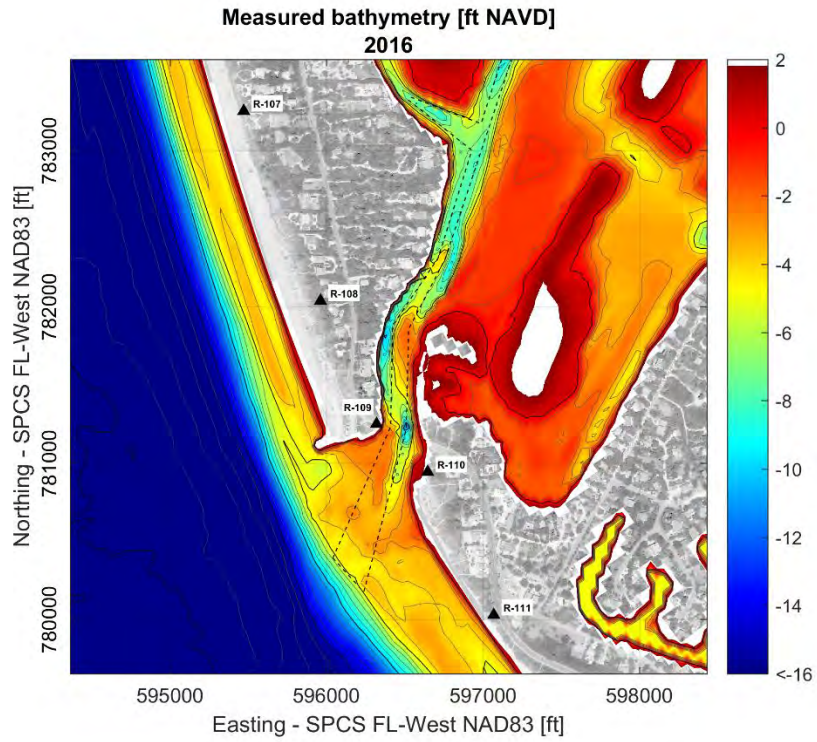


**Figure 1-5: Blind Pass 2016 before construction Bathymetry (feet NAVD).**

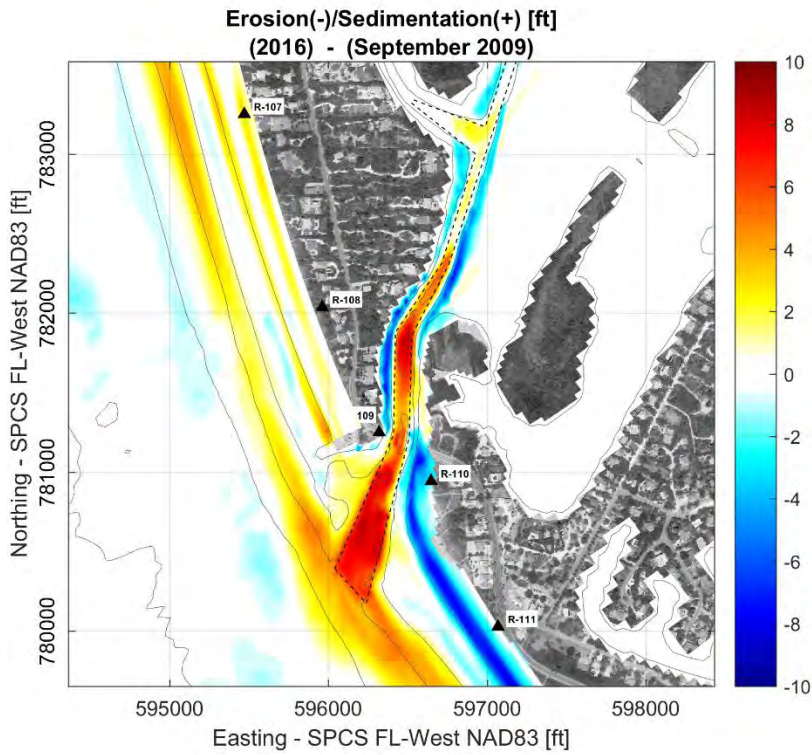


**Figure 1-6: Blind Pass bathymetry changes between 2009 and 2016 (feet).**

### **1.3. Methods**

The primary tool in this investigation is the Delft3D morphological model (Deltares, 2016a). This model determines changes in topographic and bathymetric surfaces based on the effects of waves, water levels, winds, and currents. Wave transformation from the offshore to the nearshore area is simulated using the Simulating WAVes Nearshore (SWAN) wave transformation model (Booij, et al, 2004, Deltares, 2016b). The SWAN model (version 40.72ABCDE) is coupled with the Delft3D-Flow model (version 4.02.02), which simulates currents, water levels, and sediment transport. Based on the sediment transport estimates at each flow time step, the Delft3D-Flow model calculates the subsequent elevations of the topographic and bathymetric surfaces. Typical time steps in Delft3D-Flow range from 1 second to 60 seconds. Water levels, currents, and bottom grade elevations are then provided to the SWAN model at each wave time step, which is on the order of 1 to 3 hours.

Given this study's objectives, Delft3D is the best means of evaluating the various dredging, nourishment and structural designs for Blind Pass and adjacent shorelines. By linking waves, currents, sediment transport, erosion, and deposition, Delft3D can provide valuable information regarding all of these processes within a single set of outputs. Stand-alone flow models or stand-alone wave transformation models do not offer this sort of combined capability. Delft3D can also accommodate curvilinear grids, which allows the grids to be better fitted to offshore contours and shorelines than the rectangular grids used by other models.

This inlet study will examine dredging designs of the outer and inner channels, beach nourishment and structural alternatives and evaluate the impacts on the adjacent coast. For a better representation of the flows and processes in the coastal system, use is made of a three dimensional flow and sediment transport formulation to resolve the complex flows patterns at the outer and inner areas.

### **1.4. Model Application**

While the Delft3D model is a process based model capable of replicating the morphological evolution of complex bathymetries, the strength of the model is in its ability to show the relative differences between alternatives. The model should not be solely relied on to predict the absolute shoreline position, currents, and morphological implications of a specific alternative. Also, due to the inability to predict weather and sea conditions well into the future, the Delft3D model is not used as a predictive model. Instead, the model results are given in terms of the relative difference in the model's response to simulated alternatives compared to its response to a baseline scenario (i.e., existing condition). Additionally, model results must be combined with sound coastal engineering judgment.

## 2. MODEL DATA

### 2.1. Bathymetry

The bathymetric data sources used in this model study appear in Table 2-1. The grids used in the study were constructed in meters using the Florida State Plane Coordinate System, West Zone, North American Datum of 1983 (FL-West NAD83). The bathymetric surfaces used in the model were compiled in meters relative to the North American Vertical Datum of 1988 (NAVD).

Coordinate system conversions were performed using the software Global Mapper v16.1.2 (<http://www.bluemarblegeo.com/knowledgebase/global-mapper/>). Conversions between feet and meters assumed a ratio of 1200.0 m to 3937.0 U.S. Feet. NOAA's Soundings and the Coastal Relief Model elevations are given in MLW which was converted using NOAA's VDatum (<https://vdatum.noaa.gov/>) and assumed to be -1.48 feet NAVD88.

The level of accuracy of the inlet surveys and beach profiles performed by APTIM, the County and FDEP follow the FDEP (2004) standard or similar methods. The level of accuracy of the NOAA Soundings and Coastal Relief Model (CRM) follow the International Hydrographic Organization Standards for Hydrographic Surveys (IHO, 1968; IHO, 1982; IHO, 1987; IHO, 1998) and the NOAA standards, that are based on the Hydrographic Manuals described by Adams (1942), Jeffers (1960), and Umback (1976), and the NOAA NOS Office of Coast Survey Specifications and Deliverables (<https://nauticalcharts.noaa.gov/publications/standards-and-requirements.html>). The level of accuracy of the LiDAR data sets are described in Irish *et al.* (2000).

The June-July 2010 LiDAR data presented elevation values below wading depth 0.31 feet higher than surveys taken by conventional methods around the same time. To remedy this discrepancy in the LIDAR data, points with reported elevation above 0 feet NAVD88 were used as-is and the points below 0 feet NAVD88 were lowered 0.31 feet.

The June 2015 LiDAR dataset was compared to the surveys taken by conventional methods by APTIM in December 2015. It was identified that the submerged LIDAR elevation values were higher than the conventional surveys. To remedy this discrepancy in the LIDAR data, points with a reported elevation above -1.5 feet NAVD88 were used as-is and the points with a reported elevation below -1.5 feet NAVD88 were adjusted with linear regression using the 2015 bathymetric survey performed by APTIM as baseline.

The land boundaries appearing in the document graphics are shown primarily for visual reference and were digitized from Google Earth according to the year of the period analyzed.

**Table 2-1: Bathymetric and topographic surveys used in the Delft3D modeling of Blind Pass**

<b>Date</b>	<b>Source</b>	<b>Type</b>	<b>Vertical Datum</b>	<b>Horizontal Datum</b>	<b>Location</b>
Inlet Surveys and Beach Profiles:					
Aug 2016	CEC	Survey & Beach Profiles	ft. NAVD88	FL-West NAD83 ft.	Blind Pass, Captiva and Sanibel Island
Dec 2015	CPE	Survey	ft. NAVD88	FL-West NAD83 ft.	Blind Pass
Dec 2015	CPE	Survey	ft. NAVD88	FL-West NAD83 ft.	Redfish Pass Inlet Throat and Ebb Shoal
Dec 2015	CPE	Beach Profiles	ft. NAVD88	FL-West NAD83 ft.	Captiva and North Captiva Island
Jun 2015	Lee County	Survey	ft. NAVD88	FL-West NAD83 ft.	Blind Pass, Wulfert & Roosevelt Channel
May 2015	CPE	Beach Profiles	ft. NAVD88	FL-West NAD83 ft.	Captiva & Sanibel Island
Jul 2014	Lee County	Survey	ft. NAVD88	FL-West NAD83 ft.	Blind Pass Ebb Shoal
May 2012	CEC	Survey & Beach Profiles	ft. NAVD88	FL-West NAD83 ft.	Blind Pass, Captiva and Sanibel Island
Sep 2009	CPE	Beach Profiles	ft. NAVD88	FL-West NAD83 ft.	Captiva & Sanibel Island
Sep 2009	CEC	Beach Profiles	ft. NAVD88	FL-West NAD83 ft.	Captiva & Sanibel Island
Aug 2009	CEC	Survey	ft. NAVD88	FL-West NAD83 ft.	Blind Pass & Ebb Shoal
Feb 2006	FDEP	Beach Profiles	ft. NAVD88	FL-West NAD83 ft.	Captiva & Sanibel Island
LiDAR:					
Jun 2015	JALBTCX/USACE	Topo-bathymetry	m NAVD88	GCS NAD83	Gulf Coast of Florida
Jun-Jul 2010	JALBTCX/USACE	Topo-bathymetry	m NAVD88	GCS NAD83	Gulf Coast of Florida
NOAA Soundings and Coastal Relief Model (CRM):					
1961	NCEI/NOAA	Survey	m MLW	GCS NAD27	H08363 – West of Sanibel Island
1961	NCEI/NOAA	Survey	m MLW	GCS NAD27	H08632 – North of Sanibel Island
1961	NCEI/NOAA	Survey	m MLW	GCS NAD27	H08598 – South Pine Island Sound
1960	NCEI/NOAA	Survey	m MLW	GCS NAD27	H08362 – West of North Captiva Island
1960	NCEI/NOAA	Survey	m MLW	GCS NAD27	H08555 – Mid Pine Island Sound
Compilation of Multiple Years	NCEI/NOAA	CRM	m MSL	GCS NAD83	Florida and Eastern Gulf of Mexico – Vol. 03

## **2.2. Structures**

The Blind Pass jetty located in the northern side of the inlet, on the south end of Captiva Island, was digitized from Google Earth and included in the modeling effort.

## **2.3. Seagrass, Tidal Flats and Mangroves**

Seagrass, tidal flats and mangroves in the study area were identified and used to define spatially variable bottom friction coefficients in the numerical models. The compiled data is presented in Figure 2-1 and Figure 2-2.

The seagrass and tidal flats were compiled from the South Florida Water Management District (SFWMD, 2008) and the Southwest Florida Water Management District (SWFWMD, 2012). The data from both sources was photo-interpreted from 2008 and 2012, respectively, 1: 24,000 scale natural color aerial photography and classified using the Water Management District modified from Florida Land Cover Classification System (FLUCCS).

Mangrove mapping was obtained from the Florida Fish and Wildlife Conservation Commission-Fish and Wildlife Research Institute (FWC-FWRI, 2014). The mangrove locations provided by FWC-FWRI were established using a compilation of statewide data from aerial photographs, field measurements, and other sources collected between 1987 and 2012.

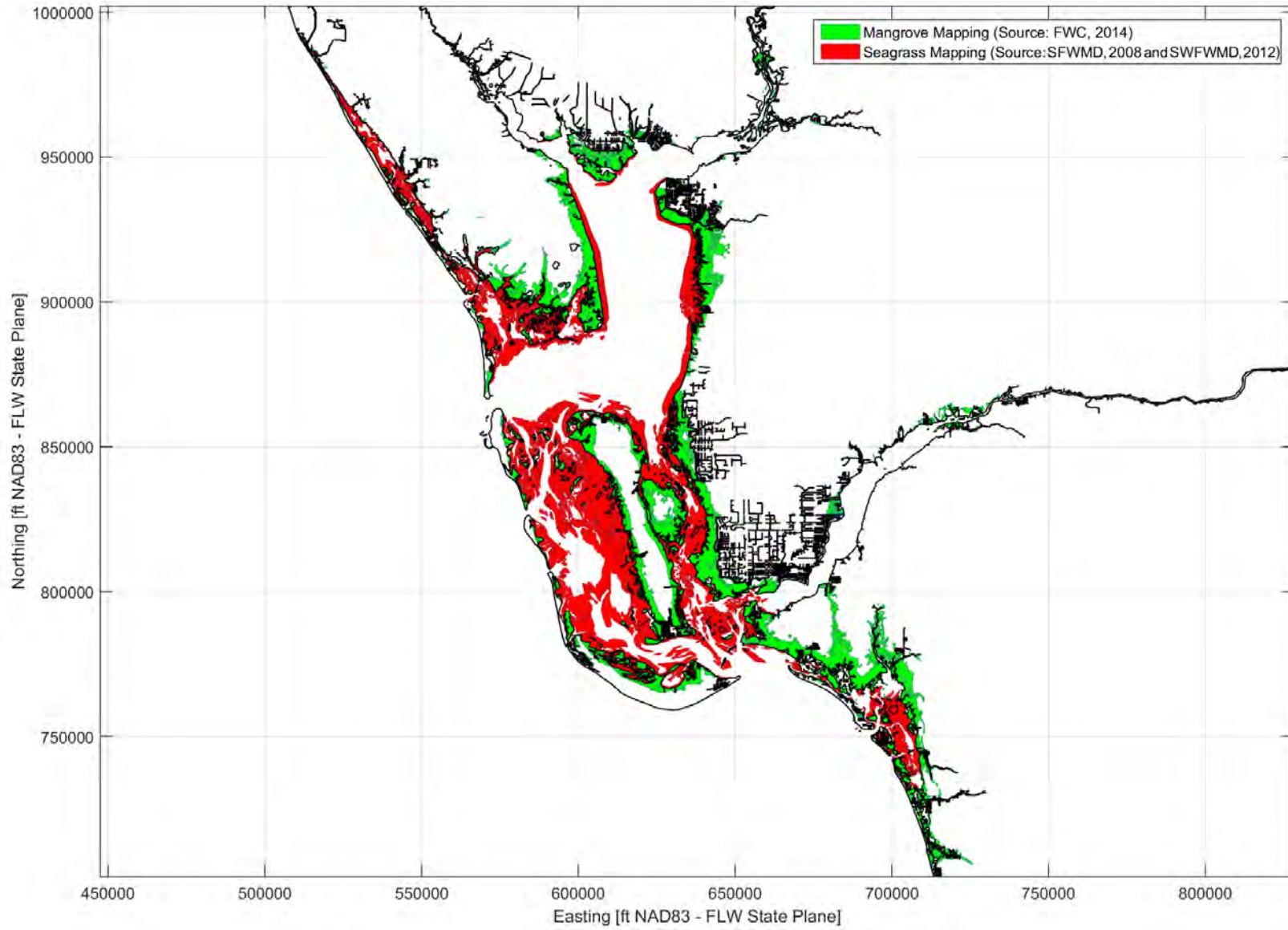


**Figure 2-1: Compiled mangrove and seagrass mapping.**

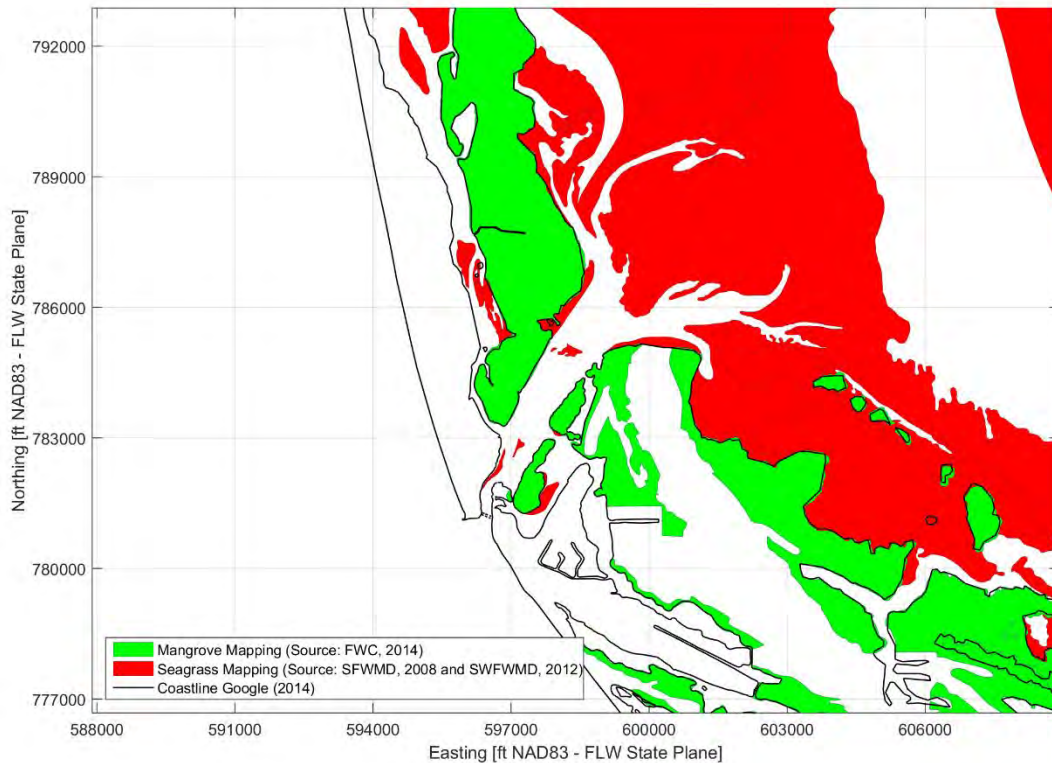


**Figure 2-2: Compiled mangrove and seagrass mapping – Blind Pass area.**

## 2.4. Waves

The source of wave data used in this modeling study was the NOAA Wavewatch III hindcast (WW3, 2015) at 26°30'20.60"N, 82°21'40.82"W (Figure 2-3) at a depth of approximately 60 feet. WW3 model performance and validation have been widely published and more information is available in Hanson *et al.* (2009), Chu *et al.* (2004), and Chawla *et al.* (2009).

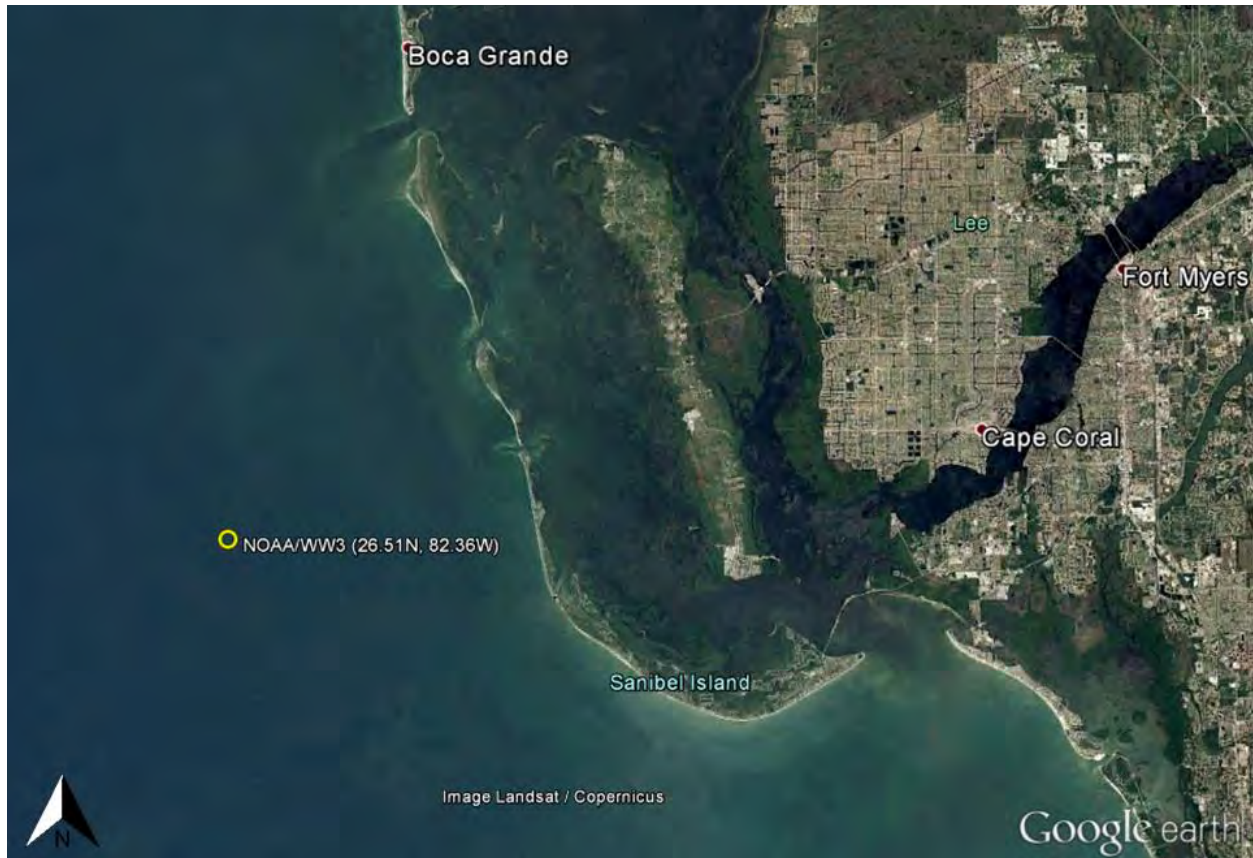


**Figure 2-3: NOAA/WW3 offshore wave data point.**

The time period extracted from the WW3 database was July 1999 through July 2015, and the data was given every 3 hours. Parametric hindcast wave data used in the study includes significant wave height ( $H_s$ ), peak wave period ( $T_p$ ), and peak wave direction (PDir). Data is originally provided in SI units, with times referenced to Greenwich Mean Time (GMT).

Typical wave statistics for the WW3 data extracted appear in Figure 2-4 and Figure 2-5. As discussed in the next section, the prevailing winds come from the east. As a result, a large proportion of time (~50%) the significant wave height is smaller than 1 ft.

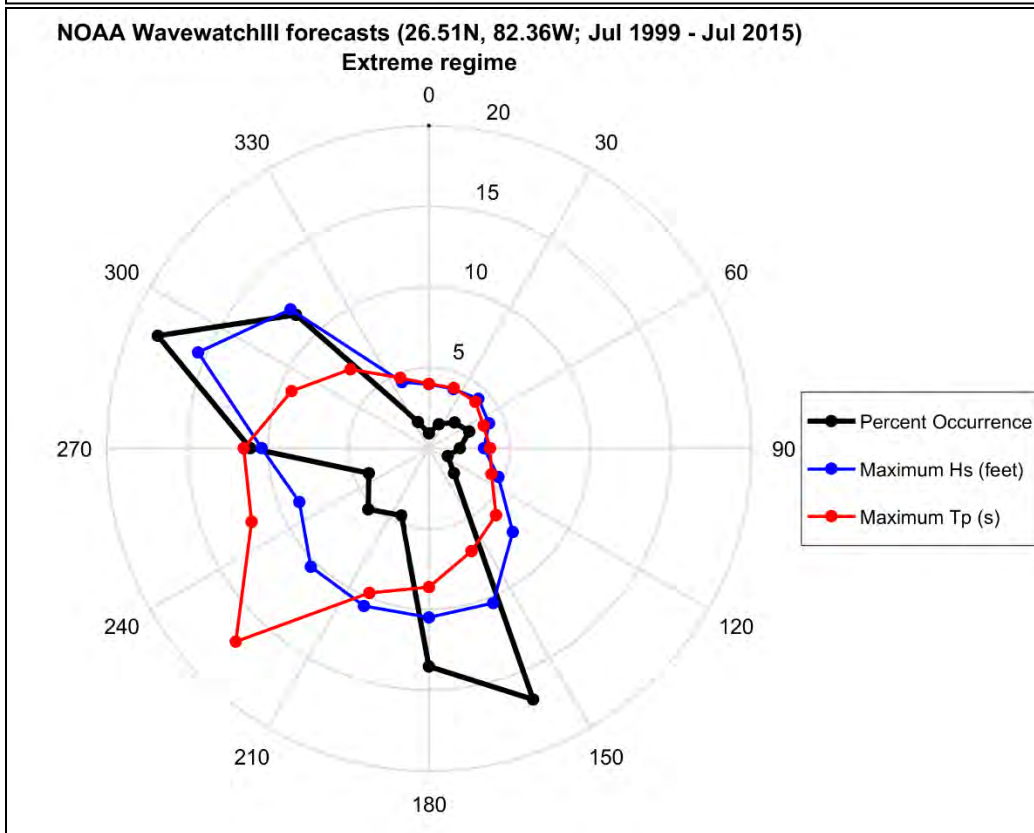
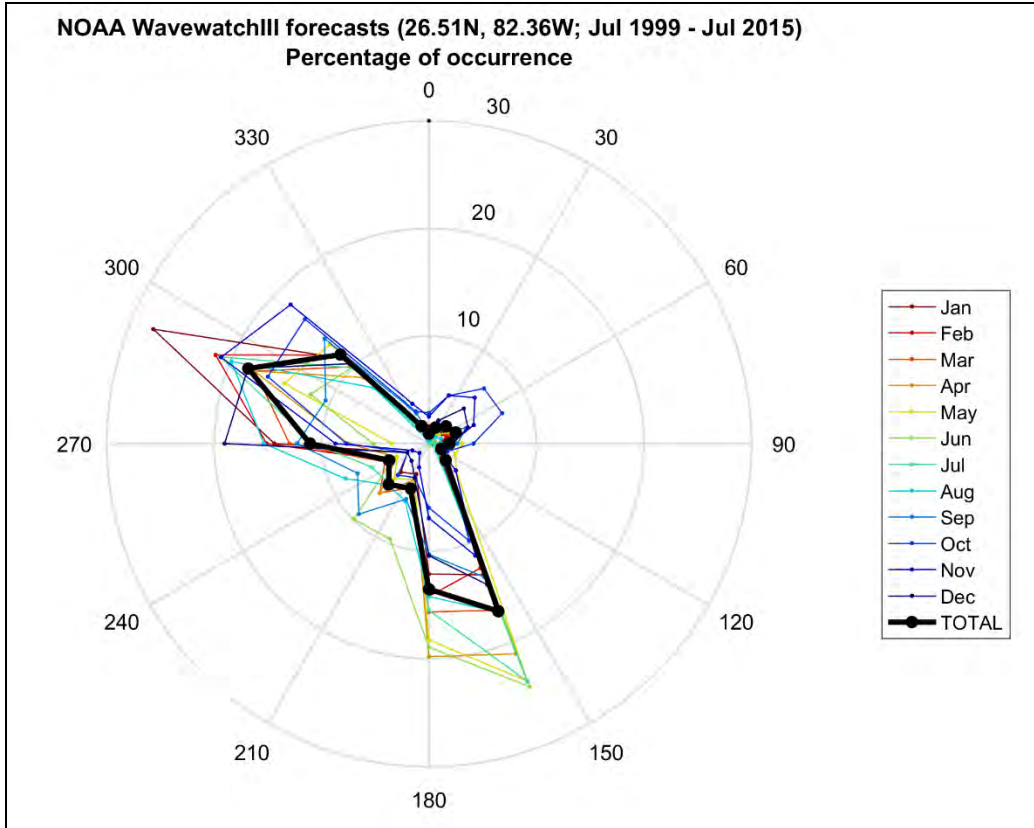
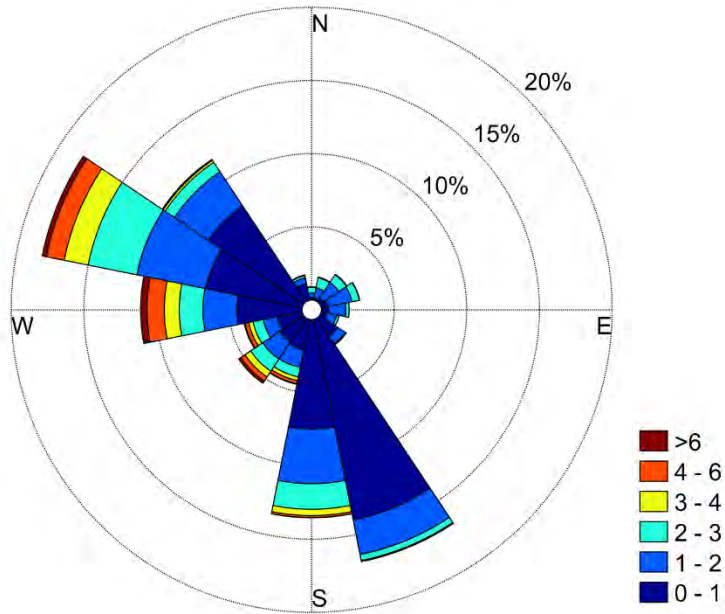


**Figure 2-4: Directional Wave Statistics at 26.51°N, 82.36°W.**

NOAA WavewatchIII forecasts (26.51N, 82.36W; Jul 1999 - Jul 2015)  
Wave height rose [ft]



NOAA WavewatchIII forecasts (26.51N, 82.36W; Jul 1999 - Jul 2015)  
Wave period rose [s]

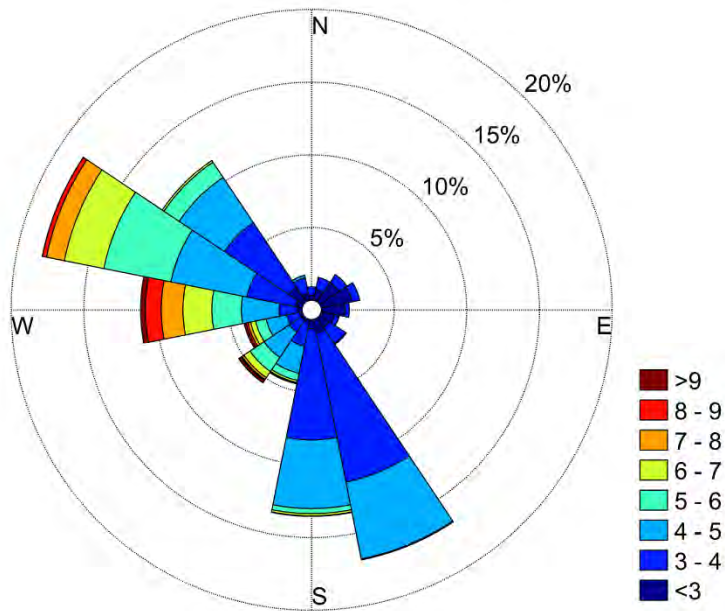


Figure 2-5: Directional Wave Statistics at 26.51°N, 82.36°W.

## 2.5. Winds

To account for wind-generated wave development, wind stress was activated in the SWAN model. The primary sources of wind data is presented below:

- August 2007 to May 2016: measured wind speed and wind direction from the Coastal Ocean Monitoring & Prediction System (COMPS), Station C10, located at 27°10'22.80"N, 82°55'26.40"W.
- July 1999 to July 2015: WW3 hindcast, same database and location described in previous section (26°30'20.60"N, 82°21'40.82"W).

All wind velocities were provided in meters per second, with times referenced to Greenwich Mean Time (GMT). The COMPS wind information were given every 30 minutes. The WW3 wind fields were given every 3 hours.

The two wind datasets were combined, and the first data source (COMPS C10 Station) was used as a primary source. At certain time periods, the COMPS C10 Station presented gaps in the time series. These were filled with WW3 data. Comparisons between the measured COMPS C10 Station and WW3 hindcast data are presented in Figure 2-7. In general, the hindcast wind speeds were consistent with the observed and accommodated the full range of wave conditions that affected the region.

Long-term wind statistics of the combined time series are summarized in Figure 2-6. In general, the prevailing wind direction is from the east. The high percentage of winds from the east and northeast is the primary reason why the waves are generally smaller than 2 feet.

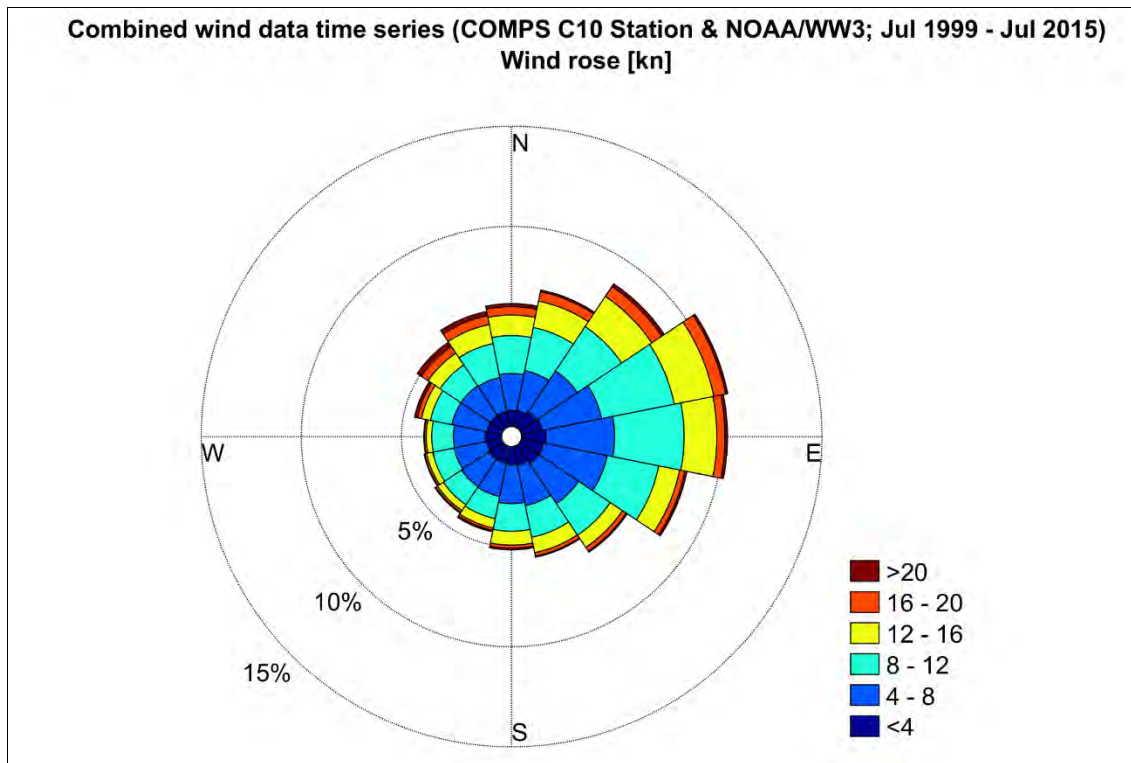
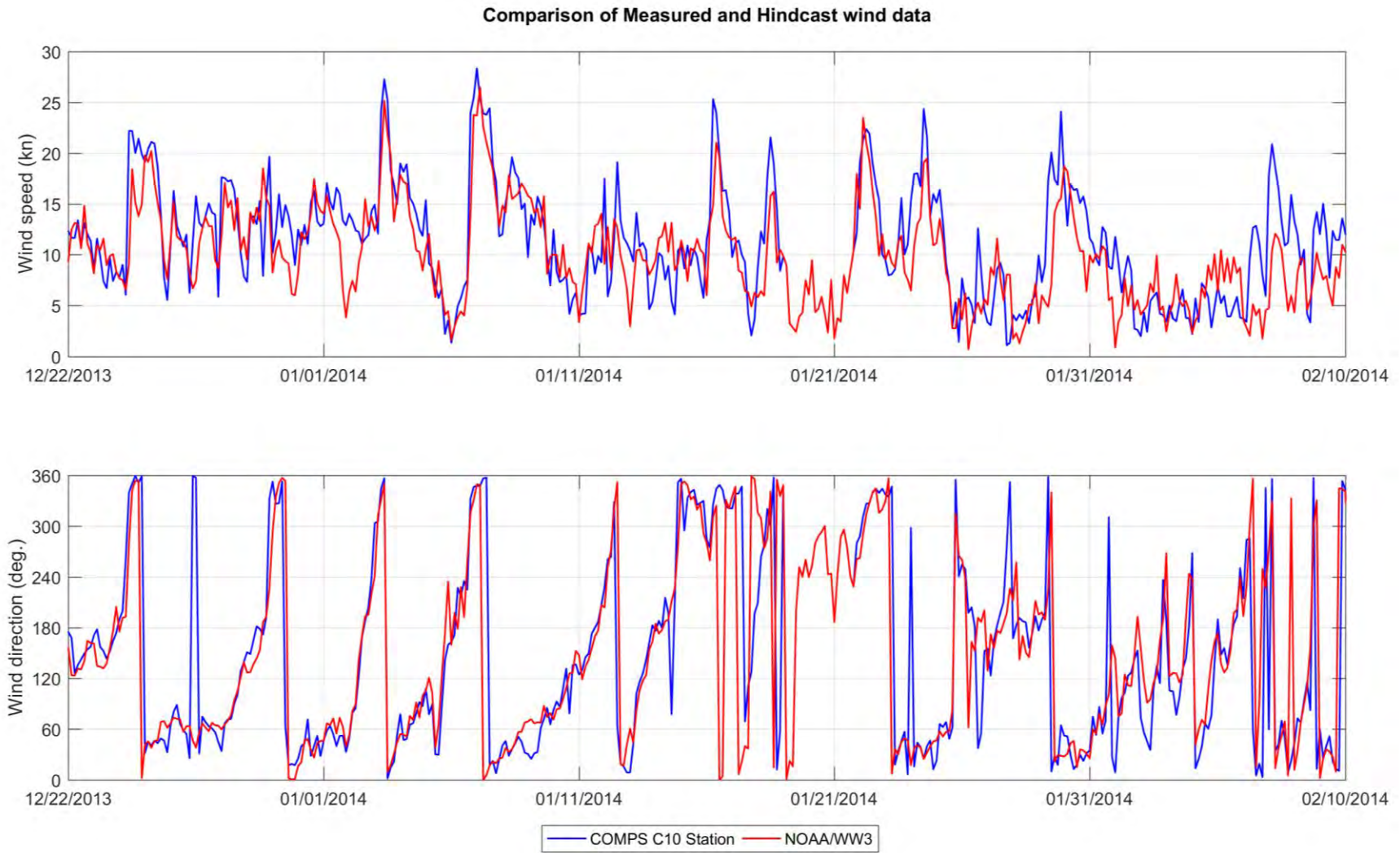


Figure 2-6: Directional wind statistics.



**Figure 2-7: Comparison of Measured wind data at COMPS C10 Station and Hindcast wind data at the selected NOAA/WW3 point (26°30'20.60"N, 82°21'40.82"W) – Dec 15, 2013 to Feb 15, 2014.**

## 2.6. Water Levels

Water levels used as input of the hydrodynamic model were obtained with the Tidal Model Driver (TMD), which uses the global model of ocean tides TPXO7.2 (Egbert & Erofeeva, 2002; Egbert et al., 1994). The tides are provided as complex amplitudes of earth-relative sea-surface elevation for eight (8) primary (M2, S2, N2, K2, K1, O1, P1, Q1), two (2) long period (Mf, Mm) and three (3) non-linear (M4, MS4, MN4) harmonic, totalizing thirteen (13) harmonic constituents that are used to predict tides along the offshore model boundary during the simulation period.

## 2.7. ADCP and Tide Gages Measurements

Three Acoustic Doppler Current Profilers (ADCPs) and two tide gages were deployed between December 11<sup>th</sup> 2015 and January 27<sup>th</sup> 2016. The locations of the ADCPs appear in Figure 2-8 and Table 2-2, and further information and details about the deployment and data processing appears in the Appendix B. The measured data was compared to the wave and flow model results during the calibration phase.

**Table 2-2: Location of the ADCP and tide gages measurements.**

Station	Latitude	Longitude	Depth (approx.)
North Pine Island Sound Tide Gage (NPIS Tide Gage)	26°33'2.20"N	82°10'12.00"W	*
South Pine Island Sound (SPIS Tide Gage)	26°29'47.80"N	82°7'11.90"W	*
Blind Pass Current meter	26°29'7.75"N	82°10'53.17"W	- 6 ft NAVD88
Redfish Pass ADCP	26°33'14.73"N	82°11'58.62"W	-39 ft NAVD88
Nearshore ADCP	26°31'0.18"N	82°12'26.05"W	-20 ft NAVD88
Offshore ADCP	26°30'20.63"N	82°21'40.59"W	-54 ft NAVD88

\*Tide gauges were strapped to channel markers poles approximately four feet below the water level. Measured data were post-processed and referenced to NAVD88.

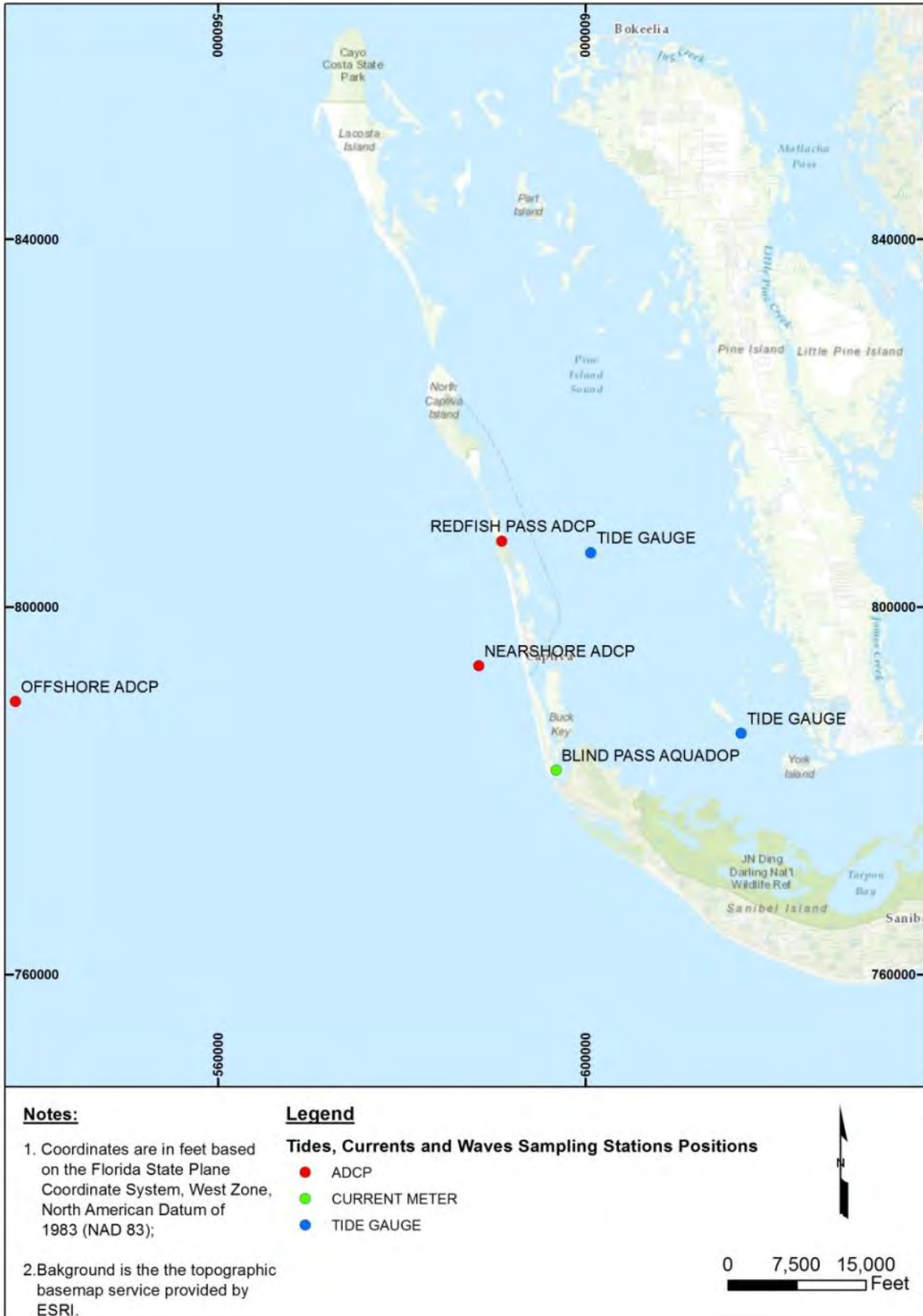


Figure 2-8: Location of the wave, current and tide gauges.

### **3. MODEL CONFIGURATION, CALIBRATION, AND PARAMETER SELECTION**

The goals of the model configuration, calibration and parameter selection were to setup a model that replicates the waves, flows and sediment transport in Blind Pass and adjacent beaches. This model will then be used in the production runs to simulate alternatives and perform comparative analysis to help the decision making in the Inlet Management Study.

#### **3.1.Grids**

Five grids were created to evaluate wave propagation, flow, sediment transport, erosion, and deposition along the study area. These grids include the following:

- Regional Wave Grid, Intermediate Wave Grid and Local Wave Grid;
- Regional Flow Grid and Local Flow Grid.

The modeling approach overview is provided in Figure 3-1. Figure 3-2, Figure 3-3 and Figure 3-4 show the extents of the model grids, while grid characteristics are summarized in Table 3-1. Detailed descriptions of the various grids used in the model study are provided below.

The Regional Wave Grid was used to examine wave propagation from the open ocean to the nearshore region. The offshore boundary of the Regional Wave Grid roughly follows the -60 feet NAVD88 depth contour and extends from Stump Pass in Charlotte County to the north end of Lovers Key in Lee County. The Local Wave Grid was used to examine wave propagation from a depth of approximately -25 feet NAVD88 offshore Blind Pass, extending from monuments R-101 through R-118. An Intermediate Wave Grid was used to facilitate the transition from the coarse Regional Wave Grid.

The Regional Flow Grid was used to reproduce the hydrodynamics of Blind Pass, and encompasses Pine Island Sound and all the water bodies interconnected that influence the hydrodynamics in the area. The grid resolution is variable, with higher resolution in areas of interest, i.e. Blind Pass, and less resolution in areas farther from the inlet. The Local Flow Grid was nested into the Regional Flow domain and is intended to simulate currents, sediment transport, erosion, and deposition within Blind Pass, the nearshore area and the adjacent beaches in Captiva and Sanibel Island. The nesting approach is adopted to make the longer term morphology simulations computationally feasible. The Local Flow Grid is similar to the Local Wave Grid.

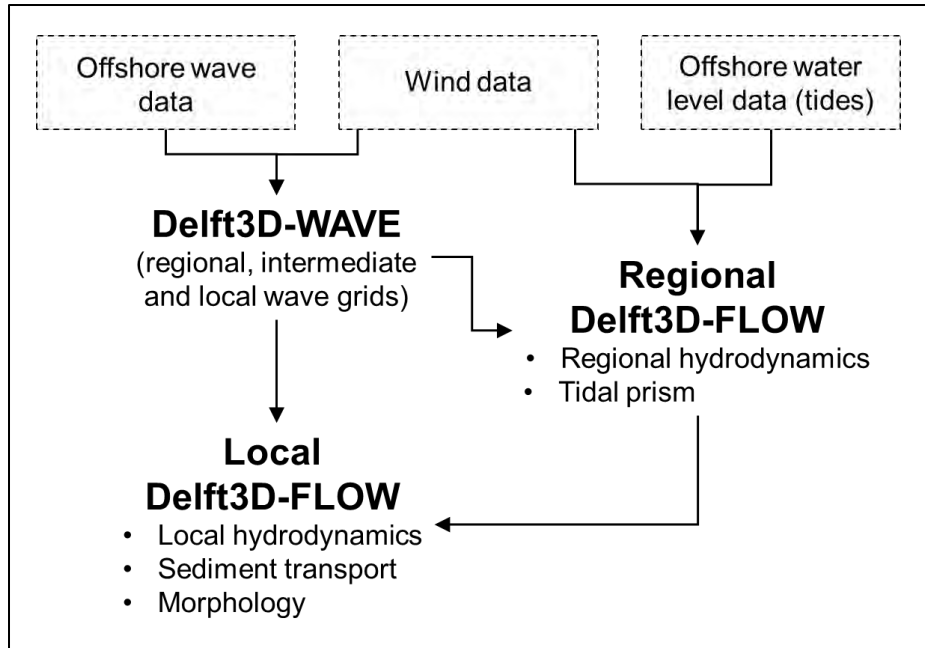


**Figure 3-1: Modeling scheme.**

The model grids generally follow the guidelines established by Deltares (2016c) for smoothing and orthogonality (Table 3-1). Smoothing values represent the change in cell size between adjacent grid cells. For example, a smoothing value of 1.1 indicates that the cell sizes between adjacent grid cells increase by 10%. The maximum smoothing value within the area of interest recommended by the model’s developer is 1.2. Orthogonality is equivalent to the angle between the longshore and cross-shore grid lines, which should be at least  $87.7^\circ$  ( $\cos \alpha < 0.04$ ) within the area of interest.

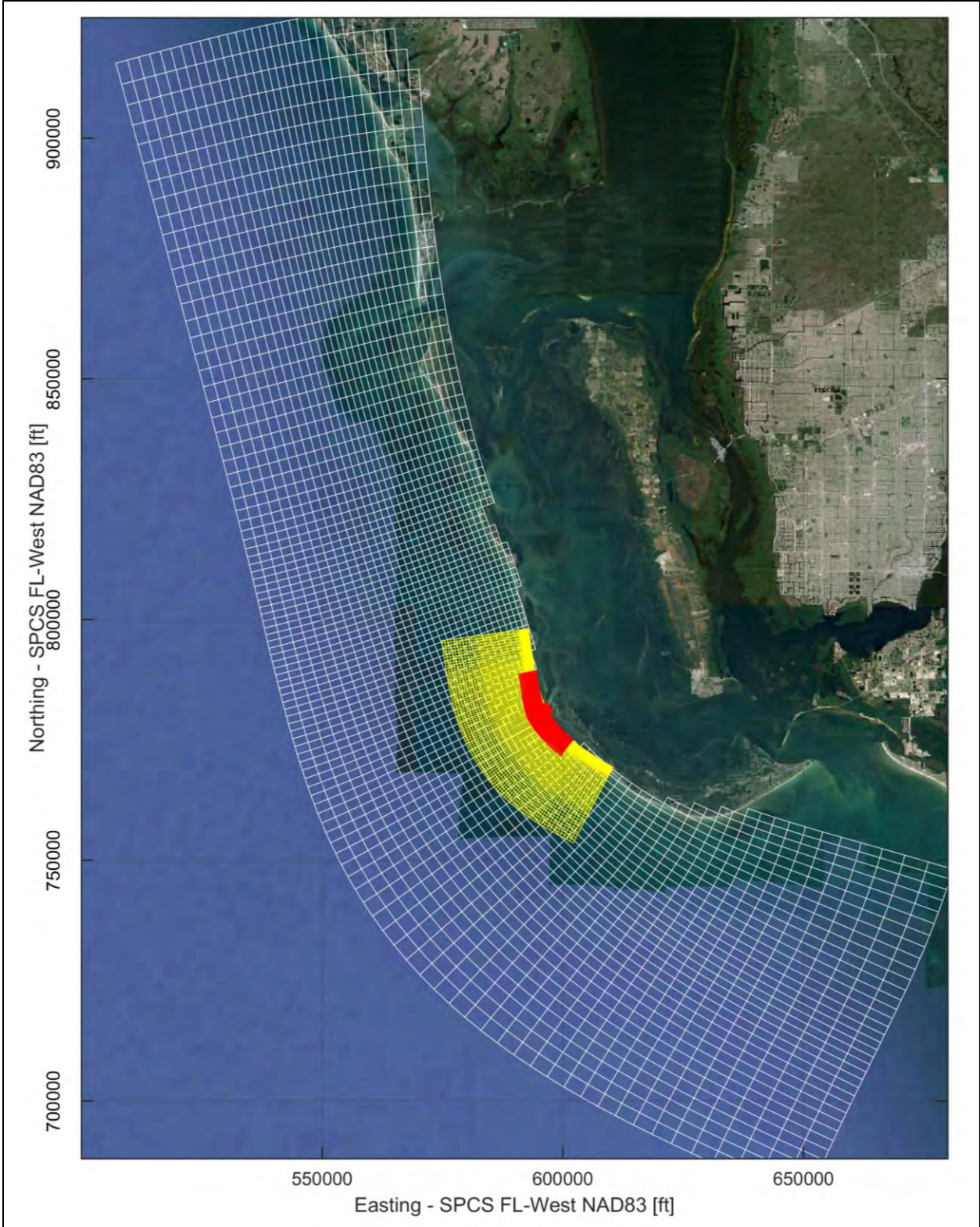
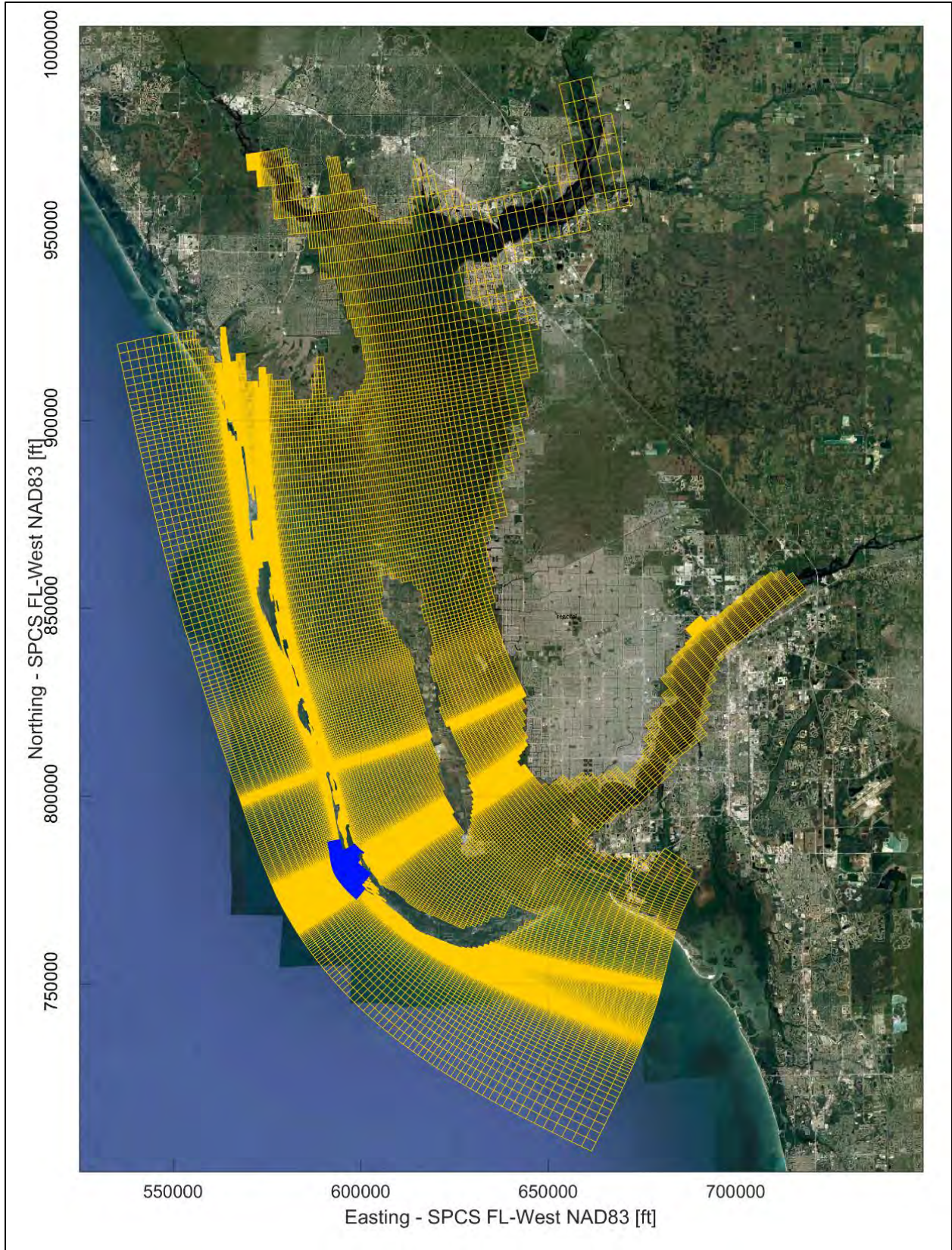
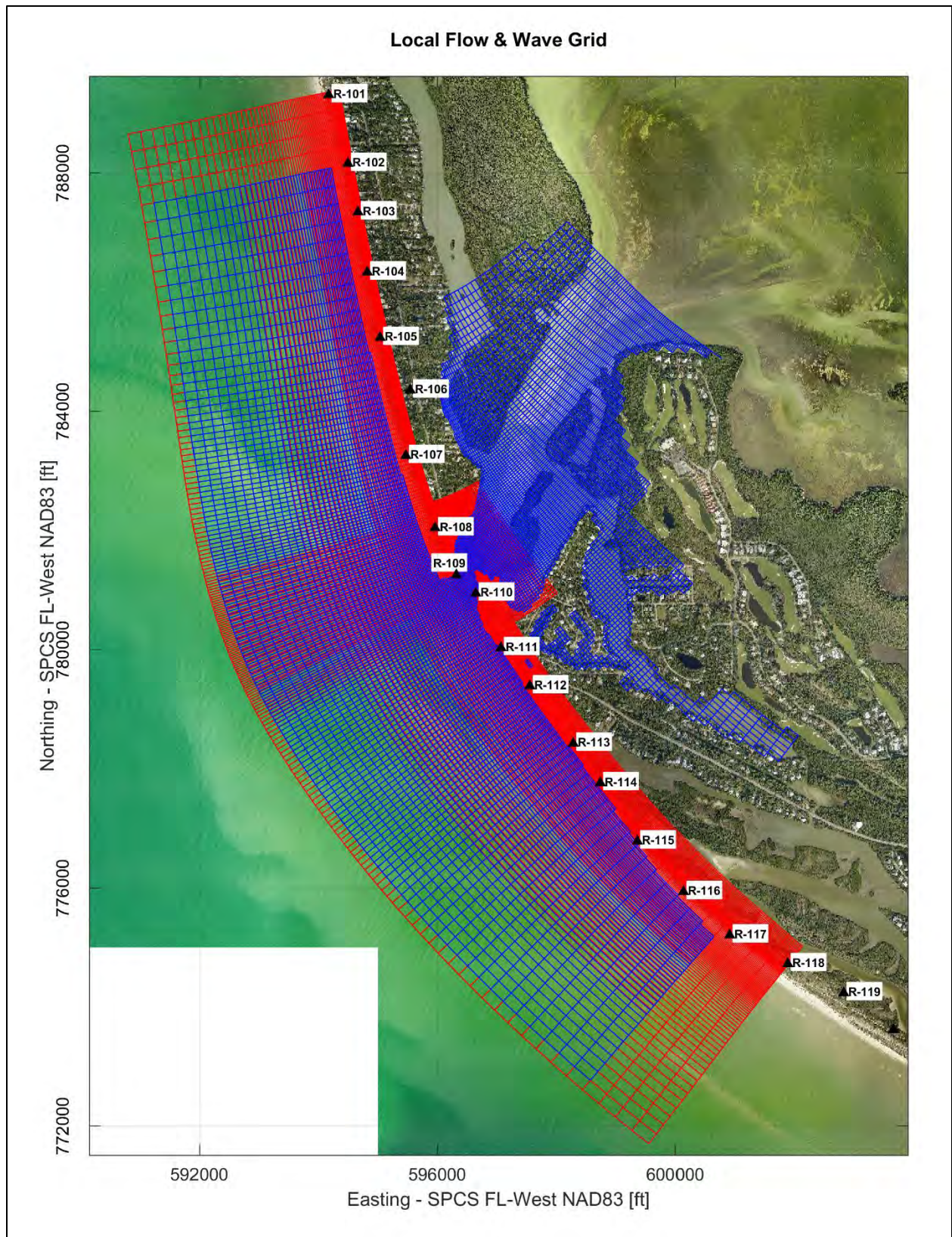


Figure 3-2: Regional Wave Grid (white), Intermediate Wave Grid (yellow) and Local Wave Grid (red).



**Figure 3-3: Regional Flow Grid (yellow) and Local Flow/Morphology Grid (blue).**



**Figure 3-4: Local Flow/Morphology Grid (blue) and Local Wave Grid (red).**

**Table 3-1: Summary of grid properties.**

Grid	Orthogonality	Smoothness		Spacing (feet)		Number of Cells	
		Long-shore	Cross-shore	Long-shore	Cross-shore	Long-shore	Cross-shore
Regional Wave	0 to 0.03	1.00 to 1.14	1.00 to 1.08	1,085 to 5,436	1,049 to 3,622	103	38
Intermed. Wave	0 to 0.04	1.00 to 1.10	1.00 to 1.02	219 to 597	351 to 623	122	73
Local Wave	0 to 0.036	1.00 to 1.09	1.00 to 1.08	21 to 361	11 to 213	181	119
Regional Flow	0 to 0.05	1.00 to 1.53	1.00 to 1.21	6 to 5,880	15 to 3,500	468	215
Local Flow	0 to 0.017	1.00 to 1.10	1.00 to 1.21	31 to 360	10 to 199	157	135
Recommended (Deltares, 2016a)	< 0.04	< 1.2	< 1.2				

### 3.2.Delft3D-WAVE Model Calibration

The numerical wave model Delft3D-WAVE (SWAN) is applied to propagate wave conditions from the offshore boundary of the model (approx. -50 ft. NAVD) to the nearshore areas adjacent to Blind Pass. In the nearshore areas, the wave model communicates and interacts with the flow/sediment transport model. Therefore, an appropriate representation of the wave regime along the study area is essential to reproduce the coastal processes that are the object of this study.

The Simulating Waves Nearshore Model (SWAN) was developed at Delft University of Technology (Netherlands) and can be used to simulate the evolution of random, short-crested wind-generated waves in coastal waters, estuaries, tidal inlets and lakes and has been validated and verified successfully in a range of complex laboratory and field experiments (Deltares, 2016b). The waves are described using the two-dimensional wave action density spectrum, even when non-linear phenomena dominate (e.g., in the surf zone). The model is capable of transforming offshore wave data into nearshore, taking into account processes such as wave refraction and diffraction due to the presence of shoals, channels or obstacles; wave generation by wind; wave dissipation by depth-induced breaking, white-capping and bottom friction; non-linear wave-wave interaction; and wave propagation through obstacles.

Inputs to the SWAN model include the bathymetry, the grid coordinates, the bottom friction factor, the wave breaking coefficients, the diffraction coefficients, the wind velocities, and the height, period, direction, and directional spreading values of each wave case. Outputs from the SWAN model include the wave height, wave peak period, and wave direction.

### 3.2.1. Boundary Conditions and Forcing

In order to assess the consistency of the wave model developed for the current application, results of the Delft3D-WAVE (SWAN) computations are compared with measured wave data at the Nearshore ADCP between December 11, 2015 and January 26, 2016. The offshore boundary conditions on the Regional Wave Grid were defined based on the observed waves the Offshore ADCP (Figure 3-5) as the wave hindcast database (NOAA/WW3) was not updated to the calibration period at the time the model calibration was performed.

During the model calibration period a wide range of distinct wave conditions were observed, representing a complete sample of the wave climate adjacent to the study area. The conditions ranged from mild to energetic sea states (1 ft – 12 ft) with a prominent energy decay/dissipation observed across the continental shelf, while waves propagate from deeper to shallower waters. The peak wave period ( $T_p$ ) varied from 3 to 12 seconds, encompassing primarily wind-sea wave conditions typically observed in the Gulf of Mexico. Waves approached the study area from different directions, with most conditions ranging from  $180^\circ$  (S) and  $360^\circ$  (N). Due to wave refraction effects, directional variability in the Nearshore ADCP gauge was less.

Time-varying wave conditions were imposed at the boundaries of the Regional Wave Grid. The boundary definitions for the Intermediate and Local Wave Grids are defined based on model results for the immediately larger domain (i.e. Regional and Intermediated Wave Grids, respectively).

In addition to the regional boundary conditions, time-varying winds and water levels were provided for the modeled area in order to account for local generation of waves and water depth variations due to tides. Wind velocities and directions were based on measured wind data at COMPS Station C10, provided at 20 minutes intervals (Figure 3-6). Water levels during the calibration period were based on the astronomical components provided by the global model of ocean tides TPXO7.2 for locations along the Gulf boundary of the model. The astronomical tides were combined with the low-frequency water level variations measured by the Nearshore ADCP (Figure 3-7). Water level signals were converted from MSL to NAVD88 using the tidal datum provided by NOAA for the station ST 8725110 in Naples, FL, where the MSL is -0.64 feet NAVD.

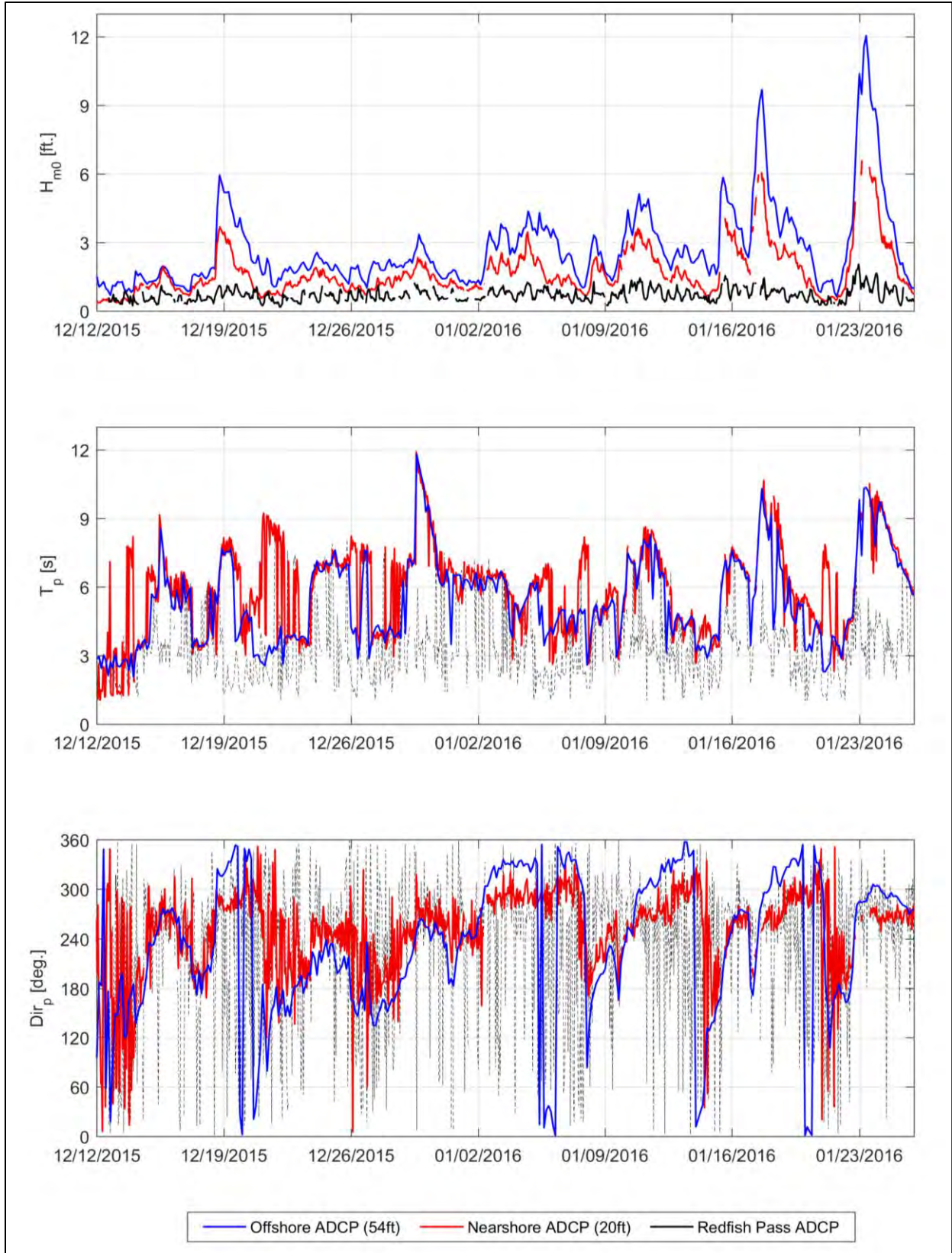


**Figure 3-5: Observed Waves during the Calibration Period. Offshore ADCP conditions were imposed along model offshore boundaries.**

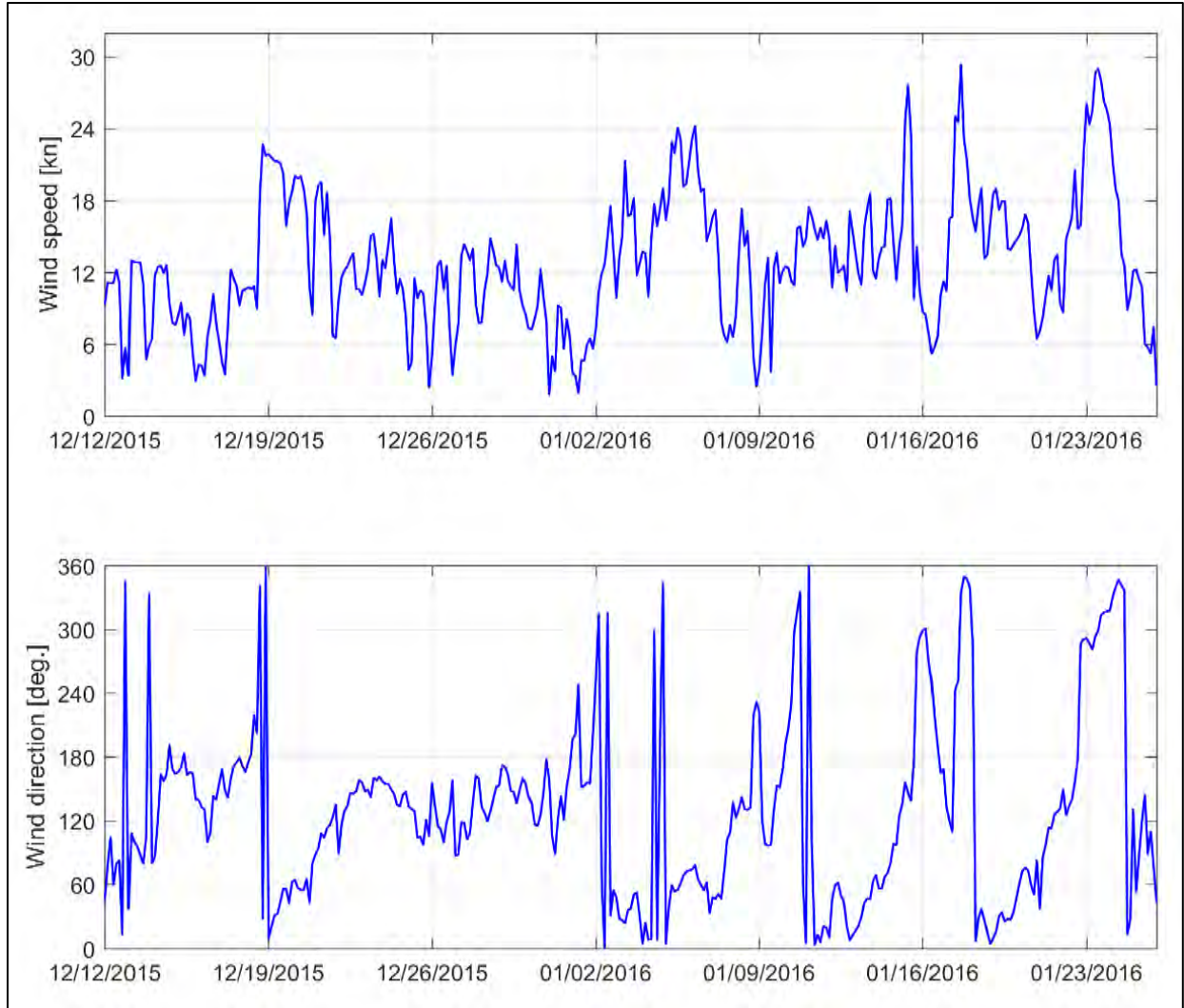


**Figure 3-6: Winds during the Calibration Period – measured at COMPS Station C10.**

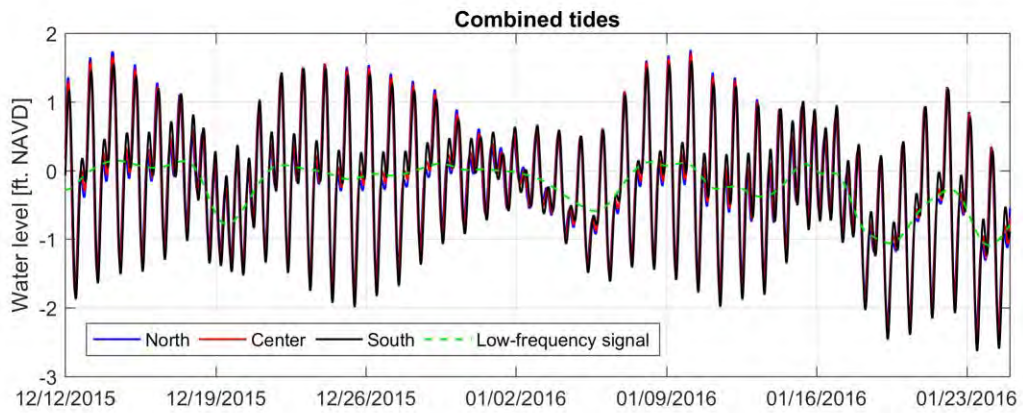
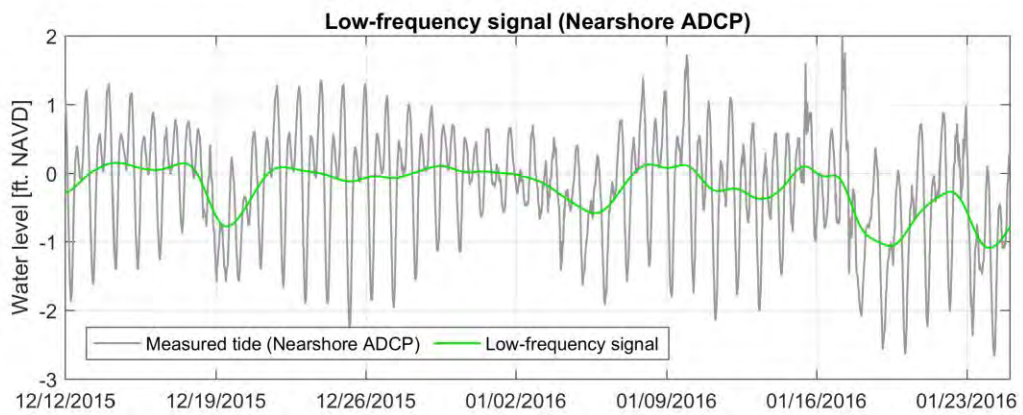
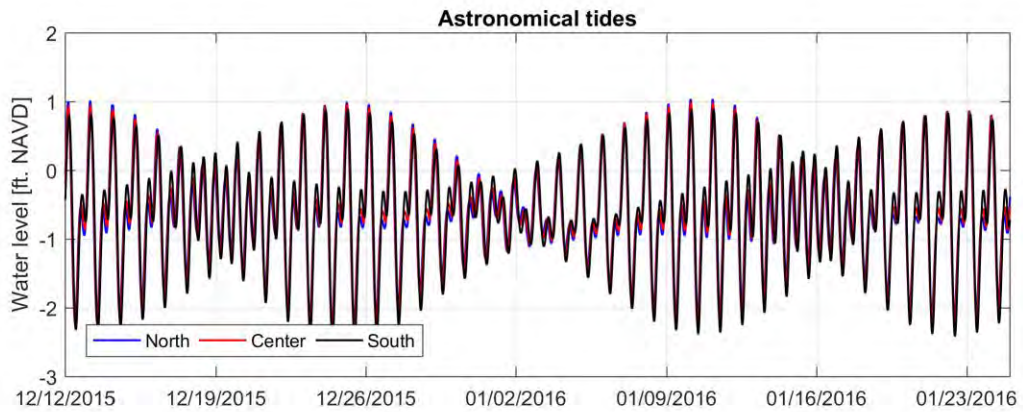


**Figure 3-7: Water Levels during the Calibration Period.**

### 3.2.2. Bathymetry

The bathymetry used in the calibration of the Delft3D-WAVE model (SWAN) was based on the bathymetric data sets between 1960 and 2015 (see Table 2-1). The 2015 surveys were used as the primary data source. Grid points outside the 2015 survey areas were filled using older data sets, using the NCEI/NOAA (NOAA Soundings and Coastal Relief Model) as the data set of last resort. Bathymetric surfaces used in the model appear in Figure 3-8 through Figure 3-10.

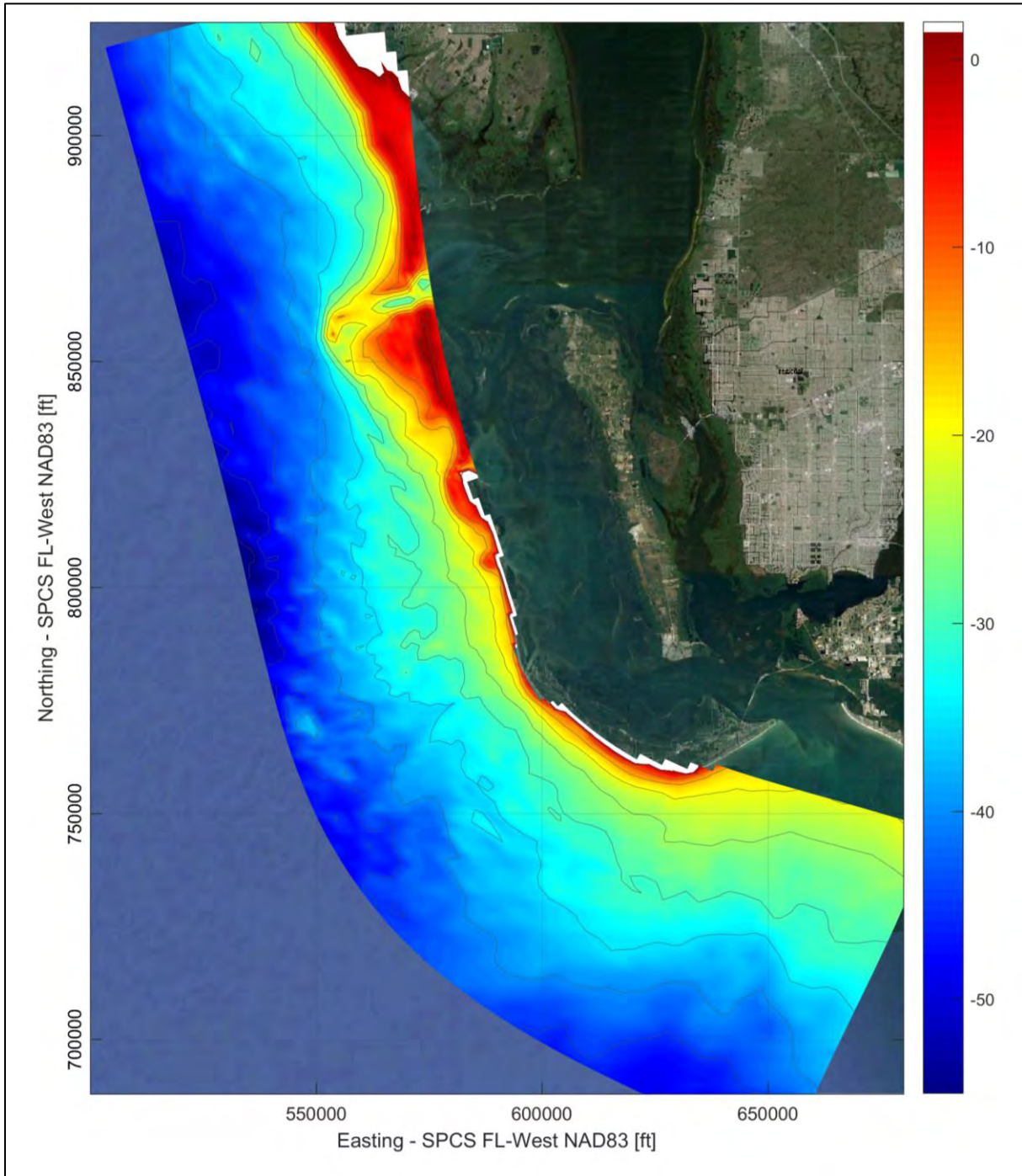


**Figure 3-8: Bathymetry over the Regional Wave Grid.**

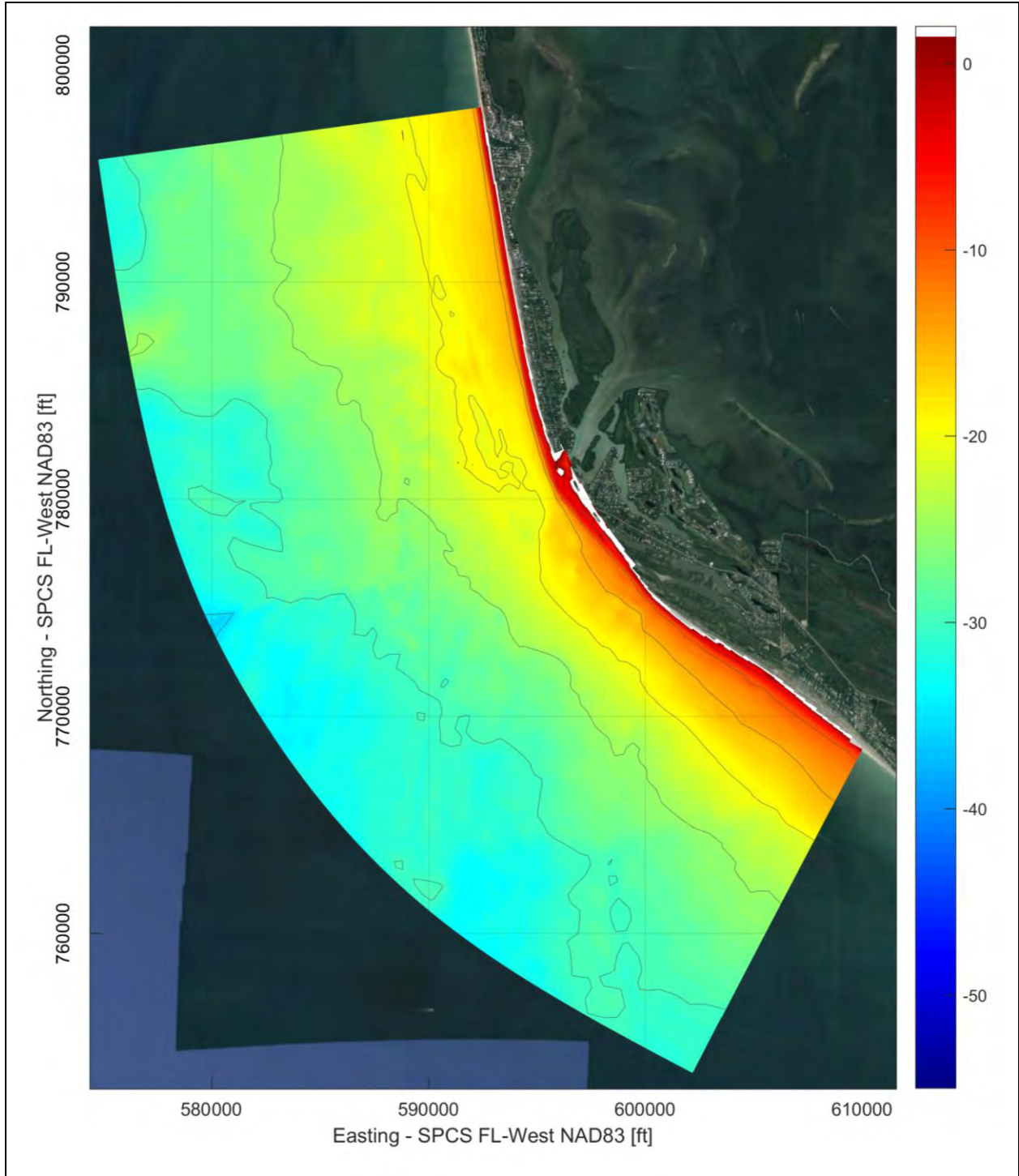


**Figure 3-9: Bathymetry over the Intermediate Wave Grid.**

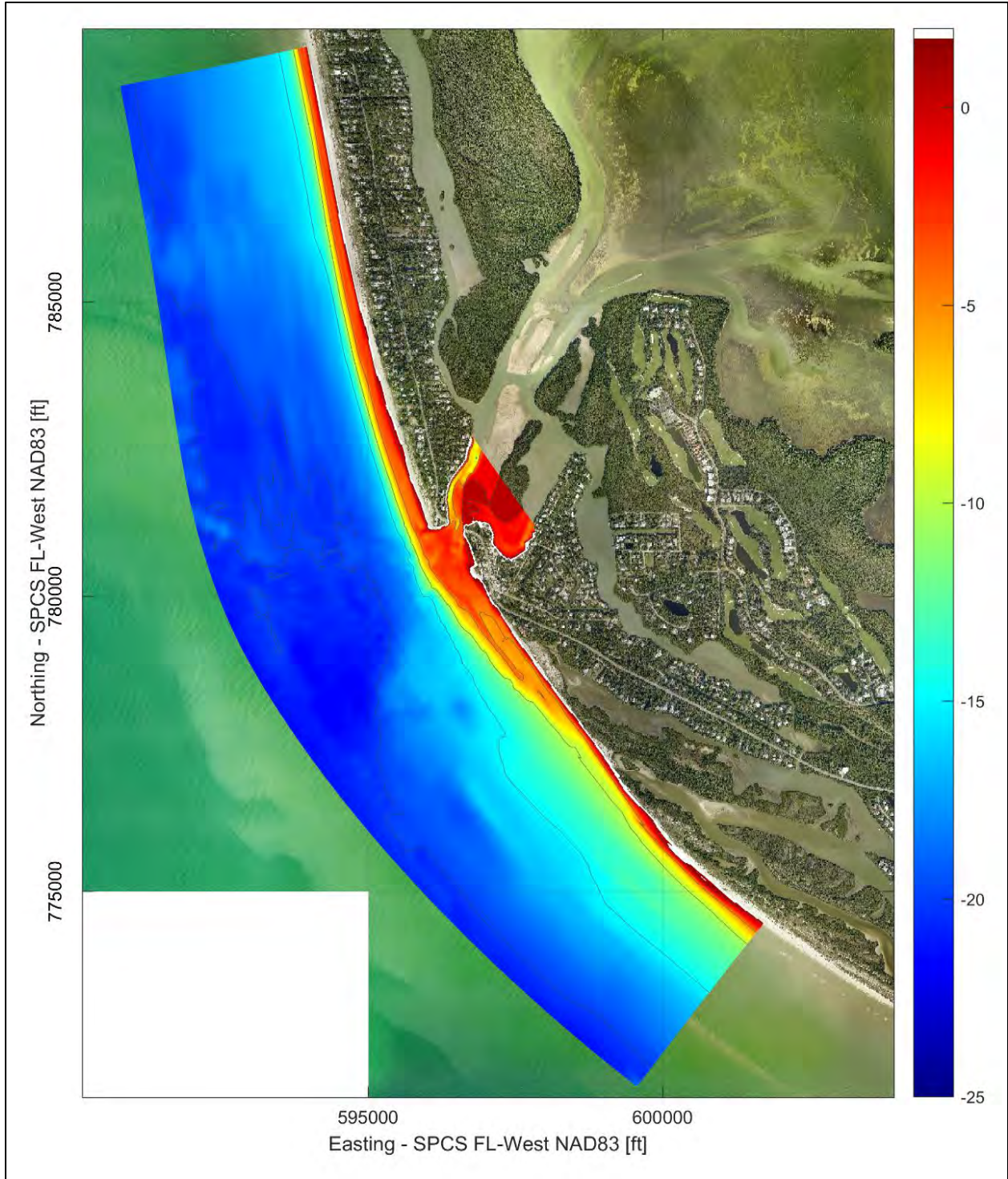


**Figure 3-10: Bathymetry over the Local Calibration Wave Grid through 2015. Color scale limits were changed relative to the maps in the previous pages to facilitate visualization.**

### 3.2.3. Model Calibration

The wave model results were compared to the measured data from the Nearshore ADCP. The Redfish Pass ADCP was deployed in the inlet throat, which is partially sheltered from waves due to local scale wave processes. As the wave model used in the Blind Pass study is not developed to resolve detailed waves processes in the Redfish Pass, assessments of the wave model performance are not made at that location.

The primary parameter examined during the SWAN calibration process was the bottom friction. This parameter had the most influence on the results at the locations of the ADCPs. To account for local wave development due to wind, SWAN's wind stress formulation was used in all calibration runs, along with the default diffraction formulation. All other model parameters were set to their default values and the computations were performed in stationary mode.

The JONSWAP (Hasselmann *et al.*, 1973) bottom friction dissipation formulation was used and three different JONSWAP coefficients for bottom friction dissipation were tested: 0.038, 0.067, and 0.096 m<sup>2</sup>/s<sup>3</sup>. Results for these tests are generally similar, with waves slightly bigger for the lower bottom friction coefficient (0.038 m<sup>2</sup>/s<sup>3</sup>) with respect to the more dissipative simulations (e.g. 0.096 m<sup>2</sup>/s<sup>3</sup>). The criteria to select the parameter that best represent the waves for the study area were based on the Root Mean Square Error (RMSE) of the three different JONSWAP coefficients simulated versus the observed data (Table 3-2). The wave transformation in the study area was better represented by using the 0.067 m<sup>2</sup>/s<sup>3</sup> JONSWAP coefficients for bottom friction dissipation, and was selected for use in subsequent simulations.

**Table 3-2: SWAN calibration summary.**

JONSWAP bottom-friction coefficient	0.038 m <sup>2</sup> /s <sup>3</sup>	0.067 m <sup>2</sup> /s <sup>3</sup>	0.096 m <sup>2</sup> /s <sup>3</sup>
NEARSHORE ADCP			
Hs(simulated) – Hs(observed) (feet)			
Mean	0.19	0.01	-0.13
Root-Mean-Square	0.40	0.32	0.37
Tp (simulated) – Tp (observed) (s)			
Mean	-0.73	-0.82	-0.89
Root-Mean-Square	1.46	1.55	1.59
Mean Dir.(simulated) – Mean Dir.(observed) (°)			
Mean	-27.1	-30.6	-31.6
Root-Mean-Square	69.2	78.1	79.8

Comparisons between the simulated and observed waves at the Nearshore ADCP location appear in Figure 3-11 to Figure 3-14. In these figures, the percentage in parentheses following the RMSE value is the RMSE value divided by the range of variation in the measured data. This percentage is a measure of the error with respect to the natural variability of the analyzed parameter.

Overall, the model results show that the SWAN model is able to realistically predict the wave parameters in the nearshore areas. During some conditions of the simulated month, the peak wave period and peak wave direction are reasonably reproduced. It is highlighted that especially for multi-modal wave spectra (e.g. superposition of swell wave condition(s) and wind sea), relatively small deviations in the wave energy distribution between the sea states may result in the selection of a different peak and therefore large differences in peak wave parameters. Such deviation does not necessarily mean, however, that the overall sea state is misrepresented.

The configuration of the Delft3D-WAVE (SWAN) model is summarized on Table 3-3. Typical wave patterns over the 3 grids used in the model appear in Figure 3-15 to Figure 3-17.

**Table 3-3: Summary of the Delft3D-WAVE (SWAN) model parameters.**

<b>SWAN Wave Transformation Model Parameters:</b>	<b>Min.</b>	<b>Default</b>	<b>Max.</b>	<b>Best Run Parameters</b>
Breaking Parameter Gamma (Hb/db)	0.55	0.73	1.2	0.73
Breaking Parameter Alpha	0.1	1	10	1
JONSWAP Friction Value (m <sup>2</sup> /s <sup>3</sup> )	0	0.067	None	0.067
Triads - Energy Transfer from low to high frequencies in shallow water	-N/A-	Off	-N/A-	On
Diffraction:	-N/A-	Off	-N/A-	On
Diffraction Smoothing Coefficient	0	0.2	1	0.2
Diffraction Smoothing Steps	1	5	999	5
Wind Growth	-N/A-	On	-N/A-	On
JONSWAP Peak Enhancement Factor (for input parametric wave conditions)	-N/A-	3.3	-N/A-	3.3

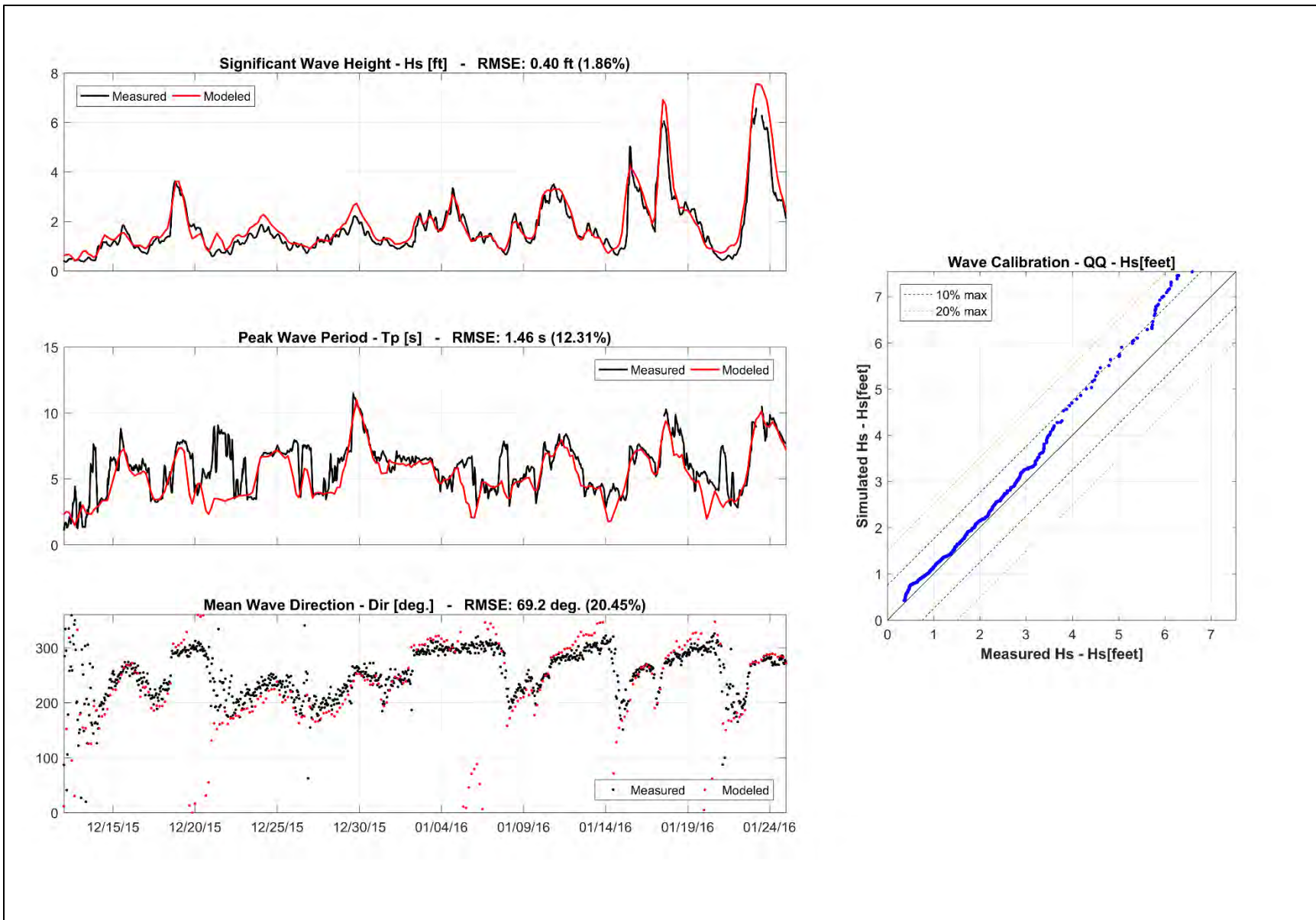


Figure 3-11: SWAN Model Results at the Nearshore ADCP. JONSWAP coefficients for bottom friction dissipation: 0.038 m<sup>2</sup>/s<sup>3</sup>.

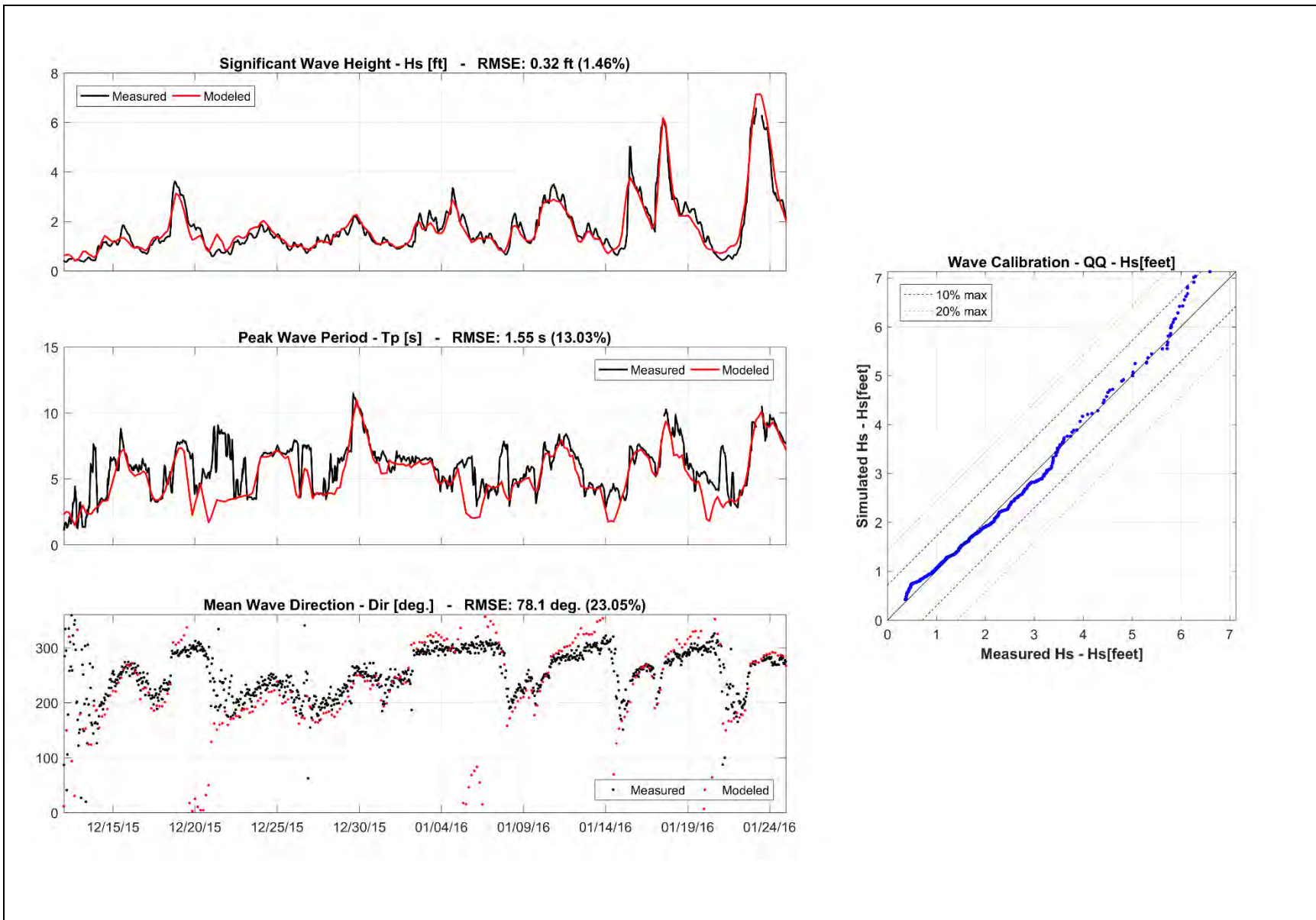


Figure 3-12: SWAN Model Results at the Nearshore ADCP. JONSWAP coefficients for bottom friction dissipation:  $0.067 \text{ m}^2/\text{s}^3$ .

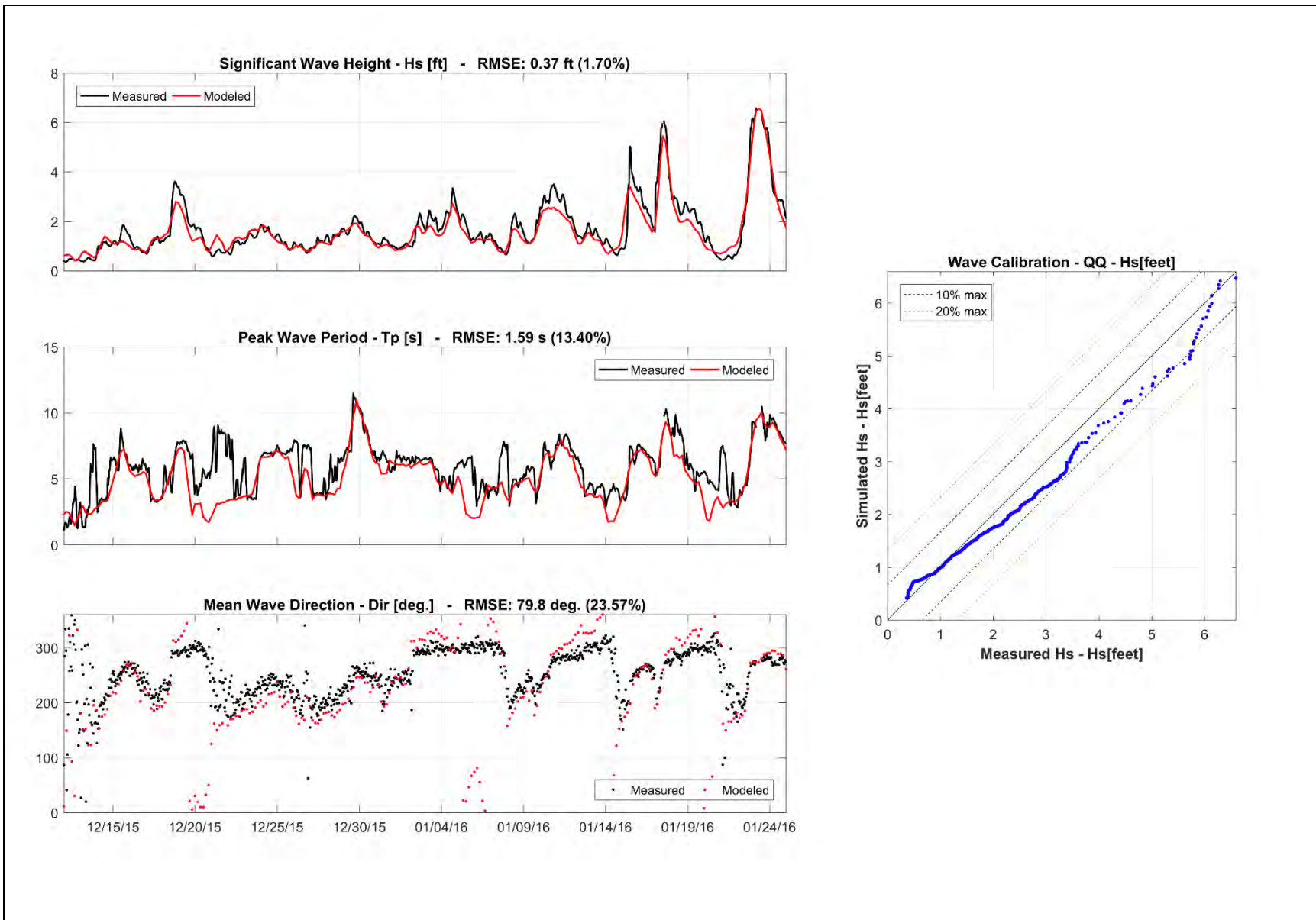


Figure 3-13: SWAN Model Results at the Nearshore ADCP. JONSWAP coefficients for bottom friction dissipation:  $0.096 \text{ m}^2/\text{s}^3$ .

Simulated, JONSWAP Bottom Friction Coef. =  $0.067 \text{ m}^2 \text{ s}^{-3}$

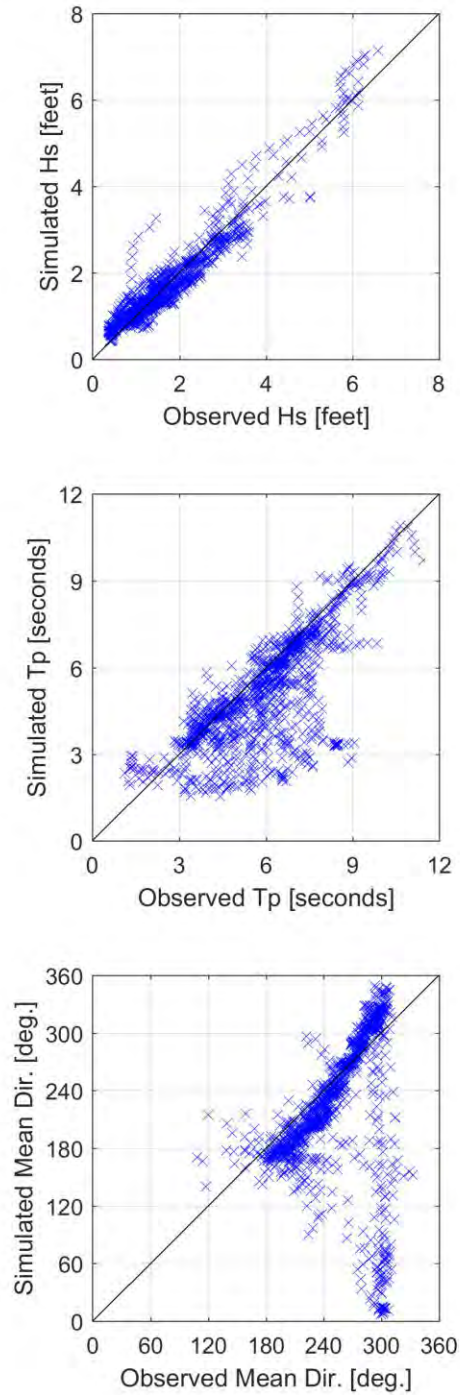
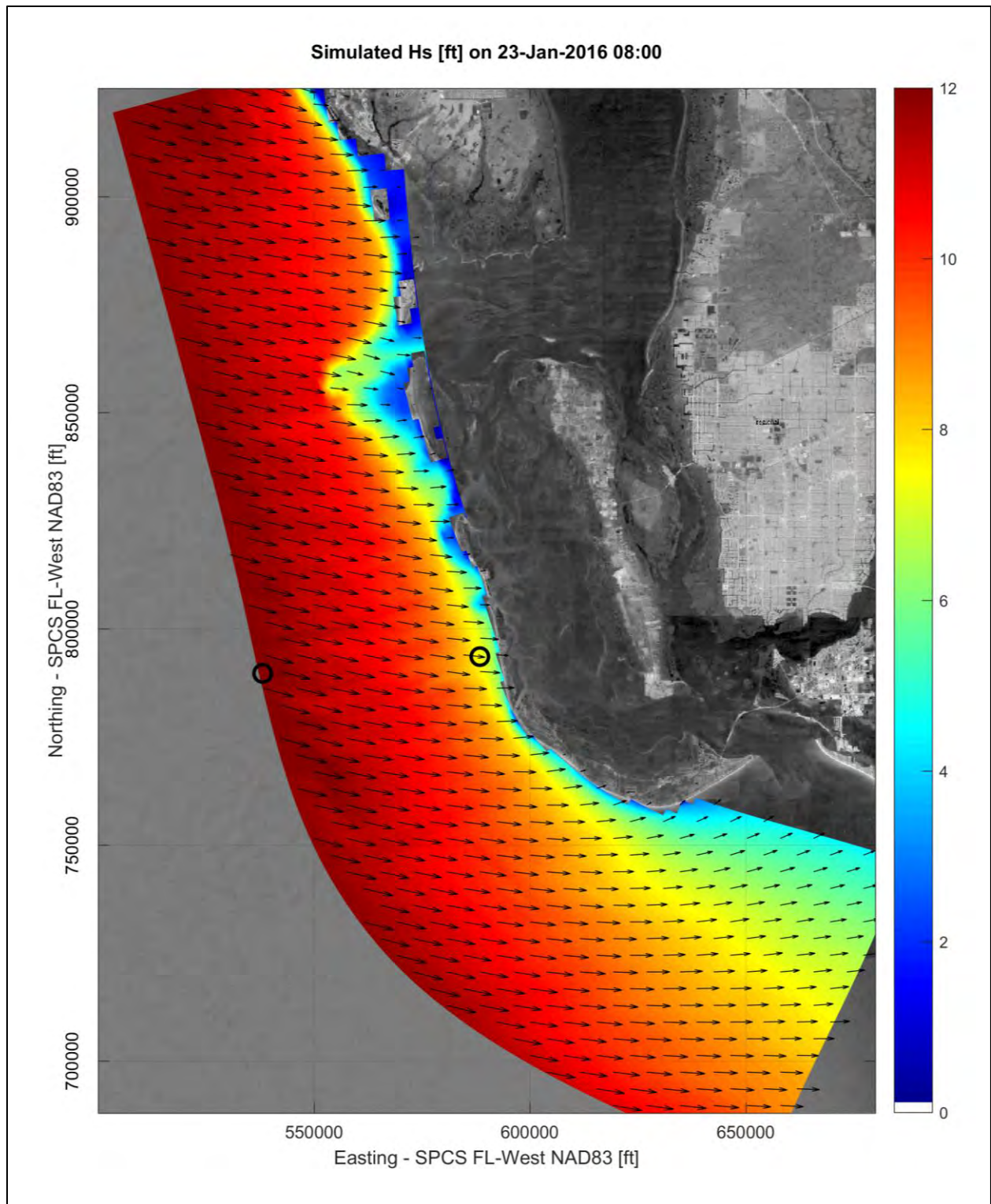
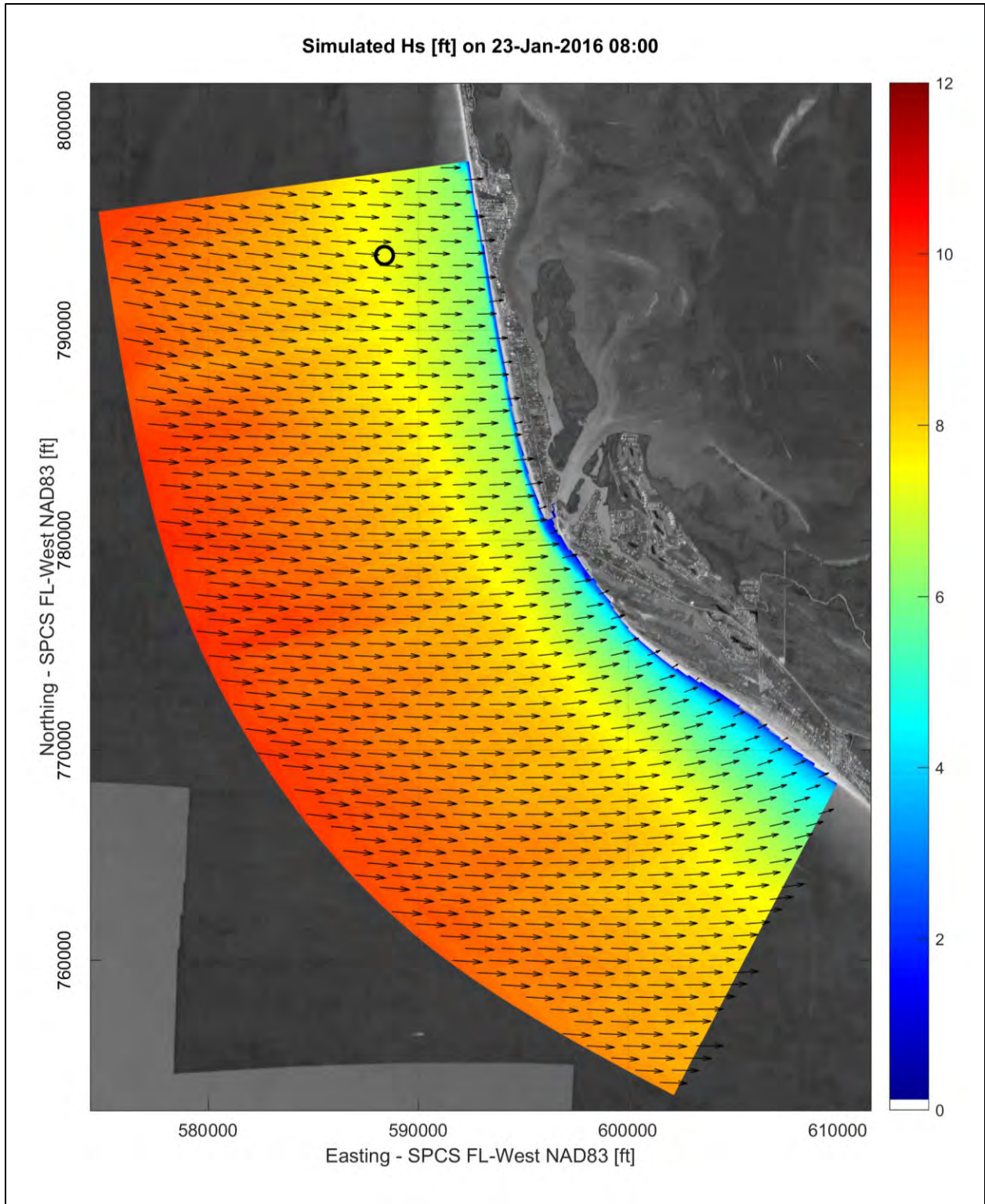


Figure 3-14: Scatter Plot of SWAN Model Results at the Nearshore ADCP.



**Figure 3-15: Typical SWAN Results during the Calibration Period over the Regional Wave Grid. Black circle indicate the location of the Offshore and Nearshore ADCPs.**



**Figure 3-16: Typical SWAN Results during the Calibration Period over the Intermediate Wave Grid. Black circle indicate the location of the Nearshore ADCP.**

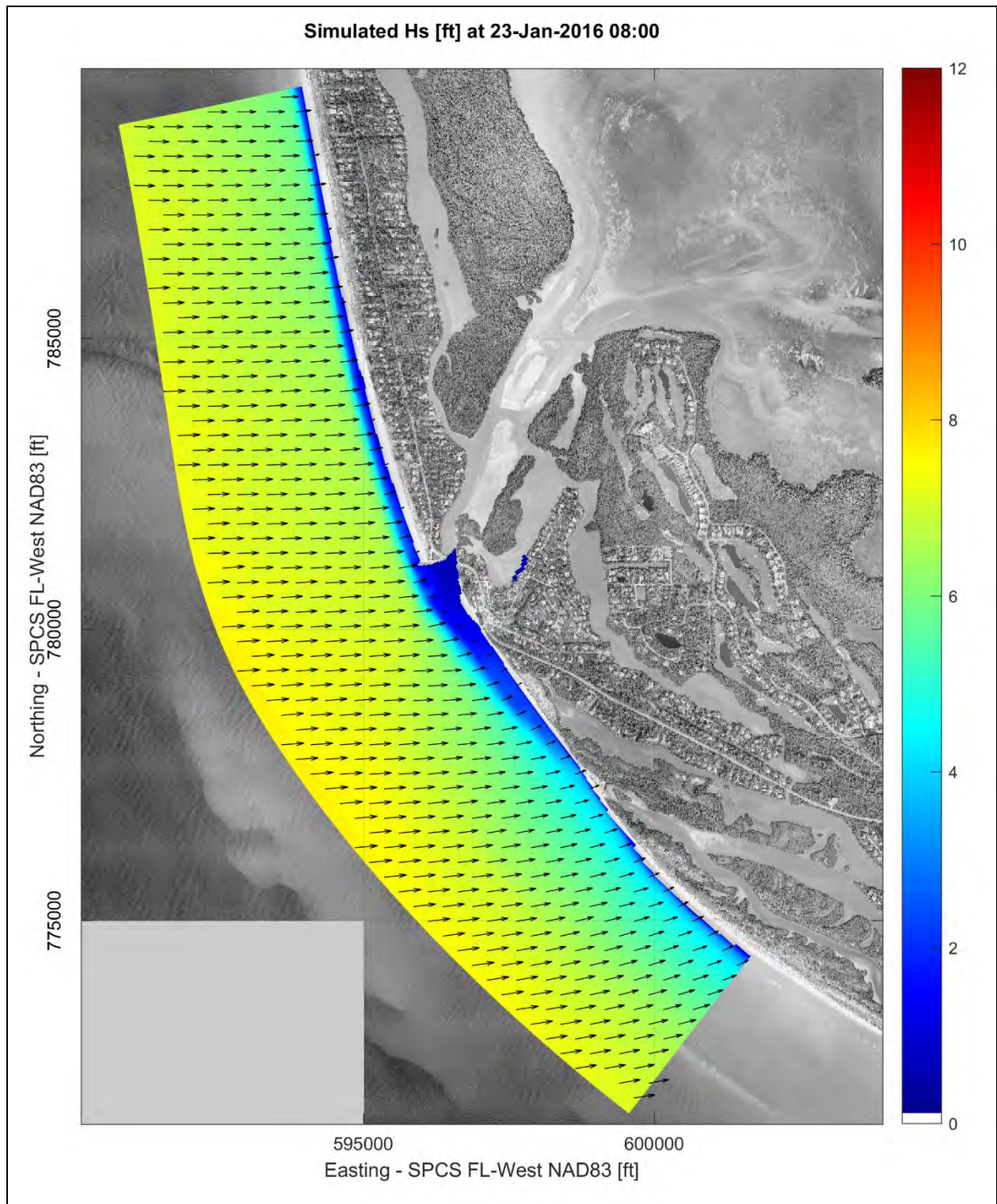


**Figure 3-17: Typical SWAN Results during the Calibration Period over the Local Wave Grid.**

### **3.3. Delft3D-FLOW Hydrodynamic Calibration**

The objective of the hydrodynamic modeling is to reproduce the patterns of the water flow through Blind Pass and adjacent areas, controlled by the ebb and flood variability of the currents and water level. Wind effects and wave-induced alongshore currents driven by radiation stress gradients are also taken into account in the hydrodynamic simulations. These are the driving processes of the evolution of the morphology of the inlet and the adjacent beaches, which is the final piece of the modeling study.

An offline nesting approach was applied in order to optimize the computational time. Two grids are used in the hydrodynamic simulations (grid specifications are provided in Section 3.1):

- Regional Flow Grid: covers a larger area and includes the whole Pine Island Sound and its connections to the Gulf of Mexico;
- Local Flow Grid: covers a smaller area, centered at the area of interest.

The Regional Flow model is run in 2DH mode (i.e. depth-averaged), while the Local Flow computations are performed considering 6 vertical sigma-layers with variable fractions of the local water depth at each computational point: 32.3%, 23.4%, 16.9%, 12.2%, 8.8%, 6.4% (from surface to bottom).

Hydrodynamic results of the Regional Model are provided as boundary conditions for the simulations using the Local Flow Grid, which makes the Local Flow model ‘nested’ into the Regional one. The information is updated every 20 minutes and include water levels along the offshore and Pine Island Sound boundaries and water discharges at the Roosevelt Channel and Dinkins Bayou boundaries.

#### **3.3.1. Boundary Conditions and Forcing**

Inlet flows were calibrated based on the 2015/2016 current and water level measurements (Table 2-2 and Figure 2-8). The calibration period was from December 10, 2015, to January 25, 2016. Two grids were utilized during the calibration – the Regional Flow Grid and the Local Flow Grid (Figure 3-3 and Figure 3-4). Results obtained with Regional Flow Grid were used to define boundary conditions of the detailed Local Flow domain using an offline nesting approach.

The hydrodynamic simulations covering the flow calibration period were forced with waves (calibrated Delft3D-WAVE setup – input data given in Figure 3-5), winds and water levels. The wind and offshore water level boundary conditions on the Regional Flow Grid are presented in Figure 3-6 and Figure 3-7, respectively. Zero-gradient boundary conditions were applied on the upcoast and downcoast boundaries of the Regional Flow Grid. In other words, water levels just outside the grid were assumed to be equal to water levels just inside. Flows within the Regional Flow Grid were estimated using a depth-averaged flow formulation. The water levels based on these results provided the offshore, upcoast, and downcoast boundary conditions on the Local Flow Grid. Water levels at the northern section of the Wulfert Channel and discharges through the

Roosevelt Channel and Dinkins Bayou were also incorporated as boundary conditions to the Local Flow simulations.

### **3.3.2. Bathymetry**

The bathymetry used in the calibration of the nearshore and inlet flow was based on the bathymetric data sets between 1960 and 2015 (Table 2-1). The 2015 surveys were used as the primary data source. Grid points outside the 2015 survey areas were filled using older data sets, using the NCEI/NOAA (NOAA Soundings and Coastal Relief Model) last. In this manner, bathymetric surfaces used in the model utilized the most recent survey available at a given location. Bathymetric surfaces used in the Regional and Local Flow models appear in Figure 3-18 through Figure 3-20.

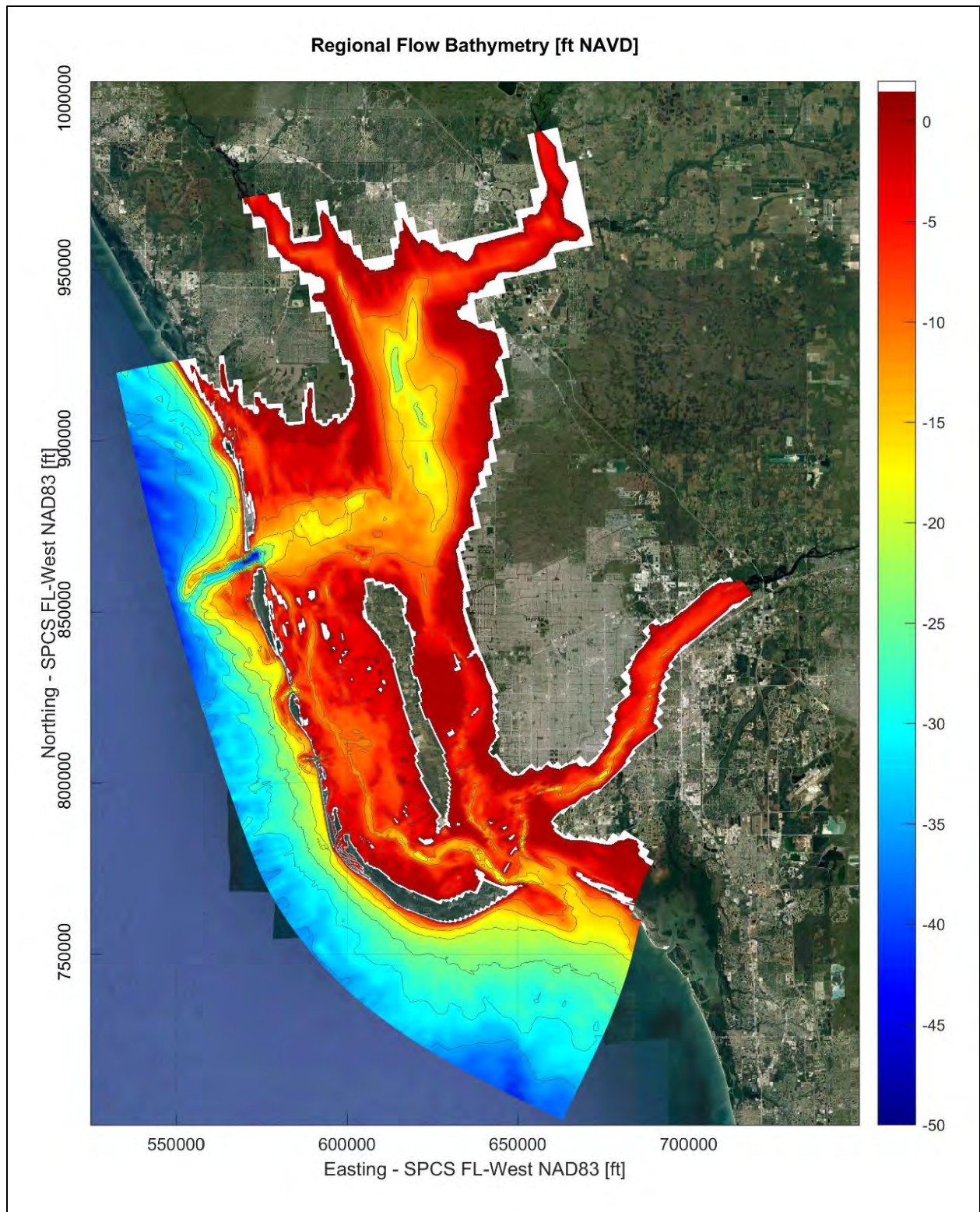


**Figure 3-18: Bathymetry over the Regional Flow Grid.**

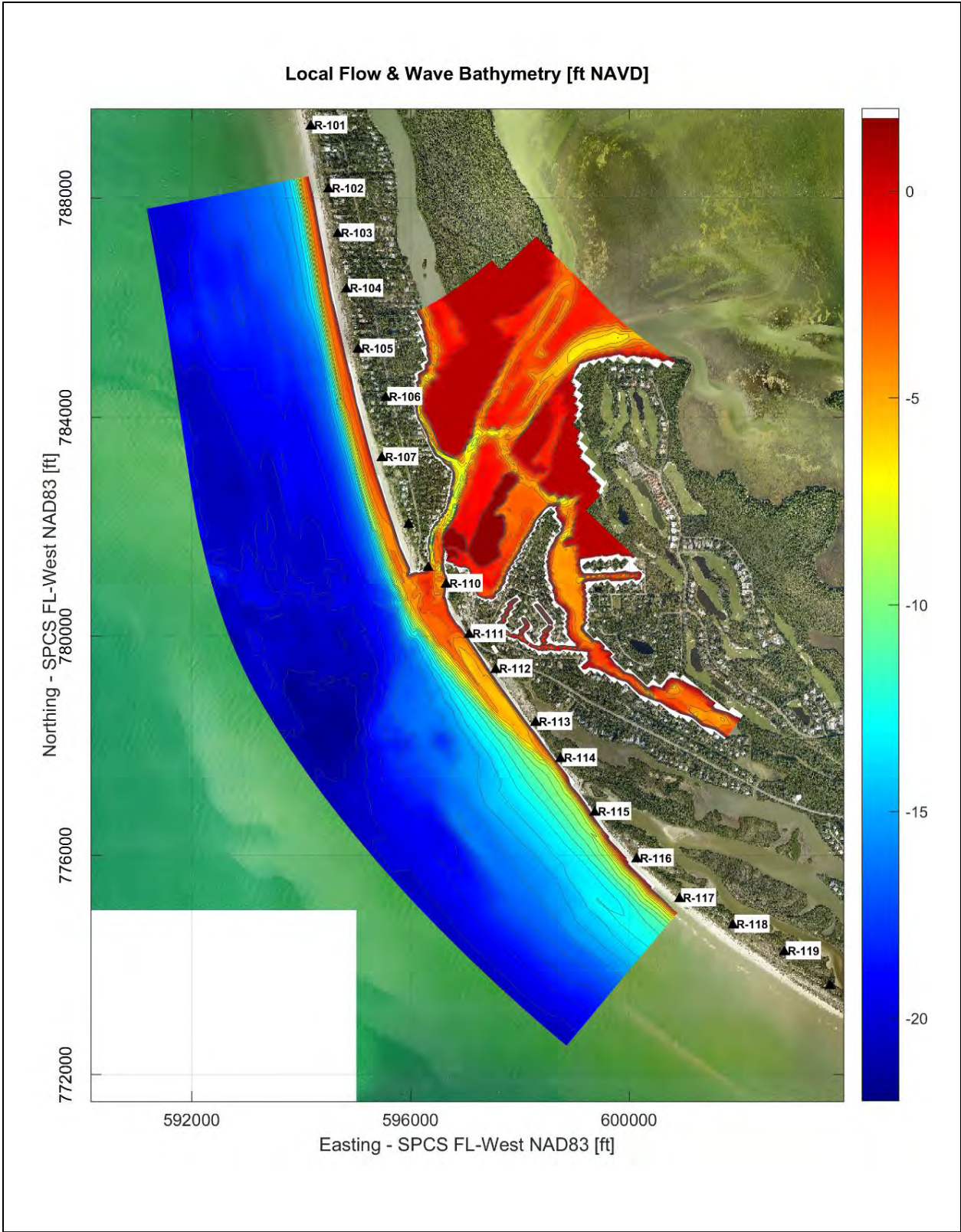


**Figure 3-19: 2015 Bathymetry over the Local Flow (1992) Grid in feet NAVD.**

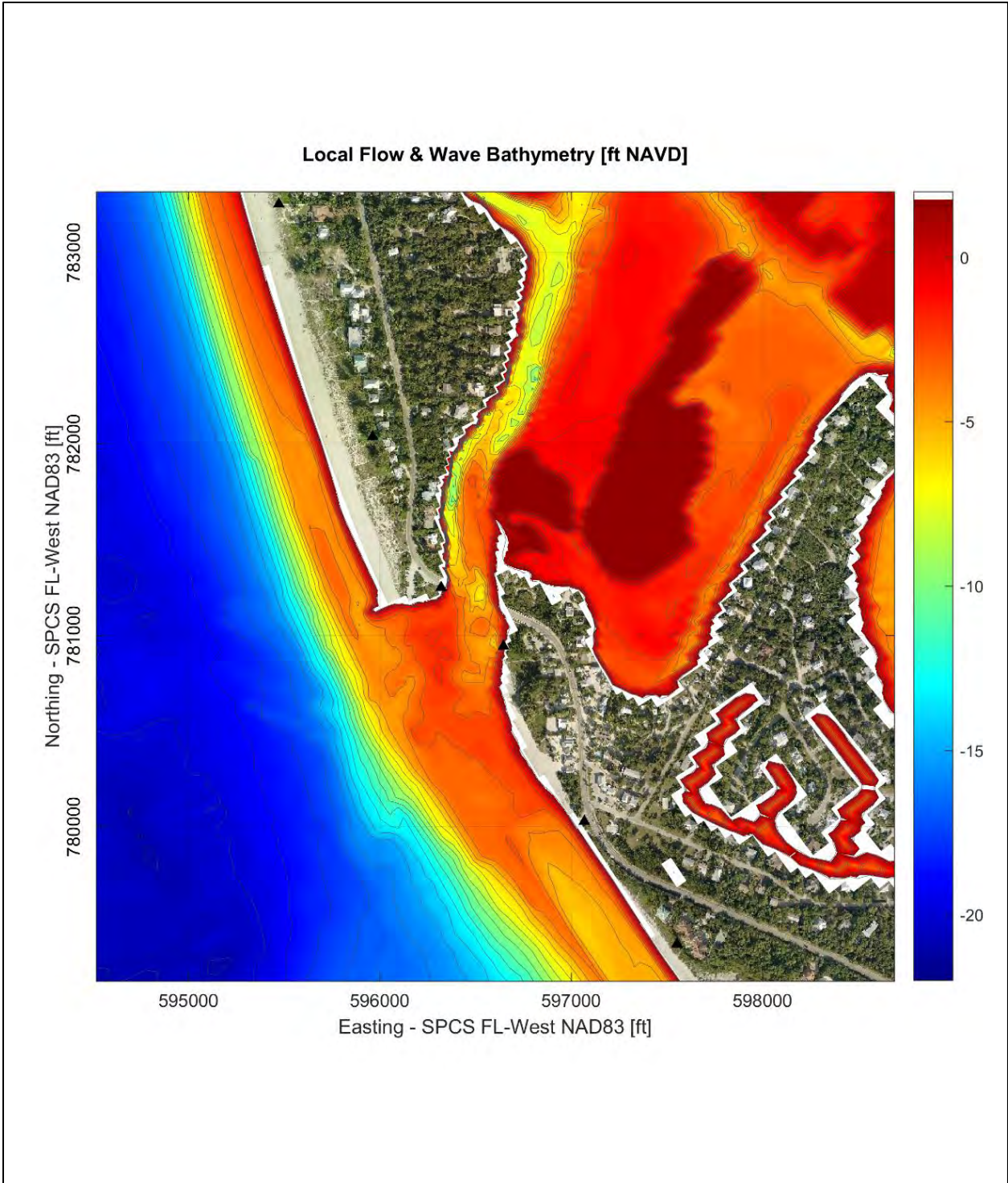


**Figure 3-20: 2015 Bathymetry over the Local Flow Grid in feet NAVD (Close-up).**

### 3.3.3. Bed Roughness

In the Delft3D model, the shear stress at the bed induced by a turbulent flow is assumed to be given by a quadratic friction law:

$$\vec{\tau}_b = \frac{\rho_0 g \vec{U} |\vec{U}|}{C_{2D}^2}$$

Where  $|\vec{U}|$  is the magnitude of the depth-averaged horizontal velocity and  $C_{2D}$  is the specified 2D Chezy's friction coefficient. A lower Chezy friction coefficient corresponds with a larger bottom roughness and thus a larger resistance; conversely a higher value corresponds with smaller roughness and less bed resistance.

Seagrasses and mangrove vegetation located inside the bay influence the currents by increasing the bed roughness. Outside of the submerged aquatic vegetation areas  $C_{2D}$  was defined as 80  $m^{1/2}/s$ . Within the submerged aquatic vegetation areas, the Chezy friction coefficient was lowered to 50  $m^{1/2}/s$ . In shallow regions with mangrove vegetation, Chezy coefficient was further reduced to 8  $m^{1/2}/s$ . The definition of the seagrass and mangrove distribution is described in Section 2.3 of this report and the Chezy coefficient map as used in the regional flow simulation is given in Figure 3-21.

A time variable bed roughness coefficient is used in the Local Flow Model, considering that this model setup is the base for the sediment transport and morphology simulations. This functionality was recently incorporated into the Delft3D model, and uses a bed roughness predictor based on the evolution of bed forms such as ripples and mega ripples over time as a function of the local water depth and hydrodynamics.

### 3.3.4. Model Calibration – Regional Flow Grid

Comparisons between the simulated and observed currents at the Nearshore ADCP, Redfish Pass ADCP, Blind Pass Current Meter, Pine Island Sound North and Pine Island South gauges appear in Figure 3-22 to Figure 3-29. Mean and average errors for the different gages and parameters are displayed in Table 3-4. Typical flow patterns during peak flood and peak ebb appear in Figure 3-32 and Figure 3-33.

The model was able to capture the average current velocities in the Nearshore ADCP, as well as the wind driven events that forced the increase in the current velocities (Figure 3-22). The model was able to replicate the differences between the velocity components in both Redfish Pass and Blind Pass gauges (Figure 3-23 and Figure 3-24). Overall, the model results show that the Delft3D-FLOW model is able to realistically simulate the typical flow patterns in the nearshore area, at Redfish Pass and Blind Pass.

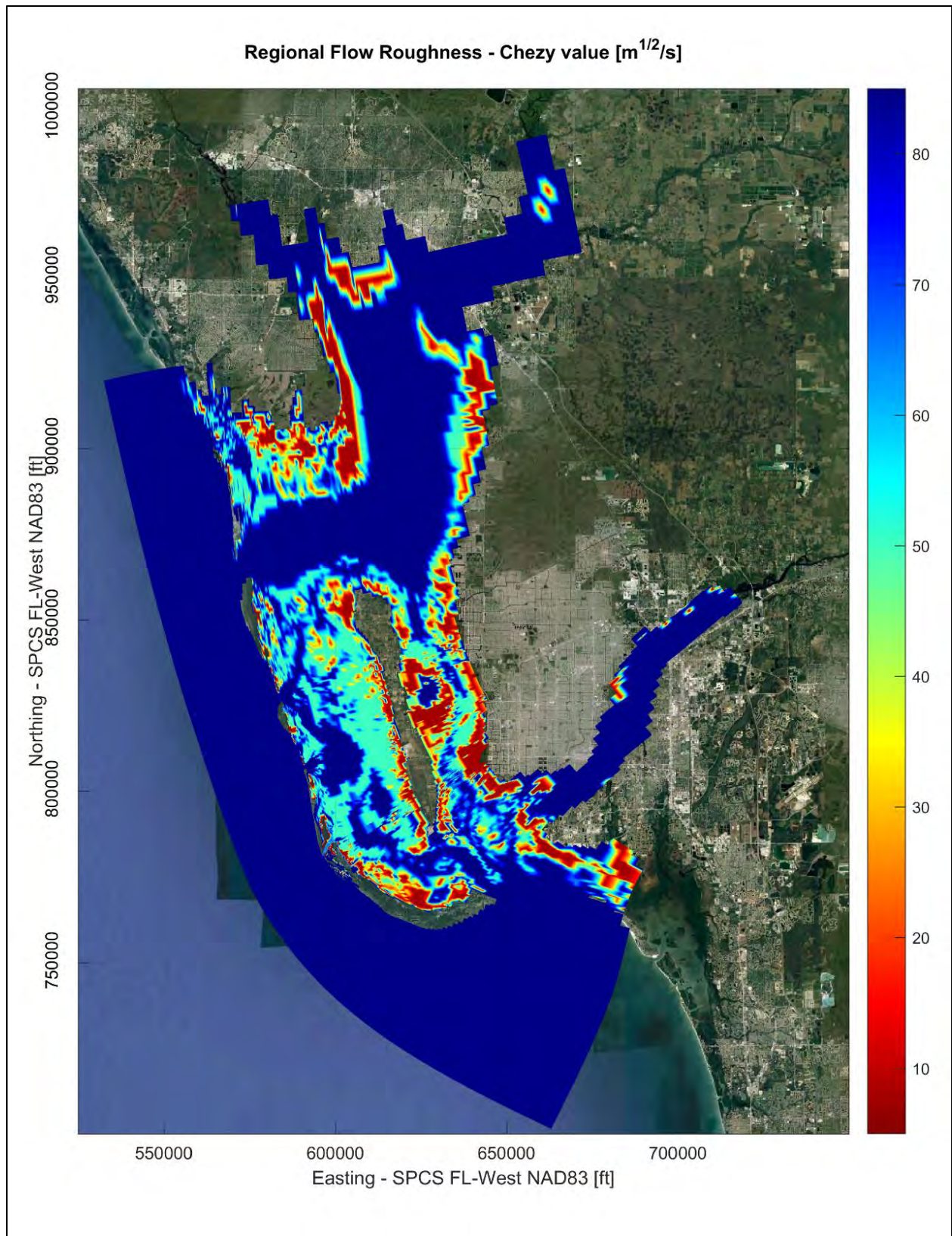


**Figure 3-21: Variation of Chezy Friction Coefficient; mangrove = 8 m<sup>1/2</sup>/s; sea grass = 50 m<sup>1/2</sup>/s; other areas = 80 m<sup>1/2</sup>/s.**

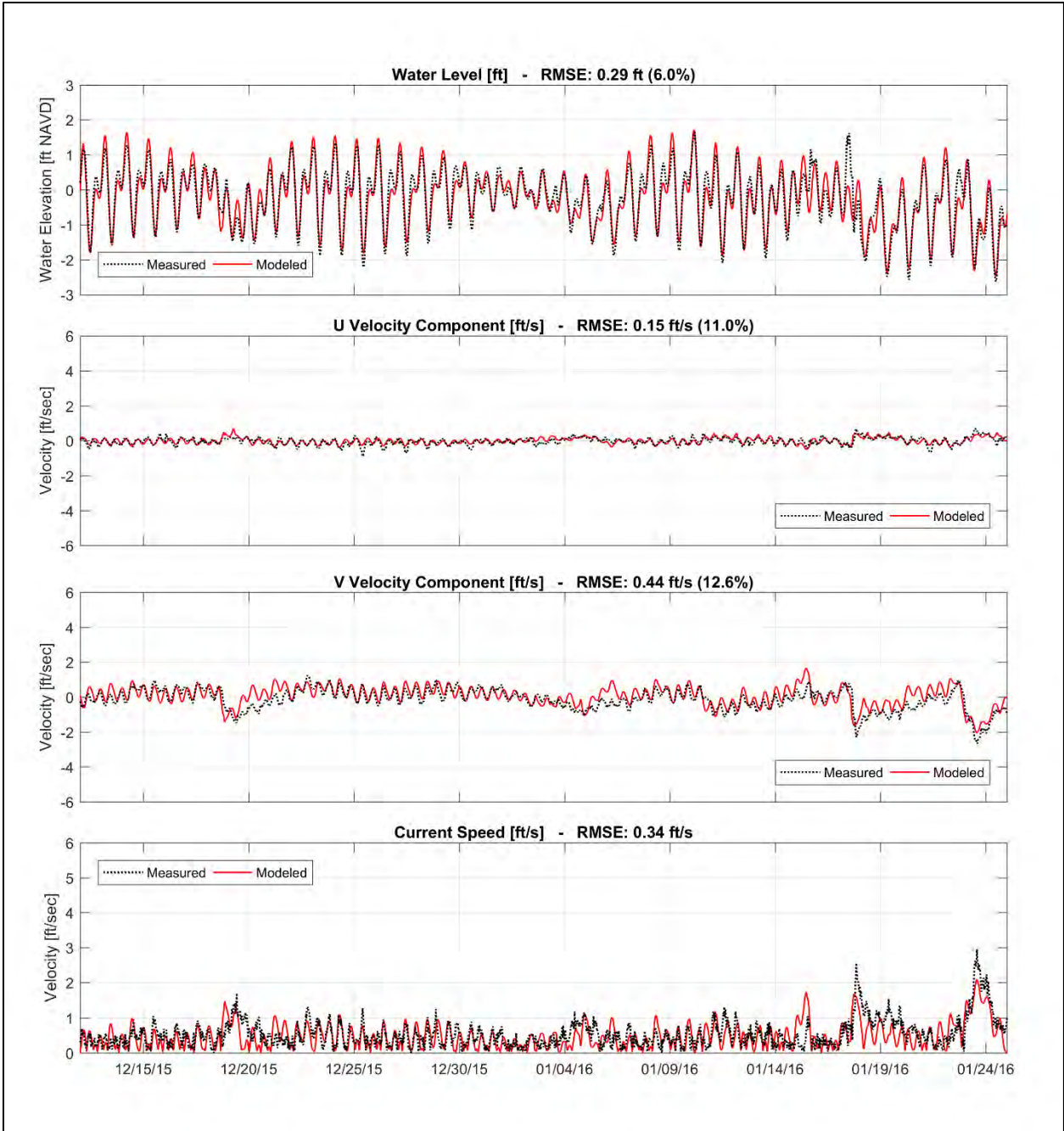


**Figure 3-22: Comparison between measured and simulated water levels and currents at the location of the Nearshore ADCP. Top: Water level; 2nd: U-velocity; 3rd: V-velocity; bottom: Velocity magnitude.**

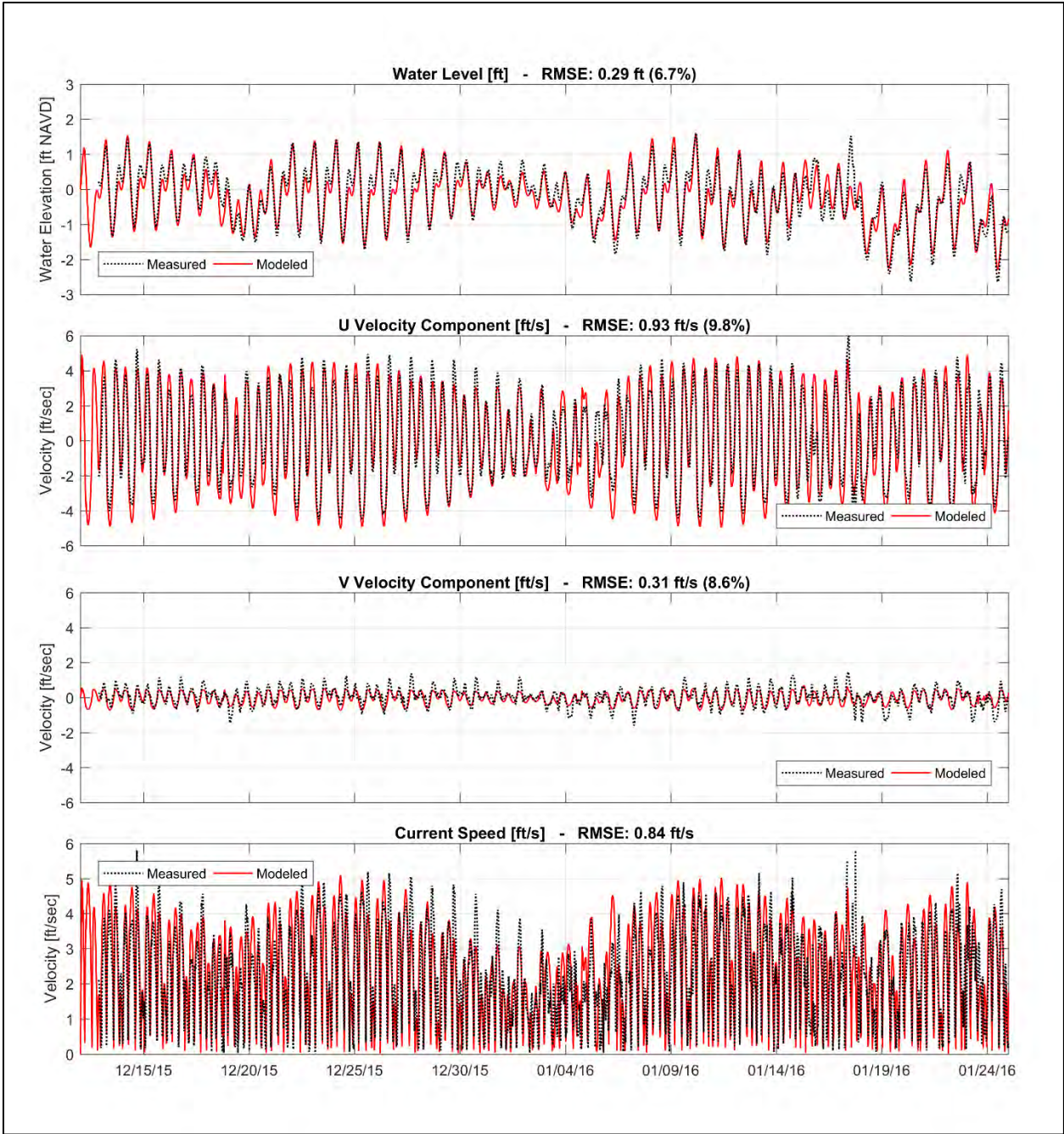


**Figure 3-23: Comparison between measured and simulated water levels and currents at the location of the Redfish Pass ADCP. Top: Water level; 2nd: U-velocity; 3rd: V-velocity; bottom: Velocity magnitude.**

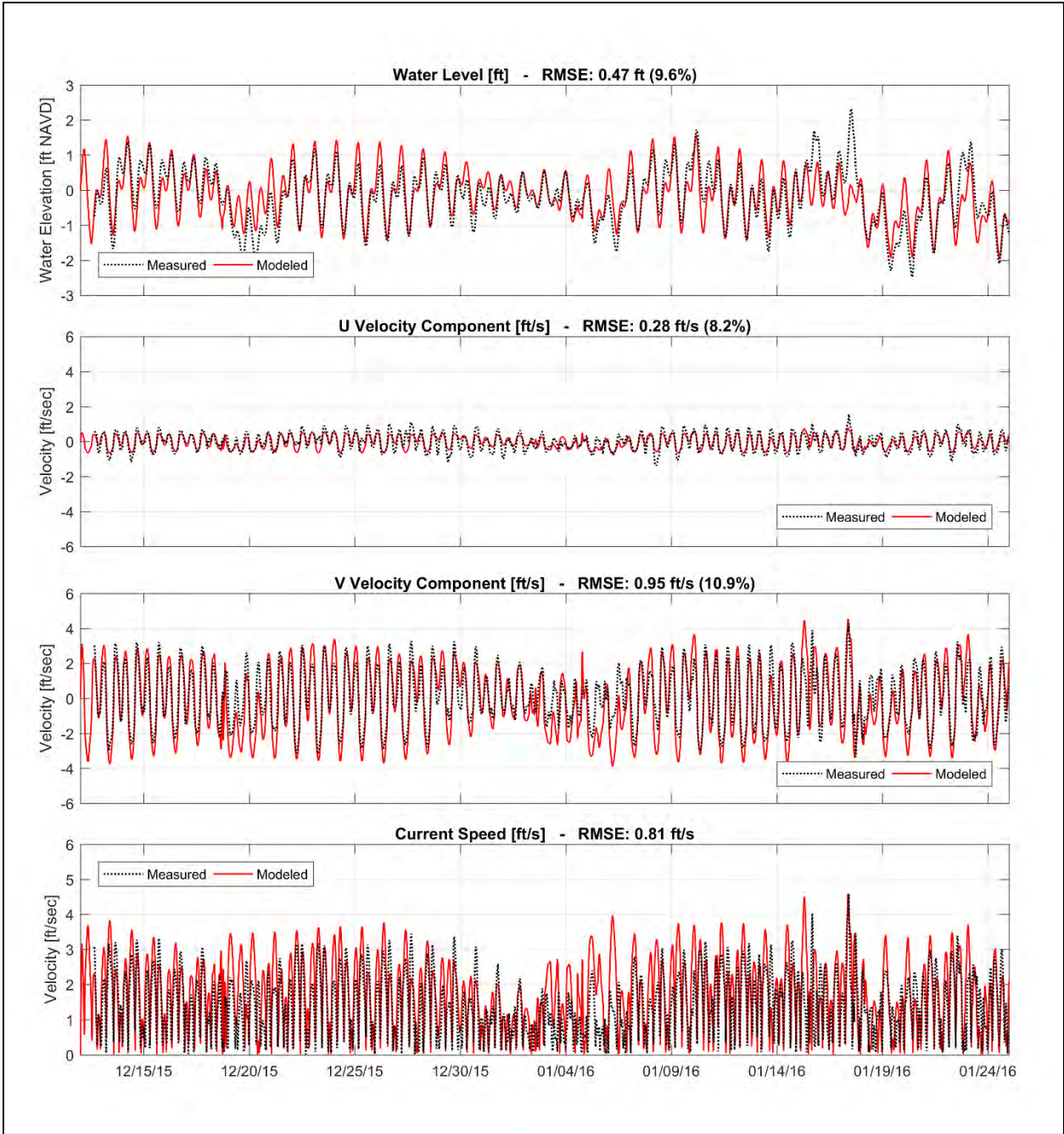


**Figure 3-24: Comparison between measured and simulated water levels and currents at the location of the Blind Pass Current Meter. Top: Water level; 2nd: U-velocity; 3rd: V-velocity; bottom: Velocity magnitude.**

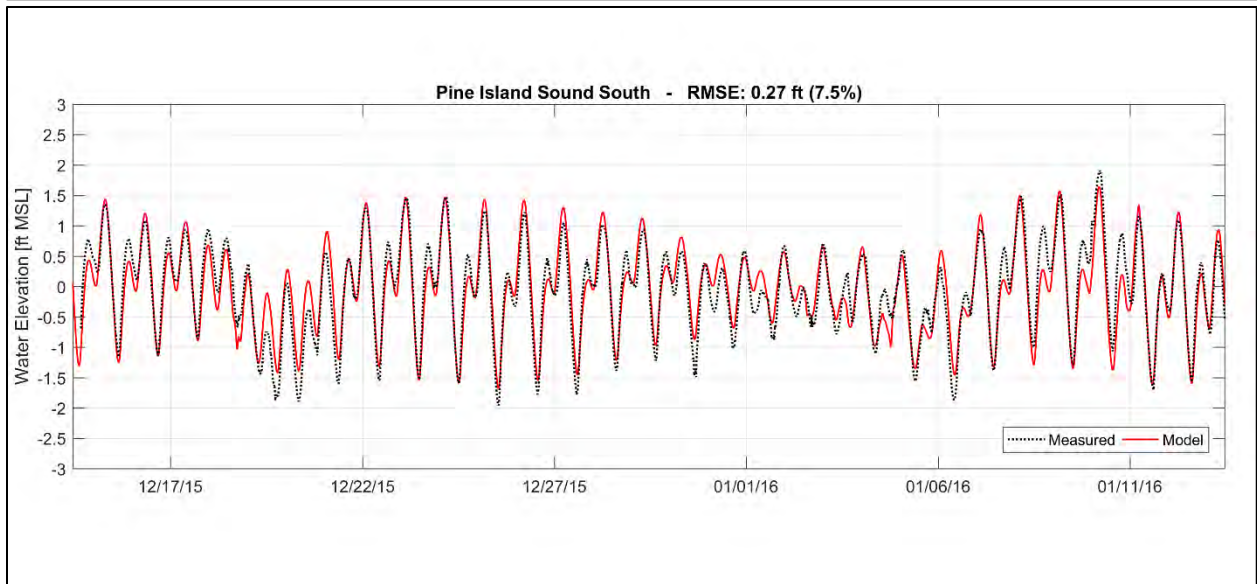
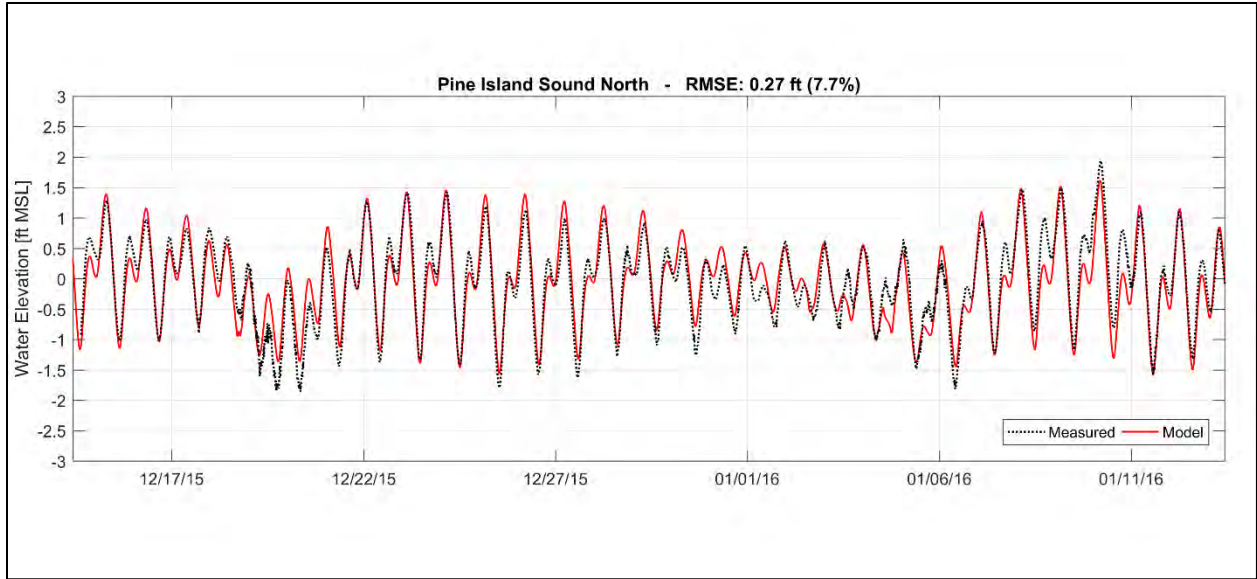


**Figure 3-25: Comparison between measured and simulated water levels at the tide gauges deployed in the Pine Island Sound. Top: northern tide gauge; bottom: southern tide gauge.**

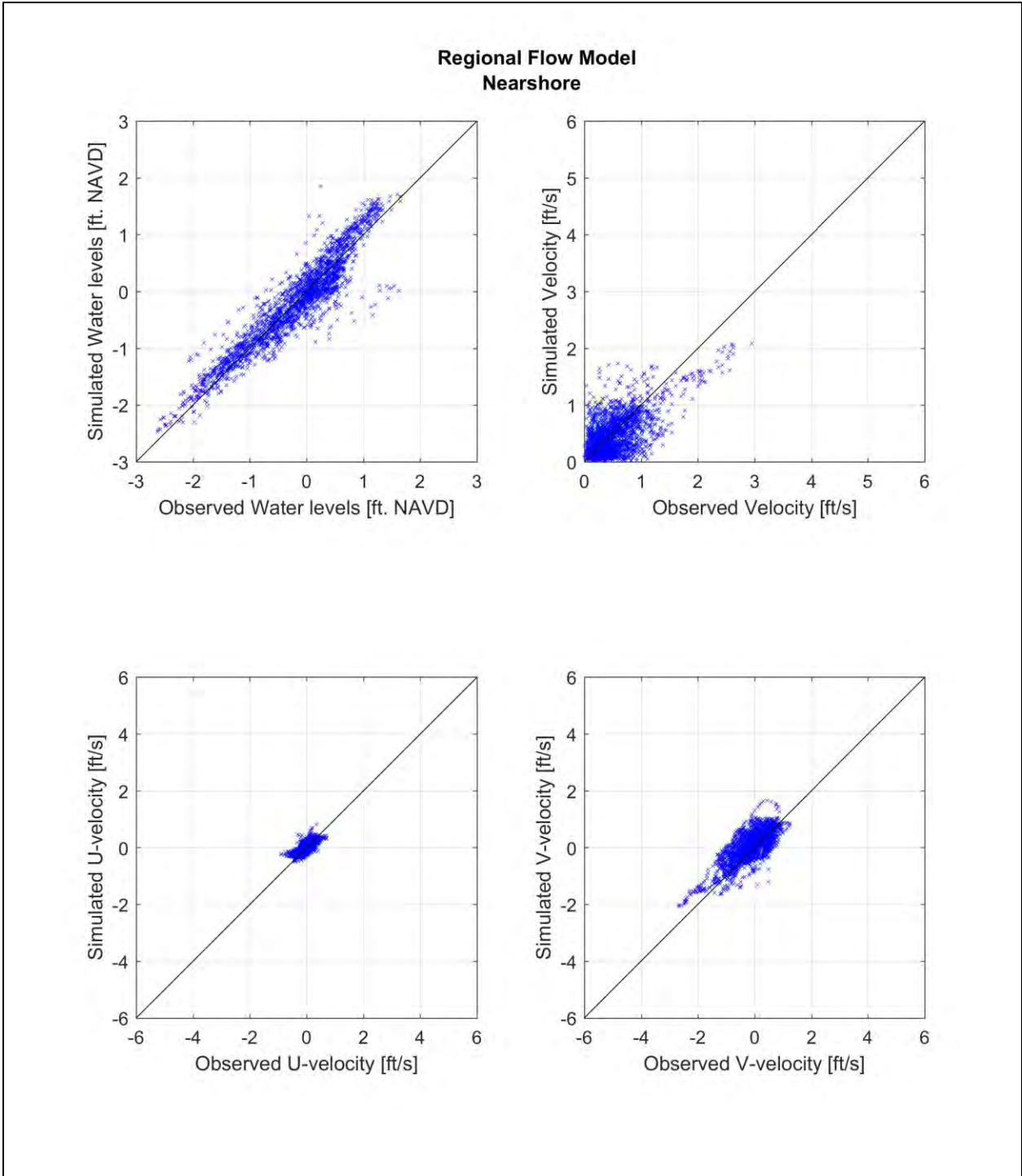


**Figure 3-26: Scatter Plot of Observed versus Simulated Water Levels and Currents – Nearshore ADCP.**

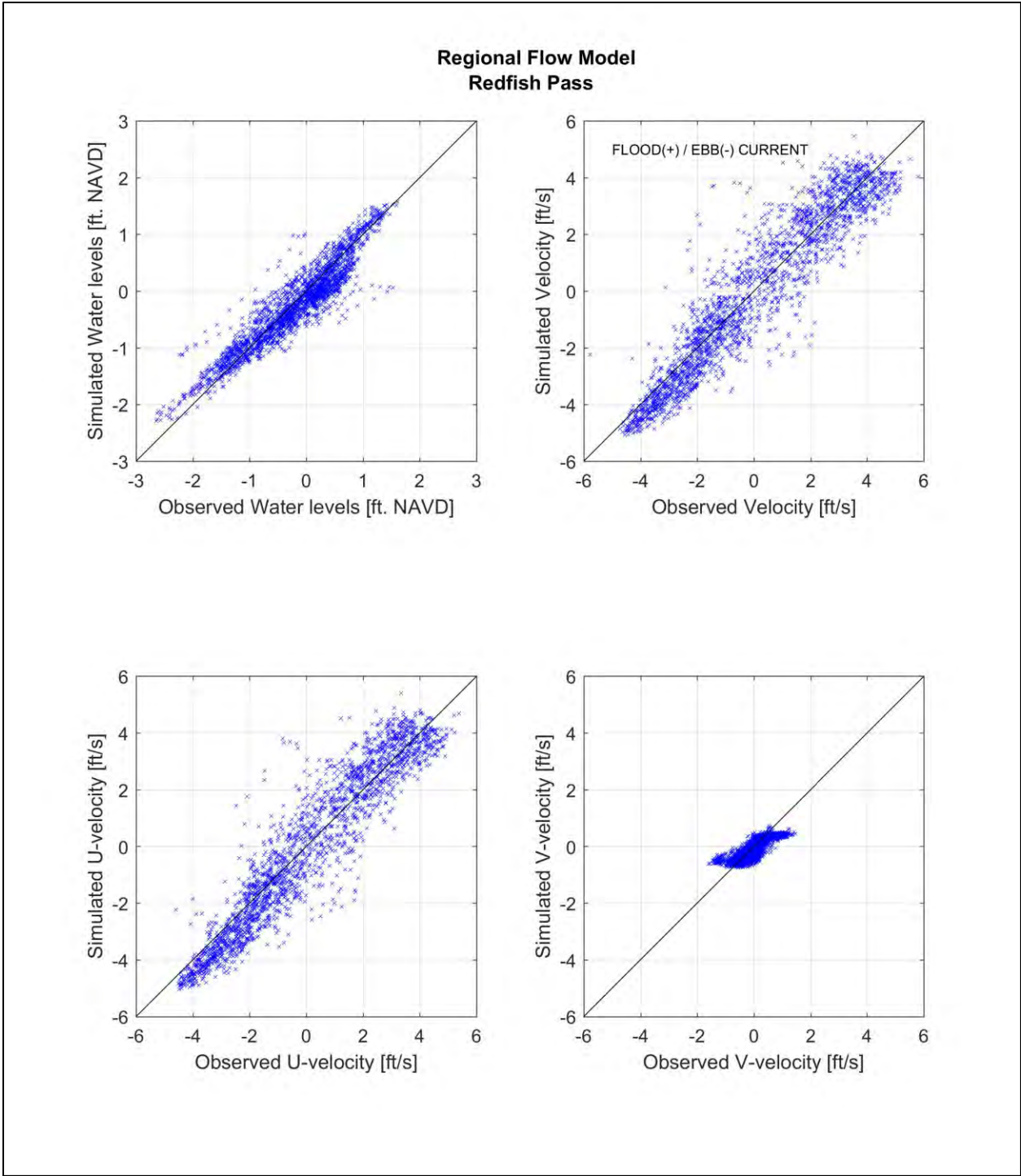


**Figure 3-27: Scatter Plot of Observed versus Simulated Water Levels and Currents – Redfish Pass ADCP.**

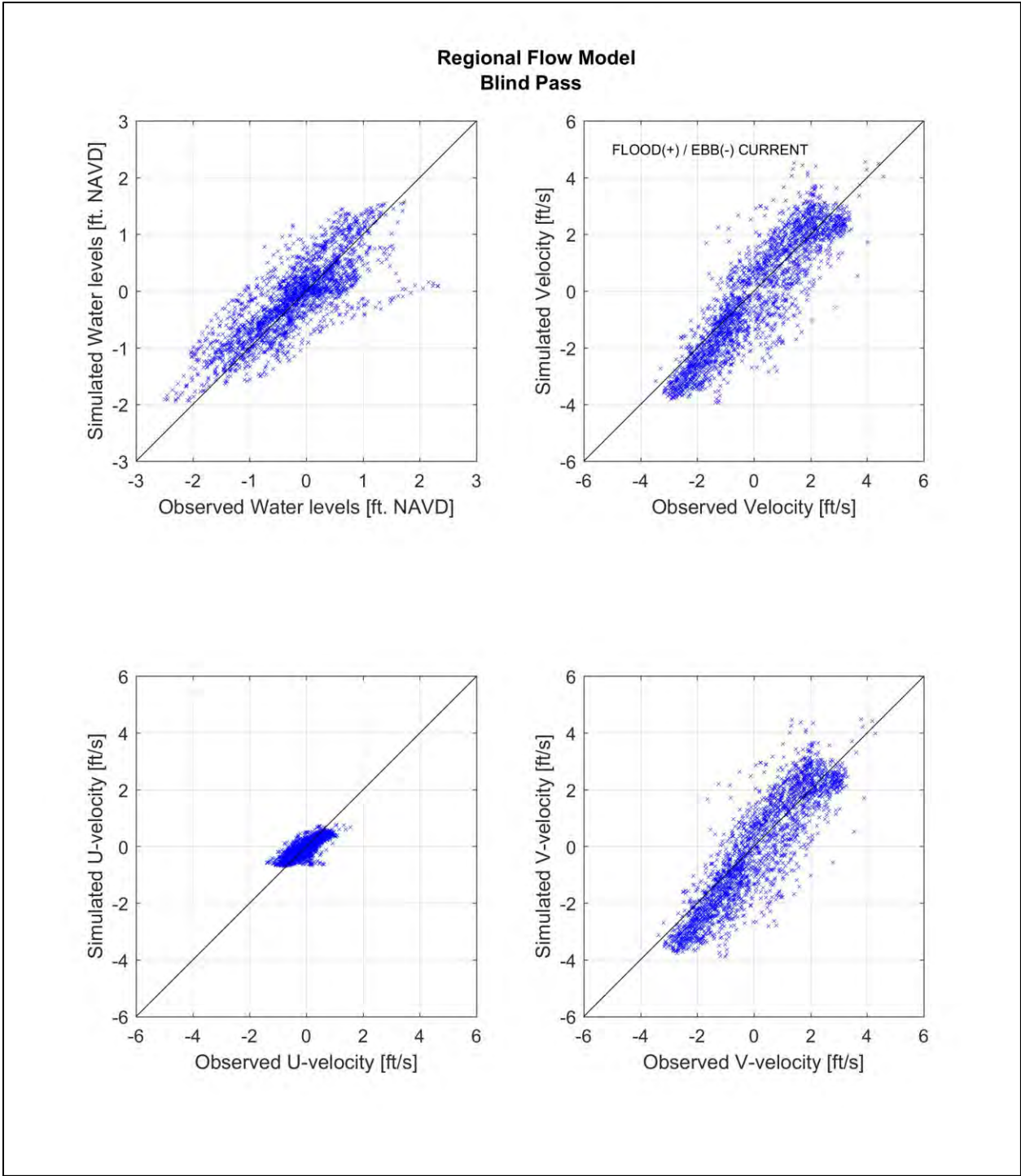


**Figure 3-28: Scatter Plot of Observed versus Simulated Water Levels and Currents – Blind Pass Current Meter.**

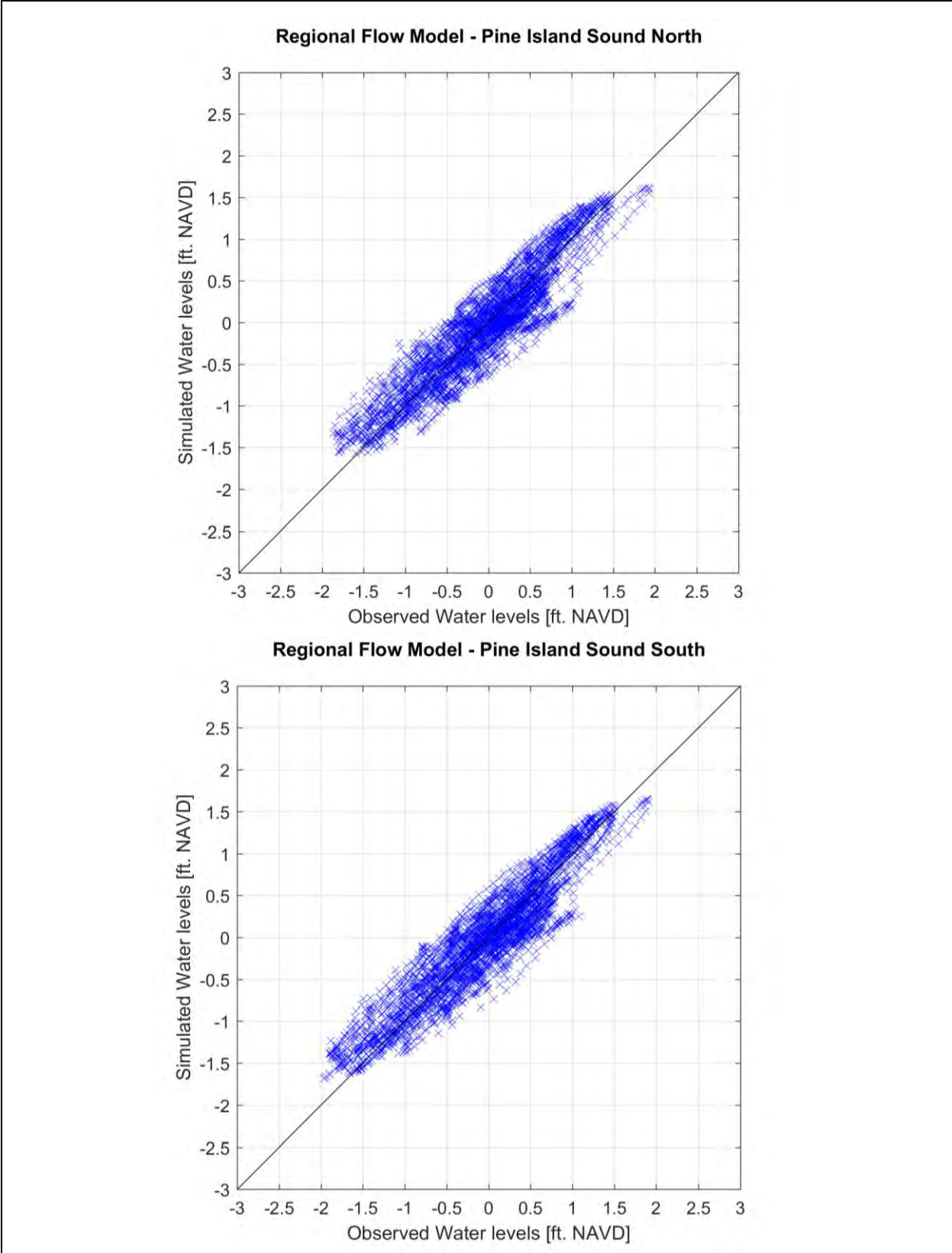


**Figure 3-29: Scatter Plot of Observed versus Simulated Water Levels – Pine Island Sound North and South tidal gauges.**

**Table 3-4: Regional flow calibration summary - Delft3D-FLOW model.**

Location	Simulated – Observed Water Level (feet)		Simulated – Observed East / West Current (feet/second)		Simulated – Observed North/South Current (feet/second)		Simulated – Observed Current speed (feet/second)	
	Mean	RMS	Mean	RMS	Mean	RMS	Mean	RMS
Nearshore	0.00	0.29	0.02	0.15	0.19	0.44	-0.06	0.34
Redfish Pass	-0.04	0.29	-0.10	0.93	-0.08	0.31	0.18	0.84
Blind Pass	0.06	0.47	-0.01	0.28	-0.23	0.95	0.32	0.81
PIS (North)	-0.01	0.27	-	-	-	-	-	-
PIS (South)	0.00	0.27	-	-	-	-	-	-

### 3.3.5. Model Calibration – Local Flow Grid

Local Flow model, developed for the computations of detailed flows, sediment transport and morphology. Hydrodynamic results obtained from the calibrated Regional Flow model were used as boundary conditions in the detailed Local domain. This includes time varying:

- Water levels along the offshore boundary (Gulf of Mexico);
- Water level gradients (i.e. Neumann boundaries) in the northern and southern boundaries normal to the coastline;
- Water levels at the connection of the Wulfert channel and the Pine Island Sound;
- Water Discharges in the Roosevelt Channel;
- Water discharges in the Dinkins Bayou.

As mentioned in section 3.3.3, the bed form and roughness predictor was applied in the Local Flow simulations. A series of simulations were performed by varying the horizontal eddy viscosity coefficient. Three values were tested: 0.2, 1.0 (default value), and 5.0 m<sup>2</sup>/s. Table 3-5 shows the associated Mean Errors and Root Mean Square Errors (RMSE) from the comparison of measured and modeled water levels and current speed at the Blind Pass Current Meter location. Water level errors are relatively small for all simulations and the contribution of the East-West velocity (U-component) to the velocity magnitude is minor as the channel is approximately North-South orientated. Therefore, the North-South Current (V-component) and the Current speed are primarily considered to rank the model performance. The horizontal eddy viscosity coefficient of 1.0 m<sup>2</sup>/s (the default value in Delft3D) resulted in the best overall comparison with measured data was selected to be used hereafter. Comparisons of measured and modeled data using the selected configuration are presented in Figure 3-30 and Figure 3-31.

Examples of current fields computed with the Local Flow model are given in Figure 3-32 and Figure 3-33, for ebb and flood tide conditions and under mild and severe waves/winds.

**Table 3-5: Local flow calibration summary (Blind Pass gage) Delft3D-FLOW model.**

Hor. Viscosity coefficient	Simulated – Observed							
	Water Level (feet)		East / West Current (feet/second)		North/South Current (feet/second)		Current speed (feet/second)	
	Mean	RMS	Mean	RMS	Mean	RMS	Mean	RMS
0.2 m <sup>2</sup> /s	0.08	0.47	-0.04	0.32	-0.17	0.92	0.34	0.78
<b>1 m<sup>2</sup>/s (default)</b>	<b>0.09</b>	<b>0.47</b>	<b>-0.02</b>	<b>0.33</b>	<b>-0.17</b>	<b>0.81</b>	<b>0.13</b>	<b>0.68</b>
5 m <sup>2</sup> /s	0.10	0.47	0.00	0.37	-0.17	0.81	-0.48	0.79

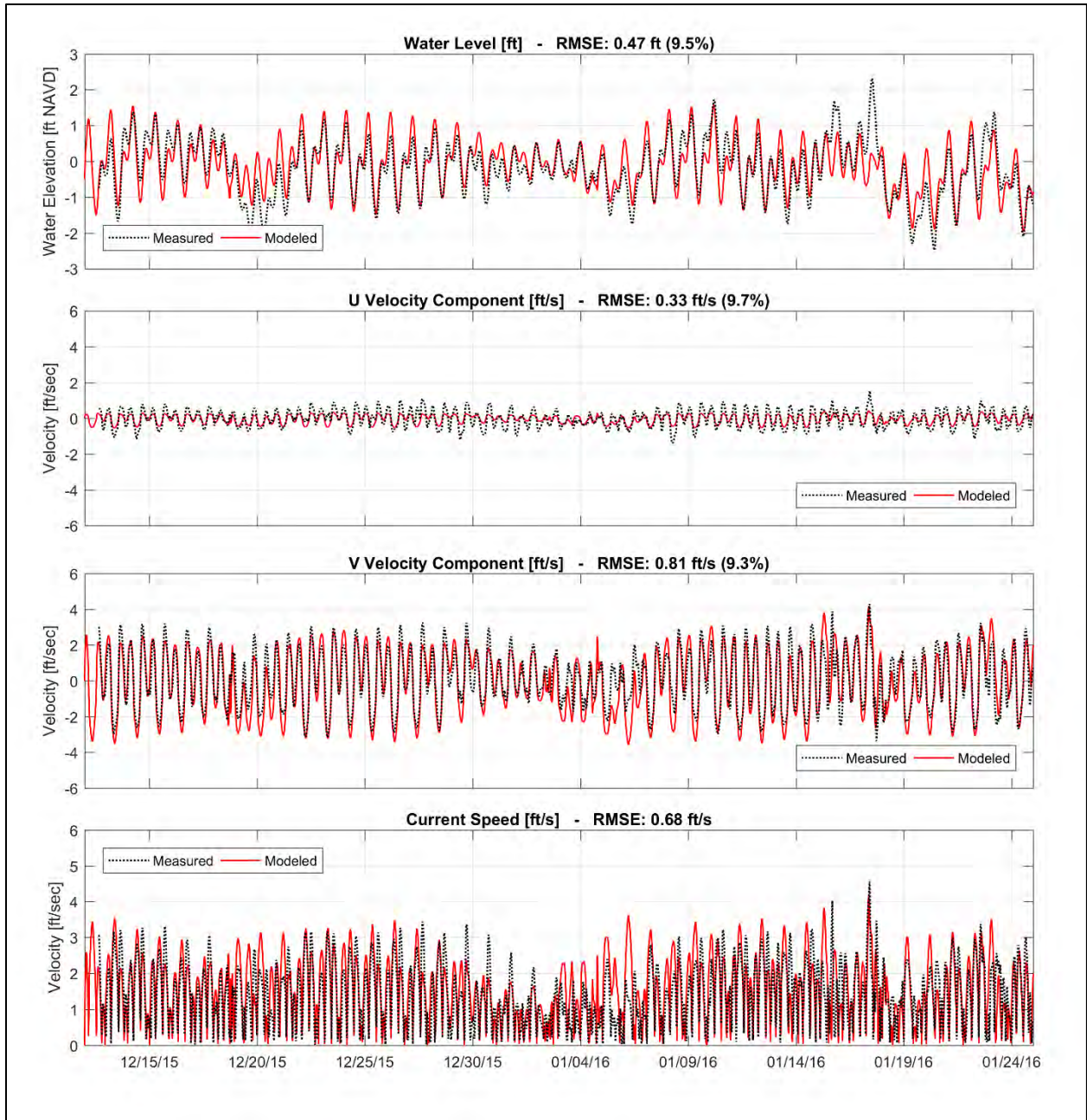


**Figure 3-30: Comparison between measured and simulated (Local Flow model, horizontal eddy viscosity coefficient = 1 m<sup>2</sup>/s) water levels and currents at the Blind Pass Gauge location. Top: Water level; 2nd: East-West velocity; 3rd: North-South velocity; bottom: Velocity magnitude.**

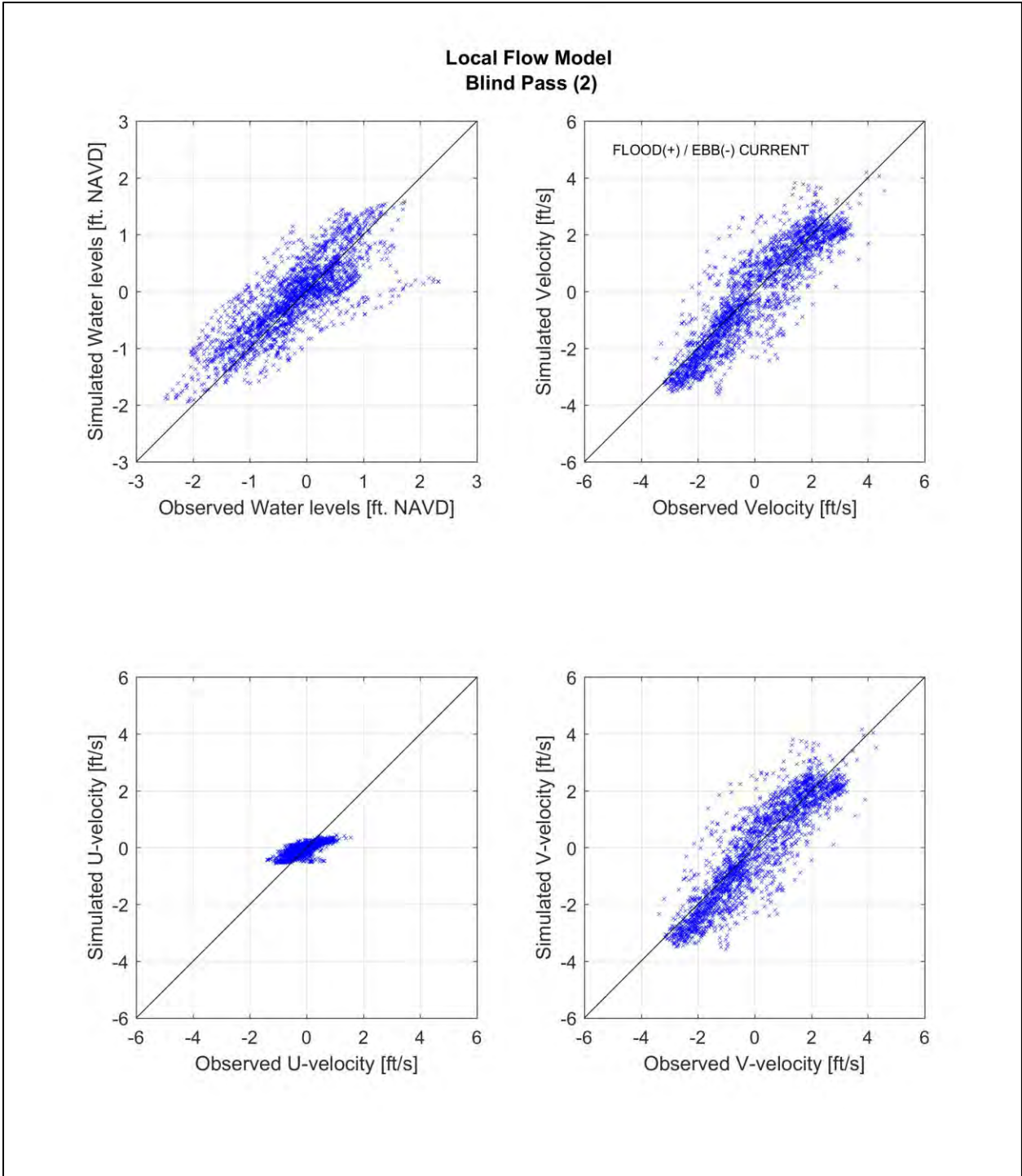
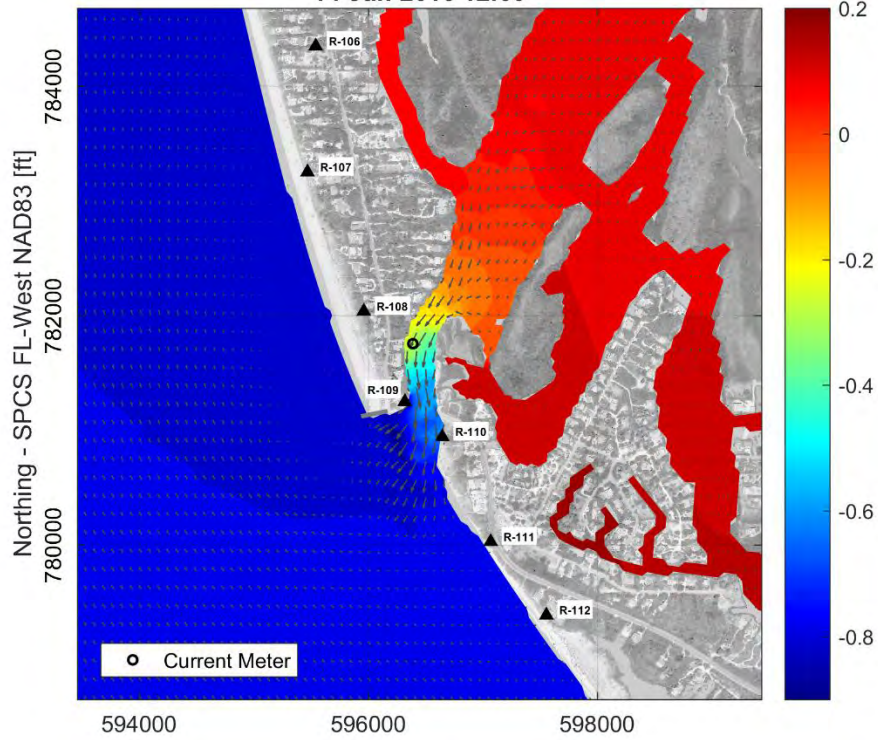


**Figure 3-31: Scatter Plot of Observed versus Simulated (Local Flow model) water Levels and currents – Blind Pass Current Meter, horizontal eddy viscosity coefficient = 1 m<sup>2</sup>/s.**

**Table 3-6: Summary of the regional and local flow model definitions- Delft3D-FLOW Model.**

<b>Model definition</b>	<b>Default Value</b>	<b>Regional</b>	<b>Local</b>
<b>Number of Layers</b>	1	1	6
<b>Wind Drag</b> <b>0 m/s</b>	0.00063	0.00072	0.00072
<b>Coefficients</b> <b>100 m/s</b>	0.00723	0.01272	0.01272
<b>Horizontal Eddy Viscosity</b>	1		
<b>Model for 3D Turbulence</b>	k-epsilon		
<b>Vertical Eddy Viscosity</b>	0	N/A (2DH)	10 <sup>-4</sup>
<b>Gravity (m/s<sup>2</sup>)</b>	9.81		
<b>Water Density (kg/m<sup>3</sup>)</b>	1025		
<b>Chezy value (roughness)</b>	65	80	Space/Time variable (Trachytopes)

Local Flow Model - Simulated water levels [ft. NAVD]  
14-Jan-2016 12:00



Local Flow Model - Simulated current velocities [ft/s]  
14-Jan-2016 12:00

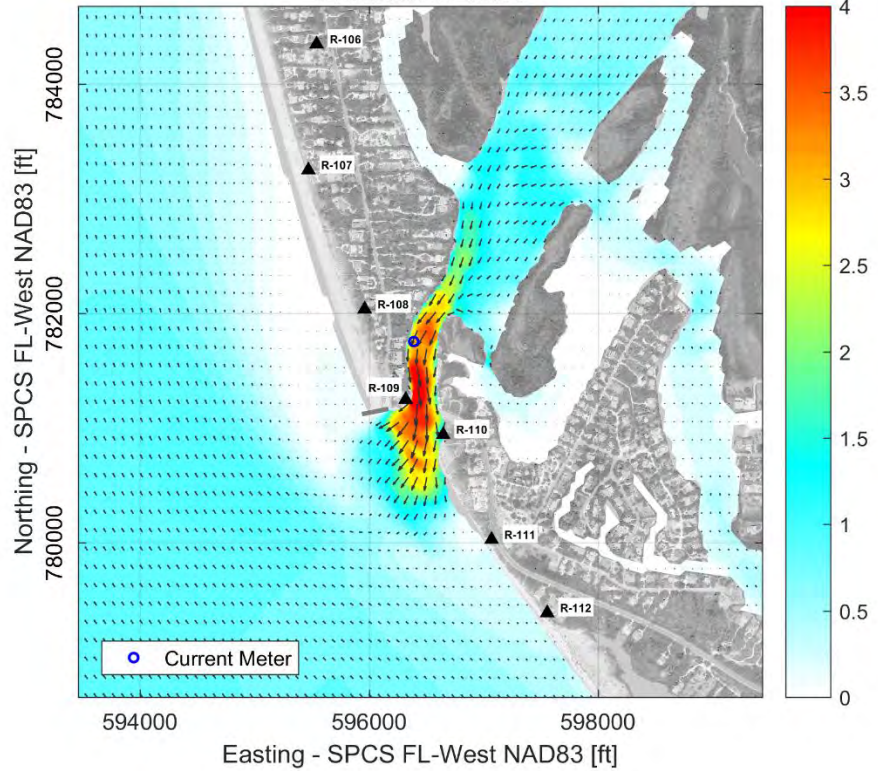
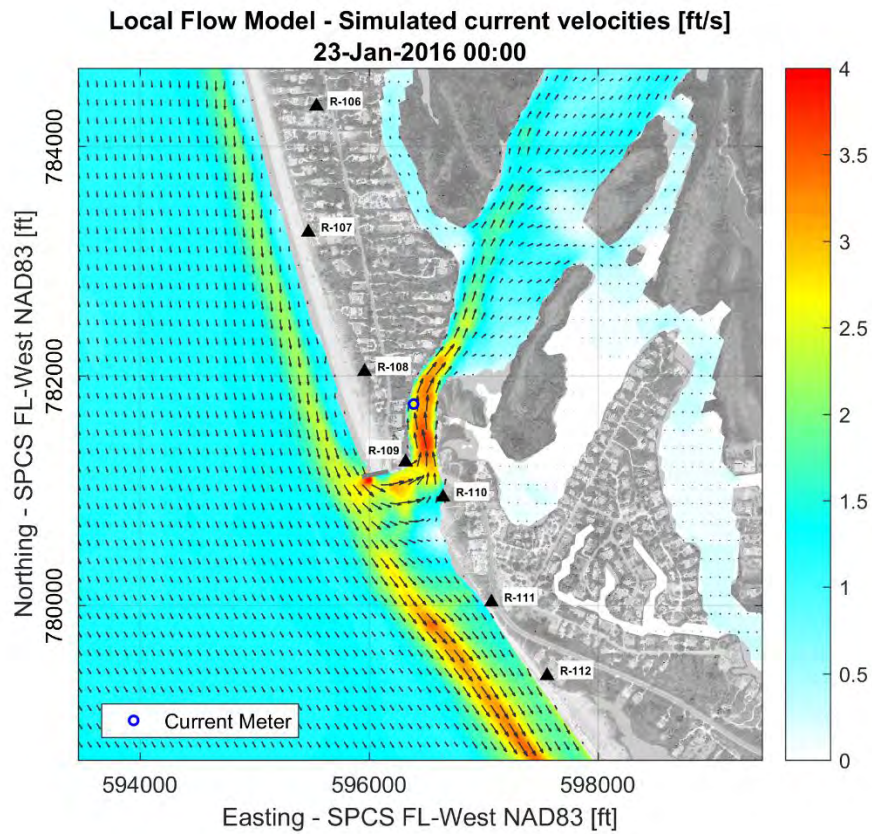
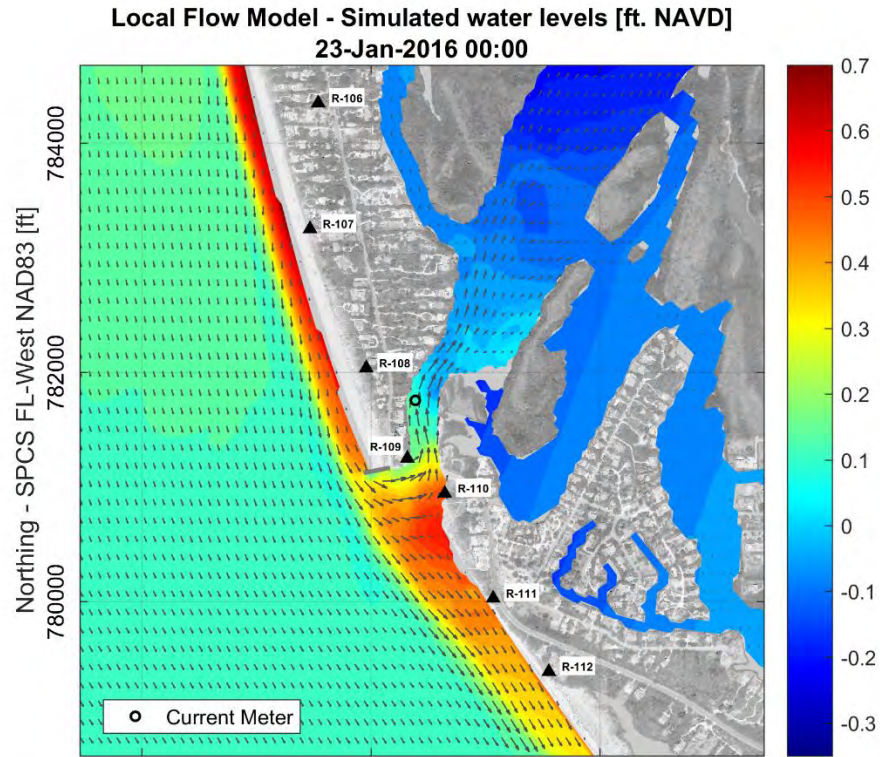


Figure 3-32: Local Flow model calibration results: ebb tide, mild waves/wind.



**Figure 3-33: Local Flow model calibration results: flood tide, strong NW waves/wind.**

### **3.4. Delft3D-FLOW Morphology Calibration**

The primary modeling tool in this investigation is the Delft3D morphological modeling package (Deltares, 2016a). This package consists of two models, which are coupled together to determine changes in a topographic and bathymetric surface based on the effects of waves, water levels, winds, and currents. Wave propagation from the offshore to the nearshore area is estimated using the Simulating Waves Nearshore Model (SWAN 40.72ABCDE, Delft University of Technology, 2008). The wave model configuration and calibration results are presented in Section 3.2. Delft3D-FLOW utilizes the output waves from SWAN, along with the varying water levels offshore and the bathymetry, to determine currents and water levels over time and space. The hydrodynamic model configuration and calibration results are presented in Section 3.3.

Delft3D-FLOW use can be extended to calculate sediment transport rates, erosion, and deposition using the wave and flow model results as input. Based on the estimated erosion and deposition at each time step, the model updates the subsequent elevations of the topographic and bathymetric surface and provides the evolved bathymetry back to the SWAN model. The time step used in the morphological simulations is 12 seconds, while wave propagation estimates in the SWAN model are performed every 2 hours. Given the interaction between waves and tidal currents near Blind Pass, Delft3D is the best means of evaluating the performance and impact of management alternatives involving dredging, beach fill and coastal structures adjacent to the pass.

The sediment transport and morphological model was calibrated based on the beachfront and inlet bathymetric and volumetric changes at the southern end of Captiva Island, Blind Pass and northern end of Sanibel Island. The morphological model calibration period, September 2009 and May 2012, was selected based on the concurrent data availability for Blind Pass channel and adjacent beaches. Details regarding the model configuration and results are presented in the coming sections.

#### **3.4.1. Initial Condition Bathymetry**

The morphological model calibration period was selected to avoid man-made changes to the simulated coastal system, such as dredging, fill placement, coastal structures construction. Upon reviewing the Blind Pass construction history after the channel reopening in 2009, no beach fill or inlet dredging occurred between September 2009 and May 2012. This period was selected as it was after the 2009 construction (Blind Pass channel re-opening and beach nourishment). Also, surveys of Blind Pass and beach profiles were available for the two periods. As such, these dates delineate the bounds of the morphology calibration period.

The numerical grid for the morphology modeling is the same as the one from the Local Flow simulation, with 6 vertical sigma layers. The bathymetry data from 2009 was interpolated to the grid and used as the initial conditions for the morphology calibration simulations. The morphological calibration model surface was created based on the following sources, which are listed in the sequence used to populate the model grid (see also Table 2-1):

1. August 2009 bathymetry survey of Blind Pass and ebb shoal.
2. September 2009 beach survey of Captiva and Sanibel Islands.

3. 2010 USACE LiDAR.
4. June 2015 bathymetry survey of Blind Pass and inner channel connections.
5. NCEI NOAA survey.
6. NCEI NOAA Coastal Relief Model (CRM).

The resulting September 2009 bathymetry interpolated to the morphology grid appears in Figure 3-34. Bathymetric data collected in 2012 was also interpolated in order to quantify the observed changes during the calibration period. The 2012 bathymetry surface and the 2009-2012 difference map (i.e. delta plot, erosion/sedimentation map) are presented in Figure 3-35.

The main bathymetry changes observed during the calibration period were the prominent accretion/sedimentation along the outer and intermediate sections of the dredged channel and beach erosion that occurred along the north end of Sanibel Island.

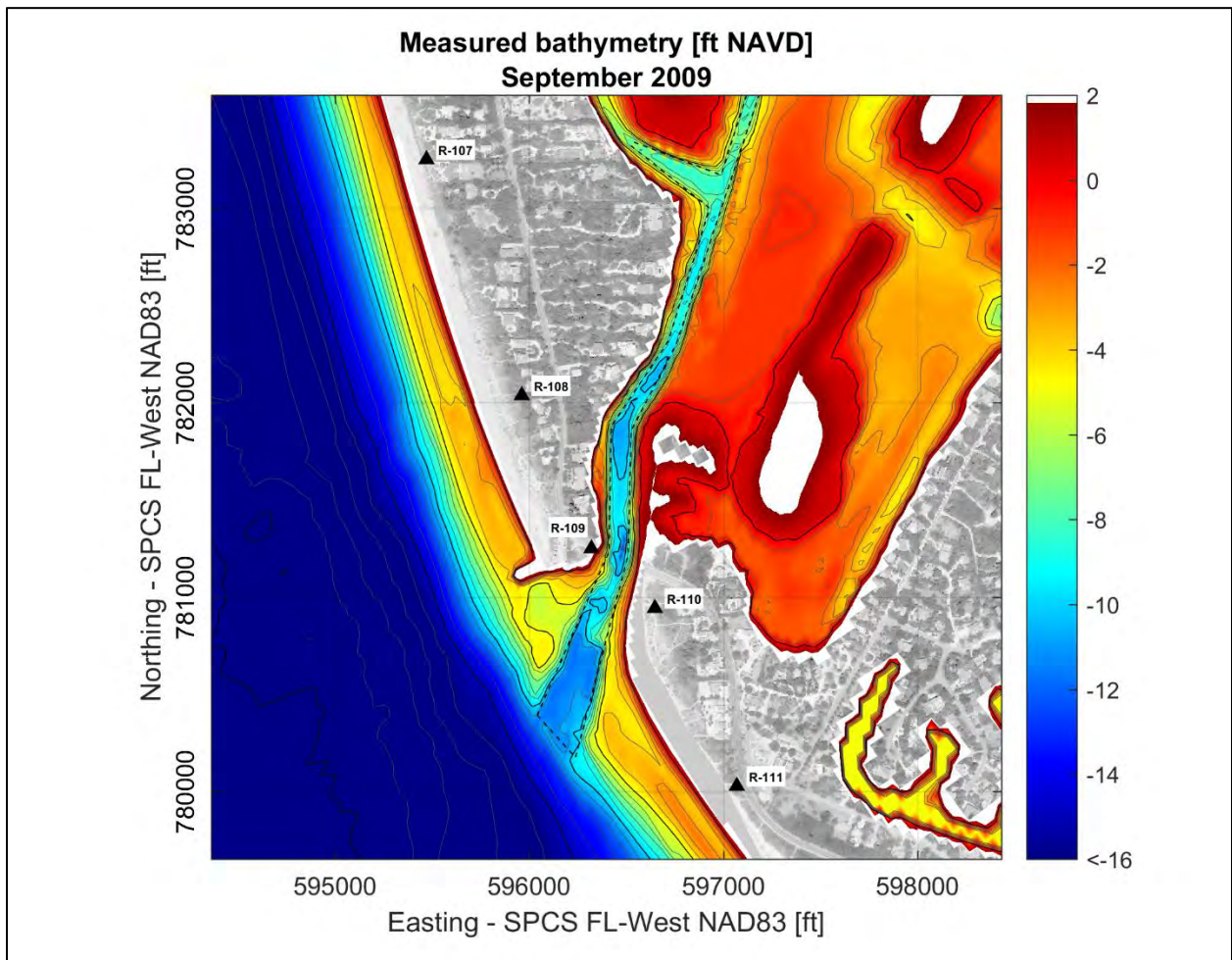


**Figure 3-34: Initial measured bathymetry for Morphology Calibration.**

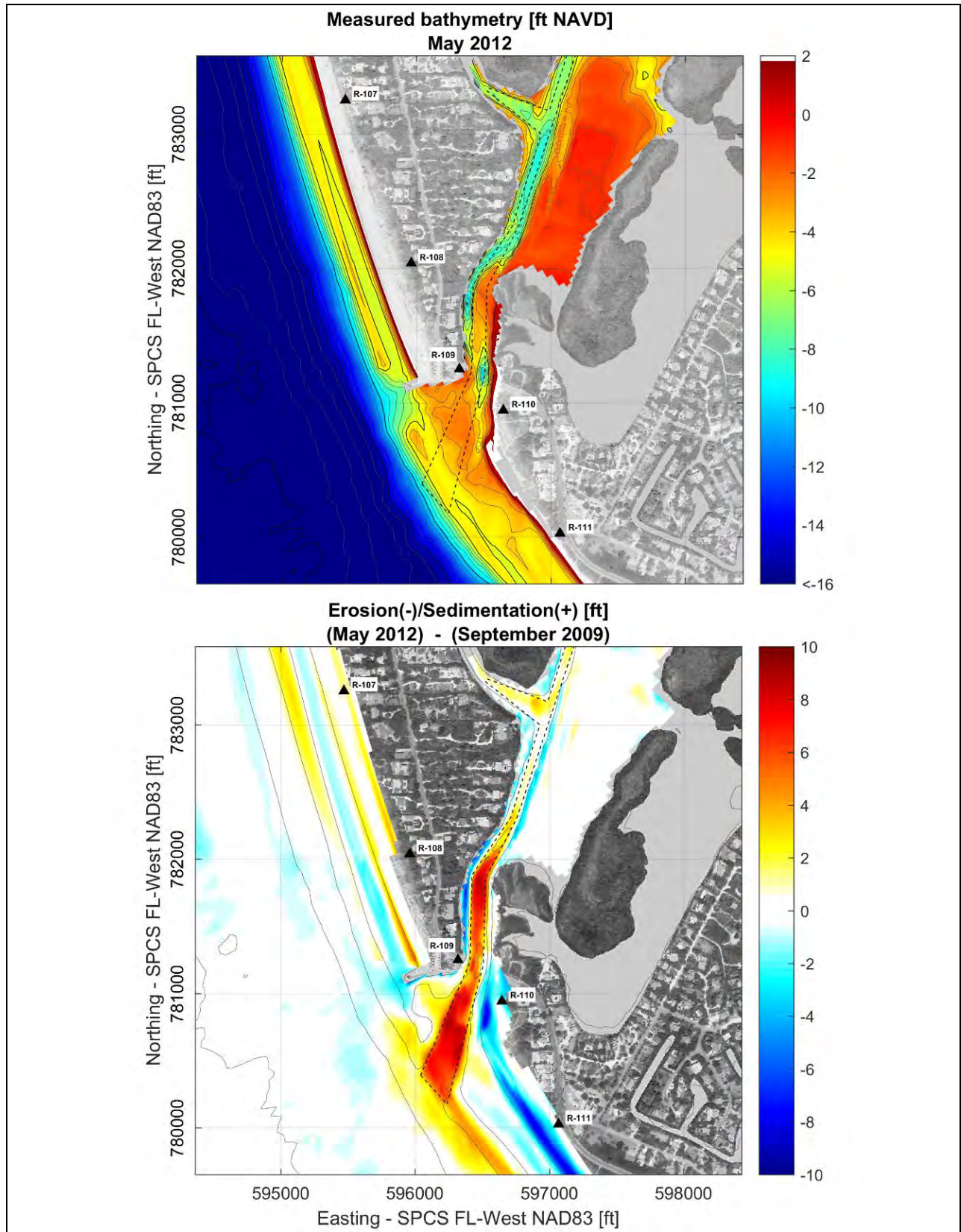


**Figure 3-35: Measured bathymetry and erosion(-)/sedimentation(+) by the end of the Morphology Calibration period (May 2012).**

### 3.4.2. Model Forcing

The time scales of morphology processes (days-years) are substantially longer than the ones of the hydrodynamic processes reproduced in the Delft3D-FLOW model (seconds-hours). In order to fill the gap between those different time scales and make it computationally feasible to use process-based morphology models for longer term simulations (i.e. years), a morphological acceleration factor (*Morfac*) is applied in the Delft3D model, as described in Lesser et al (2004). Essentially, the gradients of sediment transport and morphology changes occurred at each flow/hydrodynamic time step (in the order of 10 seconds) are multiplied by *morfac* (in the order of 10). This makes the morphology model time step ‘*morfac* times’ higher than the hydrodynamic time step.

The morphological acceleration factor “*Morfac*” was estimated according to the following procedure (Benedet and List, 2008):

$$Morfac = T_{\text{study period}} / T_{\text{model period}}$$

where

$$T_{\text{study period}} = (\text{length of the study period}) \times (\text{percent occurrence for each wave case})$$

$$T_{\text{model period}} = \text{duration of the wave case in the model simulation}$$

For example, a wave condition that occurs 14 days a year can be simulated over 24 hours with a *Morfac* value of 14. With the Delft3D modeling community, it is common practice to use lower *Morfac* values for high wave cases, when the most significant morphological changes occur, and higher *Morfac* values for smaller wave cases, where little change takes place.

However, for the application of the morphological acceleration technique based on the *Morfac* to the simulation of a whole year of morphological changes, it is necessary to apply input reduction (described below) to all the forcing variables of the model: water level, wave and wind conditions.

#### ***Waves and winds***

The wave reduction was made by selecting a number of representative wave conditions from the wave time series covering the morphology calibration period (i.e. September 2009 to May 2012), defined based on the NOAA Wavewatch III hindcast wave data (see Section 2.4). The range of incoming wave directions between 140° and 330°, with a significant wave height of 1 foot or higher, was used to select 12 main wave cases.

The representative wave conditions were selected based on the energy of each wave case and was calculated from the wave heights based on the linear wave theory.

$$E = \frac{\rho g H_{rms}^2}{8}$$

where:

E = wave energy

$\rho$  = sea water density (1025 kg/m<sup>3</sup>)  
 $g$  = gravitational acceleration (9.81 m/s<sup>2</sup>)  
 $H_{rms}$  = Root-mean-square wave height (m)

The method is described in Benedet et al. (2016) and follows the steps listed below:

- 1) Separating the wave data associated with the calibration period (September 2009 - May 2012) from the 16-year time series;
- 2) Selecting the wave conditions considered relevant for the coastal dynamics: offshore wave height ( $H_s$ ) greater than 1 ft. and offshore wave directions between 140 and 330 deg. (wave conditions propagating towards offshore regions). The filtered conditions are reserved for later consideration;
- 3) Divide the selected wave conditions into 4 directional classes (each with 1/4 of the cumulative energy flux of the whole set of conditions) and each directional class into 3 wave height classes (each with 1/3 of the energy flux of the directional class, of 1/12 of the cumulative energy flux of the whole set of conditions);
- 4) Define representative wave conditions for each of the twelve (12) directional vs. wave height classes:
  - a. representative  $H_s$  is the magnitude of the mean energy vector;
  - b. representative  $T_p$  = average period;
  - c. representative  $Dir$  = the direction of the resultant energy flux vector;
  - d. representative Wind speed = average wind speed;
  - e. representative Wind direction = the direction of the resultant wind vector;
  - f. Frequency of occurrence = number of conditions into the class relative to the total number of conditions (including calm and 'offshore-directed' sea states).

Using this method, the widths of the directional and wave height classes were not uniform. Instead, they are spaced so that within each direction band or height class would contain the same amount of wave energy. The representative wave conditions used in the morphological calibration runs were given at the seaward edge of the Regional Wave Grid in Figure 3-2.

Although the 12 wave cases (4 directional x 3 wave height classes, Figure 3-36) provide a consistent representation of the onshore wave energy, they only cover 44% of the study period (2009-2012). To account for the remaining 56%, when wave action is negligible in the study area (i.e. offshore wave height < 1 ft. or waves offshore directed) and sediment fluxes are primarily driven by tidal flows, four additional mild cases were added to represent calm conditions onshore. Therefore, the total number of wave cases for the Blind Pass morphology calibration was 16 (4 direction classes x 3 wave height classes + 4 mild cases). The list of the representative wave conditions and the associated *Morfac* values are provided in Table 3-7.

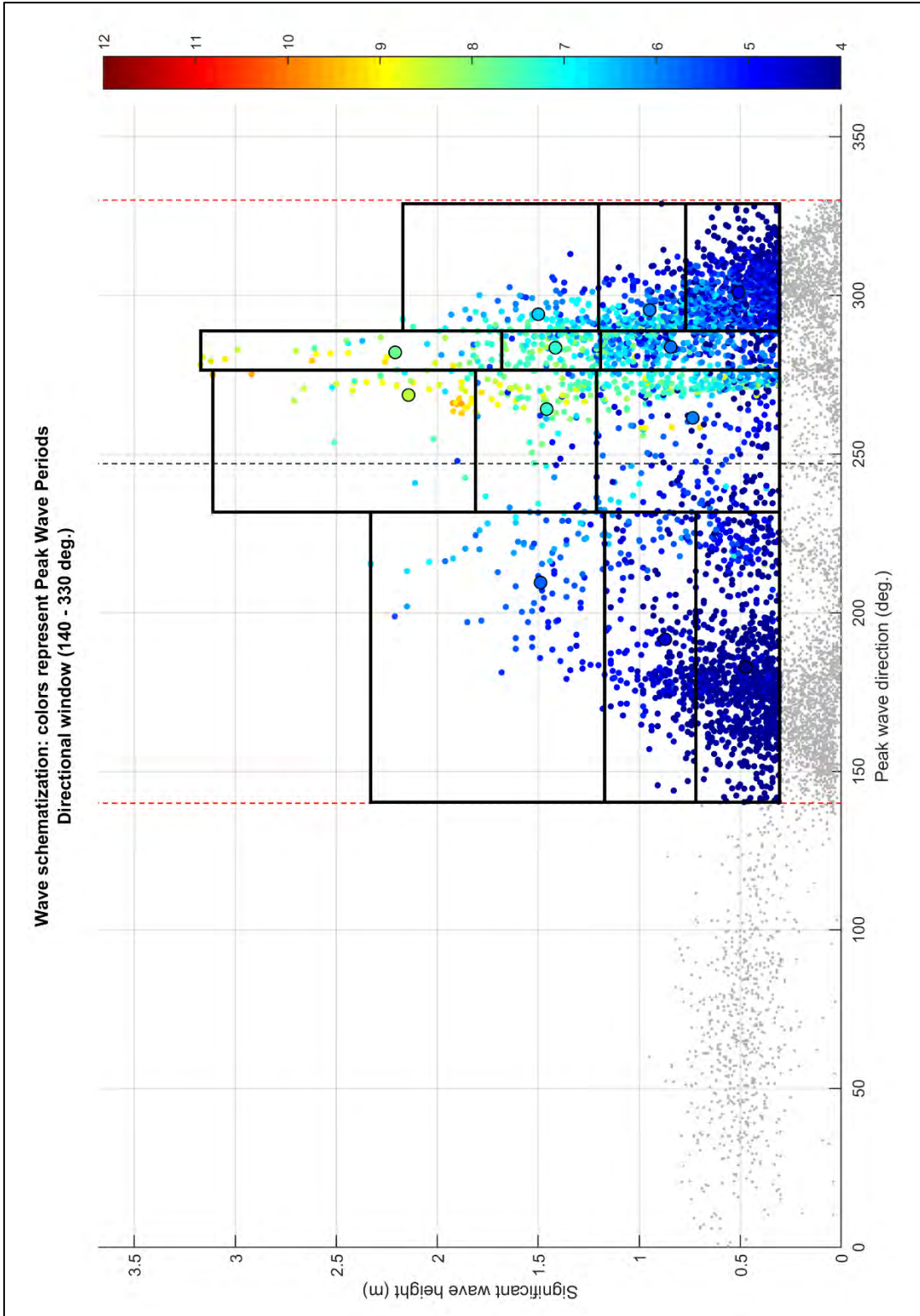


Figure 3-36: Wave climate schematization – Morphology calibration period.

**Table 3-7: Simulated wave cases and their corresponding *morfac* values.**

Wave case	H <sub>s</sub> (feet)	T <sub>p</sub> (sec.)	Dir <sub>p</sub> (deg.)	Dir. Spreading (cosine power)	Wind speed (mph)	Wind direction (deg)	Occurrence (days/yr)	Morfac
#1	1.55	4.0	183	4.1	10.8	154	42.3	28.4
#2	2.86	4.6	192	4.0	14.4	180	12.4	16.6
#3	4.88	5.6	210	4.0	18.3	216	4.4	5.9
#4	2.41	5.9	261	8.0	10.2	19	18.1	24.3
#5	4.78	7.3	264	5.0	14.4	307	4.7	6.3
#6	7.03	8.4	269	4.0	20.3	311	2.2	2.9
#7	2.77	5.9	284	6.0	11.3	339	14.0	18.9
#8	4.64	7.3	283	5.1	16.3	350	5.0	6.7
#9	7.25	7.8	282	4.0	21.1	319	2.1	2.8
#10	1.67	4.8	301	7.3	10.7	12	38.8	26.1
#11	3.12	5.9	295	5.0	14.7	1	11.2	15.0
#12	4.92	6.5	294	4.0	19.3	343	4.5	6.1
#13	0.51	3.4	163	14.0	8.1	102	56.2	25.2
#14	0.42	4.4	236	21.6	7.0	121	63.7	28.6
#15	0.56	3.9	307	15.9	7.4	27	47.1	31.7
#16	1.42	2.8	67	4.4	14.9	81	38.5	25.9

Calm

### *Tides*

Tides at Blind Pass are mixed semidiurnal tides, with both a non-uniform amplitude and non-uniform tidal period (see Figure 3-7). Simulating each wave case for a portion of the spring-neap tidal cycle introduces biases that negatively affect the model results, since the tidal component of the sediment transport would not be the same for each wave case. Ideally, each wave case could be simulated over a full, 14-day, spring-neap tidal cycle. However, given the number of wave cases, this would inflate the model’s run time to unacceptable levels. Therefore, in addition to the schematized wave cases, the tides must also be schematized to run the morphological model.

The main purpose of reducing tidal data is to replace the complex pattern of the real tide in the study area by a simplified tide, also called morphological tide. The accepted practice is to schematize the tides using one or a selected set of sinusoidal harmonics only. Tidal data reduction to a sinusoidal tide with constant periodicity allows each wave case to be propagated by at least one full tidal cycle. Thus, all wave cases are influenced by the same tidal amplitude and phase.

Ideally, the morphological tide produces the same residual sediment transport and morphological pattern of changes that the actual tide produces (Lesser, 2009). To address this theme, a sensitivity analysis was conducted considering four different tides schemes (Table 3-8).

**Table 3-8: Tested tide schemes.**

Scheme		North		Center		South	
		Amplitude (feet)	Phase (deg.)	Amplitude (feet)	Phase (deg.)	Amplitude (feet)	Phase (deg.)
# 1	K1 (diurnal)	0.45	20.4	0.46	21.5	0.48	24.8
# 2	M2 (semi-diurnal)	0.59	105.9	0.61	120.4	0.68	144.9
# 3	M2* (semi-diurnal)	0.71	105.9	0.74	120.4	0.82	144.9
# 4	M2** (semi-diurnal)	0.65	105.9	0.68	120.4	0.75	144.9
	C1 (diurnal)	0.62	15.1	0.63	16.1	0.63	18.6

\*Scheme #3 considers an amplification of 20% to the M2 component amplitude.

\*\*Scheme #4 considers an amplification of 10% to the M2 component amplitude.

The tide scheme #4 is proposed by Lesser (2009) to better represent the tidal fluxes associated with the full tide by using a simplified tidal signature with two sinusoidal harmonics. The tidal signal of the different morphological tides can be seen on Figure 3-37.

The testing approach consisted of simulating six (6) months of morphology changes in separated models considering each tide scheme along with a baseline simulation taking into account the thirteen (13) astronomical tidal constituents (see Section 2.6). In order to create the boundary conditions to the Local model used for the morphology simulations, the Regional Flow model was run for several days using the different tides. From these simulations, both the water level (offshore and northern Wulfert channel boundary of Local domain) and discharge time series (Roosevelt Channel and Dinkins Bayou boundaries) were derived. The initial condition was the bathymetry in Figure 3-34. In order to focus on tidal effects only, waves were not included in these simulations and default sediment transport parameters were used.

The morphology changes after the 6-month morphology simulation considering the full astronomical tide signal is given in Figure 3-38. The computed changes using the tested Tide Schemes appear in Figure 3-39.

The Tide Scheme #1 (diurnal tide with the amplitude of the K1 component) causes practically no morphological changes after 6 month, suggesting that this scheme is unable to reproduce the morphology processes associated with the full astronomical tides at the inlet. The Tide Scheme #4 (M2C1) provides the best correlation with the erosion/sedimentation patterns and magnitudes achieved with baseline simulation, and was selected for the subsequent model applications.

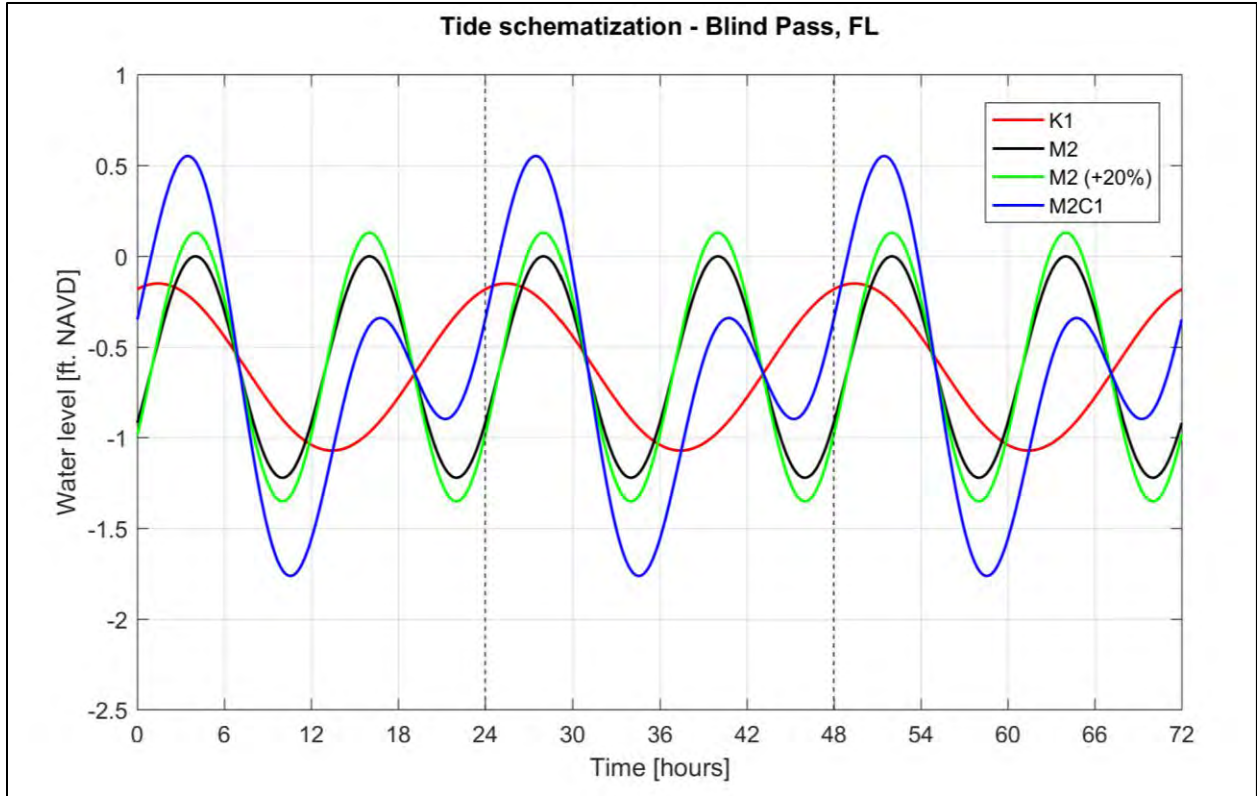


**Figure 3-37: Morphological tide schemes tested in the study.**

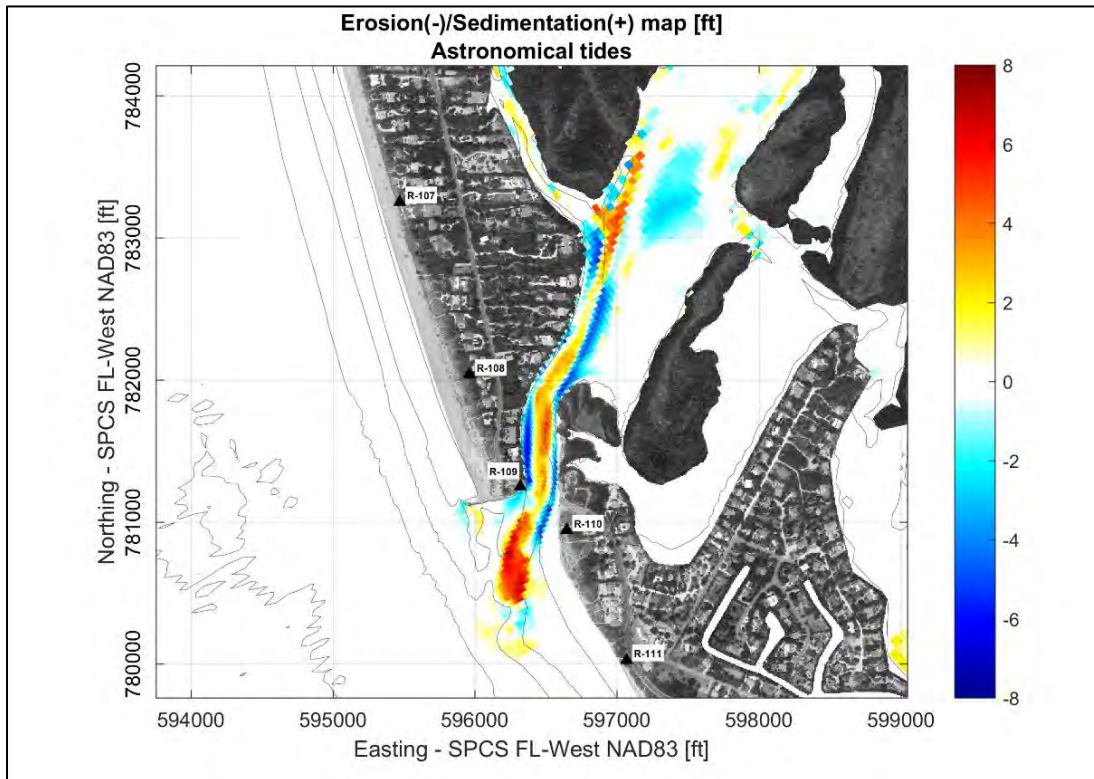


**Figure 3-38: Six Month Erosion (-feet) and Deposition (+feet) given the baseline simulation (full astronomical tides).**

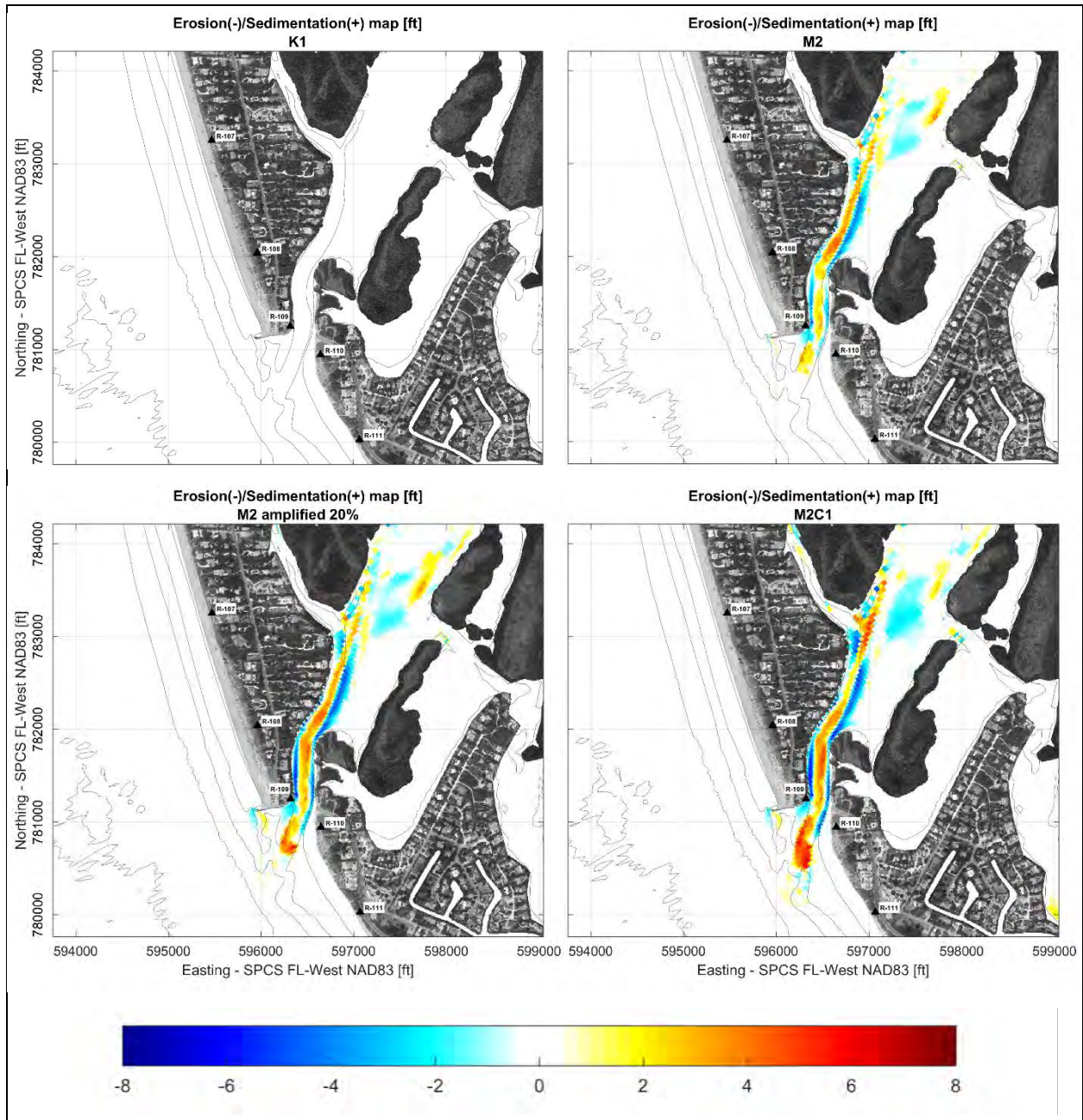


**Figure 3-39: Six Month Erosion (-feet) and Deposition (+feet) given the tested Tide Schemes: #1 one diurnal component (top left); #2 one semidiurnal component (top right), #3 one semidiurnal component amplified 10% (bottom left); and #4 the so called M2C1 tide composed of both a diurnal and a semidiurnal component (bottom right)**

### **3.4.3. Morphology Calibration**

The primary goal of the morphology calibration was to approximate the observed morphology changes at a sufficient level to simulate the overall coastal processes and sediment budget. The resulting morphology calibration was based on qualitative and quantitative analysis of the bed level changes (i.e. erosion and sedimentation) and sediment transport in the inlet and adjacent beaches. Several morphology simulations were performed for the calibration period in which different parameters of the model were tested and sensitivity analyses were performed.

The morphology calibration runs used the calibrated model configuration of the flow and wave conditions (described in Section 3.2.3 and Section 3.3.5, respectively). The final parameters used in the calibrated model can be seen in Table 3-9. The model calibration was successfully completed by analyzing qualitative and quantitative results.

The measured and modeled erosion/sedimentation maps are given in Figure 3-40 (qualitative results). The model was able to replicate the morphology trends in the dredged channel and its margins, and the erosion of the active profile in the north end of Sanibel. Overall changes at the south end of Captiva Island and the stability of other areas were represented by the model. The quantitative comparison presented on Figure 3-41 shows the integrated volume changes inside along sectors of the system, including different sections of the channel and adjacent areas that corroborate the qualitative analysis.

The net sediment transport map calculated by the calibrated Delft3D model for the morphology calibration period is shown in Figure 3-42. It shows predominance of alongshore sediment transport throughout the area, its path across the tip of Blind Pass jetty followed by an onshore movement immediately south of the structure, import of sand towards inner channel sections, and the bypassing path southward towards Sanibel beaches.

**Table 3-9: Summary of Delft3D calibration parameters.**

	Default	Selected Value
<b>SWAN Wave Transformation Model Parameters:</b>		
Breaking Parameter $\square$ (Hb/db)	0.73	0.73
Breaking Parameter $\square$	1.0	1.0
Bottom Friction Coef. for Waves (Optional): JONSWAP Friction Value ( $m^2/s^3$ )	0.067	0.067
Collins Friction Value	0.015	Not used
Madsen Roughness Scale (m)	0.0500	Not used
Triads - Energy Transfer from low to high frequencies in shallow water	Off	On
Diffraction:	Off	On
Diffraction Smoothing Coefficient	0.2	0.2
Diffraction Smoothing Steps	5	5
Wind Growth	On	On
JONSWAP Peak Enhancement Factor (for input waves specified in terms of height, period, and direction)	3.3	3.3
<b>Delft3D-FLOW Model, Flow Parameters:</b>		
Bottom Friction Coef. for Flow: Chezy's Friction Coef. C	65	Time variable (Trachytopes)
Manning's n	None	
Horiz. Eddy Viscosity ( $m^2/s$ )	1	1
Vertical Eddy Viscosity ( $m^2/s$ )	0	$1 \times 10^{-4}$
<b>Delft3D-FLOW Model, Sediment Transport Parameters:</b>		
Spin-up Interval - # of hours between the start of the simulation and the initiation of erosion & deposition estimates	6	6 hours
Density of sediment grains ( $kg/m^3$ )	2650	2200
Dry bed density ( $kg/m^3$ )	1600	1600
Median Grain Size (mm)	0.200	0.27
Horiz. Eddy Diffusivity ( $m^2/s$ )	10	0.01
Vertical Eddy Diffusivity ( $m^2/s$ )	0	$1 \times 10^{-4}$
Maximum Dry Cell Erosion Factor	0.5	0.2
BED - Current-Related Bedload Transport Factor (including wave-driven currents)	1	1
SUS - Current-Related Suspended Load Transport Factor (including wave-driven currents)	1	1
BEDW - Wave-Related Bedload Transport Factor	1	0.55
SUSW - Wave-Related Suspended Load Transport Factor	1	0.55
Transverse bed gradient factor (AlfaBn)	1.5	10

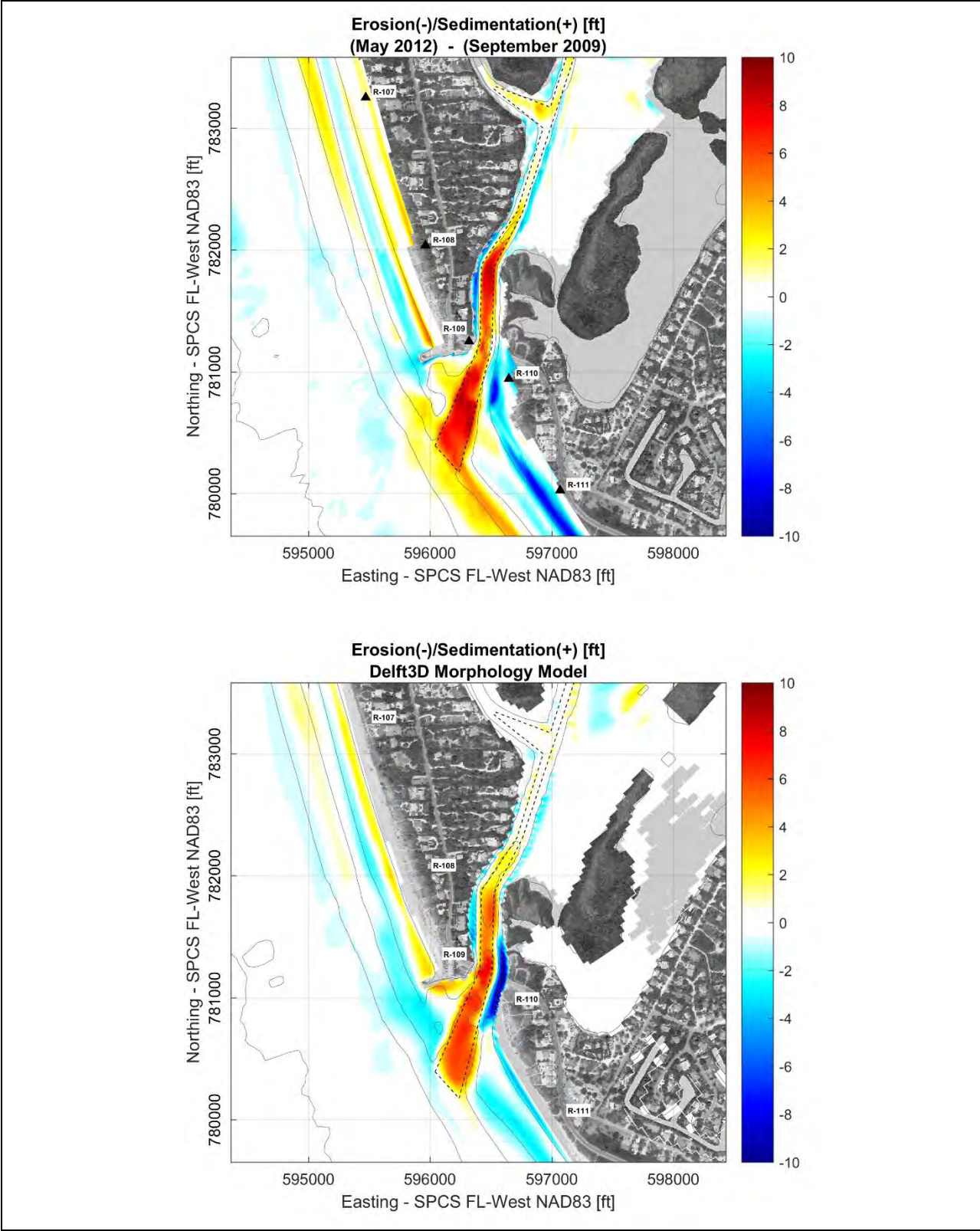
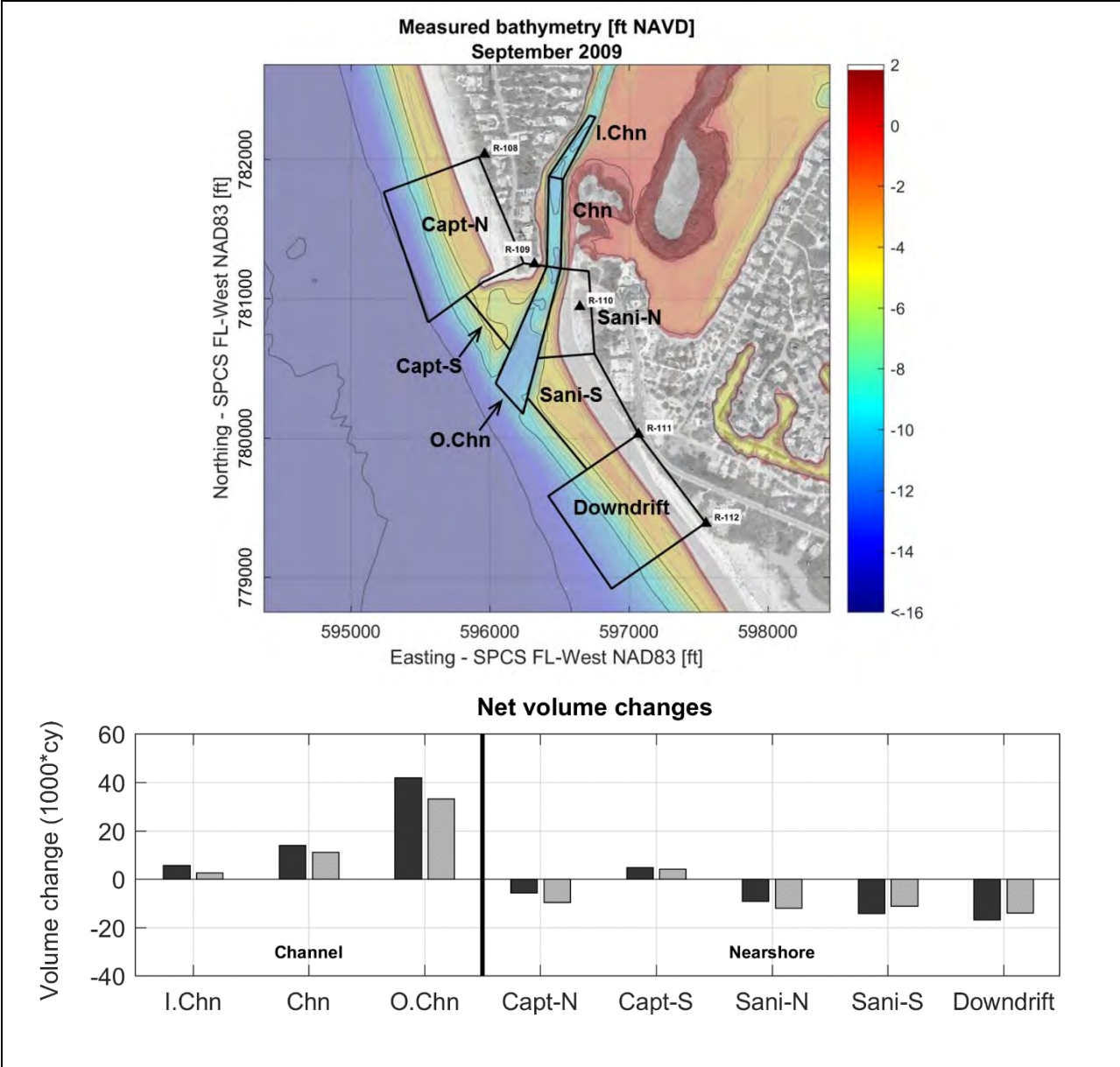
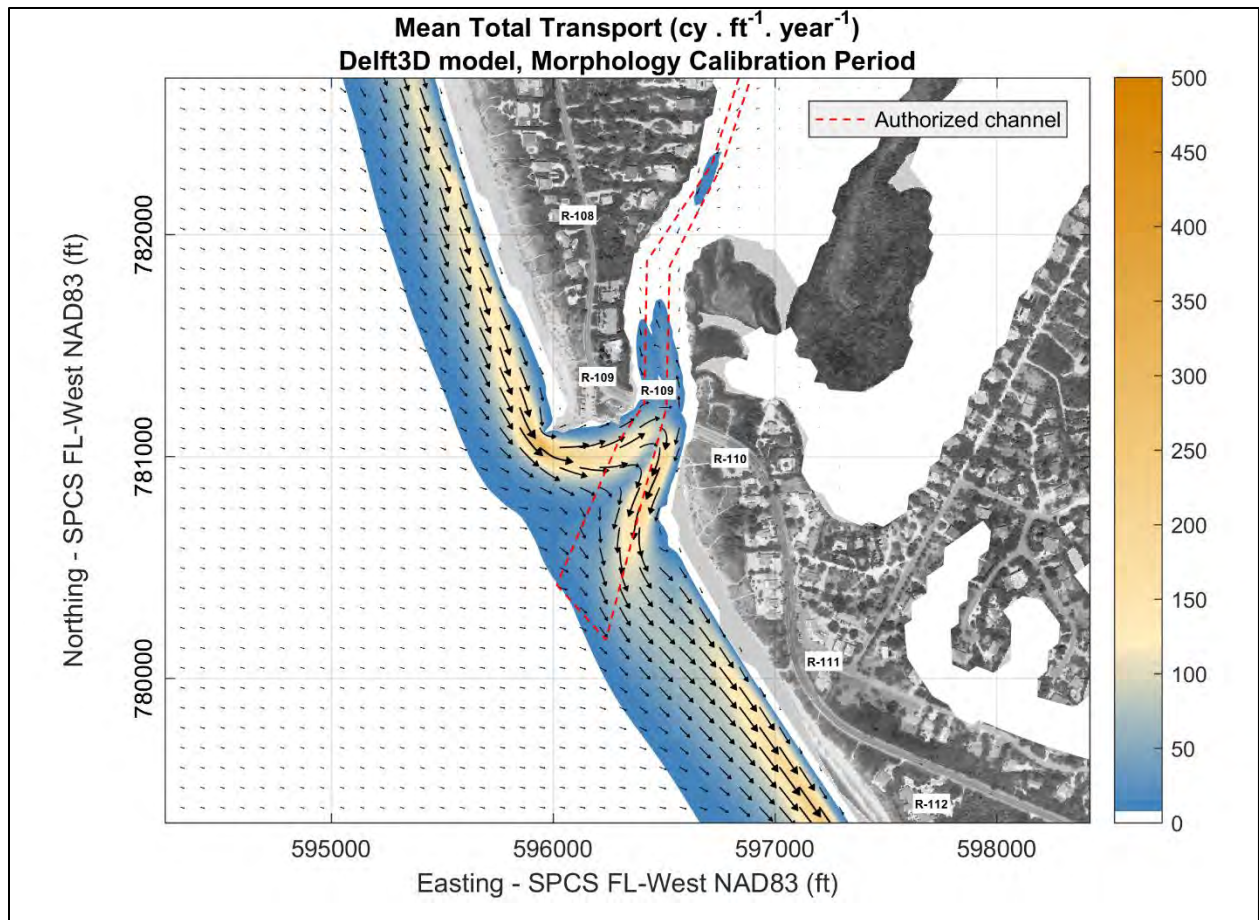


Figure 3-40: Measured and modeled erosion/sedimentation map.



**Figure 3-41: Measured and modeled volume changes for the morphology calibration period. Darker bars: Measured data; lighter bars: Delft3D model.**



**Figure 3-42: Net sediment transport map – Delft3D model, morphology calibration period.**

## 4. PERFORMANCE OF INLET MANAGEMENT ALTERNATIVES

In order to evaluate the inlet processes and the performance of alternatives, several dredging, structural and beach fill designs were developed and analyzed through model simulations. First, eighteen (18) preliminary alternatives were evaluated under average conditions (5-year simulation). Based on this initial analysis and its findings, three (3) scenarios combining multiple design elements from the preliminary analysis were evaluated under average conditions (5-year simulation) and under two storm conditions. The two storm conditions were selected to represent winter conditions (January 2016 cold front) and summer conditions (Hurricane Charley, 2004).

### 4.1 Model Setup

All simulations utilized the Regional, Intermediate and Local Wave Grids, and the Local Flow Grid. The initial bathymetry used for the alternatives was based on the bathymetric data sets of 2016, which represented the most recent available surveys at the time the study was performed (see Table 2-1). The 2016 survey data was used as the primary data source. Grid points outside the 2016 survey areas were filled using older data sets, beginning with the 2015 surveys and ending with the NCEI/NOAA data (see Table 2-1). The resulting 2016 bathymetry interpolated to the morphology grid appears in Figure 4-1.

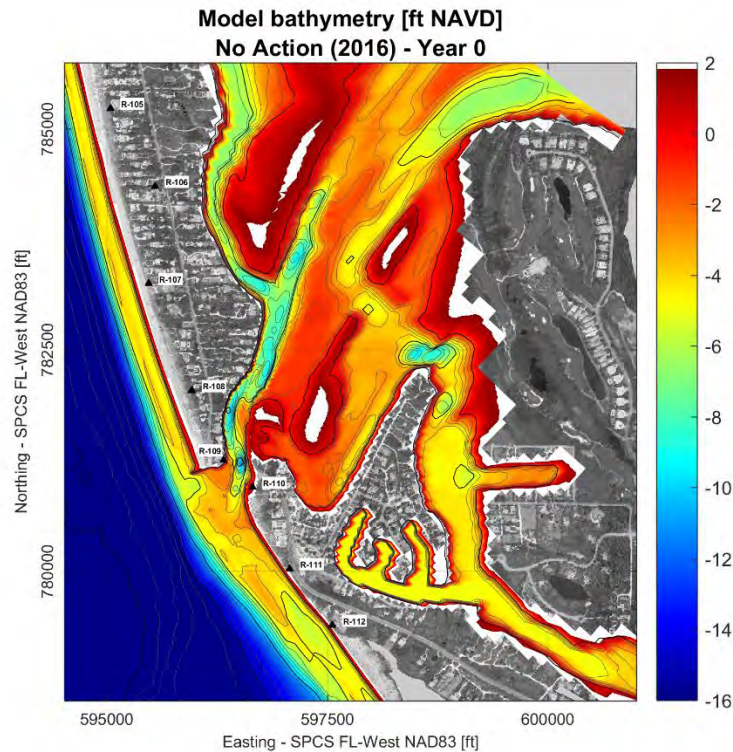


Figure 4-1: 2016 Model bathymetry used as baseline in production runs - No Action.

The forcing conditions for the production runs vary when simulated for average conditions (5-year simulation) or for storm conditions. The details of the average conditions set up are provided below. The configuration and results of the storm simulations (i.e. Cold Front and Hurricane Charley) are provided in Sub-Appendix A-5.

For the simulations of the scenarios under average conditions (5 years), the model forcing approach was identical to the final morphology calibration run. For the morphology calibration simulations, the representative waves were selected from the wave data time series covering the morphology calibration period (2009-2012, see Section 3.4.2). For the production runs, the 16 wave conditions were re-defined considering the whole wave data time series from 1999 to 2015. The representative wave cases are listed in Table 4-1:

**Table 4-1: Representative wave conditions used in the production runs.**

Wave case	Hs (feet)	T <sub>p</sub> (sec.)	Dir <sub>p</sub> (deg.)	Dir. Spreading (cosine power)	Wind speed (mph)	Wind direction (deg)	Occurrence (days/yr)	Morfac
#1	1.51	4.0	183	4.4	10.6	151	36.7	18.3
#2	2.83	4.7	193	4.0	14.9	175	10.6	10.6
#3	5.43	6.2	207	4.0	21.5	177	2.9	2.9
#4	2.11	5.3	255	6.7	9.9	261	19.5	19.5
#5	4.23	6.9	257	5.0	13.9	299	4.8	4.8
#6	6.45	8.2	259	4.3	19.3	289	2.1	2.1
#7	2.31	5.7	282	7.6	10.0	342	16.8	16.8
#8	4.52	7.2	282	5.3	15.6	343	4.4	4.4
#9	6.76	7.8	281	4.0	21.2	320	2.0	2.0
#10	1.67	4.7	301	7.0	11.0	4	32.0	16.0
#11	3.11	5.7	297	4.5	15.7	353	9.2	9.2
#12	5.56	6.5	295	4.0	22.3	331	2.9	2.9
#13	0.51	3.7	162	15.9	7.0	102	62.2	31.1
#14	0.45	4.3	231	20.7	6.6	112	60.5	30.2
#15	0.56	3.9	305	16.2	7.4	29	51.0	25.5
#16	1.43	2.8	58	4.5	14.1	65	47.4	23.7

Calm

## 4.2 Preliminary Alternatives

The eighteen (18) preliminary alternatives including No Action are presented in Table 4-2. The initial surfaces for all alternatives are provided in Sub-Appendix A-1.

The alternatives were developed to test options to address the challenges in the behavior of the pass and adjacent beaches. This includes (1) the instability of Blind Pass channel position and cross-sectional area caused by high sedimentation rates around the bridge and seaward causing a tendency of inlet closure over time and requiring frequent maintenance dredging, and (2) the unstable downdrift beach behavior and erosion at the north end of Sanibel Island related to the pass and dredge/fill activities.

For the initial alternative screening, the Blind Pass dredge template (Alt 3a) was a simplified version of the permitted dredge template considering a uniform dredging depth of -10 ft NAVD.

The alternative does not include beach fill placement, which allows the effects of the inlet dredging to be easily isolated. In the final phase of the study presented in Section 4.3, where the most effective alternative components are combined, the Blind Pass dredge template is refined to represent the existing inlet management approach (i.e. including variable dredging depths in the inner sections and beach fill placement in two locations south of the Pass).

Dredge and fill quantities for the tested alternatives appear in Table 4-2. The simulations for Alternatives 6a-6d assumed that the dredged material would be placed (a) on Sanibel Island (R-110.5 to R-117), (b) on Captiva Island (R-102 to R-109), (c) adjacent to the inlet as an ebb shoal enhancement, and (d) nearshore disposal at Sanibel Island (R-110.5 to R-117).

**Table 4-2: Summary of the preliminary alternatives.**

• Alt 0: No Action (2016 bathymetry as initial condition).	NO ACTION
• Alt1b: Blind Pass dredge template + Wulfert Channel extension to Pine Island Sound	
• Alt3a: Blind Pass dredge template (-10 ft NAVD)	DREDGING
• Alt3c: Truncated Blind Pass dredge template (-10 ft NAVD)	ALTERNATIVES
• Alt4: Alt3a + Restore connection to Sunset Bay (1995 condition)	
• Alt5a: Alt3a + Blind Pass jetty: Remove	BLIND PASS
• Alt5b: Alt3a + Blind Pass jetty: Shorten by 50 ft	JETTY
• Alt5c: Alt3a + Blind Pass jetty: Lengthen by 100 ft	ALTERNATIVES
• Alt6a: Alt3a + Beach fill*: north end of Sanibel Island	
• Alt6b: Alt3a + Beach fill*: south end of Captiva Island	BEACH FILL
• Alt6c: Alt3a + Beach fill*: Ebb shoal enhancement	ALTERNATIVES
• Alt6d: Alt3a + Beach fill*: Nearshore placement at Sanibel Island	
• Alt7: Alt3a + Deposition Basin (interior and exterior)	DEPOSITION BASINS
• Alt8b: Alt3a + Angled (Z) structure on Sanibel Island	
• Alt8South: Alt3a + Straight structure (tip at similar location as 8b)	SANIBEL
• Alt8Center: Alt3a + Straight structure north of previous	STRUCTURE
• Alt8North: Alt3a + Straight structure north of previous	
• Alt9: Alt3a + 200 ft Spur at Blind Pass jetty	SPUR

\*Beach fill volume = 102,000 cy for all Alt6 variations.

**Table 4-3: Simulated alternatives - dredge and fill volumes.**

Alternatives	Volumes (1,000 * cy)	
	Dredge	Fill
Alt1b	264	-
Alt3a	102	-
Alt3c	66	-
Alt4	184	-
Alt5a	102	-
Alt5b	102	-
Alt5c	102	-
Alt6a	102	102
Alt6b	102	102
Alt6c	102	102
Alt6d	102	102
Alt7	181	-
Alt8b	102	-
Alt8South	102	-
Alt8Center	102	-
Alt8North	102	-
Alt9	102	-

The Blind Pass jetty and its variations (Alts 5a-c) were represented in the model bathymetry similarly to the definition in the final morphology calibration run (i.e. rising the bed elevation at the structure location and setting the bed material as non-erodible). The tested structures in the north end of Sanibel Island (Alternative 8) and the Blind Pass jetty spur (Alt 9) were simulated as “Thin Dams” in the Delft3D-FLOW model and “Sheets” in the SWAN model, with no wave reflection and transmission through the structures.

Each preliminary alternative was simulated for a period of 5 years. Model results were analyzed qualitatively and quantitatively using several model outputs to evaluate the multiple objectives of the study. Absolute model results are presented for two baseline scenarios: Alternative 0 (No Action) and Alternative 3a (Blind Pass dredge template, -10 ft NAVD). Results for all other alternatives are analyzed relative to Alternative 3a, which is a baseline condition for the other alternatives. Therefore, these relative results represent the net effects associated with each tested component. The following graphics were generated:

a) Bathymetric Map results:

- i. Simulated bathymetry after 5 years for baseline alternatives (No Action and Alt 3a)
- ii. Net bathymetry changes after 5 years relative to Alternative 3a (alternative “minus” Alt 3a)

- b) Minimum inlet cross-sectional area over time
  - i. Absolute (minimum) cross sections over 5 years for baseline alternatives (No Action and Alt 3a)
  - ii. Net changes after 5 years relative to Alternative 3a baseline scenarios (alternative “minus” Alt 3a)
- c) Volume changes along adjacent Captiva and Sanibel Island beaches
  - i. Net changes after 5 years relative to Alternative 3a after 1 and 5 years (alternative “minus” Alt3 a)
- d) Volume changes over time at R-monument 111 (R-111)
  - i. Net changes after 5 years relative to Alternative 3a (alternative “minus” Alt 3a)

Considering the large number of alternatives and prepared model results, a subset of model plots is provided in this appendix to facilitate the discussion of the performance of each alternative. The plots presented within this appendix are the net changes in minimum inlet cross-sectional area over time, the net volume changes alongshore, and the net changes at R-111, which is an area of narrow width fronting the roadway. The remaining model plots can be found in Sub-Appendix A-2.

Bathymetric changes are plotted in feet. For the relative (net) change plots, positive changes (warm colors) indicate that the alternative is shallower than No Action; negative changes (cool colors) indicate that the alternative is deeper than No Action.

Volumetric changes are calculated in cubic yards per foot (cy/ft) above the depth of closure, -13 feet NAVD. For the relative (net) change plots, positive changes (to the left of the 0-axis) indicate that the alternative has more volume than No Action; negative changes (to the right of the 0-axis) indicate that the alternative has less volume than No Action.

The minimum inlet cross-sectional area over time results are calculated considering the southern-end of the channel, an approximately 1,200 feet longitudinal section that spans either side of the bridge and represents the most constricted area of the channel. For each bathymetry output from the model along the 5-year simulations (260 maps), a large number of cross-sectional areas are calculated along the considered channel section (>370 cross sections). The minimum cross-section at each time is stored and plotted in square feet (sq. ft.).

The results for the preliminary alternatives are described below, and are grouped categorically as presented in the beginning of Section 4 for comparison purposes by dredging, Blind Pass jetty, beach fill, and Sanibel structure. The baseline scenarios, No Action and Alternative 3a (Blind Pass dredge template at -10 ft NAVD), are presented first.

#### **4.2.1 Baseline Conditions: Alternative 0 (No Action) and Alternative 3a**

The effects of dredging (Alt 3a) versus No Action is shown in Figure 4-2, which is the difference between Alternative 3a and No Action after 5 years of simulation. In the figure, positive changes

(warm colors) indicate that Alternative 3a is shallower than No Action; negative changes (cool colors) indicate that Alternative 3a is deeper than No Action.

The most evident differences between the final bathymetries of Alternative 3a and No Action occur along the dredged channel and immediately south of the channel limits (between R-110 and R-111). The channel dredging increases the tidal prism and channel stability, resulting in a deeper final bathymetry for Alternative 3a relative to No Action (blue colors along the channel in Figure 4-2). The more stable channel and stronger tidal currents also builds and maintains an ebb shoal immediately south of the inlet (orange and yellow colors in Figure 4-2). Although still modest, the final ebb shoal feature associated with the Alternative 3a simulation is more prominent than the one observed at the final stage of the No Action simulation.

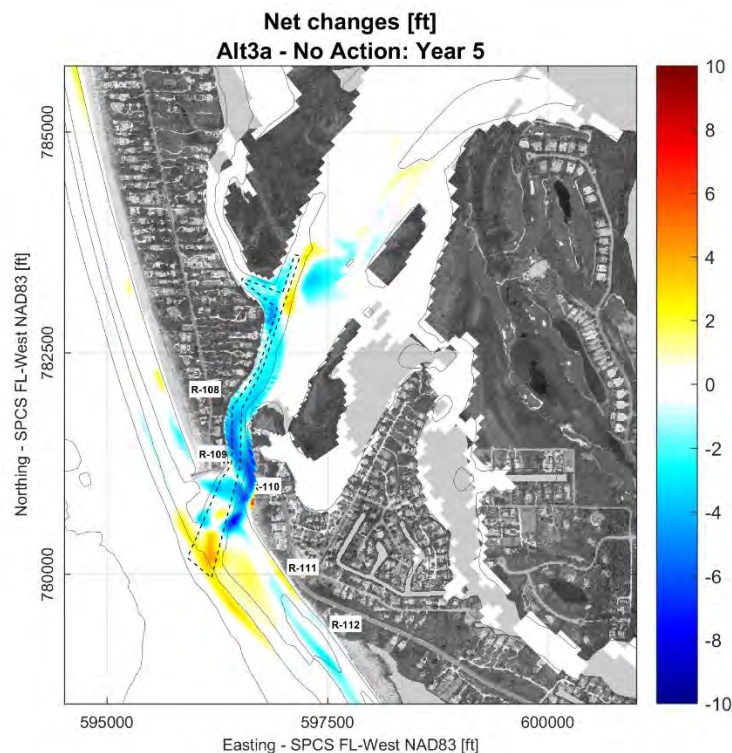


**Figure 4-2: Net bathymetry changes relative to No Action (difference between year 5 bathymetries). Dashed line represents dredge template boundary.**

The model indicates bathymetry changes associated with the channel dredging adjacent to the northern limits of the dredge template. This is supported by the observed changes that have occurred in the region after channel opening in 2009 (Figure 4-3). The connection to Pine Island Sound through Wulfert Channel, across a shallow bar north of the connection to Roosevelt Channel, has naturally expanded due to the increased tidal currents resulting from the channel dredging. The development of deeper channels results in a cumulative enhancement of the tidal flows and ultimately increased inlet stability. However, since this area is out of the dredging template, the net changes in sediment volume are expected to be small, and proportional shallowing at adjacent areas is also expected.



**Figure 4-3: Observed changes in Wulfert Channel (images: Google Earth). Red line: Blind Pass dredge template; white line: reference contour.**

Figure 4-4 presents the minimum cross-sectional area of Blind Pass channel over the 5-year simulations for No Action and Alternative 3a. Due to the relatively small size of the Blind Pass channel, its morphodynamic response is fast and the channel cross-sectional area changes considerably over time. These fluctuations in the channel cross-sectional area are shown in the time series: the channel reduces drastically during high wave events when alongshore sediment transport overcomes the tidal forces, and re-establishes during calmer periods when restoring tidal forces prevail.

For No Action, the initial minimum cross-sectional area is approximately 500 sq. ft., and gradually reduces along the simulation time. Episodic channel closures occur after approximately 3 and 5 years of simulation. For the Alternative 3a scenario, the initial cross section is in the order of 1400 sq. ft. It varies over the simulation, but the trend is relatively stable, unlike No Action which has a negative trend.

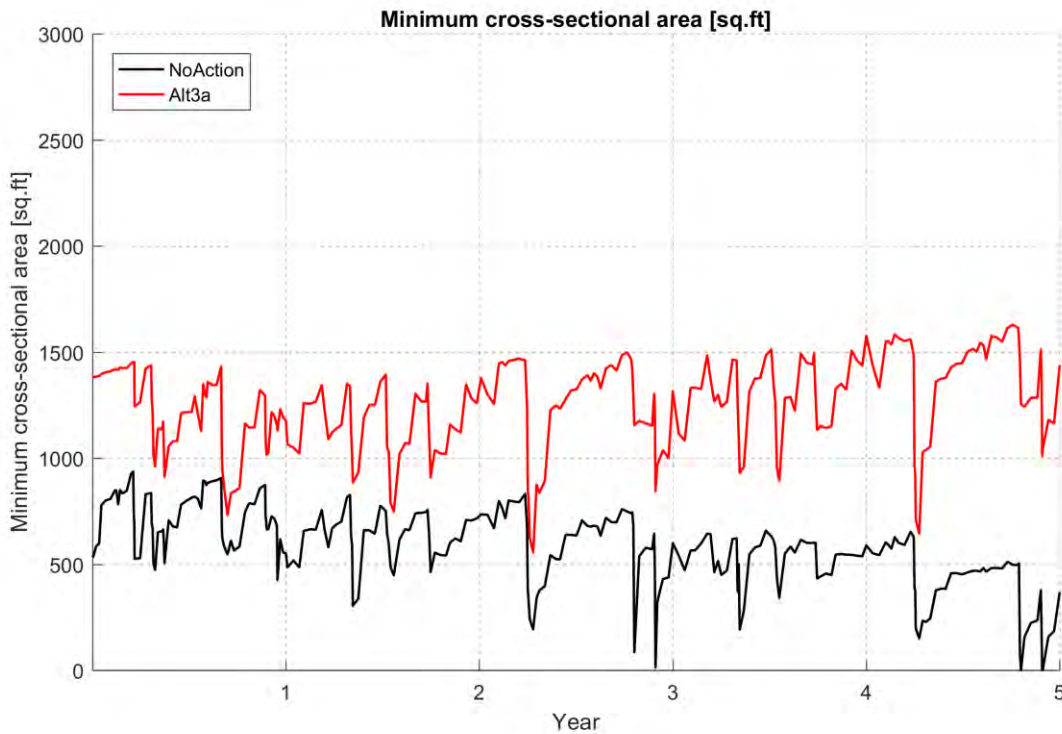


**Figure 4-4: Minimum Blind Pass channel cross-sectional area over the simulated period.**

Figure 4-5 and Figure 4-6 present the net volumetric changes along Captiva and Sanibel Islands for Alternative 3a relative to No Action, after 1 and 5 years of simulation. Alternative 3a starts with a relative reduction of 102,000 cy of sand from the channel dredging. It is noted that Alternative 3a does not include beach nourishment placement, allowing for the isolated comparison of channel dredging alone.

On the shorter time-frame (1 year), the volume changes on Captiva Island for Alternative 3a are generally the same as No Action, with a negative effect at the south end near Blind Pass (~7 cy/ft). On Sanibel Island channel dredging causes negative effects on the adjacent beaches between R-110 and R-113. These effects peak immediately downdrift of the channel around R-110.5 (~30 cy/ft).

The longer term behavior of the simulated section of Captiva Island remains similar after 5 years (Figure 4-6). However, different patterns are noticed on Sanibel Island in Figure 4-6: the effects of channel dredging are negative next to the channel due to its migration, positive at the north end of the island, and negative south of R-112. This is related to the more stable channel and its (modest) ebb tide shoal protecting the adjacent shoreline. These results indicate that the stability of Blind Pass benefits the beaches adjacent to the inlet. The results south of R-112 are related to the migration/diffusion of the direct effects of channel dredging (observed in year 1 results), development of the ebb shoal features, and the diminished erosion at the north end of the island, which reduces sediment mobilized southward.

For a better understanding of the dredging effects on the north end of Sanibel Island, net volume changes at profile R-111 are analyzed over the 5 year period (Figure 4-7). At this location, negative effects of channel dredging peak after 1 year (~25 cy/ft) and become positive after 3 years.

To summarize, the channel dredging causes an immediate downdrift effect on Sanibel Island caused by removing the bypassing bar, which is the sediment transport pathway from north to south, and creating a sediment 'sink'. The adjacent downdrift beach experiences the effect of the interruption in sediment transport first, and over time the effects migrate further down Sanibel Island. As the dredge template refills and the bypassing bar reforms, the downdrift effects from lack of transport are reduced. However, the refilling causes the channel to migrate south and causes erosion on the beach adjacent to the channel.

The results indicate that the beach fill placement may need to be shifted north to address the immediate effect of the inlet dredging. The current practice is to place the material starting at R-112, which bypasses the area to the north that is immediately effected by dredging. The beach fill placed further north would benefit areas to the south in the subsequent years via littoral drift (i.e. feeder beach).

The presented results are generally consistent with observed behavior of the channel and adjacent beaches over the last decade. Multiple dredging projects were required to ultimately maintain Blind Pass open, and erosion was observed south of the Pass.

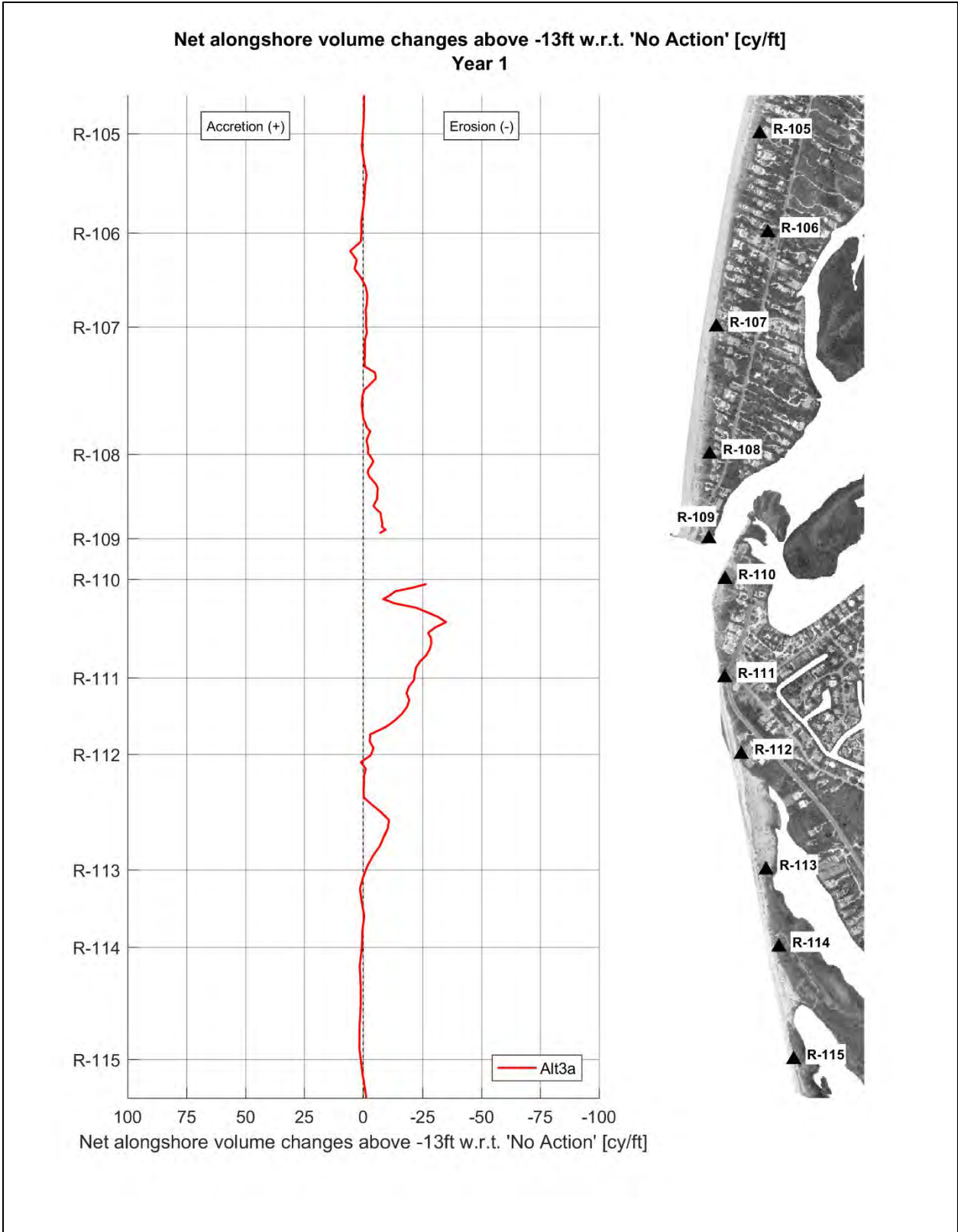


**Figure 4-5: Simulated net beach volume changes relative to No Action, after 1 year.**

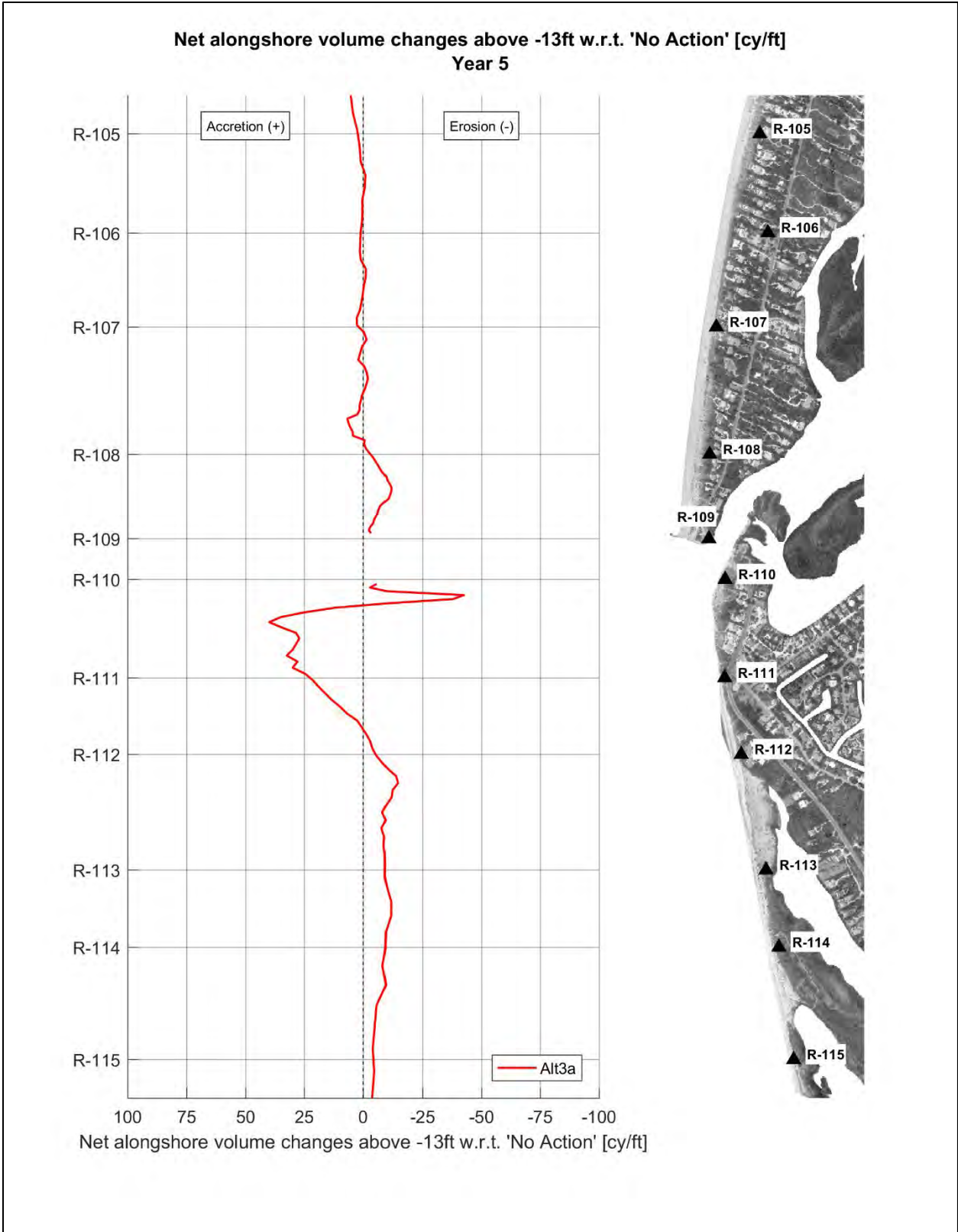


**Figure 4-6: Simulated net beach volume changes relative to No Action, after 5 years.**

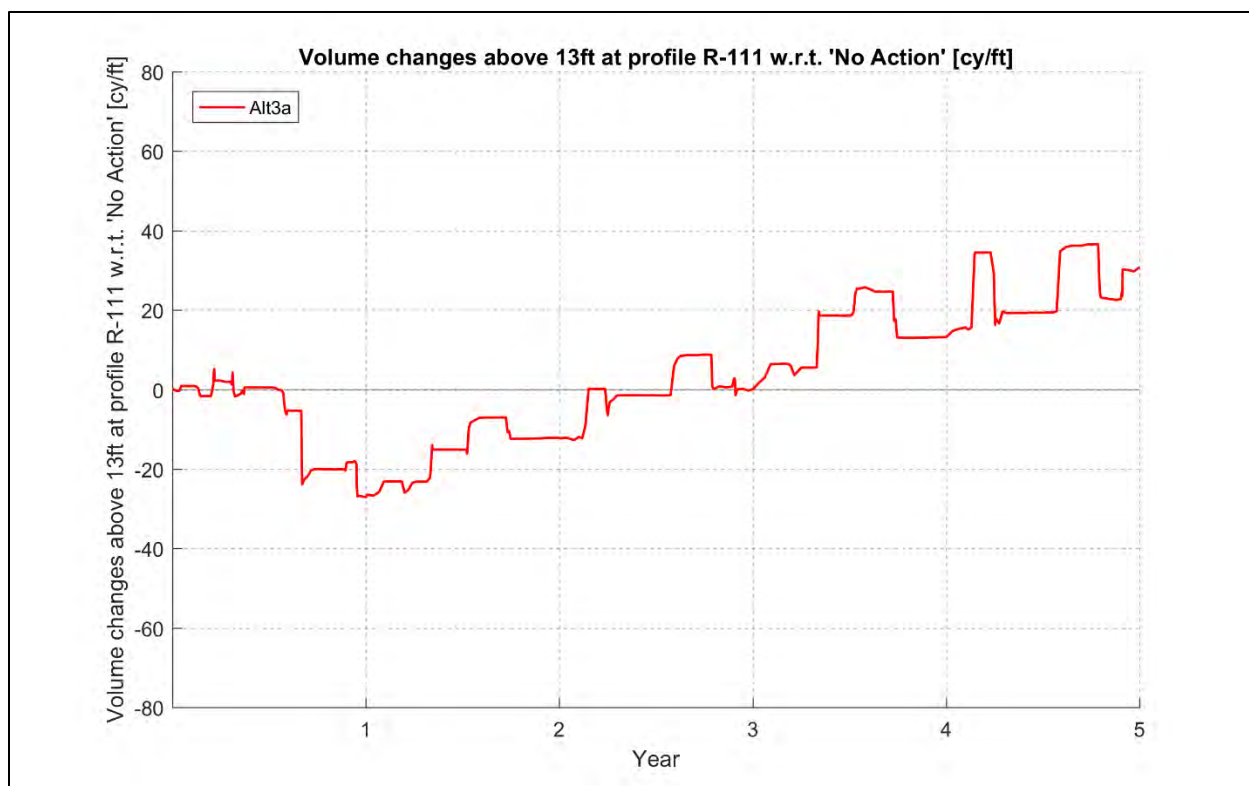


Figure 4-7: Simulated beach volume changes at profile R-111.

#### 4.2.2 Dredging Alternatives (1b, 3c, 4, 7)

The results for the dredging alternatives relative to Alternative 3a are summarized in Figure 4-8 to Figure 4-11. The net bathymetry change maps comparing the final simulated bathymetries (year 5) for each alternative relative to Alternative 3a are given in Sub-Appendix A-2. Net changes with respect to Alternative 3a represent relative effects of the tested design elements on the coastal system. The dredging alternatives and their general description are listed below.

Baseline Condition: Alt 3a: Blind Pass dredge template (-10 ft NAVD)

- Alt 1b: Blind Pass dredge template + Wulfert Channel extension to Pine Island Sound
- Alt 3c: Truncated Blind Pass dredge template
- Alt 4: Alt 3a + Restore connection to Sunset Bay (1995 condition)
- Alt 7: Alt 3a + Deposition Basin (interior and exterior)

The model suggests that channel stability is enhanced by improving connections to the inland waterbodies: Sunset Bay, Dinkins Bayou, and Pine Island Sound (Figure 4-8). This is specifically shown in the results for Alternative 1b and Alternative 4. Alternative 7 considers additional dredging of 80,000 cy from the Pass and immediately adjacent areas for deposition basins, which directly increases channel's cross-section area. Alternative 3c considers a shorter, "truncated"

dredging template, which has a slightly negative effect on channel's cross-sectional area, especially after the third year of simulation.

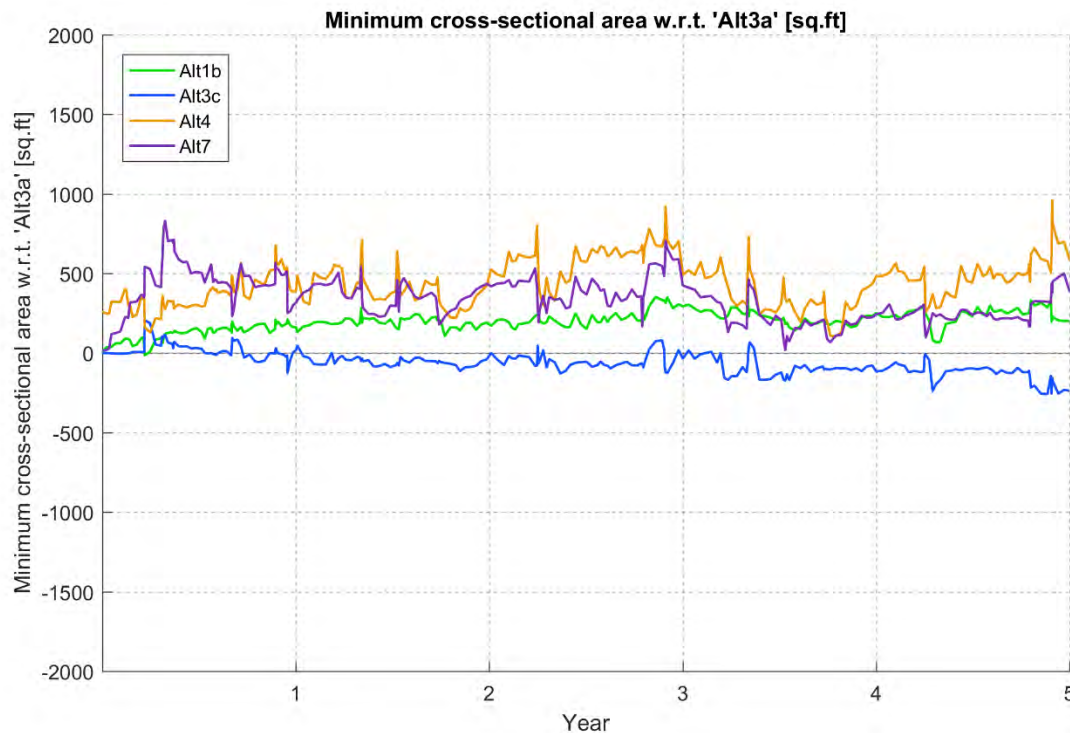


**Figure 4-8: Minimum Blind Pass channel cross-sectional area over the simulated period – dredging alternatives.**

The shorter term (1 year) effects of the dredging alternatives on adjacent beaches indicate negligible effects on Captiva Island relative to Alternative 3a (Figure 4-9). On Sanibel Island, effects are mostly concentrated north of R-112, and are remarkably positive for Alternative 3c (~25 cy/ft) and negative for Alternative 7 (~45 cy/ft), whereas Alternative 1b and 4 have less of an effect. The positive effect of Alternative 3c is caused by maintaining a portion of the bypassing bar, which is the sediment transport pathway from north to south and allows more sand to be transported to the south to Sanibel Island vs. Alternative 3a. The negative effect of Alternative 7 is due to the deposition basins trapping more sand from the littoral drift causing less sand to be transported downdrift of the inlet. In comparison, the shorter channel (Alt 3c) partially maintains the bypassing bar benefiting downdrift beaches, while the deposition basins magnify negative downdrift effects.

After five years of simulation, the net effects of the dredging alternatives relative to Alternative 3a remain small at Captiva Island (Figure 4-10). Alternatives 1b and 3c benefit the north end of Sanibel Island, Alternative 7 produces negative effects, and Alternative 4 has a variable influence, but is mostly negative. It is highlighted that tidal fluxes through the inlet are significantly increased with Alternative 4, and consequently the ebb tidal shoals develop further and store additional sand in front of the inlet that would otherwise be transported to feed the beaches to the south.

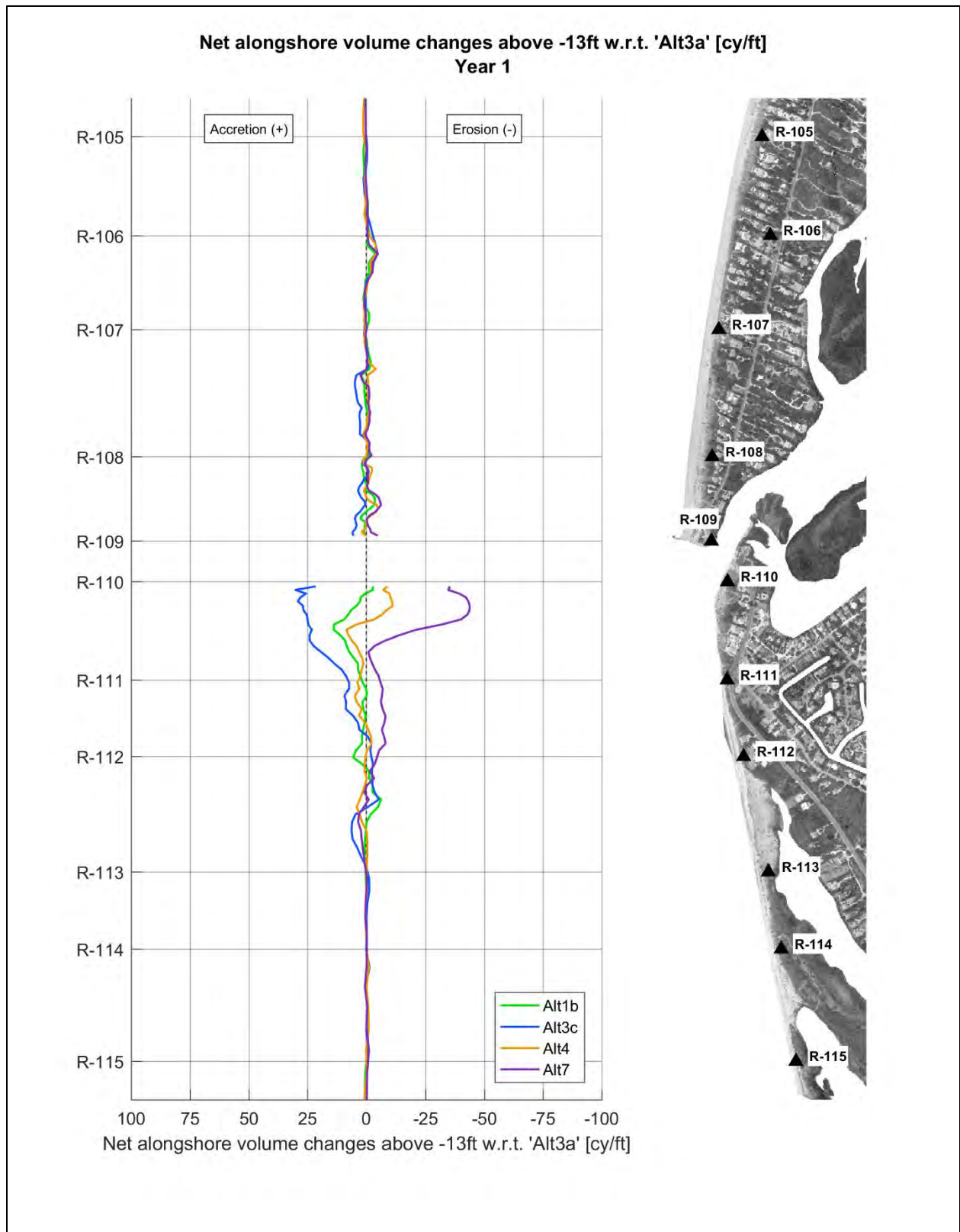


**Figure 4-9: Simulated beach volume changes after 1 year – dredging alternatives.**

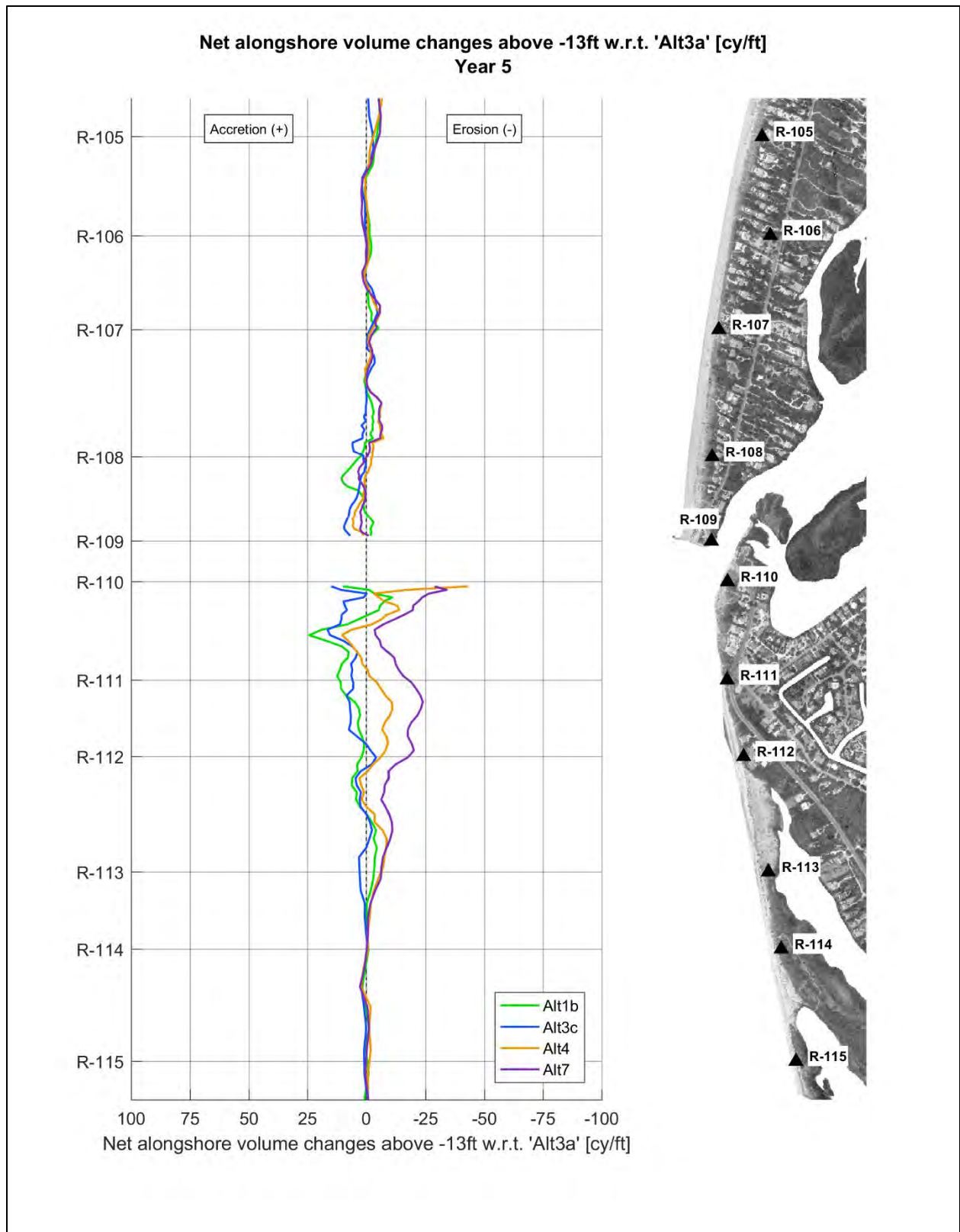


**Figure 4-10: Simulated beach volume changes after 5 years – dredging alternatives.**

The volume changes at R-111 on Sanibel Island are shown in Figure 4-11. The model indicates that Alternative 3c has the most benefit relative to Alternative 3a in the first couple years at R-111 due to the intact bypassing bar enabling sediment transport. Alternative 7 generally causes a deficit of sand at this location over the 5 year time period, while Alternatives 1b and 4 are generally beneficial due to an enhanced tidal prism, channel area and ebb shoal features.

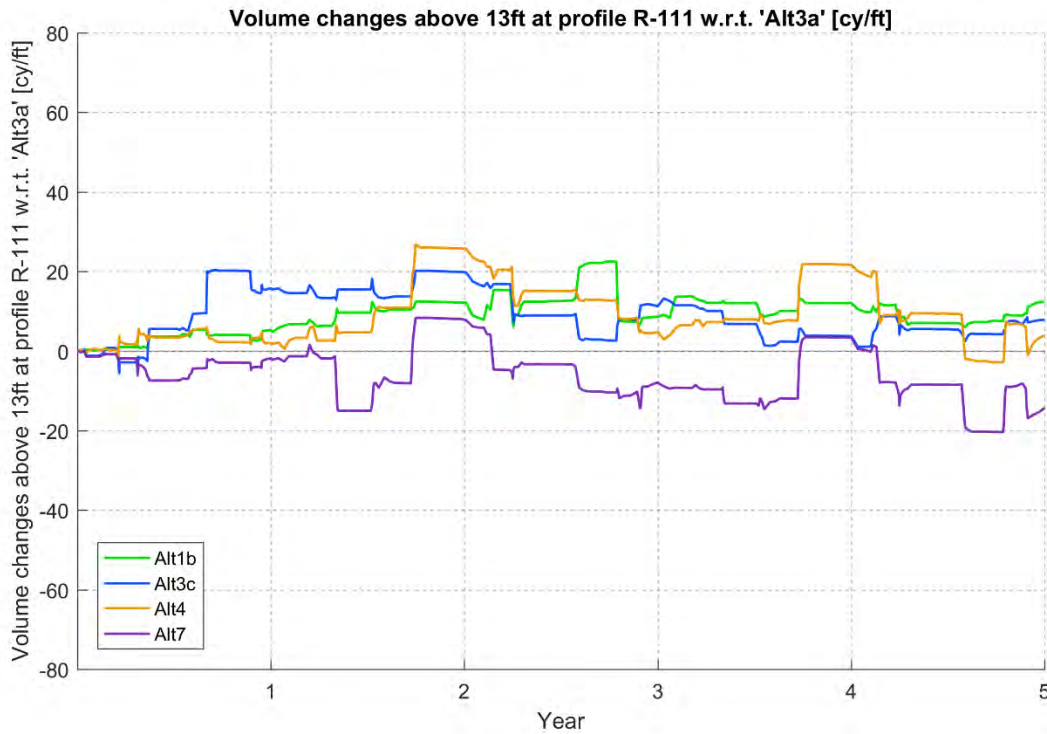


Figure 4-11: Simulated beach volume changes at profile R-111 – dredging alternatives.

#### 4.2.3 Blind Pass Jetty Alternatives (5a, 5b, 5c, 9)

The results for the Blind Pass jetty alternatives are summarized in Figure 4-12 to Figure 4-15. The net bathymetry change maps comparing the final simulated bathymetries (year 5) for each alternative relative to Alternative 3a are given in Sub-Appendix A-2. Net changes with respect to Alternative 3a represent relative effects of the tested design elements on the coastal system. The Blind Pass jetty alternatives and their general description are listed below.

Baseline Condition: Alt3a: Blind Pass dredge template (-10 ft NAVD)

- Alt 5a: Alt 3a + Blind Pass jetty: Remove
- Alt 5b: Alt 3a + Blind Pass jetty: Shorten by 50 ft
- Alt 5c: Alt 3a + Blind Pass jetty: Lengthen by 100 ft
- Alt 9: Alt 3a + 200 ft Spur at Blind Pass jetty

The minimum cross-sectional area results (Figure 4-12) indicate that shortening or removing the existing Blind Pass jetty is detrimental to channel's stability. According to model results, the jetty removal (Alt 5a) leads to permanent channel closure after 3.8 years (i.e. the negative effects equal the cross sectional area of Alt 3a, shown in Figure 4-4). On the other hand, lengthening (Alt 5c) or creating a southward spur (Alt 9) benefits the channel cross-sectional area over time. Alt 5c (lengthening) benefits the inlet by reducing the transport to the south. Alt 9 (spur) benefits the inlet by redirecting the sediment transport in a more southerly direction, reducing the transport and sedimentation in the inlet. Bypassing is improved, and channel migration is reduced.

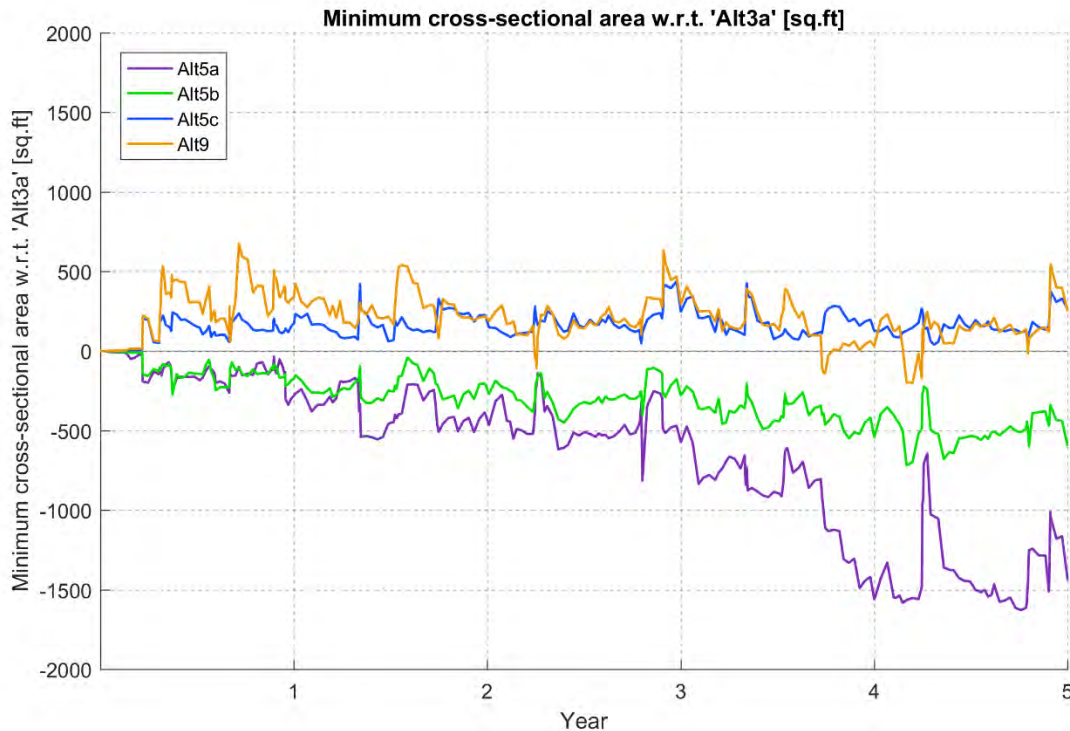


**Figure 4-12: Minimum Blind Pass channel cross-sectional area over the simulated period – Blind Pass jetty alternatives.**

The simulated volume changes presented in Figure 4-13 and Figure 4-14, 1 and 5 years respectively, suggest that jetty removal (Alt 5a) or shortening (Alt 5b) lead to significant erosion of Captiva Island. The negative changes increase over time in both magnitude and the affected area.

During the first year of simulation, both Alternative 5a (removal) and 5b (shortening) produce positive effects on the southern side of the inlet (north end of Sanibel Island) due to a release of sand from Captiva Island. Alternative 5c (lengthening) negatively affects the area north of R-111 by reducing the sediment transport from Captiva Island. Overall effects of Alternative 9 (spur) are negligible.

Over the longer time term (5 years), Alternative 5a (removal) and 5b (shortening) cause additional infilling of the inlet, inlet weakening or closure, and a less developed ebb shoal. These processes counter-act potential benefits of the enhanced littoral drift from Captiva Island, and as a result Alternatives 5a and 5b cause negative effects north of R-112. Alternative 5a benefits the area further south, between R-112 and R-115, due to the increased sand transport from the south end of Captiva Island, channel closure after 3.8 years ceasing import of sand into the inlet, and consequent ebb shoal retreat supplying sand to downdrift areas. Alternative 5c has negative effects in the area between R-110.5 and R-113 due to the reduced sand transport from Captiva Island. Finally, Alternative 9 (spur) has positive effects in Captiva Island, balancing the negative effects of channel dredging (see Figure 4-6). In Sanibel Island, positive effects occur in the area north of R-111 (ebb shoal enhancement) and negative effects between R-111 and R-113, as a consequence of the described updrift benefits.

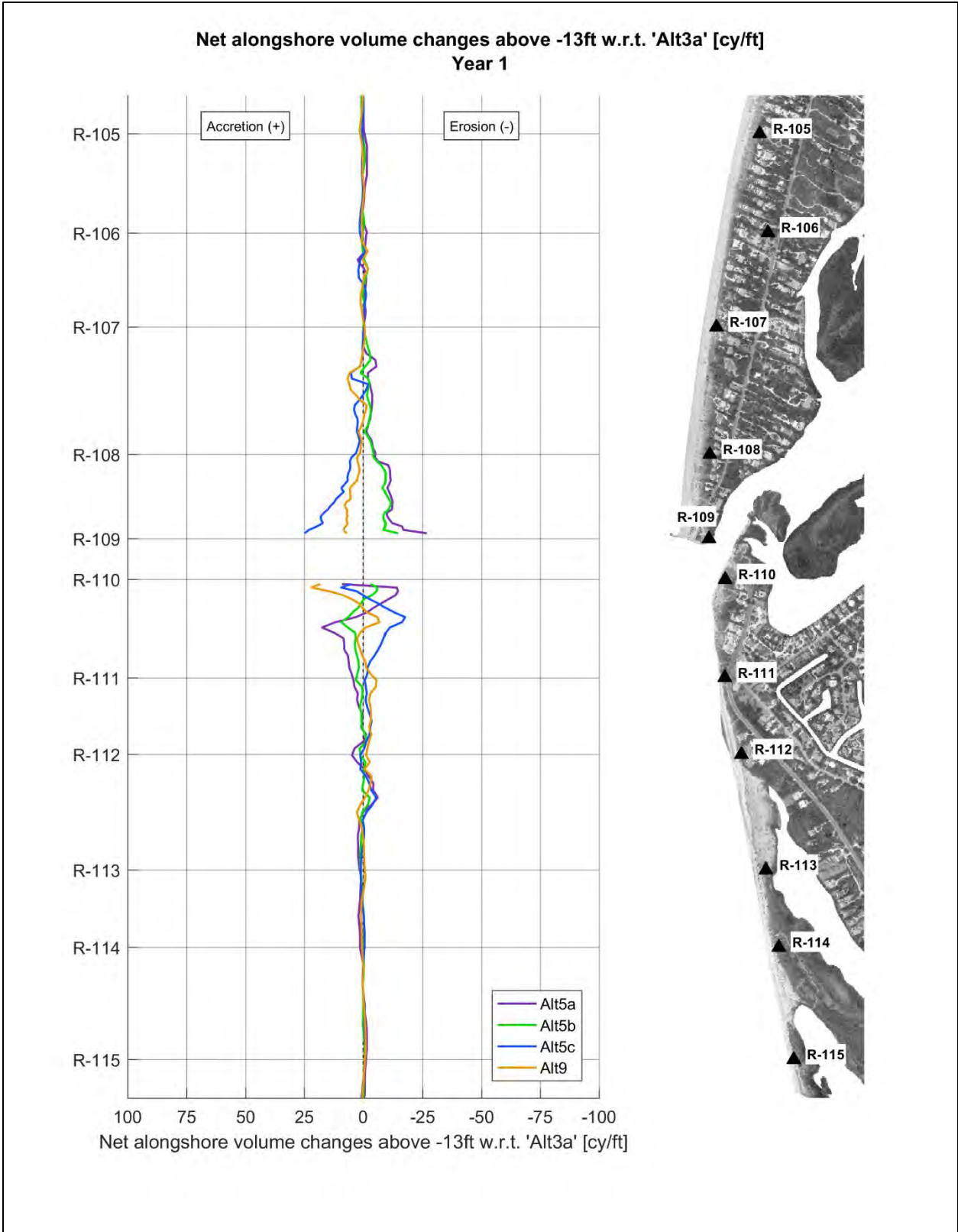


**Figure 4-13: Simulated beach volume changes after 1 year – Blind Pass jetty alternatives.**

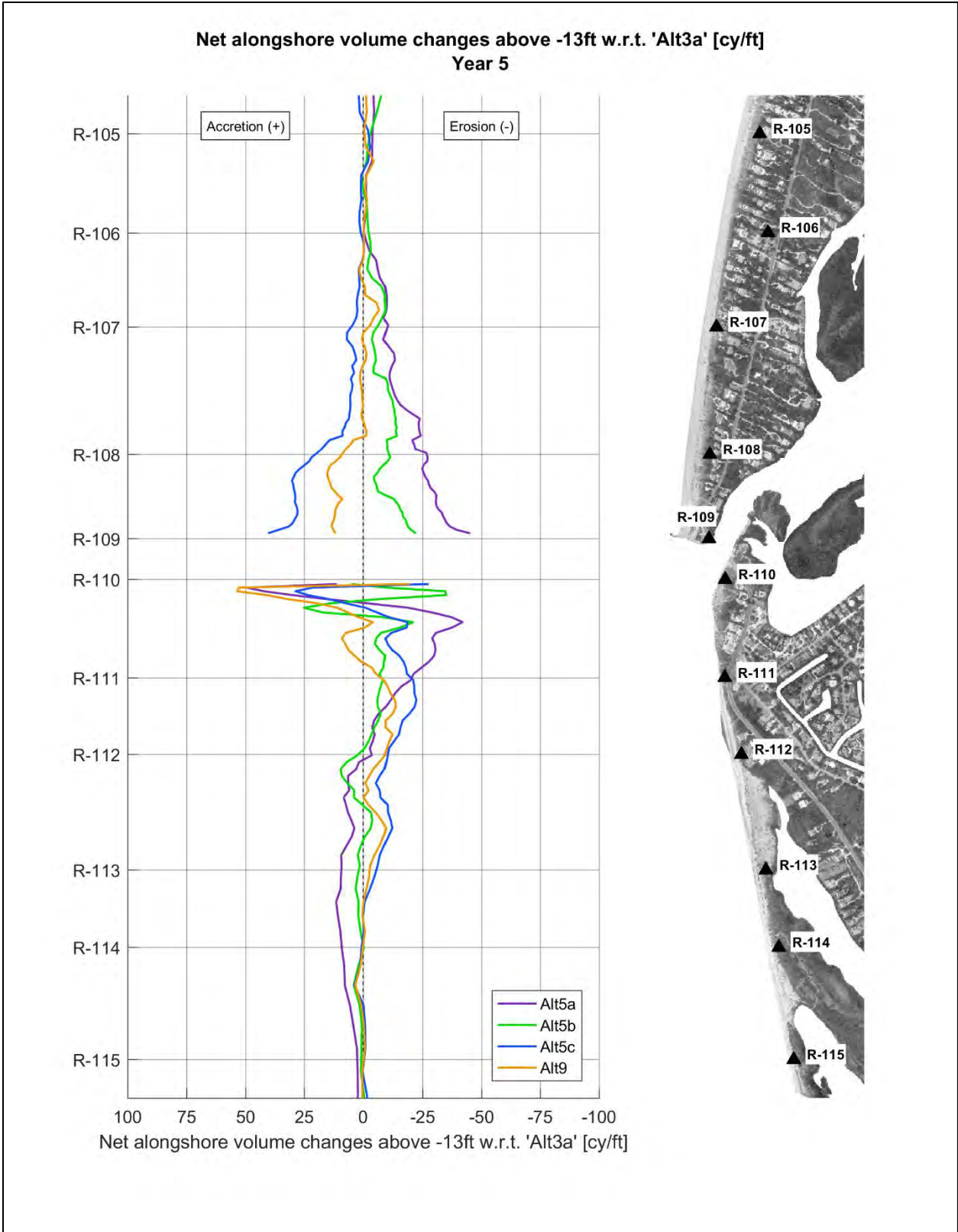


**Figure 4-14: Simulated beach volume changes after 5 years – Blind Pass jetty alternatives.**

The volume changes over time at R-111 indicate that positive effects of Alternatives 5a (jetty removal) and 5b (jetty shortening) occur up to about the third year of simulation. After that, the side effects associated with weakening the inlet prevail. Negative effects of Alternative 5c (jetty lengthening) increase over the simulation period, while the negative effects of Alternative 9 (spur) develop within the first two years and maintain the magnitude through the simulation.

To summarize, both the spur (Alt 9) and lengthening the jetty (Alt 5c) benefit the inlet stability and also the updrift beach on Captiva Island. However, the spur (Alt 9) benefits the inlet stability without having as significant of an effect on the downdrift shoreline as lengthening the jetty (Alt 5c). The jetty removal (Alt 5a) and shortening (Alt 5b) have negative effects on the channel stability and the south end of Captiva Island, although jetty removal (Alt 5a) has some benefit to further downdrift of the inlet on Sanibel Island (south of R-112, after 5 years).

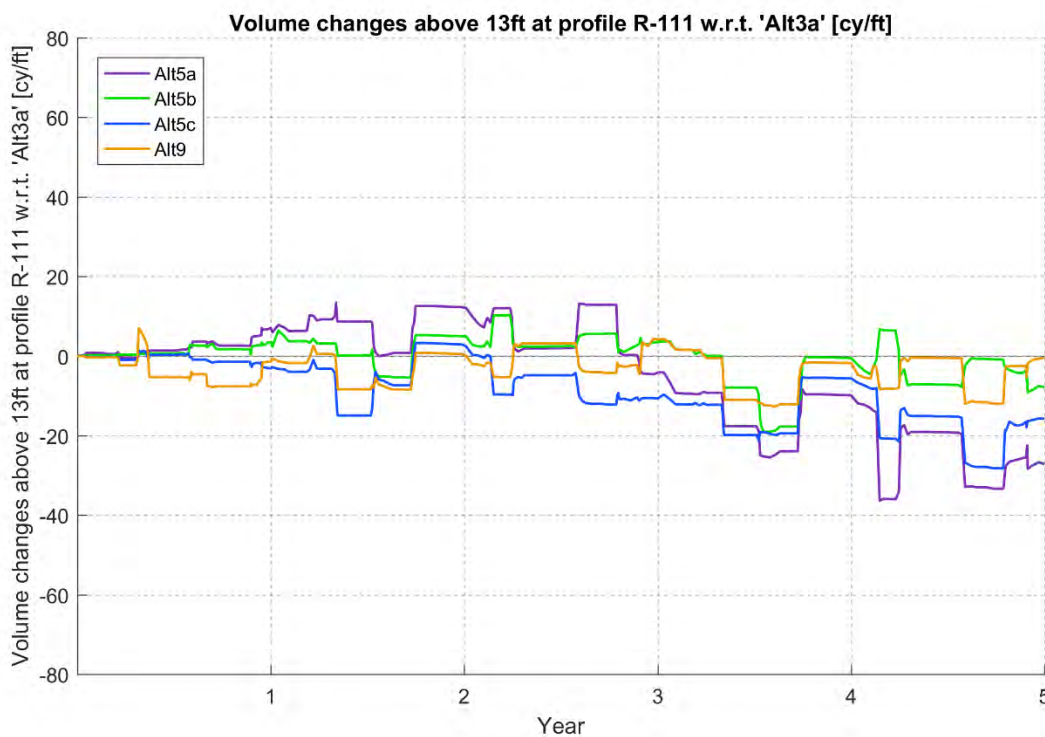


Figure 4-15: Simulated beach volume changes at profile R-111 – Blind Pass jetty alternatives.

#### 4.2.4 Beach Fill Alternatives (6a, 6b, 6c, 6d)

The results for the Beach Fill alternatives are summarized in Figure 4-16 to Figure 4-19. The net bathymetry change maps comparing the final simulated bathymetries (year 5) for each alternative relative to Alternative 3a are given in Sub-Appendix A-2. Net changes with respect to Alternative 3a represent relative effects of the tested design elements on the coastal system. All Beach Fill alternatives consider an initial placement of 102,000 cy. Their general description is listed below.

Baseline Condition: Alt 3a: Blind Pass dredge template (-10 ft NAVD)

- Alt 6a: Alt 3a + Beach fill\*: north end of Sanibel Island (R-110.5 to R-117)
- Alt 6b: Alt 3a + Beach fill\*: south end of Captiva Island (R-102 to R-109)
- Alt 6c: Alt 3a + Beach fill\*: Ebb shoal enhancement
- Alt 6d: Alt 3a + Beach fill\*: Nearshore placement at Sanibel Island (R-110.5 to R-117)

\*Beach fill volume = 102,000 cy for all Alt6 variations.

The Captiva Island beach fill represented by Alternative 6b has the most effect on channel stability compared to the other beach fill alternatives, likely due to the placement of fill updrift in the system, which has a dominant north to south transport. Therefore, the effects are negative, but are relatively small (Figure 4-16). Alternative 6a (beach fill on Sanibel) and 6d (nearshore placement) have smaller effects, which occur mostly after the third year of simulation and are slightly negative. The little to no effect on the cross-sectional area from the Sanibel Island beach fill alternatives are likely due to the limited occurrence of south to north transport over time. Effects of Alternative 6c (ebb shoal enhancement) on channel stability are negligible.

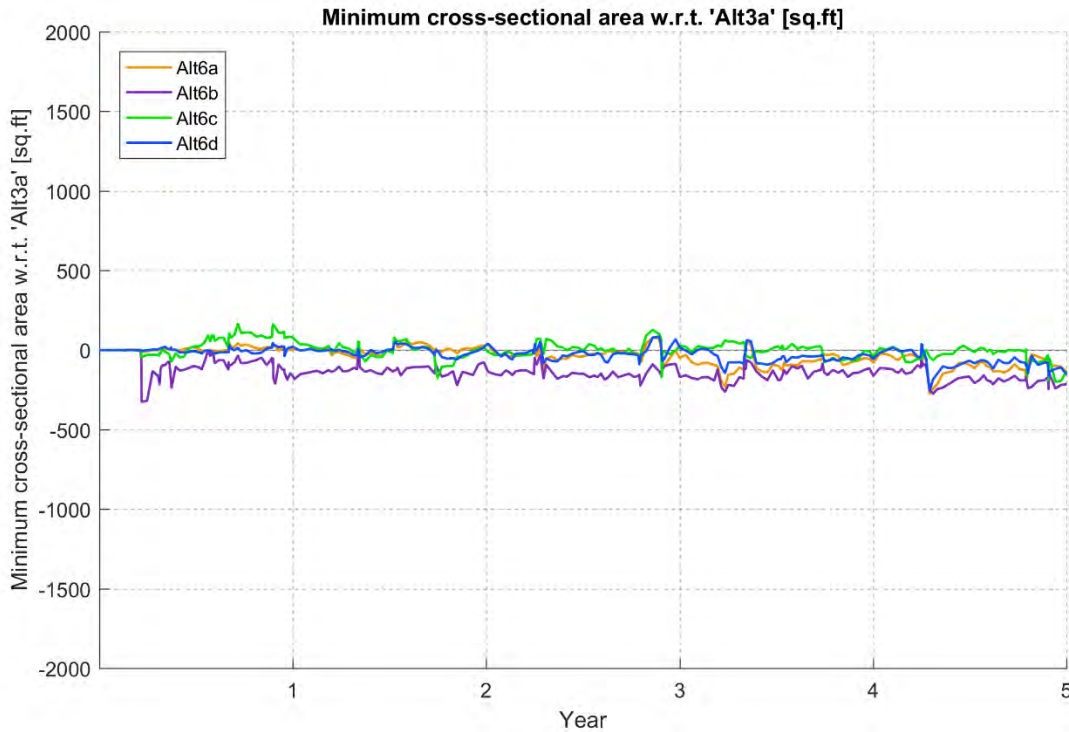
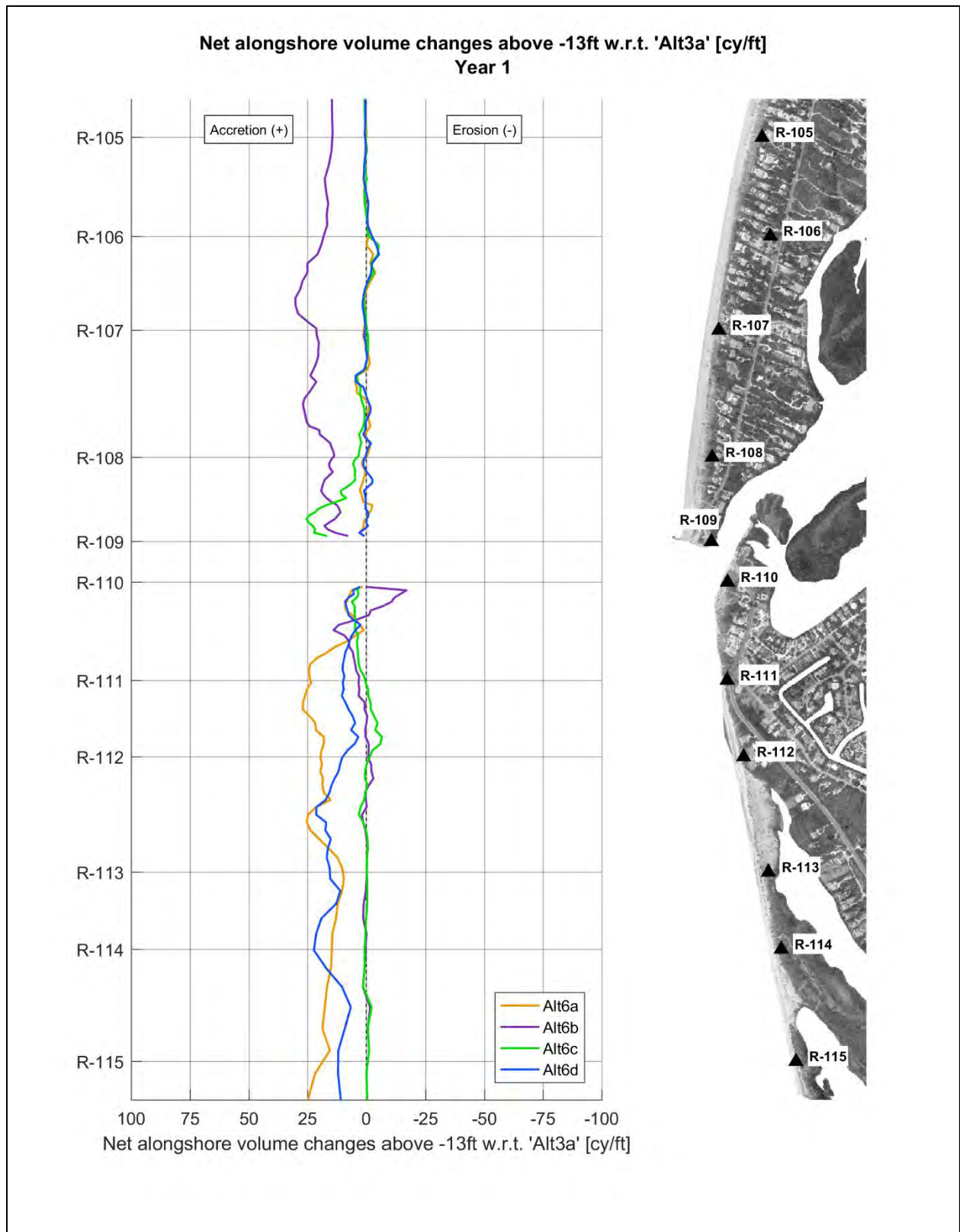
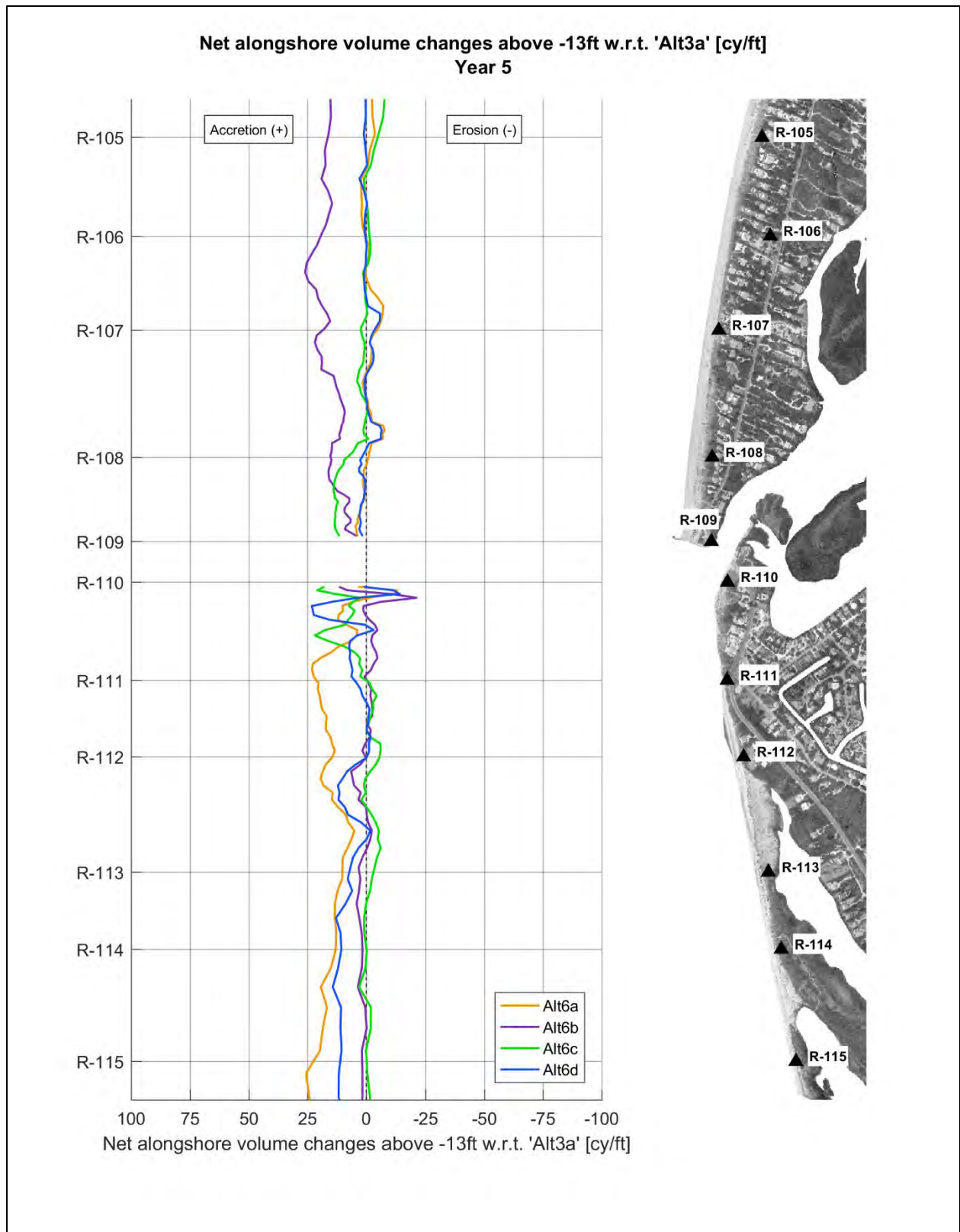


Figure 4-16: Minimum Blind Pass channel cross-sectional area over the simulated period – Beach Fill alternatives.

On both short (1 year) and long term (5 years), the effects of beach fill on the adjacent beaches are generally positive, especially along and adjacent to the fill placement areas (Figure 4-17 and Figure 4-18). For Alternative 6b (Captive Island beach fill), local effects to channel position/migration occur, which are seen as negative effects in the area closer to the inlet (Sanibel Island, north of R-110.5). In the long term, effects of Alternative 6b on Sanibel Island are small. The conventional approach to beach fill, Alternative 6a (Sanibel beach fill), benefits the beaches longer when compared to Alternative 6d (nearshore placement). This is expected since the nearshore fill material is more exposed to the driving transport mechanisms. The effects of Alternative 6c (ebb shoal enhancement) are less pronounced.



**Figure 4-17: Simulated beach volume changes after 1 year – Beach Fill alternatives.**



**Figure 4-18: Simulated beach volume changes after 5 years – Beach Fill alternatives.**

The net volume changes over time at profile R-111 are shown in Figure 4-19. As seen at time 0, the initial distribution of beach fill material differs between Alternatives 6a and 6d; and the initial fill density specifically at R-111 for Alternative 6d is about half of the density associated with Alternative 6a.

Alternative 6a (Sanibel beach fill) provides the most benefit to R-111 as a result of the direct sand placement, which is apparent over the 5-year simulation period. In the first two years, the other alternatives are beneficial as well, and 6d (nearshore Sanibel placement) is more beneficial than 6b (Captiva beach fill) and 6c (ebb shoal enhancement). The performance of Alt 6b, 6c and 6d relative to one another fluctuate after about 2 years. The increasing benefits of Alternative 6b (Captiva beach fill) gradually reduce over after the second year due to the equilibration of the bypassing rate relative to Alt 3a. The effect of Alt 6c (ebb shoal enhancement) fluctuates over time, but is generally positive. Alt 6d (nearshore placement) has an immediate benefit as a result of the direct fill placement, which reduces over the time period due to longshore transport and diffusion of fill material.

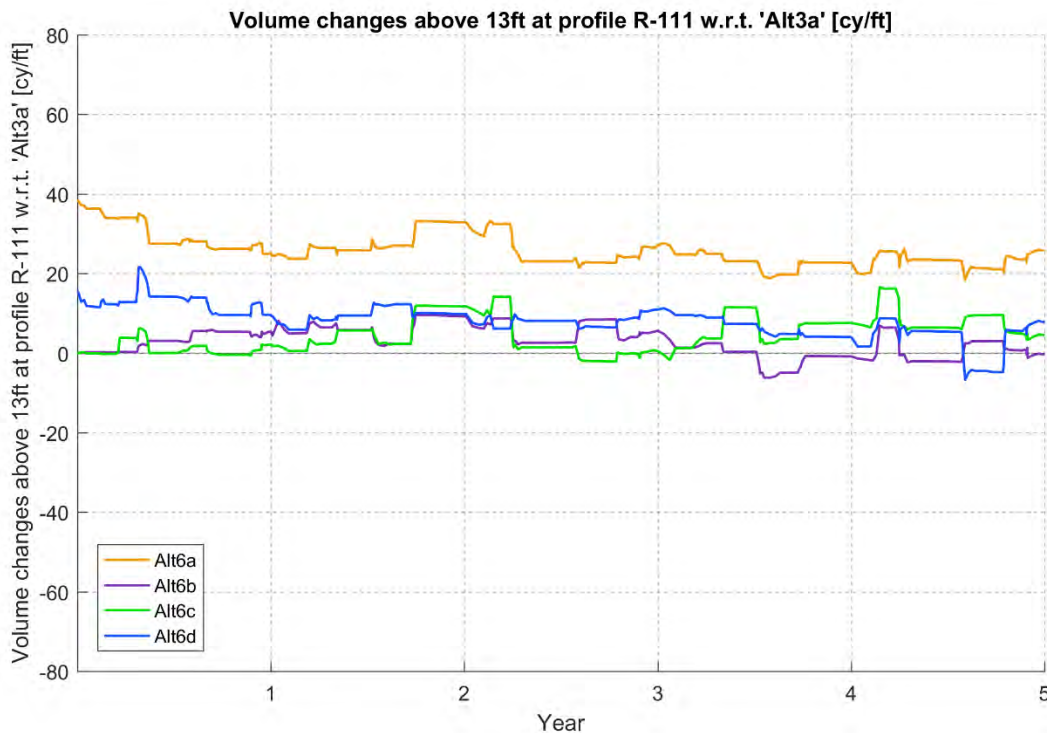


Figure 4-19: Simulated beach volume changes at profile R-111 – Beach Fill alternatives.

#### 4.2.5 Sanibel Structure Alternatives (8b, 8N, 8C, 8S)

The results for the Sanibel Structure alternatives are summarized in Figure 4-20 to Figure 4-23. The net bathymetry change maps comparing the final simulated bathymetries (year 5) for each alternative relative to Alternative 3a are located in Sub-Appendix A-2. Net changes with respect

to Alternative 3a represent relative effects of the tested design elements on the coastal system. The Sanibel Structure alternatives and their general description are listed below.

Baseline Condition: Alt 3a: Blind Pass dredge template (-10 ft NAVD)

- Alt 8b: Alt 3a + Angled (Z) structure on Sanibel Island
- Alt 8South: Alt 3a + Straight structure (tip at similar location as 8b)
- Alt 8Center: Alt 3a + Straight structure north of previous
- Alt 8North: Alt 3a + Straight structure north of previous

The minimum cross sectional area results (Figure 4-20) indicate that Alternative 8North provides benefits to channel stability for about the first year, and the results are negative through the rest of the simulation time. According to the model results, the other variations of Sanibel structures have little to no negative effect on channel stability. The limited effects of these alternatives is likely related to the sediment transport patterns. The net sediment transport in the region is from north to south, and due to the absence of a developed ebb shoal, a transport nodal point is not pronounced in the downdrift side of the inlet. Consequently, after dredging projects, the channel migrates to south. Therefore, a structure on the south side of the inlet would primarily provide a barrier to channel migration and shoreline retreat, but not significantly change the channel's stability. Also, the structures do not provide enough of a constriction to create an ebb tidal jet that would increase the channel's ability to scour and maintain stability.

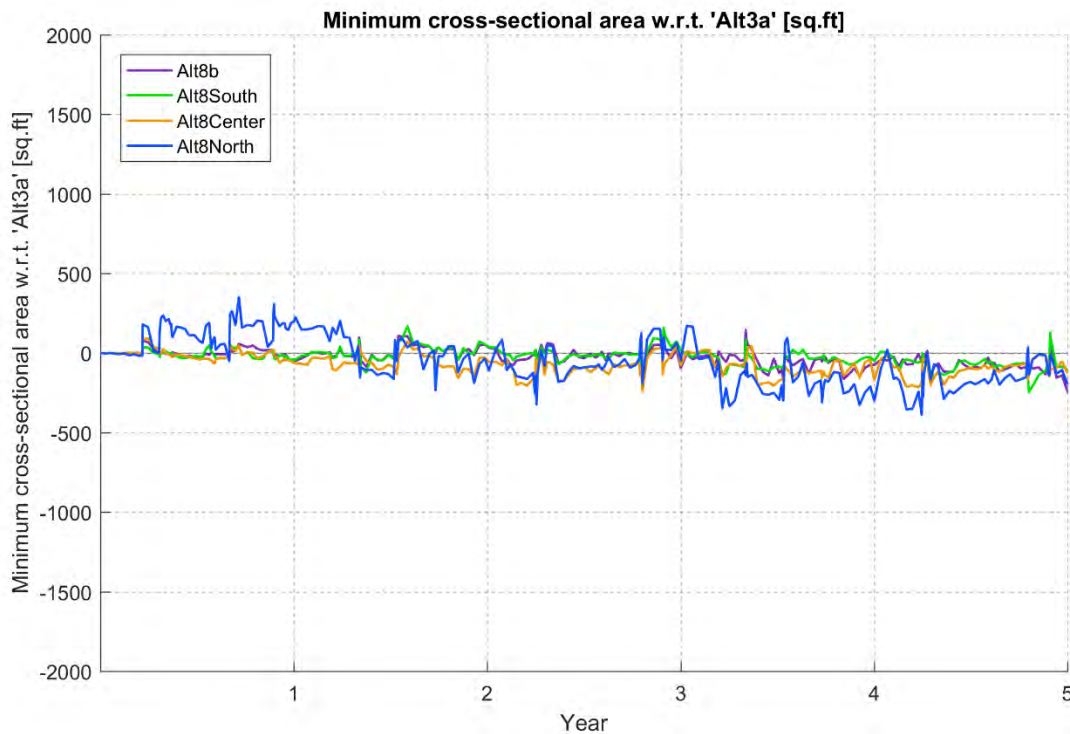


**Figure 4-20: Minimum Blind Pass channel cross-sectional area over the simulated period – Sanibel Structure alternatives.**

Particularly after 5 years, the alongshore curves of net volume changes show a similar pattern: positive effects north of R-110.5 and negative effects between R-110.5 and R-113 (Figure 4-22). The effects are larger for Alternatives 8Center and 8North, relative to Alternative 8b and 8South. This is likely due to the location of Alt 8Center and Alt 8North closer to the inlet.

Accordingly, negative effects are observed in the net volume changes at R-111 over time (Figure 4-23). Effects of Alternative 8b and 8South are less pronounced relative to Alt 8Center and Alt 8North.

The positive effect that occurs near the inlet for all Sanibel Structure alternatives is due to the reduction in both the channel migration to the south and the erosion of its southern margin (i.e. region adjacent to the bridge). Further south, the structures cause downdrift effects on Sanibel Island due to various reasons. The ebb shoal features, although not pronounced in this inlet, are shifted north, and the erosion on the north end of Sanibel is reduced, and therefore reduces the sand supply to other areas downdrift (as observed for Alternative 3a). Also, a stable fillet development associated with the structures does not occur because of the net north to south sediment transport; instead, the response in this area is more typical of coastal structure's downdrift effects and a negative signature occurs.

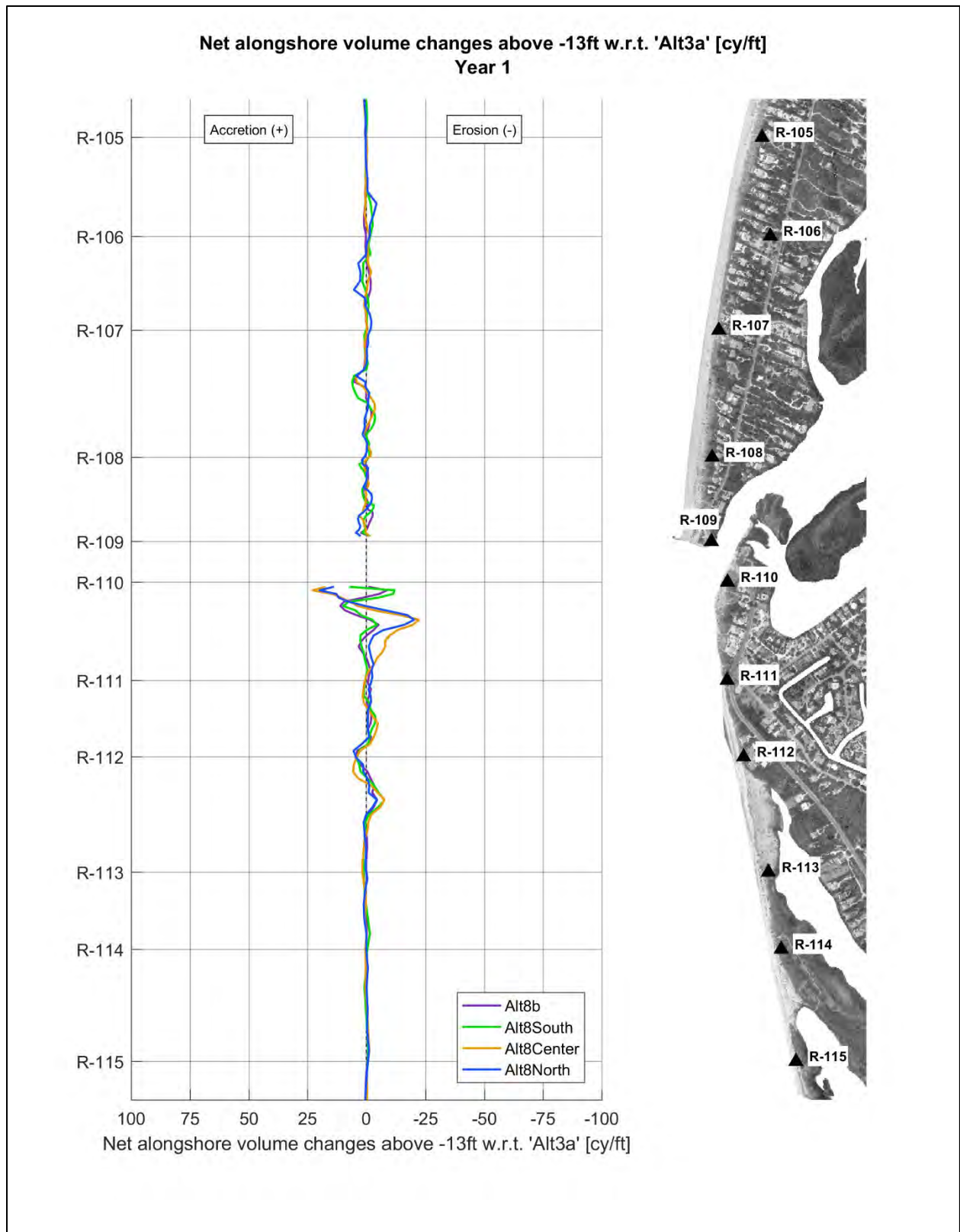


**Figure 4-21: Simulated beach volume changes after 1 year – Sanibel Structure alternatives.**

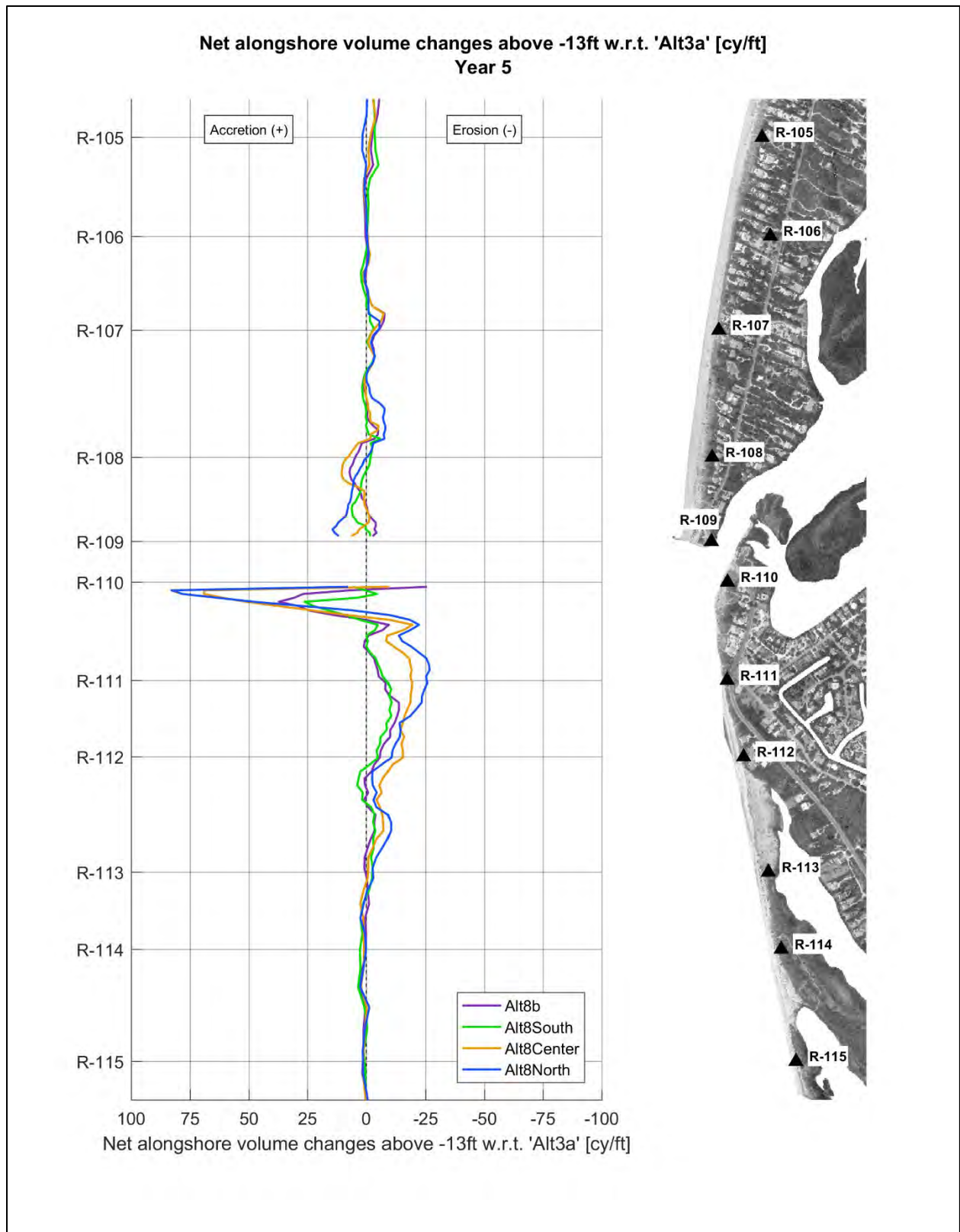


**Figure 4-22: Simulated beach volume changes after 5 years – Sanibel Structure alternatives.**

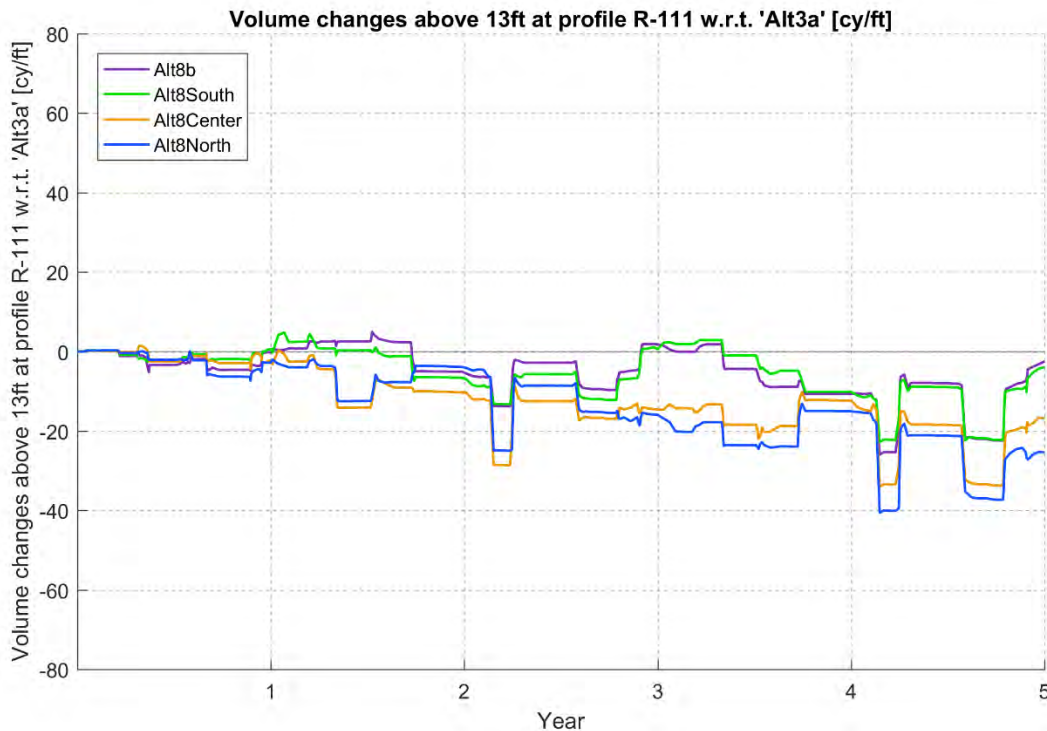


Figure 4-23: Simulated beach volume changes at profile R-111 – Sanibel Structure alternatives.

#### 4.2.6 Preliminary Alternatives Findings

Overall, the model results of the preliminary alternatives suggest the following:

- Dredging through the bypassing bar does not significantly improve the performance of the inlet. Model results indicate that dredging the outer channel section does not directly benefit channel stability, but disrupts the alongshore sediment transport affecting immediately downdrift areas.
- The truncated dredging template partially maintains the bypassing bar, minimizing the negative effects of channel dredging on the downdrift beach (north end of Sanibel Island); however, it has a slightly negative effect on the channel stability.
- Improving the inner tidal connections to Pine Island Sound is beneficial to the stability of the inlet channel due to increased tidal prism. Re-establishing the connection to Sunset Bay was the most beneficial to channel stability.
- Removing, lengthening or shortening the existing Blind Pass jetty significantly effects the distribution of sand through the study area, taking the system out of the quasi-equilibrium state. The effects of each of these alterations to the jetty varies throughout the study area, but all result in an adverse effect on an adjacent shoreline.

- The addition of a southward oriented spur at the tip of the Blind Pass jetty benefits the channel stability by reducing the transport into and sedimentation in the inlet. This is a result of redirecting flow and sediment transport in a more southerly direction past the inlet. After 5 years, this option also provides benefits to the south end of Captiva Island and the north end of Sanibel Island (north of R-111), and as a result, negative effects occur further south between R-111 and R-113.
- The beach fill alternatives provide benefits at the fill areas as a result of the direct placement of material, which expands to adjacent areas over time, particularly downdrift. Conventional placement of fill directly on the beach performed better than nearshore placement or ebb shoal enhancement alternatives.
- The model results indicate that the effect of beach nourishment in south Captiva Island is slightly negative to Blind Pass channel stability, as additional sand is entered into the system updrift that moves down the coast through the pass. The Sanibel Island beach fill alternatives produced only marginal effect to channel stability, likely due to limited periods of south to north sediment transport over time.
- The nearshore sand placement option shows higher diffusion rates compared to the conventional fill placement, as the material is more exposed to the transporting forces.
- The structures tested at the north end of Sanibel Island do not effectively improve channel stability. This is due to a limited influence on the ebb tidal flow to overcome the dominant north to south longshore sediment transport.
- The structures tested at the north end of Sanibel protect the inlet shoreline from channel migration, but have a downdrift effect particularly between R-110.5 and R-112.
- A combination of preliminary alternatives may be necessary to balance and/or combine the effects of individual design features to improve the performance of the inlet and adjacent beaches.

### **4.3 Combined Scenarios**

Several preliminary alternatives identified as positive measures were adapted and combined into three ‘Combined Scenarios’ for comparison of inlet management strategies. The Combined Scenarios are simulated in order to evaluate the collective effects of the multiple design features on the system. The scenarios include combinations of the truncated Blind Pass dredge template, connections to Pine Island Sound, beach fill on Sanibel Island and the spur at the Blind Pass jetty.

The Combined Scenarios include the truncated Blind Pass dredge template to reduce downdrift effects of dredging. The slightly negative effect on channel stability may be moderated and overcome by combination with other alternatives, such as improvements of inner tidal connections to increase tidal fluxes and inlet stability (i.e. the connection to Pine Island Sound through Wulfert

Channel, connection to Pine Island Sounds through Sunset Bay and the spur at the Blind Pass jetty).

The Combined Scenarios include Sanibel Island beach fill. Placing the sand dredged from the inlet downdrift contributes to mitigating the negative effects of channel dredging. From this perspective, fill placement at the north end of Sanibel Island was adopted (R-110.5 – R-112), which is the primarily affected area and also serves as a feeder beach to area further downdrift (south of R-112). For the purposes of this study, conventional beach fill is considered in the combined scenarios due to the performance. However, if higher diffusion rates are acceptable or the dredged material is not suitable for direct placement on the beach, nearshore placement of dredged material may be a viable option.

The specific design features considered in each alternative are listed in Table 4-4, and further detailed below with objective for selecting the features:

**Table 4-4: Design features considered in the Combined Scenarios.**

Design feature	Combined Sc. #1	Combined Sc. #2	Combined Sc. #3
Truncated template	✓	✓	✓
Connection to Pine Island Sound (Wulfert)	✓	✓	✓*
Sanibel Island beach fill	✓	✓	✓
Connection to Pine Island Sound (Sunset Bay)		✓	✓*
Spur at Blind Pass jetty			✓

\* Smaller connection than Combined Sc. #2.

### **Combined Scenario #1:**

---

- **Truncated dredge template:** based on Alt 3c; variable dredging depth at inner channel  
Objective: Maintain the bypassing bar in order to reduce the disruption of the alongshore sediment transport and the negative effects in downdrift beaches
- **Connection to Pine Island Sound (Wulfert Channel extension):** based on Alt 1b; 100 ft wide, 8 ft NAVD deep channel  
Objective: Enhance connection between Blind Pass and Pine Island Sound in order to increase the tidal flux and inlet stability
- **Sanibel Island beach fill:** based on Alt 6a; template between R-110.5 and R-112.5 (60,000 cy, average density of approximately 38 cy/ft)  
Objective: Bypass the dredged material that has accumulated in the channel to the north end of the island creating a buffer to absorb the inlet-induced dynamics

### **Combined Scenario #2:**

---

- **Combined Scenario #1**
- **Connection to Pine Island Sound (Sunset Bay):** based on Alt 4; 75 ft wide channel, transitioning depths from Blind Pass to inland sections (10, 9 and 8 ft NAVD)  
Objective: Unload the restriction in the main inner channel (south of the Roosevelt channel intersection) and reduce hydraulic losses in order to increase tidal flux and inlet stability

### **Combined Scenario #3:**

---

- **Truncated dredge template:** based on Alt 3c; variable dredging depth at inner channel  
Objective: Maintain the bypassing bar, reducing the disruption of the alongshore sediment transport and the negative effects in downdrift beaches
- **Connection to Pine Island Sound (Sunset Bay and Wulfert Channel extension):** based on Alt 1b and 4; narrower channel (20 ft wide), and shallower (-5 ft MLLW, -7.29 ft NAVD) channel  
Objective Enhance connection between Blind Pass and the Pine Island Sound, and therefore the tidal flux and inlet stability
- **Sanibel beach fill:** based on Alt 6a; template moved north and concentrated between R-110.5 and R-112.5 (60,000 cy, average density of approximately 38 cy/ft)  
Objective: Bypass the material accumulated in the channel creating a buffer to absorb the inlet-induced dynamics at the north end of the island
- **Spur at Blind Pass Jetty:** based on Alt 9; shorter structure extension (100 ft long)  
Objective: Redirect flow/sediment transport in a more southerly direction past the inlet, reducing the transport and infilling into the inlet, the channel migration to the south (erosion at Sanibel), and enhancing inlet stability

The initial bathymetry maps for the Combined Scenarios #1, #2 and #3 are given in Figure 4-25 through Figure 4-27 in Section 4.3.2 below.

#### **4.3.1 Baseline for Combined Scenario Comparison: Permitted Template**

The Combined Scenarios are analyzed relative to the ‘Permitted Template’ as the baseline, which is the dredge template and beach fill based on the currently permitted Blind Pass maintenance project. This allows for the comparison of the current project approach in order to identify benefits or adverse effects in making alternations to the design. The modeled Permitted Template is described below:

- Variable channel depth: 10 ft NAVD at seaward to middle section, transitioning to 9 and 8 ft NAVD at inner sections (closer to the intersection with the Roosevelt Channel).
- Inclusion of beach fill: the 90,000 cy from the dredge template (based on initial bathymetry) is split between the north and south fill areas. 70,000 cy were placed between R-112 to R-114+200 (average density of approximately 34 cy/ft); 20,000 cy between R-116 to R-118. The south fill area is located out of the morphology model boundaries and therefore was not included in the simulation.

Note that the differences between the permitted template and Alternative 3a (used as baseline for comparisons of preliminary alternatives) are the variable dredging depth and the inclusion of the beach fill.

The initial bathymetry for the Permitted Template scenario are shown in Figure 4-24.

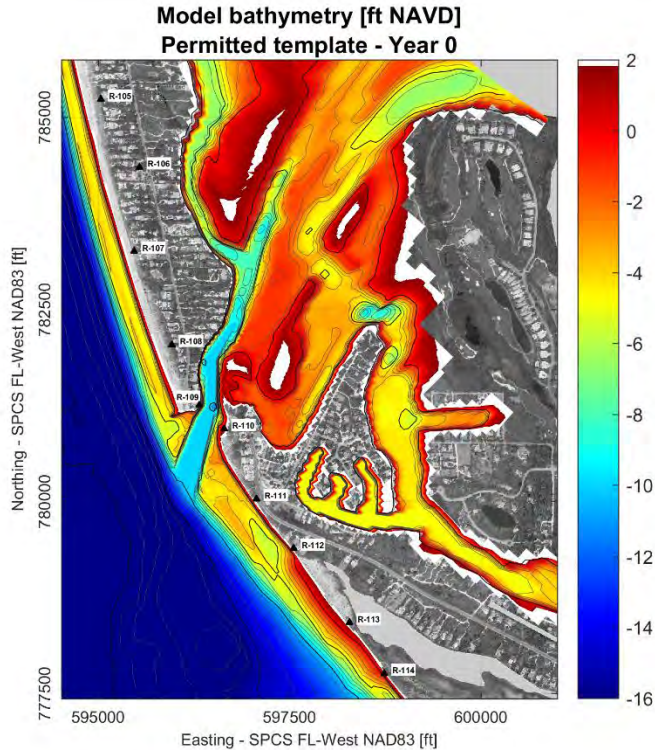


Figure 4-24: Initial bathymetry for the Permitted Template.

### 4.3.2 Average Conditions (5-years)

The initial bathymetry maps for the Combined Scenarios #1, #2 and #3 are given in Figure 4-25 through Figure 4-27. The modeled changes relative to the baseline condition (Permitted Template) are presented herein.

The effect of the Combined Scenarios on sedimentation/erosion in the system compared to the effect of the Permitted Template based on the model results is represented in Figure 4-28. The figure shows the differences between the final bathymetry of the Combined Scenarios and the Permitted Template after 5 years of simulation. Positive changes (warm colors) indicate that the Combined Scenario is shallower than Permitted Template; negative changes (cool colors) indicate that the Combined Scenarios is deeper than Permitted Template. The most pronounced effect of all of the Combined Scenarios is the deepening of Blind Pass (near the bridge) and the enhancement of the ebb shoal feature seaward of the dredge template. The inner section of the extended channels remain deeper than the Permitted Template after five years of simulation. These effects are directly related to the increased tidal prism due to improved connections to inner water bodies. The largest system response is seen with Combined Scenarios #2 and #3, due to re-establishing the connection to Sunset Bay which creates an additional path for tidal flows, increasing tidal fluxes and inlet stability.

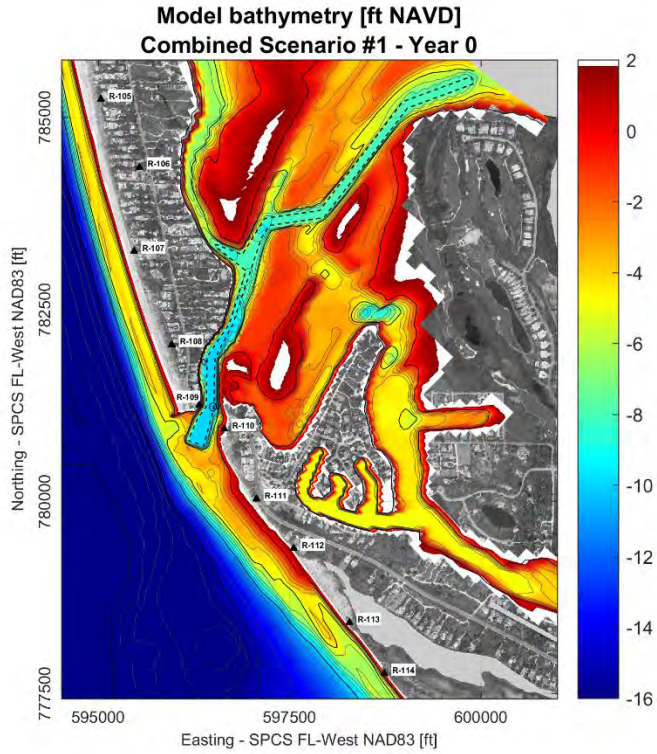


Figure 4-25: Initial bathymetry given the Combined Scenario #1 (Dashed line represents dredge template boundary).

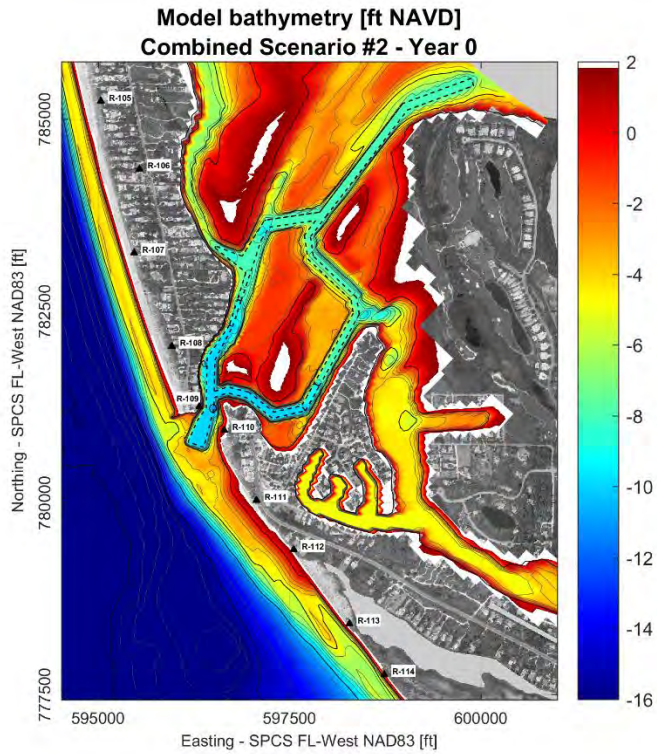
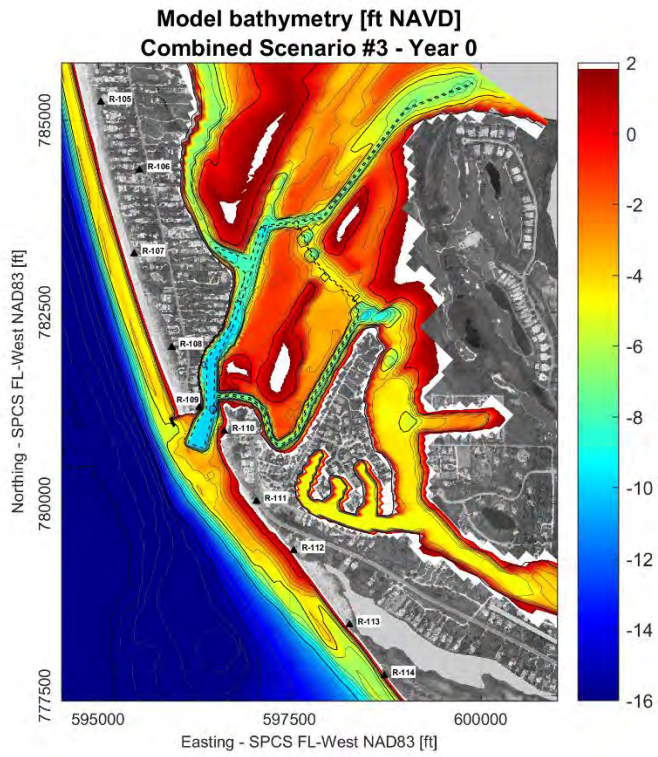
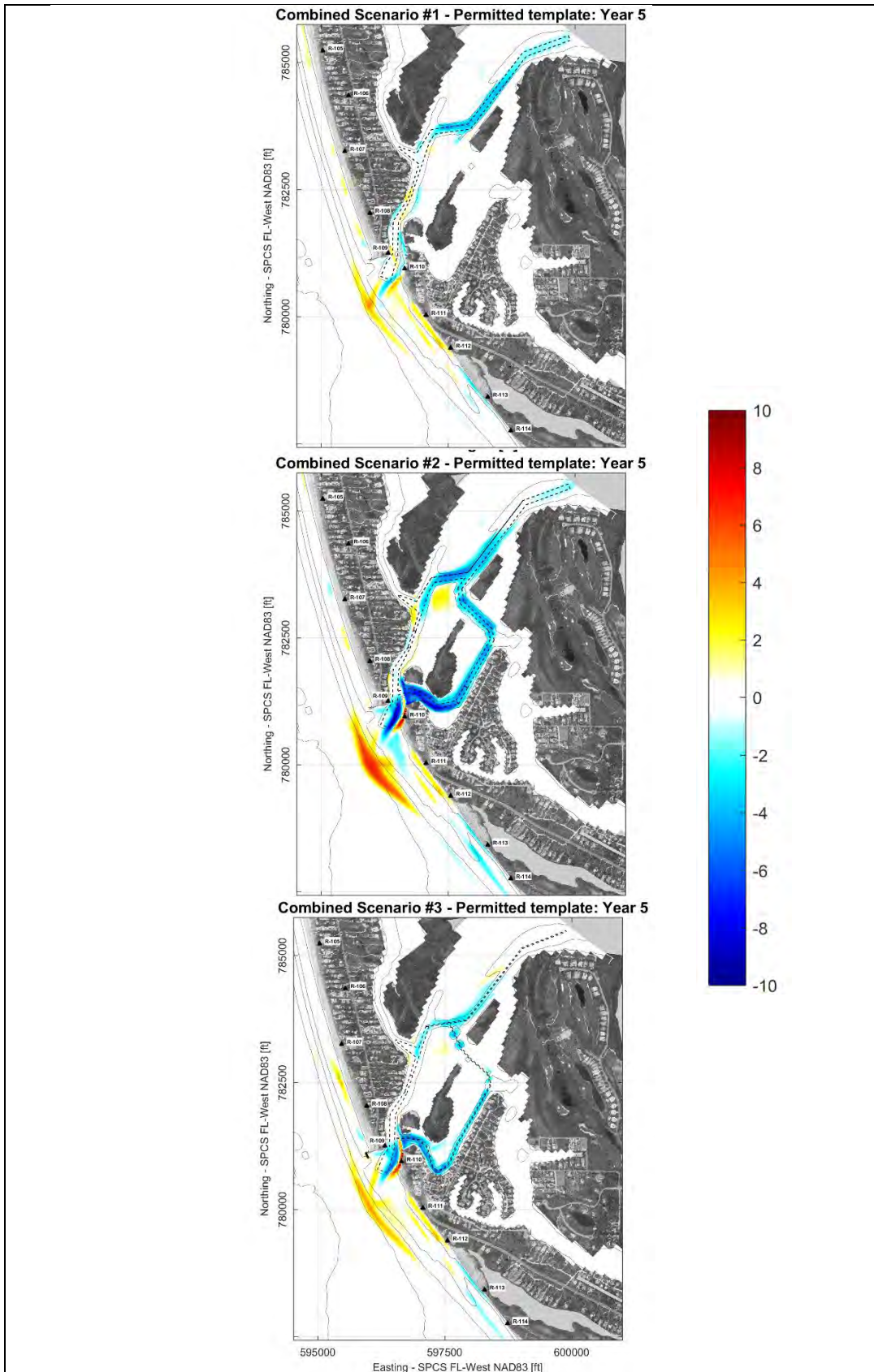


Figure 4-26: Initial bathymetry given the Combined Scenario #2 (Dashed line represents dredge template boundary).

boundary).



**Figure 4-27: Initial bathymetry given the Combined Scenario #3 (Dashed line represents dredge template boundary).**



**Figure 4-28: Net bathymetry changes relative to Permitted Template after 5.**

For Combined Scenarios #2 and #3, model results indicate erosion of the interior channel shoreline where the connection to Sunset Bay intersects the Blind Pass main channel, in the southern (Sanibel) side of the inlet just north of the bridge (Figure 4-28).

The influence of the Combined Scenarios on the stability of the Blind Pass channel is shown by comparing the changes in the minimum cross-sectional area of the channel over the simulation time (Figure 4-29). The minor positive effects associated with Combined Scenario #1 are mainly related to the channel extension north towards Pine Island Sound through Wulfert Channel. These relatively small benefits were already expected based on the results for the initial alternative simulations, which indicated that the dredging template extension through the Wulfert Channel by itself is slightly beneficial. The truncated channel and beach fill moderates those benefits to some extent, which is supported by the slight negative effects observed for Alternatives 3c and 6a (see Preliminary Alternatives Section 4.2).

The connection through Sunset Bay included in Combined Scenario #2 results in the largest increase in the channel cross-sectional area for the modeled scenarios (Figure 4-29). For this scenario, the equilibrium cross-sectional area after the second year is nearly twice as large as the Permitted Template simulation (increase of approximately 900 sq. ft. over an approximately 1000 sq. ft. cross-section from Figure 4-4). In the Combined Scenario #3, the inner connections were scaled down in terms of channel width and depth, and the spur was added to the Blind Pass jetty. The resulting effect on the cross-sectional area is in between that of the Combined Scenarios #1 and #2.

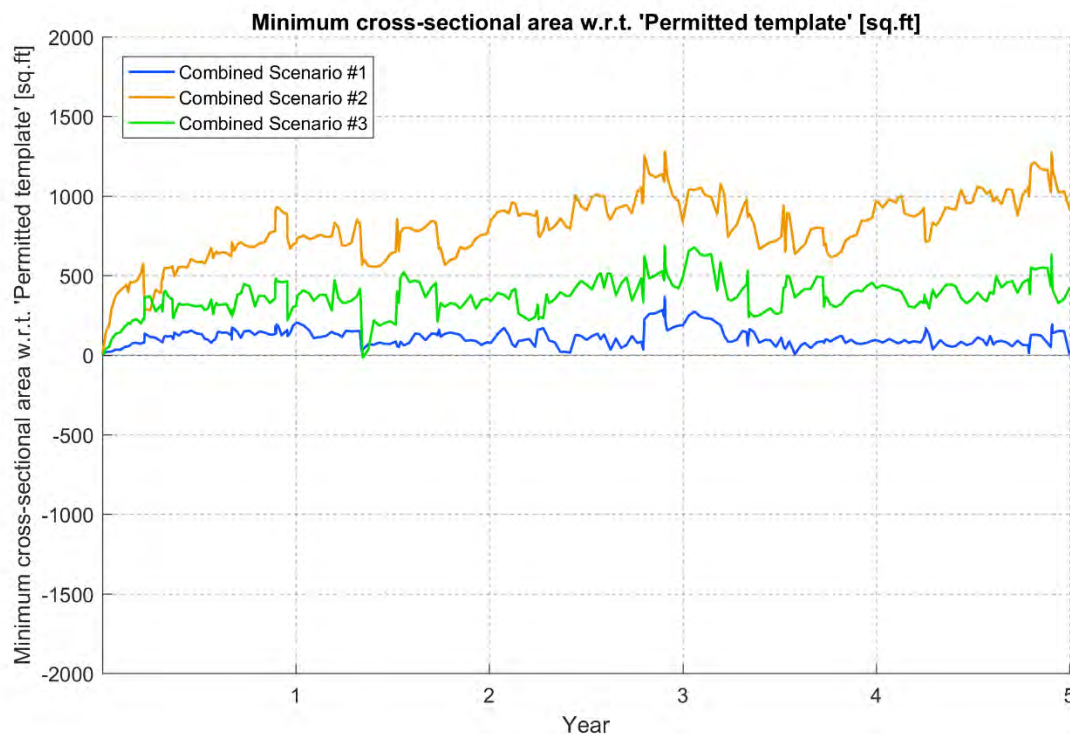


**Figure 4-29: Minimum Blind Pass channel cross-sectional area over the simulated period – Combined Scenarios.**

The influence of the Combined Scenarios on the adjacent beaches is shown in Figure 4-30 and Figure 4-31, the net alongshore volume changes after 1 and 5 years of simulation. The Combined Scenarios do not substantially affect the south end of Captiva Island. The changes in beach erosion/accretion relative to the Permitted Template are primarily on Sanibel Island and are related to the channel truncation (reducing downdrift effects) and the location of the beach fill. All Combined Scenarios have a truncated template, whereas the Permitted Template cuts through the bypassing bar. Also, the Combined Scenarios place fill further north than the Permitted Template to mitigate the immediate downdrift effects from the inlet. For the Permitted Template, 70,000 cy are initially placed between R-112 and R-114 (average density of approximately 34 cy/ft). In the three Combined Scenarios, 60,000 cy are initially placed between R-110.5 and R-112.5 (average density of approximately 38 cy/ft). Relative to the Permitted Template, this offset creates an initial benefit at the north end of Sanibel Island and negative result between R-112.5 and R-114.

After one year of simulation, overall alongshore patterns are similar between the Combined Scenarios, with relatively small differences near the inlet related to the ongoing system response to the different tidal prisms (Figure 4-30). After 5 years, the overall shape of the curve is maintained, but the effects of the enhancement of the ebb shoal are more prominent between R-110.5 and R-112 (Figure 4-31). As the ebb shoal growth draws sand from the system, it affects the overall sediment transport and leads to negative effects south of R-112. Because the Combined Scenarios and the Permitted Template consider approximately the same volume of fill, but placed at different locations, the benefits north of R-112.5 are somewhat counter-balanced by negative effects south of R-112.5.

The volumetric buffer provided by the beach fill at R-111, along with the truncated template, provide a benefit for the three Combined Scenarios (Figure 4-32). The benefits increase over time for the Combined Scenario #2 due to ebb shoal growth, are relatively stable for Combined Scenario #3, and slightly reduce for Combined Scenario #1.

Additional plots of net volume changes relative to the Permitted Template over the 5 year simulation period for profiles R-110.5, R-112 and R-113 are provided in Sub-Appendix A-4.

In general, the model analyses indicates that Combined Scenario #2 has the most pronounced effect on the system, followed by Combined Scenario #3, then Combined Scenario #1.

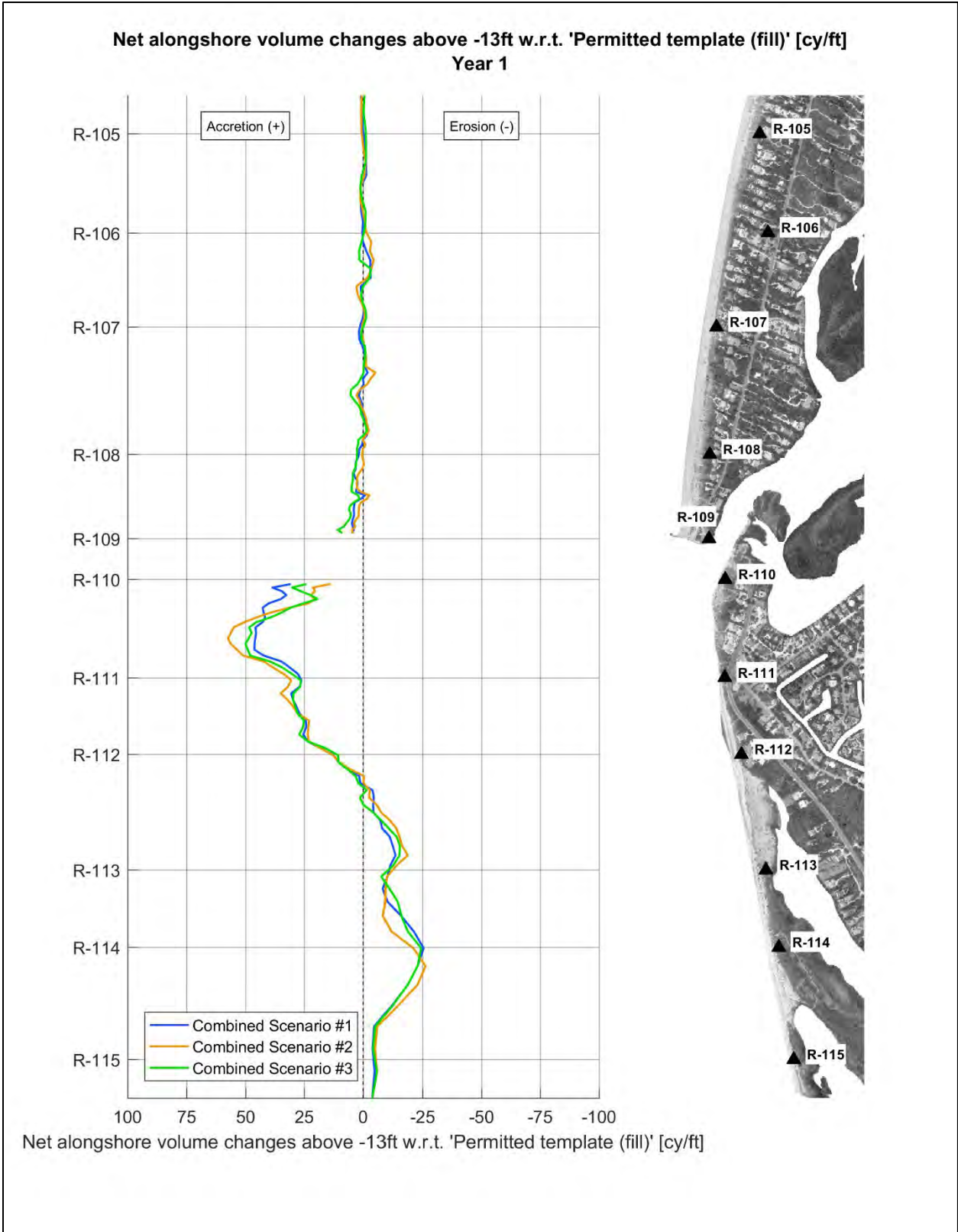


**Figure 4-30: Simulated beach volume changes after 1 year – Combined Scenarios.**

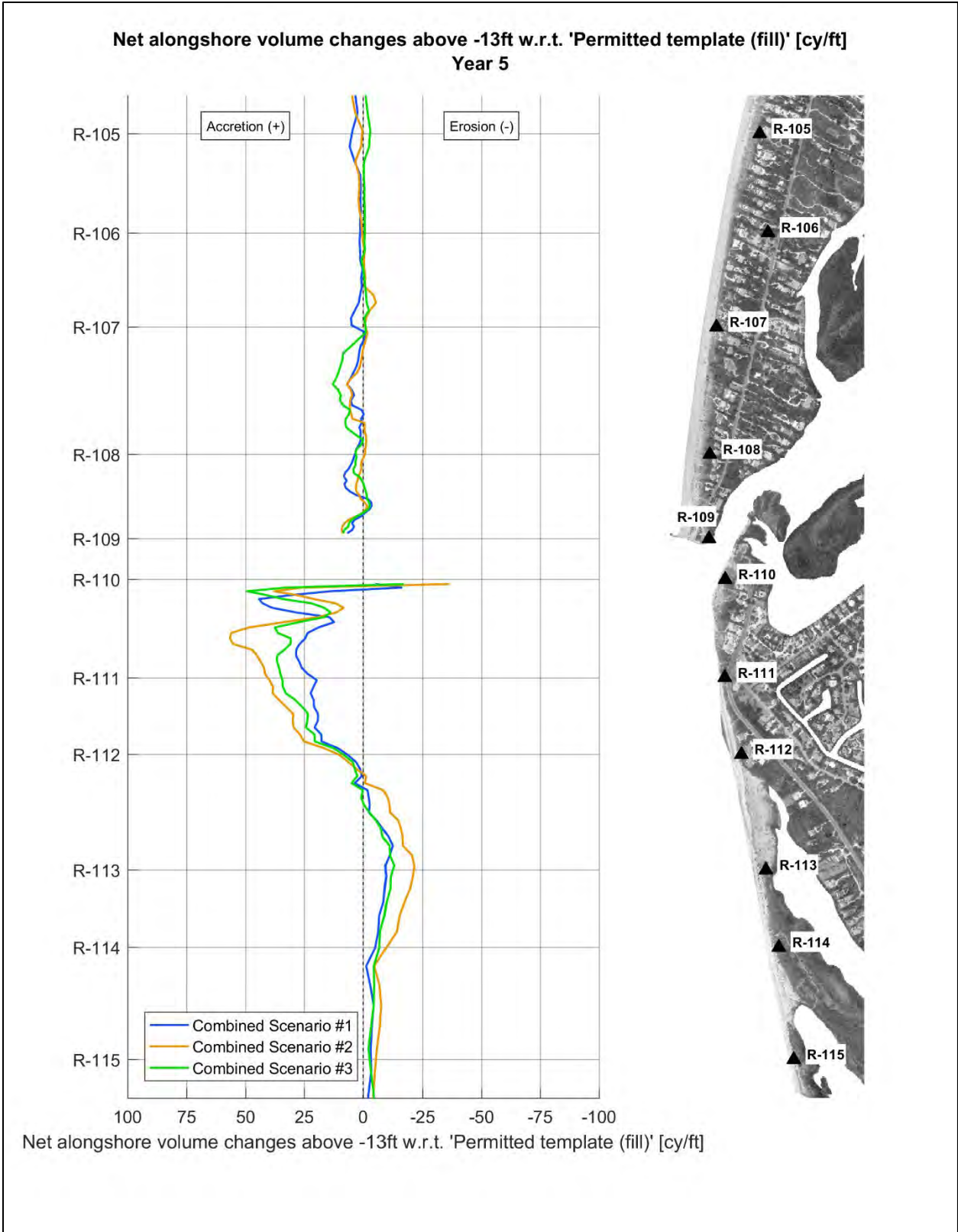


**Figure 4-31: Simulated beach volume changes after 5 years – Combined Scenarios.**

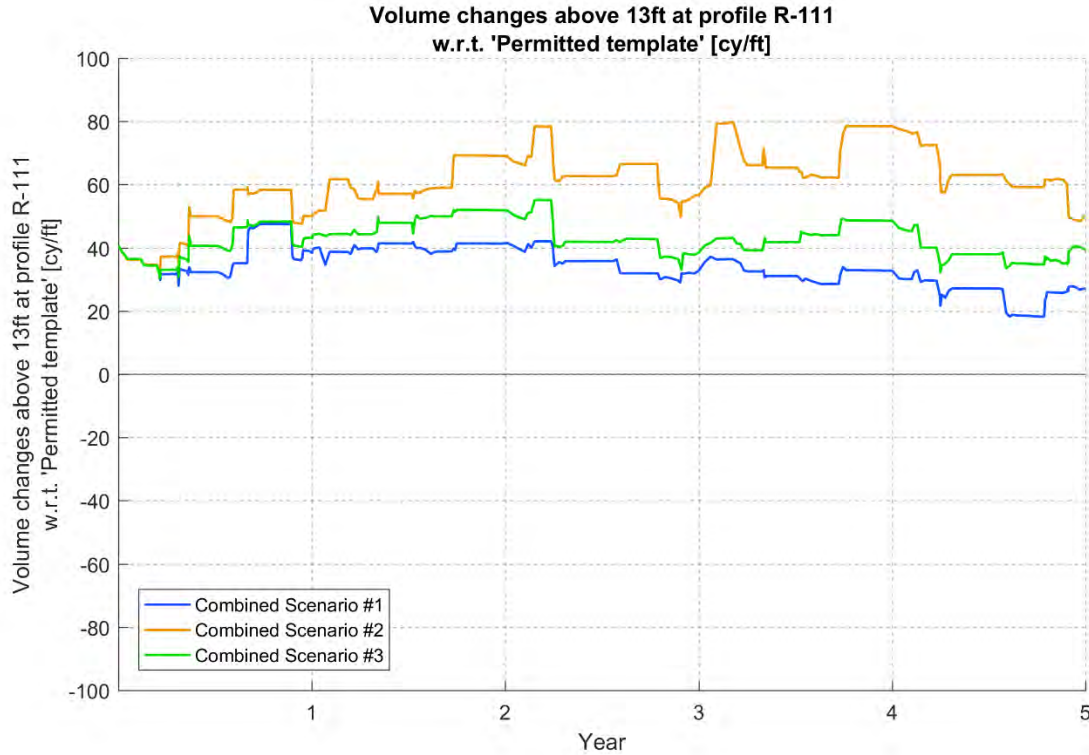


**Figure 4-32: Simulated beach volume changes at profile R-111 – Combined Scenarios.**

### 4.3.3 Storm Conditions

Two short-term simulations were performed to evaluate the performance of the Combined Scenarios under specific storm conditions: 2016 Cold Front and 2004 Hurricane Charley. Detailed discussion on model setup and results are provided in Sub-Appendix A-5.

In summary, the cold front is an energetic, but relatively small event that caused isolated changes and had a similar effect on the scenarios. Under all scenarios including No Action, the cold front effects are seen seaward of the bridge (outer section of the channel) and downdrift. The truncated template remains deeper than the permitted dredge template. The bypassing bar feature of the truncated template results in benefits downdrift and does not affect the channel stability under cold front conditions.

Hurricane Charley is an extreme event (Category 4) with the capability to cause widespread changes that caused effects throughout the entire domain, and had a similar effect on the scenarios. The effects of the storm overwhelm the incremental changes compared to the permitted template (especially between Combined Scenarios #2 and #3). Under all scenarios including No Action, Charley scours the channel. The cross-sectional area of the channel increases by double or more.

The main findings from these simulations are listed below.

### 2016 Cold Front:

- The cold front causes a similar effect on the system as the average conditions but on a more accelerated timeline.
- Significant accretion occurred in the outer channel section of the Permitted Template during the cold front.
- The cold front effects on the inlet's minimum cross-sectional area (near the bridge) and especially the inner channel sections (landward of bridge) were small.
- The infilling of the outer section of the Permitted Template draws sand from the natural littoral drift, resulting in proportional negative effects at immediate downdrift areas (R-110 to R-112). Net negative effects are indicated by the model in the north end of the island.
- The truncated template and the beach fill relocation northward (between R-110.5 and R-112.5), both included in all Combined Scenarios, minimize the downdrift negative effects of outer channel accretion and provide additional buffer for erosion, considerably improving the condition of the north end of the island as compared to the Permitted Template. The shift of the beach fill results in net negative effects south of R-112.5, although beach fill diffusion to the south over time is expected.
- Model results indicate that, under the specific simulated conditions, the truncated channel template does not interfere with the controlling cross-sectional area of Blind Pass, but minimizes downdrift effects associated with channel dredging. In other words, dredging the outer channel section disrupts the alongshore sediment transport affecting immediate downdrift areas and does not directly benefit channel stability.

### 2004 Hurricane Charley:

- Model results of Hurricane Charley simulations show significant storm impacts to both beach and channel areas. This applies for all simulated scenarios (No Action, Permitted Template, and Combined Scenarios #1, #2 and #3).
- Model results indicate that beach areas are affected by the combination of extreme waves and positive storm surge.
- The discharges associated with Hurricane Charley caused significant channel scour, on the order of 10 ft. This process is increased in the Combined Scenarios due to enhanced connections to inner water bodies.
- The effect of channel scouring is supported by the effect of historic storm events on Blind Pass. The channels are primarily affected by extreme discharges due to sharp water level changes induced by winds and storm surges. The existence of the connections between water bodies concentrates flows and enhances channel scour.
- The truncated template affects the location of the outer channel developed during the storm, resulting in a northward shift.
- The northward location of the beach fill in the Combined Scenarios as compared to the Permitted Template provided additional protection for the region adjacent to profile R-111, where the Sanibel Captiva Road is closer to the shore. Negative net effects occur south of this area at the permitted beach fill location (R-112 to R-114+200). Other beach areas are not affected by the Combined Scenarios, meaning the storm effects are equally extreme.

#### 4.3.4 Combined Scenario Findings

Overall, the model results of the Combined Scenarios relative to the Permitted Template suggest the following:

- The most pronounced effect of all of the Combined Scenarios is the deepening of Blind Pass (near the bridge) and the enhancement of the ebb shoal feature seaward of the dredge template.
- The largest system response is seen with Combined Scenarios #2 and #3, due to re-establishing the connection to Sunset Bay which creates an additional path that is created for tidal flows, increasing tidal fluxes and inlet stability.
- Negligible effects occurred on the south end of Captiva Island.
- The scenarios benefit the Blind Pass channel, which remains larger after simulation.
- The scenarios had mixed effects on Sanibel Island, which are seen in the model results by changes in erosion/sedimentation patterns.
  - Reduced channel migration to the south (near R-110, immediately southwest of the bridge).
  - Erosion just northeast of the bridge when connections to Sunset Bay are made (Combined Scenarios #2 and #3).
  - Benefits at the north end between R-110 and R-112.5 in the short term (~1 year) related to the beach fill and truncated channel, and longer term (5 years) due to the enhanced channel stability and ebb shoal persistence/build-up.
  - Benefits north of R-112.5 are somewhat counter-balanced by negative effects south of R-112.5, because the Combined Scenarios and the Permitted Template consider approximately the same volume of fill, but placed at different locations.

## 5. MODELING SUMMARY AND FINDINGS

To assist in the formulation of a management plan for Blind Pass, the Delft3D-FLOW and Delft3D-WAVE (SWAN) models were applied. These models were utilized to examine wave propagation, flow patterns, sediment transport, and morphology changes given the existing conditions and a number of potential alternatives. The designed alternatives focused on balancing the sediment budget of the inlet and adjacent beaches, improving the performance of channel maintenance projects and the stability of the north end of Sanibel Island.

The Delft3D modeling package was setup using a large collection of survey data from APTIM, FDEP, NOAA, and USACE. Grids were delineated to examine wave propagation and flow on both a regional and local basis. Wave propagation within the SWAN model was calibrated using measured wave data, regional wind fields, and recently collected wave measurements between December 11<sup>th</sup> 2015 and January 27<sup>th</sup> 2016 close to the pass. Currents and water levels within the Delft3D-FLOW model were calibrated using water level and current measurements collected during the same period, along with data summarizing the extent of the submerged aquatic vegetation near Blind Pass. Finally, sediment transport, erosion, and deposition were calibrated using the 2009 and 2012 Blind Pass channel and beach surveys, concurrent wave and wind data, and numerous test runs to examine the most appropriate values of the tidal amplitude, sediment transport and morphology coefficients.

Following the calibration effort, the Delft3D modeling package was applied to evaluate various alternatives. The effects on morphology was analyzed for each alternative. First, 19 preliminary alternatives including No Action were designed to evaluate the individual performance of different alternative components to channel stability and the adjacent beaches. The preliminary alternatives included dredging, beach fill, modifications to the existing Blind Pass jetty, and structures at the north end of Sanibel Island. These alternatives were simulated under average conditions (5 year simulation period).

Based on the results for the preliminary alternatives, three Combined Scenarios were developed. The Combined Scenarios were simulated under average conditions (5 years) and under two different storm conditions (2004 Hurricane Charley and 2016 Cold Front).

The summarized findings of the modeling effort are:

- Dredging Blind Pass creates immediate downdrift effect on Sanibel Island. This is specially related to the outer channel section across the shallow bypassing bar. A major part of dredging volume is excavated from the outer section, which infills at faster rates relative to inner sections.
- From an inlet performance standpoint, dredging through the bypassing bar does not result in significant improvements.
- The truncated template partially maintains the natural bypassing bar, and reduces the disruption of sediment transport, and therefore reduces the negative effect on the downdrift beaches that occur after dredging; however, it has a slight negative effect on the channel stability. This can be moderated or overcome by combination with other alternatives.

- Bypassing the material that accumulates in the channel to the north end of Sanibel Island creates a buffer to absorb the inlet-induced dynamics at the north end of the island.
- The beach fill alternatives provide benefits at the fill areas as a result of the direct placement of material, which expands to adjacent areas over time, particularly downdrift (south). Conventional placement of fill directly on the beach performed better than nearshore placement or ebb-shoal enhancement alternatives.
- The nearshore sand placement option shows higher diffusion rates compared to the conventional fill placement, as the material is more exposed to the transporting forces. If higher diffusion rates are acceptable or the dredged material is not suitable for direct placement on the beach, nearshore placement of dredged material may be a viable option.
- The effect of beach nourishment in south Captiva Island is slightly negative to Blind Pass channel stability, as additional sand is entered into the system updrift that moves down the coast through the pass. The Sanibel Island beach fill alternatives produced only marginal effects to channel stability, likely due to limited periods of south to north sediment transport over time.
- Enhancing the connection between the Gulf of Mexico and Pine Island Sound by extending the channel template north through Wulfert Channel and more so by re-establishing the connection to Sunset Bay, increases the tidal flux, and therefore the inlet stability.
- Removing, lengthening or shortening the existing Blind Pass jetty significantly effects the distribution of sand through the study area. The effects of each of these alterations to the jetty varies throughout the study area, but all result in an adverse effect on an adjacent shoreline.
- The influence of a jetty structure on the north end of Sanibel Island has little effect on the channel stability. The structure would function as a revetment to protect the north end from erosion during channel migration and stabilize the north end of Sanibel in times of fluctuations in channel location. However, a downdrift effect would be expected particularly between R-110.5 and R-112.
- A spur at the end of the Blind Pass jetty enhances channel stability. The spur redirects some flow (and sediment transport) away from the inlet, thereby reducing channel infilling and migration to the south.
- The beach fill placement zone can be optimized based on erosion signature.
- The Combined Scenarios relative to the Permitted Template have negligible effects on the south end of Captiva Island, benefit the channel stability as a result of improved tidal exchange, and have mixed effects on Sanibel Island, shown by the changes in erosion/sedimentation patterns. In general, the effect of Combined Scenario #3 on the system lies between Combined Scenarios #1 and #2.
- Storms can have a variety of effects on Blind Pass. Storms may cause infilling and/or scour.

The findings of both the preliminary alternatives and the Combined Scenarios analyses are used to support the overall findings of the study and the inlet management recommendations presented in the main study text. The results of this numerical modeling study should be used in conjunction with other coastal engineering assessments and prudent engineering judgment. Further engineering is recommended prior to implementation.

## 6. REFERENCES

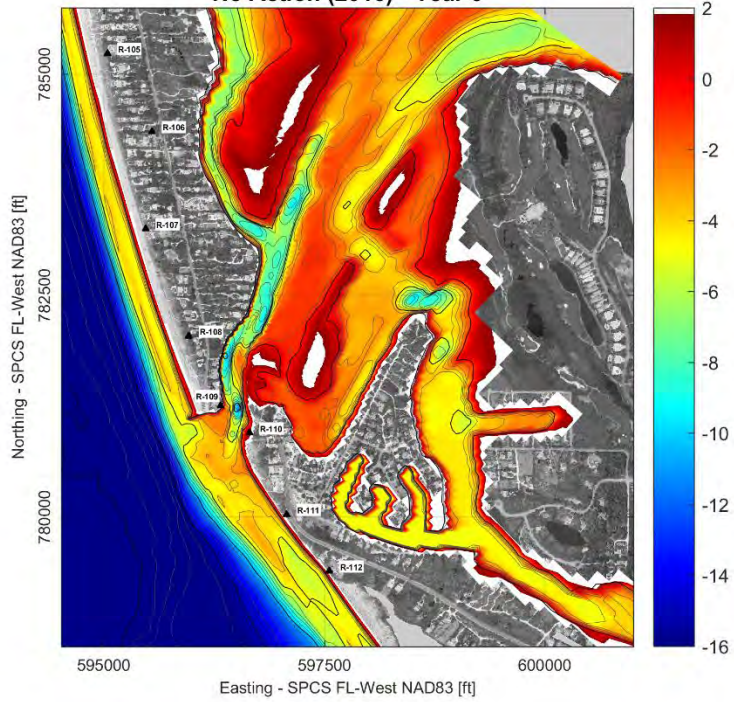
- Adams K.T., 1942. Hydrographic manual (Edition 2). U.S. Department of Commerce, U.S. Coast and Geodetic Survey, U.S. Government Printing Office, Washington, DC, 940 pp.
- Benedet, L., List, J.H., 2008. Evaluation of the physical process controlling beach changes adjacent to nearshore dredge pits. Coastal Engineering volume 55(12). 1224-1236.
- Benedet, L., Dobrochinski, J.P.H., Walstra, D.J.R., Klein, A.H.F., Ranasinghe, R., 2016. A morphological modeling study to compare different methods of wave climate schematization and evaluate strategies to reduce erosion losses from a beach nourishment project. Coastal Engineering 112 (2016). 69-86.
- Booij, N., Haagsma, I.J.G., Holthuijsen, L.H., Kieftenburg, A.T.M.M., Ris, R.C., van der Westhuysen, A.J., Zijlema, M., 2004. SWAN Cycle III version 40.41 User Manual, Delft University of Technology, Delft, The Netherlands.
- Adele M. Buttolph, Christopher W. Reed, Nicholas C. Kraus, Nobuyuki Ono, Magnus Larson, Benoit Camenen, Hans Hanson, Ty Wamsley, and Alan K. Zundel, 2006. Two-Dimensional Depth-Averaged Circulation Model CMS-M2D: Version 3.0, Report 2, Sediment Transport and Morphology Change, U.S. Army Corps of Engineers, Vicksburg, MS.
- Chawla, A., Tolman, H.L., Lanson, J.L., Devaliere, E.M., Gerald, V.M. 2009. Validation of a Multi-Grid WAVEWATCH III™ modeling system. NOAA/MMAB Contribution no. 281
- Chu, P.C., Y. Qi, Chen, Y.C., Shi, P., Mao, Q.W. 2004. South China Sea Wind-Wave Characteristics. Part I: Validation of Wavewatch-III Using TOPEX/Poseidon Data. Journal of Atmospheric and Oceanic Technology, 21(11), 1718-1733.
- Coastal Engineering Consultants, 2010. Lee County Blind Pass Restoration Project – Post-construction and 6-month monitoring report. Coastal Engineering Consultants, Naples, FL.
- Coastal Engineering Consultants, 2013. Blind Pass maintenance dredging project - 2013 post-construction report. Coastal Engineering Consultants, Naples, FL.
- Coastal Engineering Consultants, 2017. Blind Pass maintenance dredging project - 2017 post-construction report. Coastal Engineering Consultants, Naples, FL.
- Deltares, 2016a. Delft3D-FLOW, Simulation of Multi-Dimensional Hydrodynamic Flows and Transport Phenomena, Including Sediments, User Manual, Part of Hydro-Morphodynamics, Deltares, Rotterdam, Netherlands.
- Deltares, 2016b. Delft3D-WAVE, Simulation of Short-Crested Waves with SWAN, User Manual, Deltares, Rotterdam, Netherlands.

- Deltares, 2016c. RGFGRID, Generation and manipulation of structured and unstructured grids, suitable for Delft3D-FLOW, Delft3D-WAVE or D-Flow Flexible Mesh, User Manual, Deltares, Rotterdam, Netherlands.
- Egbert, A. F. Bennett, and M. G. G. Foreman, 1994. TOPEX/Poseidon Tides Estimated Using a Global Inverse Model. *J. Geophys. Res.*, 99, 24 821–24 852.
- Egbert, G.D. & Erofeeva, S.Y, 2002. Efficient Invert Modeling of Barotropic Ocean Tides. *J. Atmos. Oceanic Technol.*,19(2), 183-204.
- Florida Department of Environmental Protection, 2010. Historic Shoreline Database, <http://www.dep.state.fl.us/beaches/data/his-shore.htm>.
- Florida Department of Environmental Protection, 2009. Guidelines for Documenting Numerical Model Studies in Submittals to the FDEP Bureau of Beaches and Coastal Systems (BBCS). Tallahassee, FL.
- Florida Fish and Wildlife Conservation Commission - Fish and Wildlife Research Institute (FWC-FWRI). 2014. Mangrove Habitat in Florida. [http://geodata.myfwc.com/datasets/a78a27e02f9d4a71a3c3357aefc35baf\\_4](http://geodata.myfwc.com/datasets/a78a27e02f9d4a71a3c3357aefc35baf_4)
- Hanson, J. L., Tracy B. A., Tolman H. L. and Scott R. D. 2009. Pacific Hindcast Performance of Three Numerical Wave Models. *Journal of Atmospheric and Oceanic Technology*, 26, 1614 – 1633.
- Hanson, H., Kraus, N.C., 1989. GENESIS: Generalized Model for Simulating Shoreline Change, Report 1, Technical Reference. US Army Corps of Engineers, Washington, DC, 185 p. with appendices.
- Hasselmann, K., T. P. Barnett, E. Bouws, H. Carlson, D. E. Cartwright, K. Enke, J. Ewing, H. Gienapp, D. E. Hasselmann, P. Kruseman, A. Meerburg, P. Müller, D. J. Olbers, K. Richter, W. Sell and H. Walden, 1973. Measurements of wind wave growth and swell decay during the Joint North Sea Wave Project (JONSWAP). *Deutsche Hydrographische Zeitschrift*.
- IHO - International Hydrographic Organization. 1998. Standards for Hydrographic Surveys, Special Publication 44, 1<sup>st</sup> Edition.
- IHO - International Hydrographic Organization. 1982. Standards for Hydrographic Surveys, Special Publication 44, 2<sup>nd</sup> Edition.
- IHO - International Hydrographic Organization. 1987. Standards for Hydrographic Surveys, Special Publication 44, 3<sup>rd</sup> Edition.

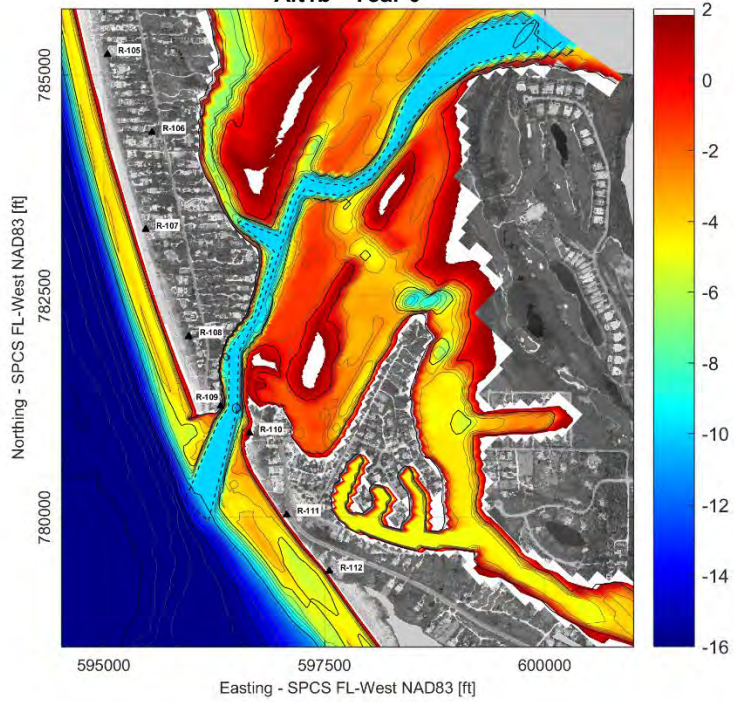
- IHO - International Hydrographic Organization. 1998. Standards for Hydrographic Surveys, Special Publication 44, 1<sup>st</sup> Edition 1968, 2<sup>nd</sup> Edition 1982, 3<sup>rd</sup> Edition 1987, 4<sup>th</sup> Edition 1998
- Irish, J.L., McClunk, J.K., Lillycrop, W.J., 2000. Airborne lidar bathymetry: the SHOALS system. PIANC Bulletin, No. 103-2000, 45-53.
- Jeffers, K.B., 1960. Hydrographic manual. U.S. Department of Commerce and U.S. Coast and Geodetic Survey. Publication 20-2. Washington, DC, 196 pp.
- Lesser G.R., Roelvink J.A., Van Kester J.A.T.M., Stelling G.S. 2004. Development and validation of a three-dimensional morphological model. Coastal Engineering 51 (2004) 883– 915.
- Lesser, G.R., 2009. An Approach to Medium-term Coastal Morphological Modelling. PhD thesis, UNESCO-IHE & Delft Technical University, Delft. CRC Press/Balkema. ISBN 978-0-415-55668-2.
- South Florida Water Management District, 2008. Estero Bay, Lower Charlotte Harbor Seagrass 2008. <https://www.arcgis.com/home/item.html?id=d0440b0700f54e0287f7ea8b35ac47c9>
- Southwest Florida Water Management District, 2012. Seagrass data for St. Joseph Sound, Clearwater Harbor, Tampa Bay, Sarasota Bay, Lemon Bay and Charlotte Harbor. [http://data.swfwmd.opendata.arcgis.com/datasets/619bd267e4c54e70968abd86eb92318e\\_17](http://data.swfwmd.opendata.arcgis.com/datasets/619bd267e4c54e70968abd86eb92318e_17)
- WW3, 2015. NOAA WavewatchIII. <http://polar.ncep.noaa.gov/waves/index2.shtml>

**SUB-APPENDIX A-1**  
**INITIAL MODEL BATHYMETRY: ALTERNATIVES 0 TO 9**

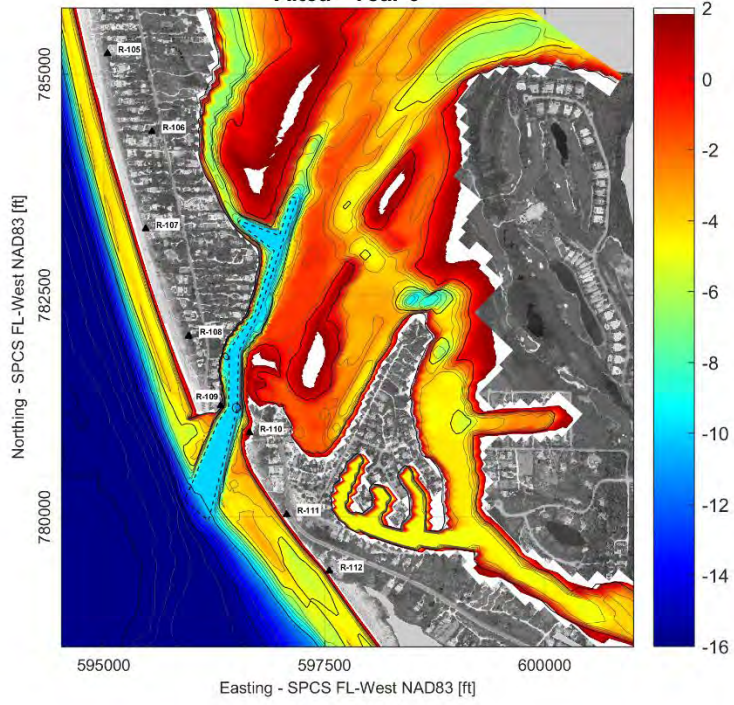
**Model bathymetry [ft NAVD]  
No Action (2016) - Year 0**



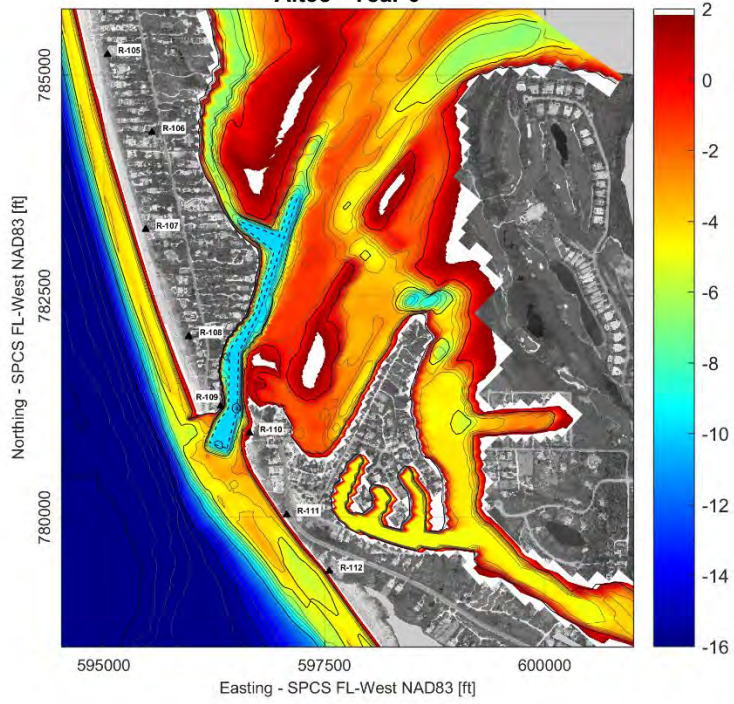
**Model bathymetry [ft NAVD]  
Alt1b - Year 0**



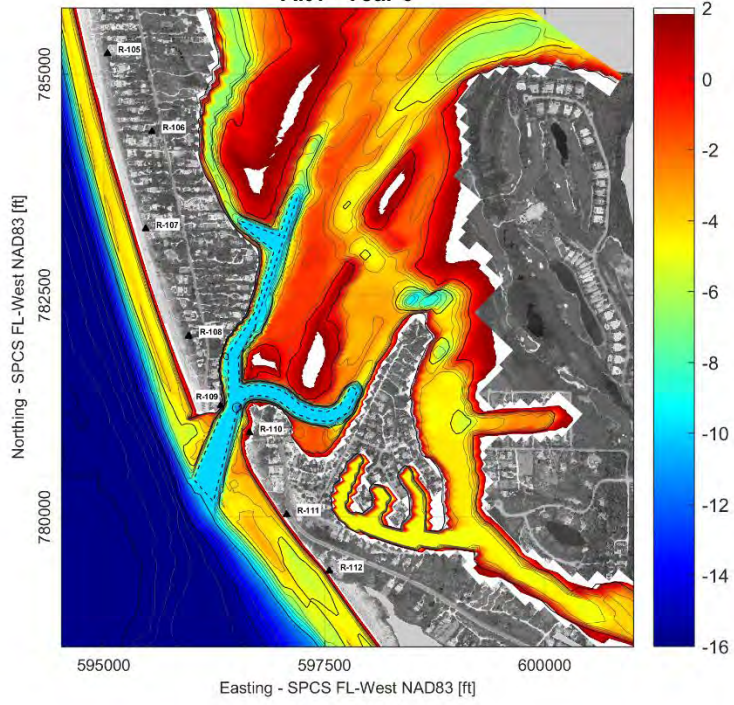
**Model bathymetry [ft NAVD]  
Alt3a - Year 0**



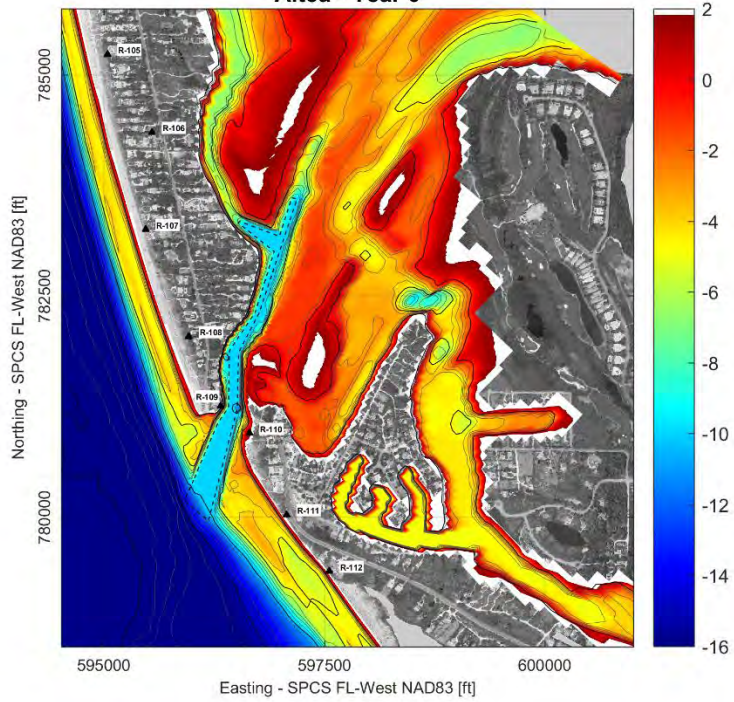
**Model bathymetry [ft NAVD]  
Alt3c - Year 0**



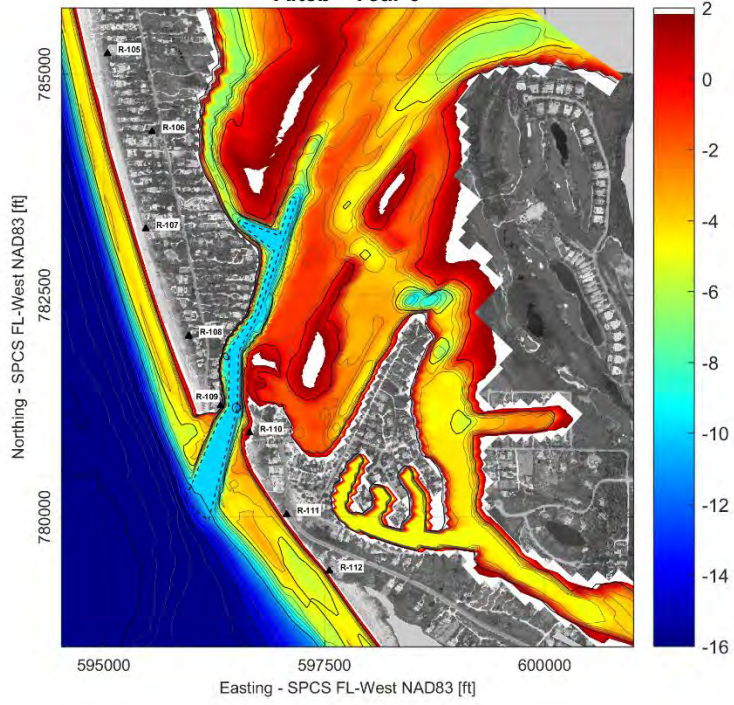
**Model bathymetry [ft NAVD]  
Alt4 - Year 0**



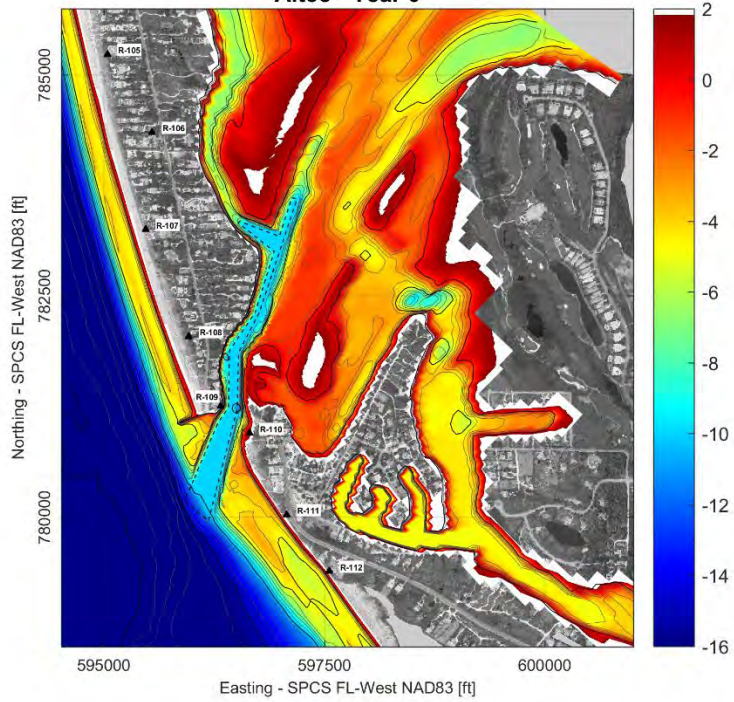
**Model bathymetry [ft NAVD]  
Alt5a - Year 0**



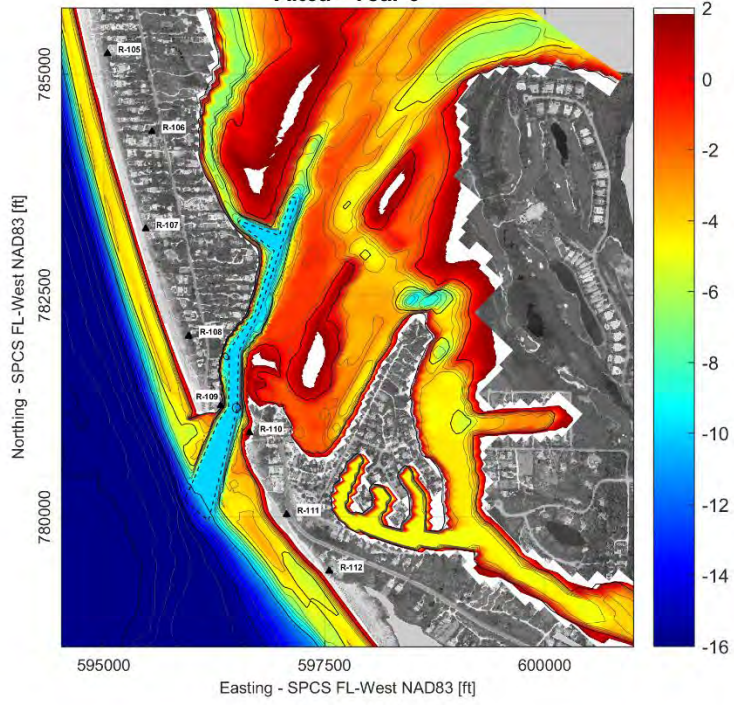
**Model bathymetry [ft NAVD]  
Alt5b - Year 0**



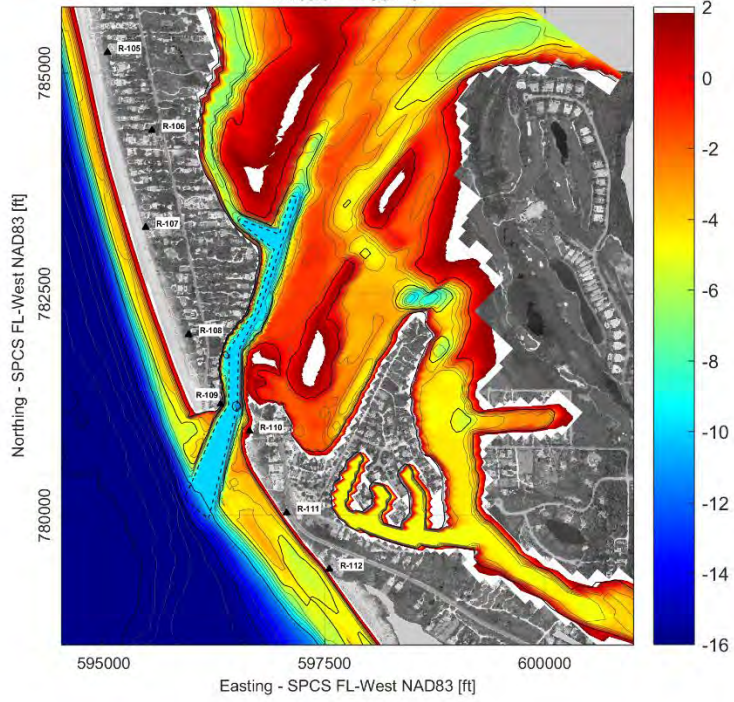
**Model bathymetry [ft NAVD]  
Alt5c - Year 0**



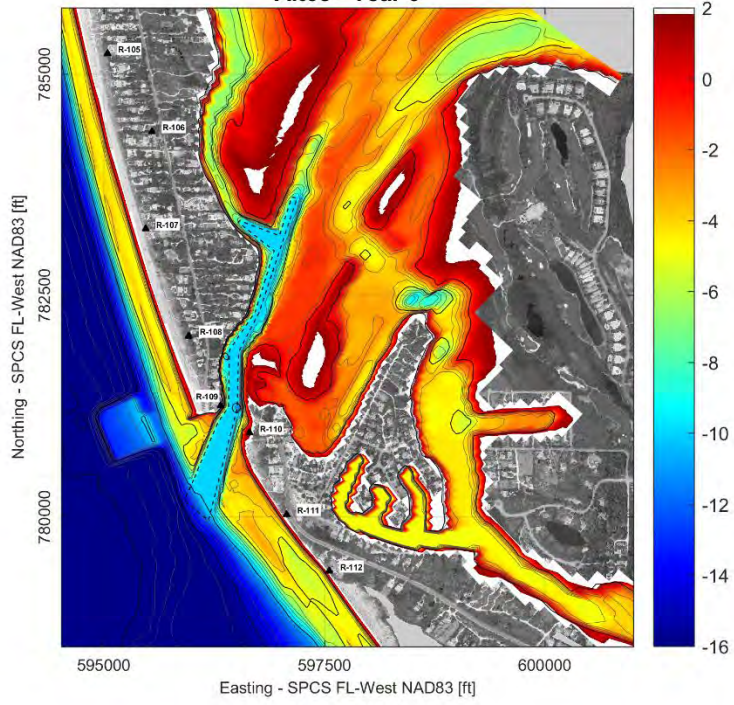
**Model bathymetry [ft NAVD]  
Alt6a - Year 0**



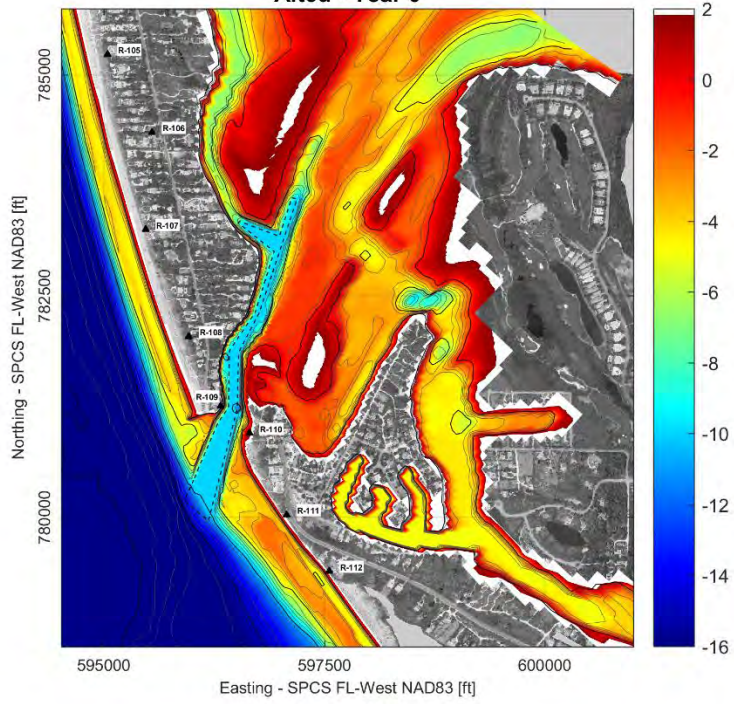
**Model bathymetry [ft NAVD]  
Alt6b - Year 0**



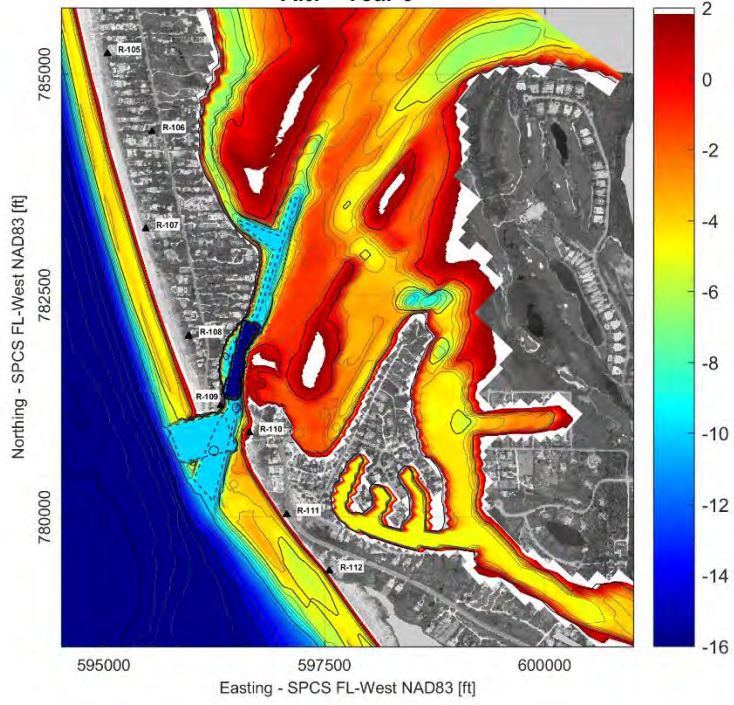
**Model bathymetry [ft NAVD]  
Alt6c - Year 0**



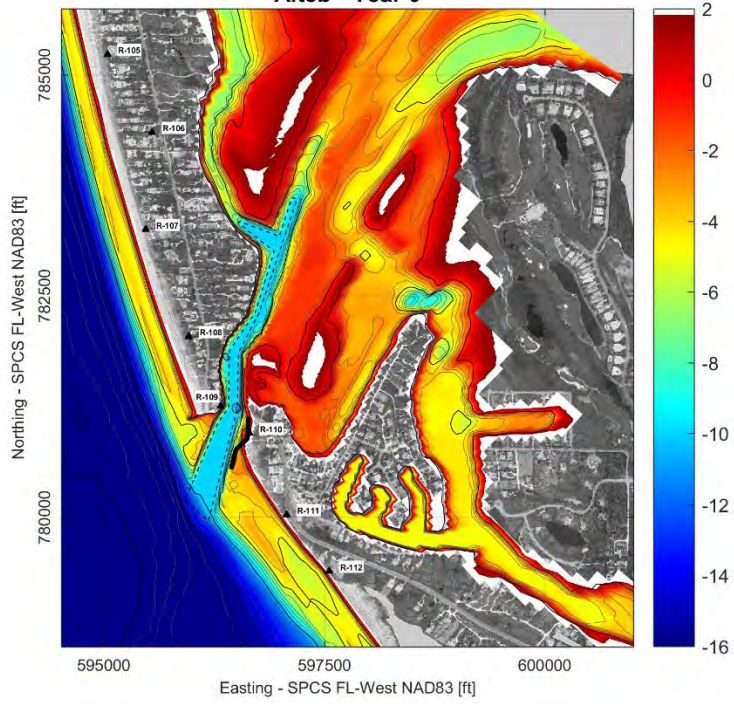
**Model bathymetry [ft NAVD]  
Alt6d - Year 0**



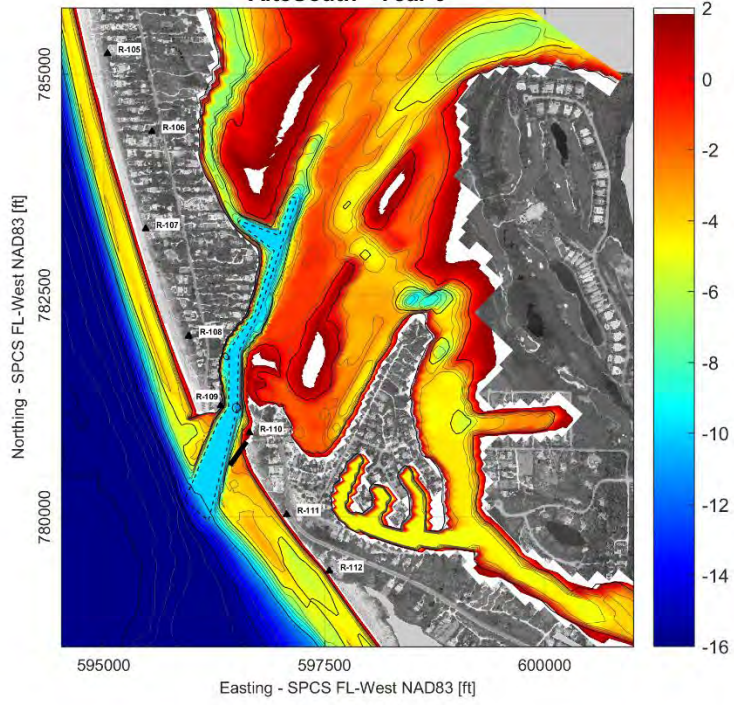
**Model bathymetry [ft NAVD]  
Alt7 - Year 0**



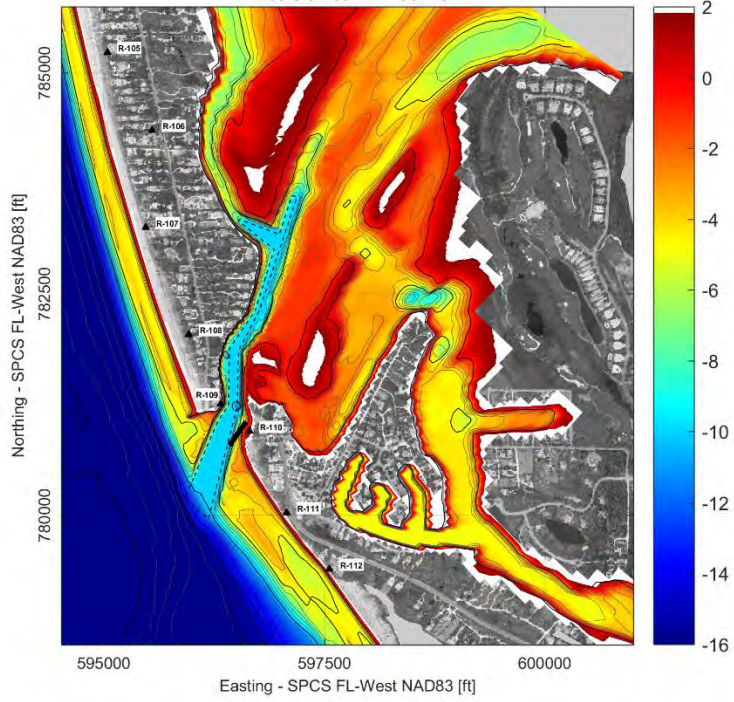
**Model bathymetry [ft NAVD]  
Alt8b - Year 0**



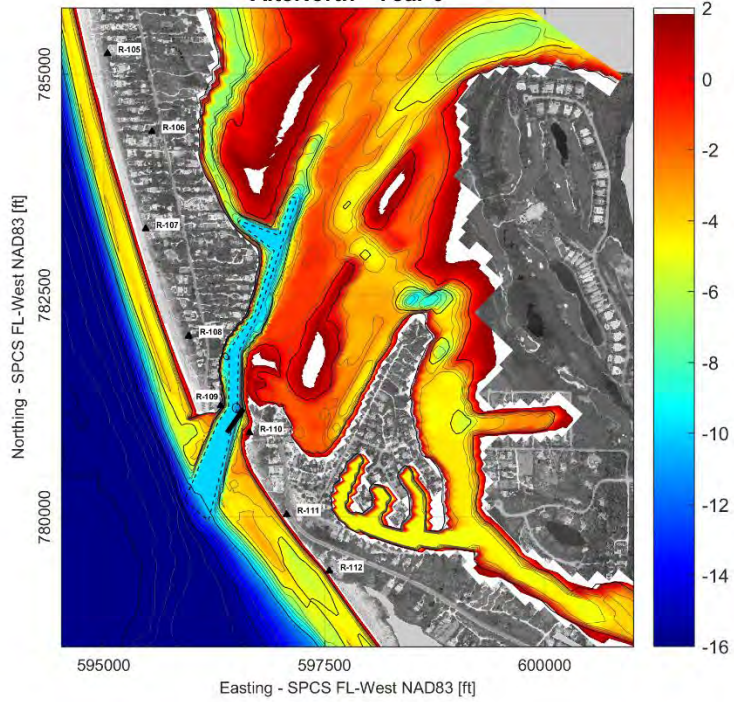
**Model bathymetry [ft NAVD]  
Alt8South - Year 0**



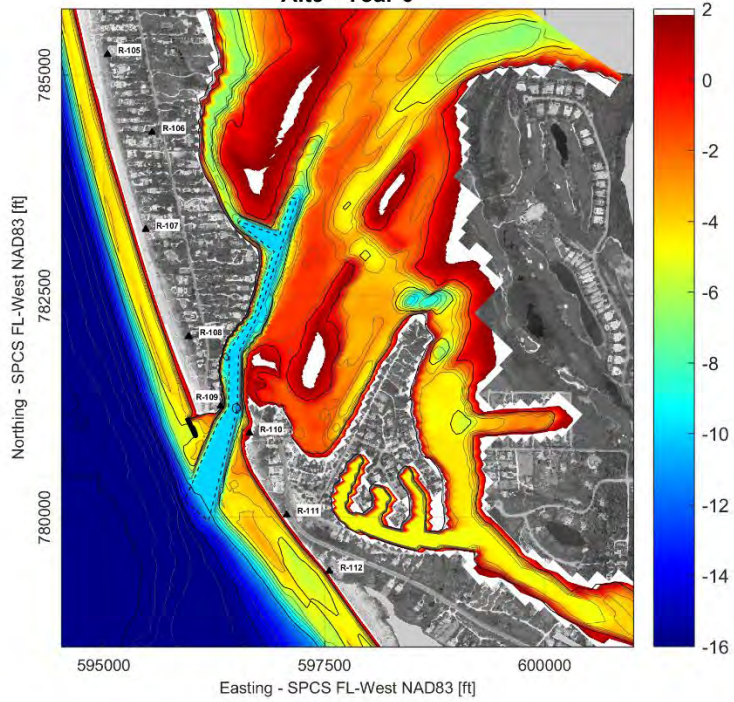
**Model bathymetry [ft NAVD]  
Alt8Center - Year 0**



**Model bathymetry [ft NAVD]  
Alt8North - Year 0**



**Model bathymetry [ft NAVD]  
Alt9 - Year 0**

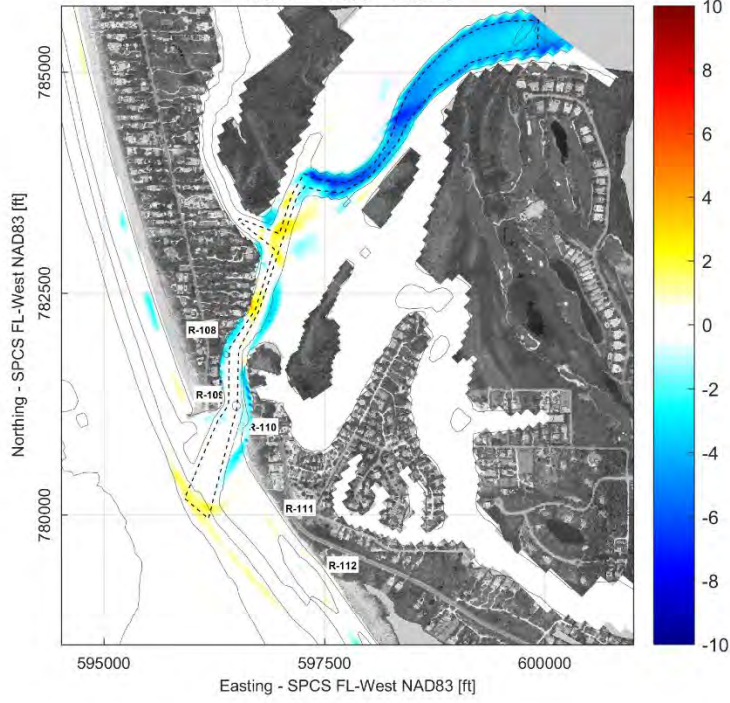


**SUB-APPENDIX A-2**

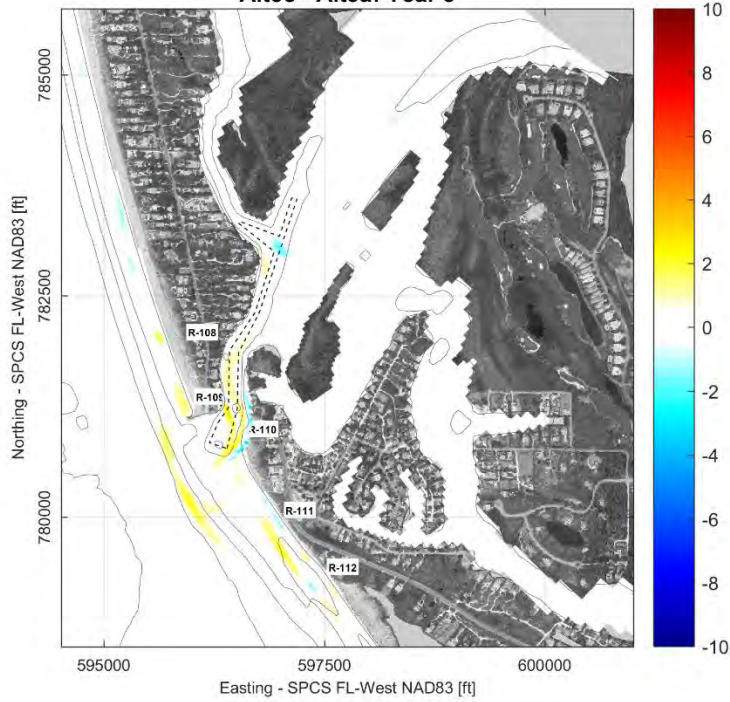
**NET BATHYMETRY CHANGES RELATIVE TO ALTERNATIVE 3A**

**Alternative 1b to 9 (Year 5)    *Minus*    Alternative 3a (Year 5)**

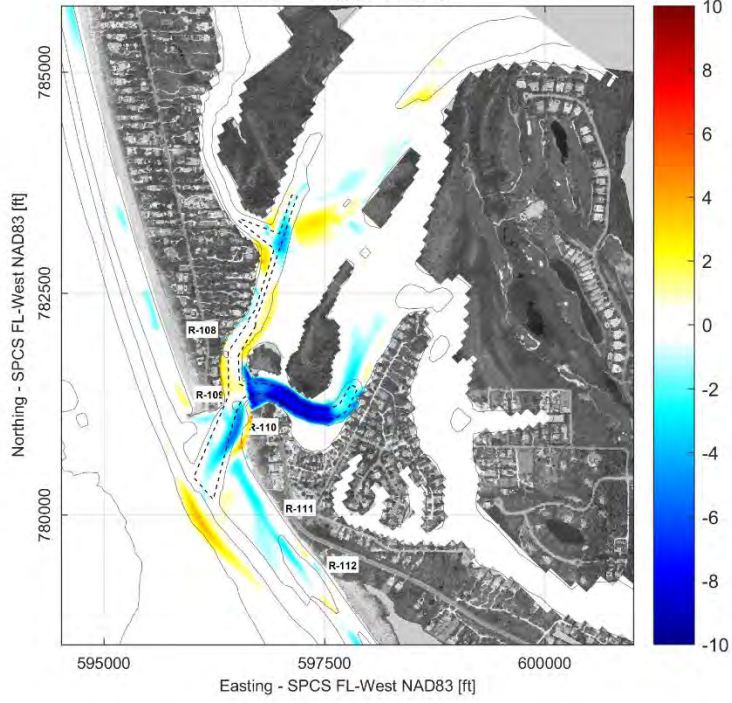
**Net changes [ft]**  
**Alt1b - Alt3a: Year 5**



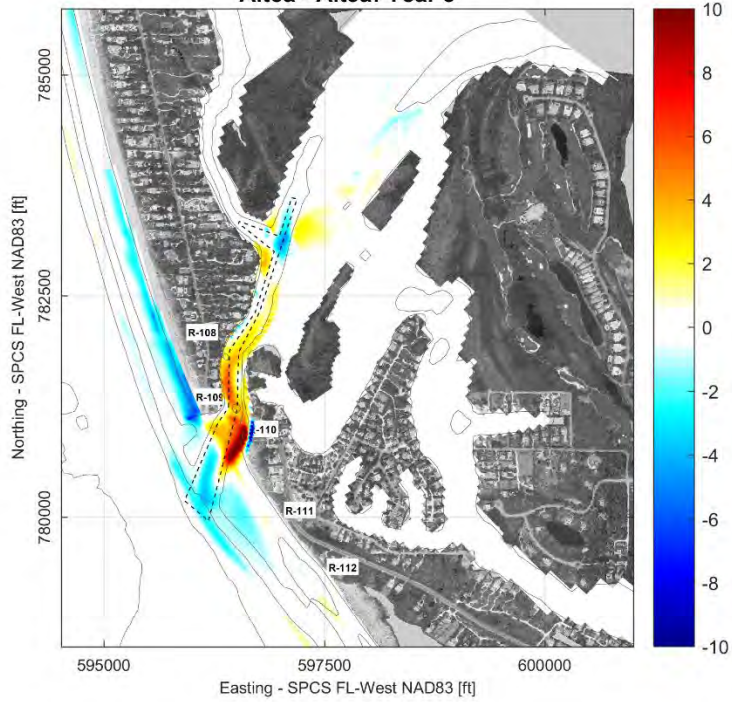
**Net changes [ft]**  
**Alt3c - Alt3a: Year 5**



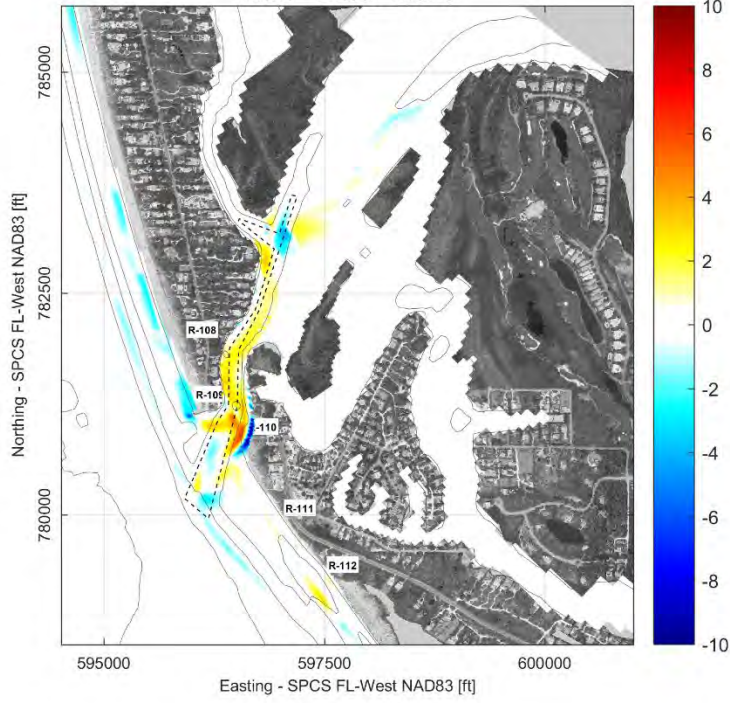
**Net changes [ft]**  
**Alt4 - Alt3a: Year 5**



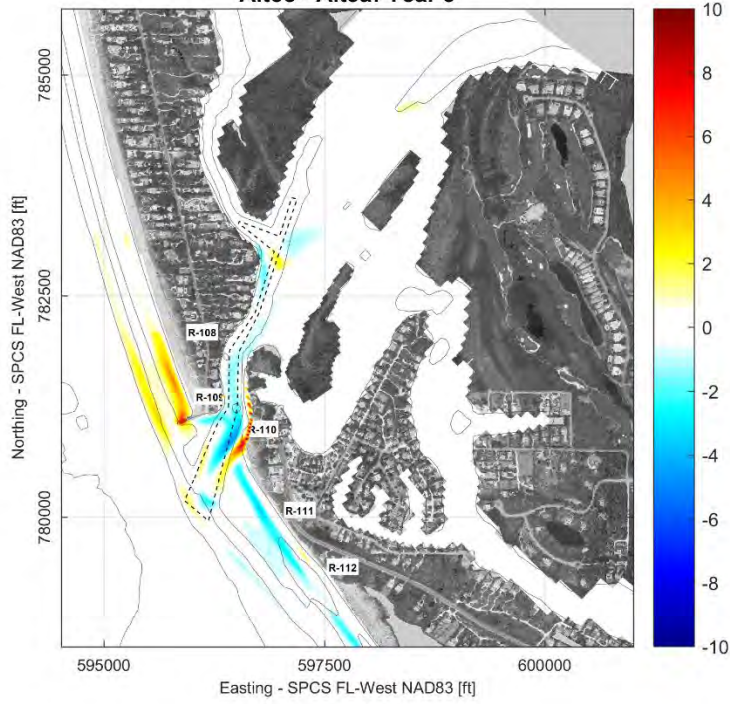
**Net changes [ft]**  
**Alt5a - Alt3a: Year 5**



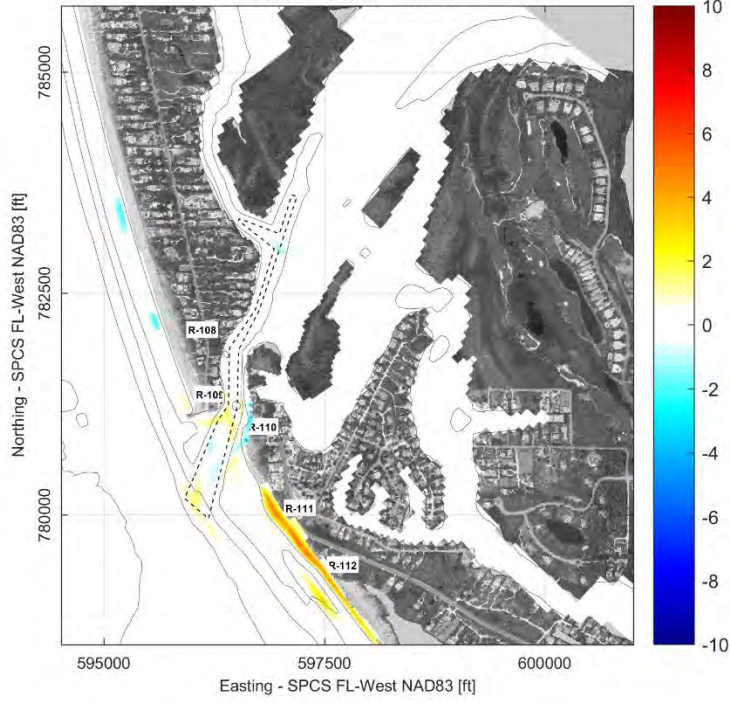
**Net changes [ft]**  
**Alt5b - Alt3a: Year 5**



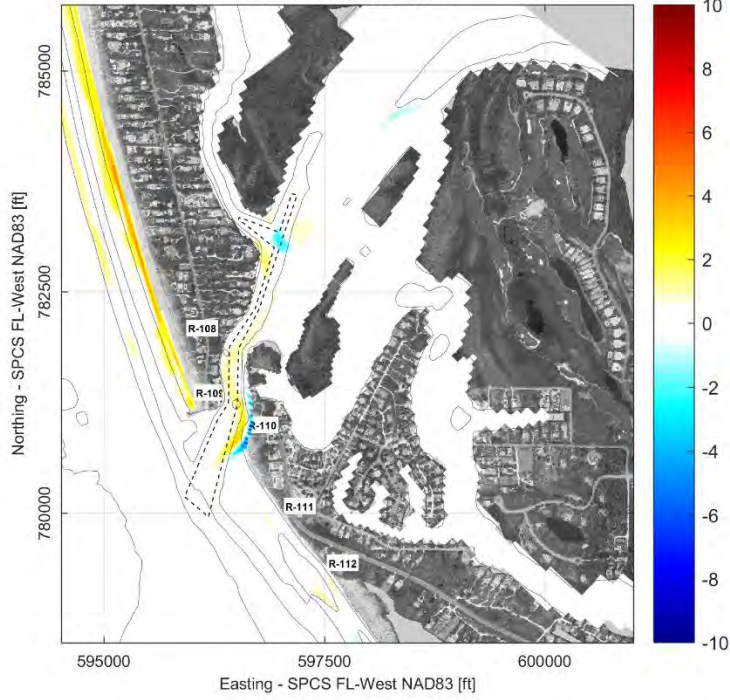
**Net changes [ft]**  
**Alt5c - Alt3a: Year 5**



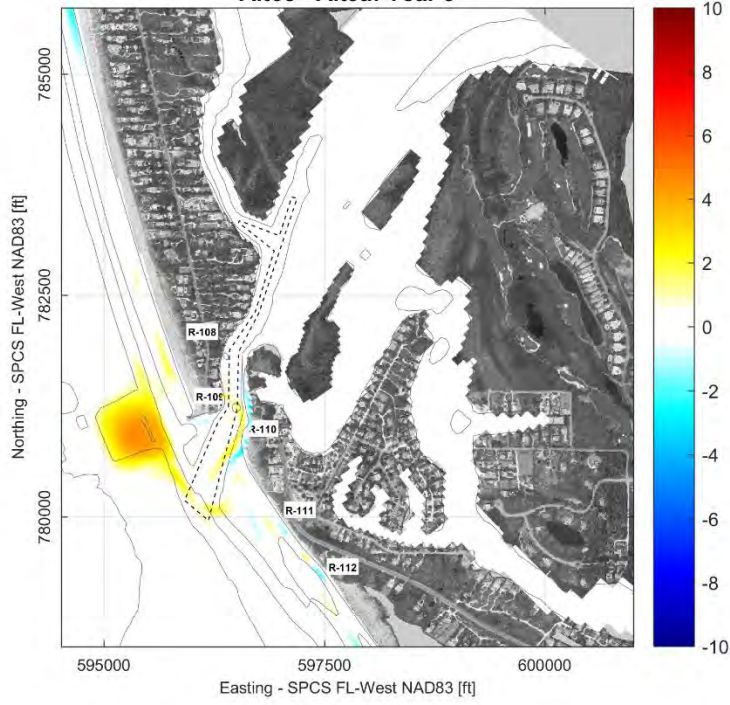
**Net changes [ft]**  
**Alt6a - Alt3a: Year 5**



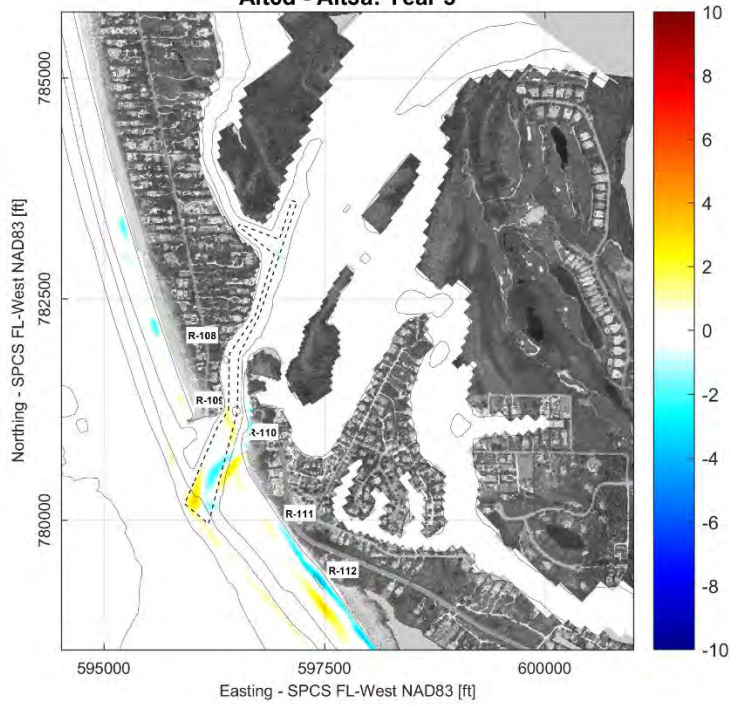
**Net changes [ft]**  
**Alt6b - Alt3a: Year 5**



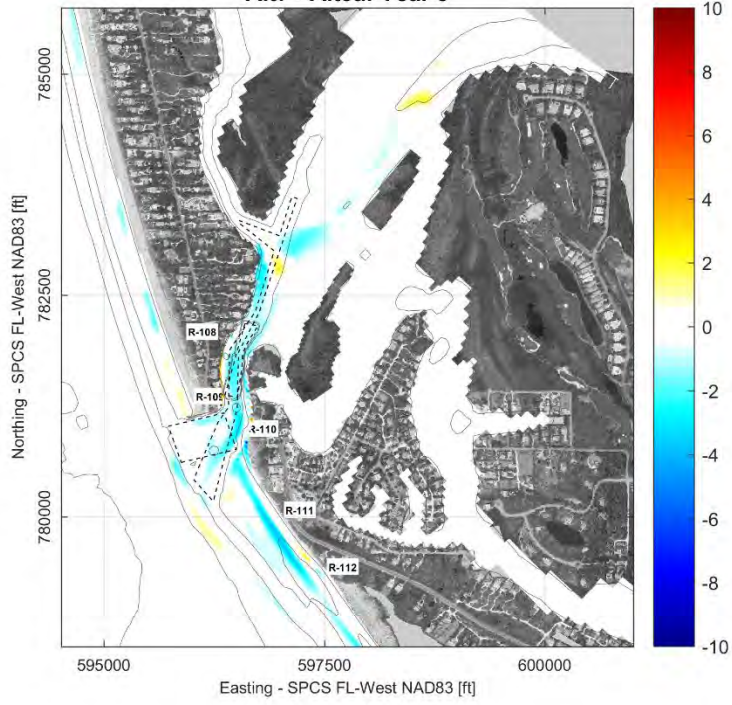
**Net changes [ft]**  
**Alt6c - Alt3a: Year 5**



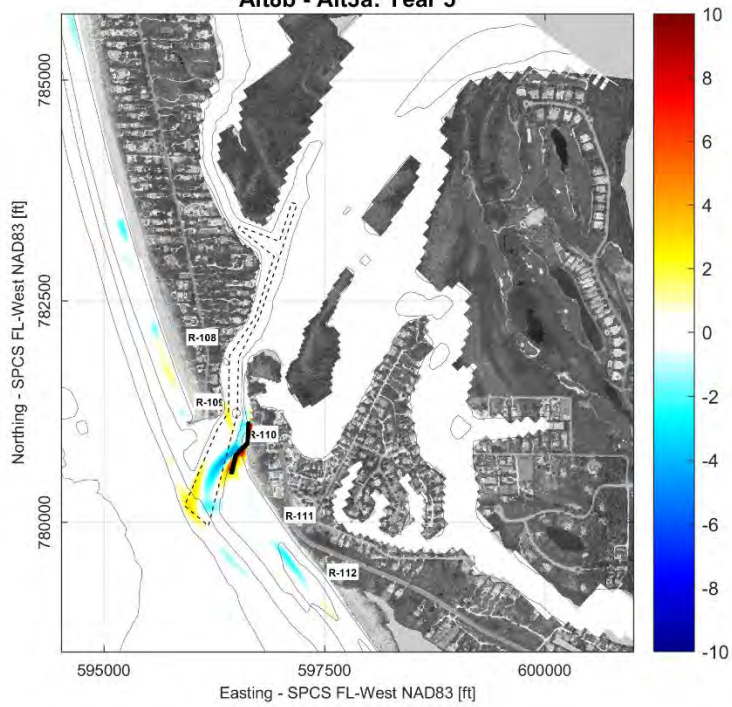
**Net changes [ft]**  
**Alt6d - Alt3a: Year 5**



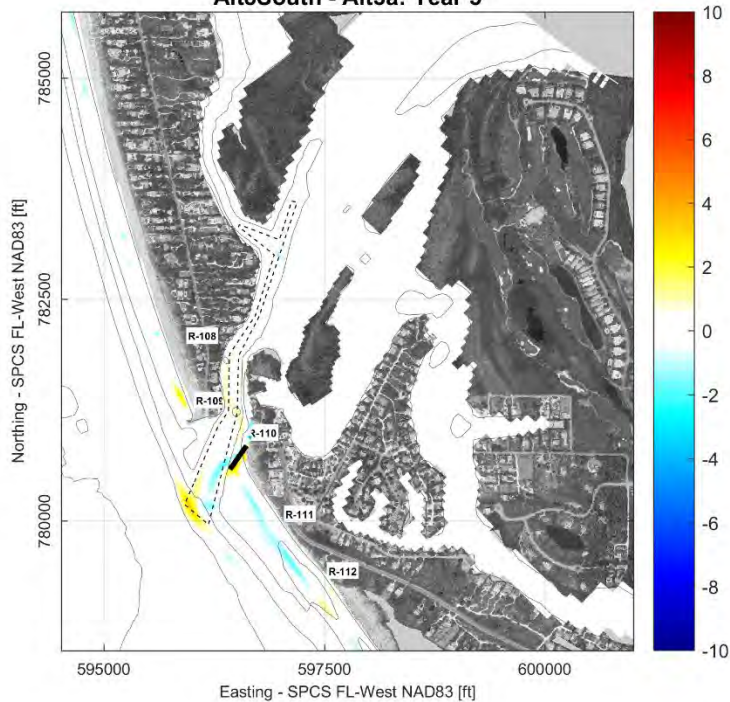
**Net changes [ft]**  
**Alt7 - Alt3a: Year 5**



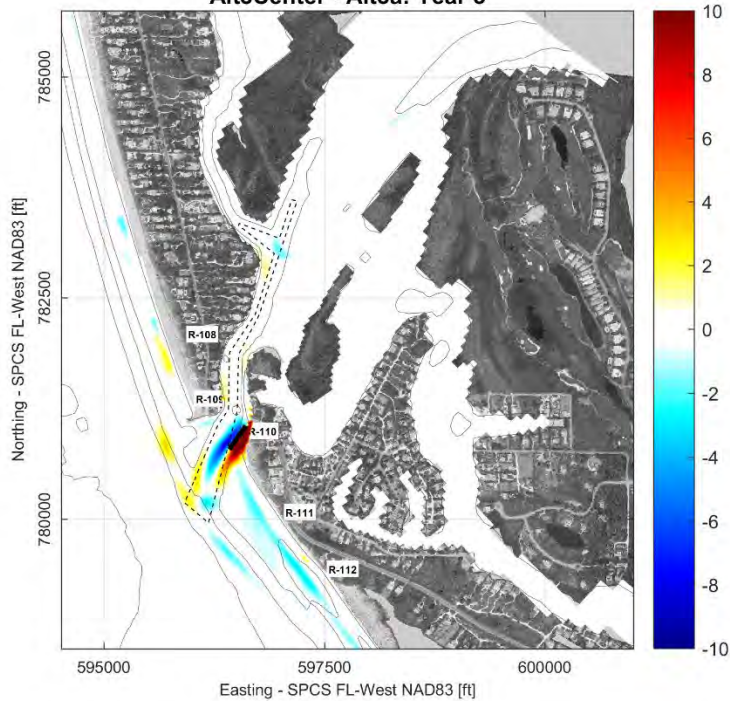
**Net changes [ft]**  
**Alt8b - Alt3a: Year 5**



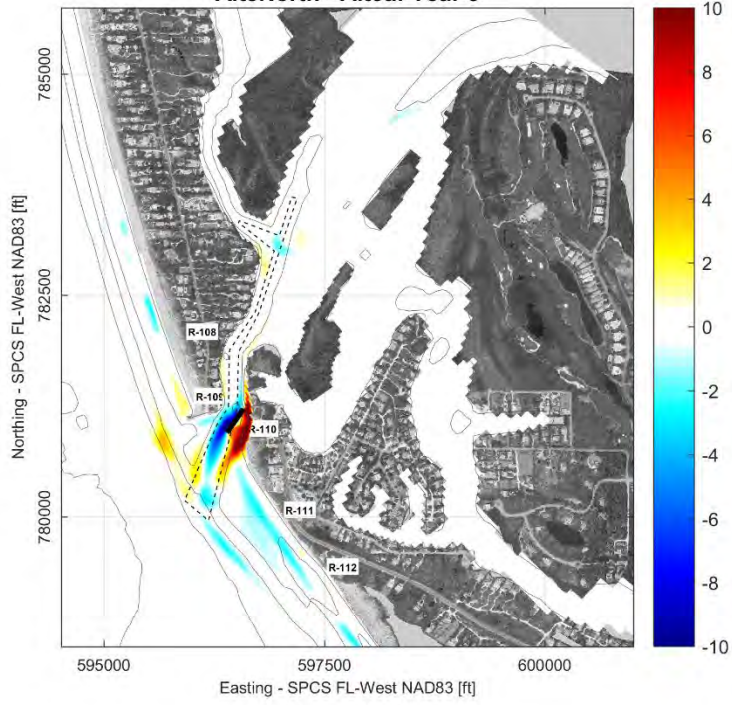
**Net changes [ft]**  
**Alt8South - Alt3a: Year 5**



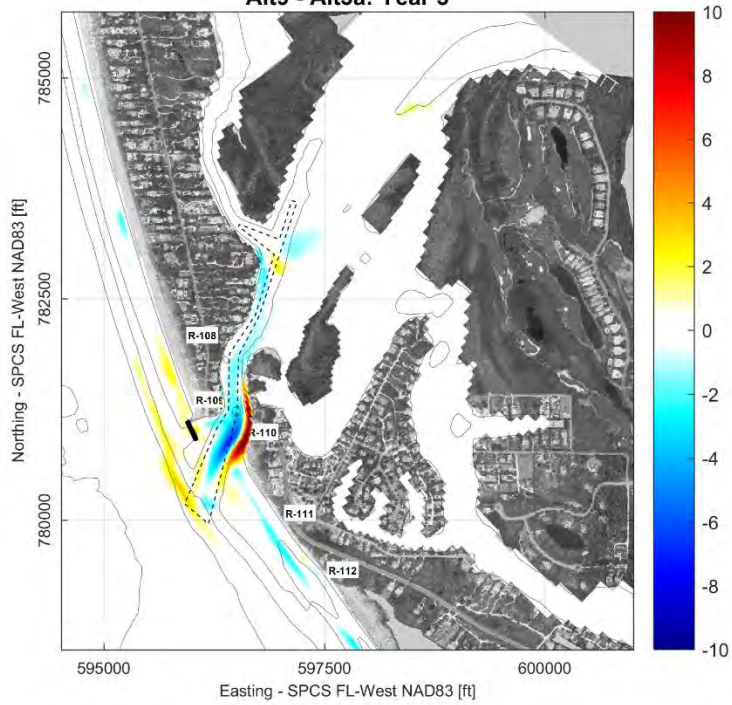
**Net changes [ft]**  
**Alt8Center - Alt3a: Year 5**



**Net changes [ft]**  
**Alt8North - Alt3a: Year 5**



**Net changes [ft]**  
**Alt9 - Alt3a: Year 5**



**SUB-APPENDIX A-3**  
**ADDITIONAL BLIND PASS JETTY SPUR ANALYSIS**

## ADDITIONAL BLIND PASS JETTY SPUR ANALYSIS

Following the beneficial results of Alternative 9 (210 ft Spur at the tip of Blind Pass Jetty), additional model simulations were performed of shorter spurs in order to evaluate the sensitivity of the coastal system compared to spur length. The baseline simulation used in these tests is the Combined Alternative #1, which does not include a spur. The simulated spur lengths are:

- 210 feet
- 170 feet
- 130 feet
- 100 feet
- 60 feet

One additional simulation considers a 130 ft spur relocated eastward, closer to the bridge on the interior side of the jetty. The purpose of this run was to evaluate the location of a spur with an intermediate length. The results of the six runs are shown on the attached plots of transport, net morphology changes and minimum cross-sectional area.

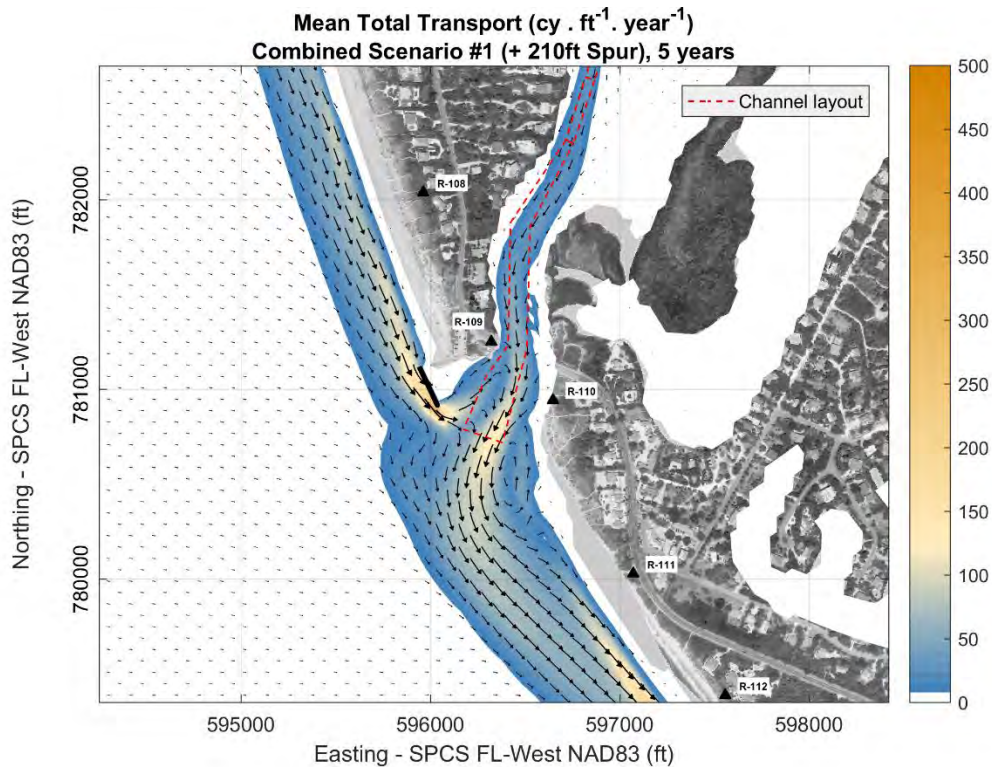
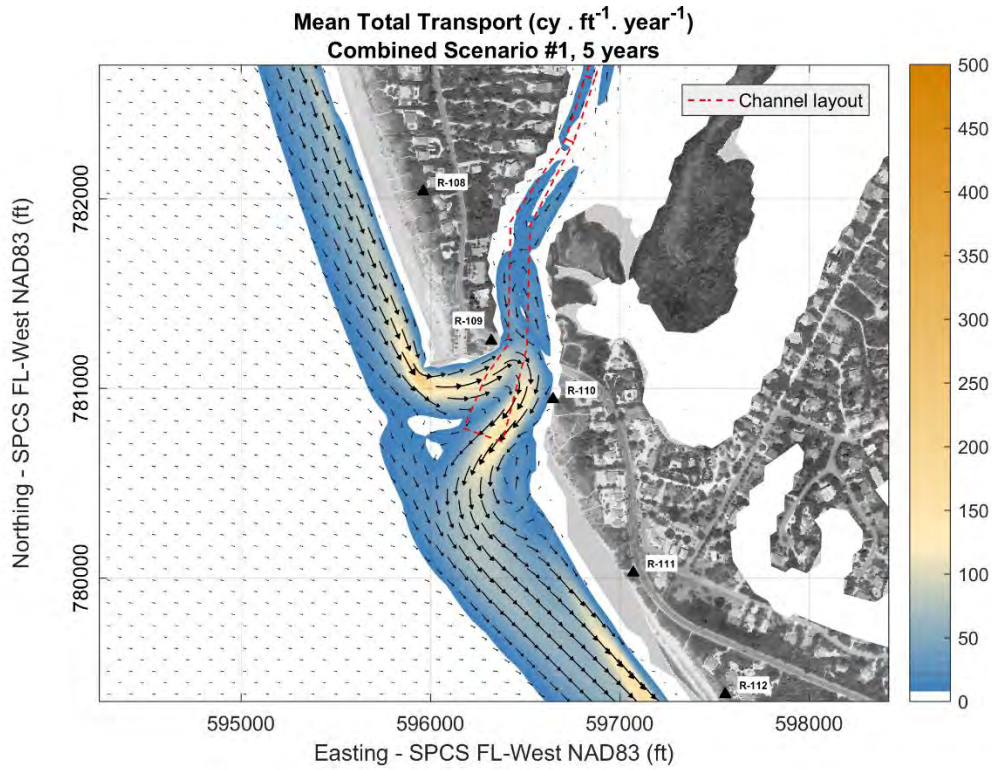
The model results suggest that the spur reduces the sediment transport immediately south of the jetty towards the channel, favoring a more direct bypassing across the outer section of the channel. This reduces channel accretion near the bridge, limits the southward channel migration and slows the consequential shoreline retreat at the southern channel margin (north-end of Sanibel Island). Sediment transport towards inner sections of the channel is also reduced.

The net change maps compare the final simulated bathymetries (Year 5) with and without the simulated spurs. These results represent isolated effects of the tested structures compared to the sensitivity of the coastal system. The simulations show that the longest (210 ft) spur produces more pronounced effects, while the shortest (60 ft) spur causes negligible changes to the system. The effects of the spur are primarily observed in the channel depth (less migration and accretion) and its southern margin (less erosion). The simulation of the 130 ft spur relocated eastward produced the opposite effects: a shallower channel and increased channel migration southward after 5 years, indicating that the better spur location is at the tip of the existing jetty.

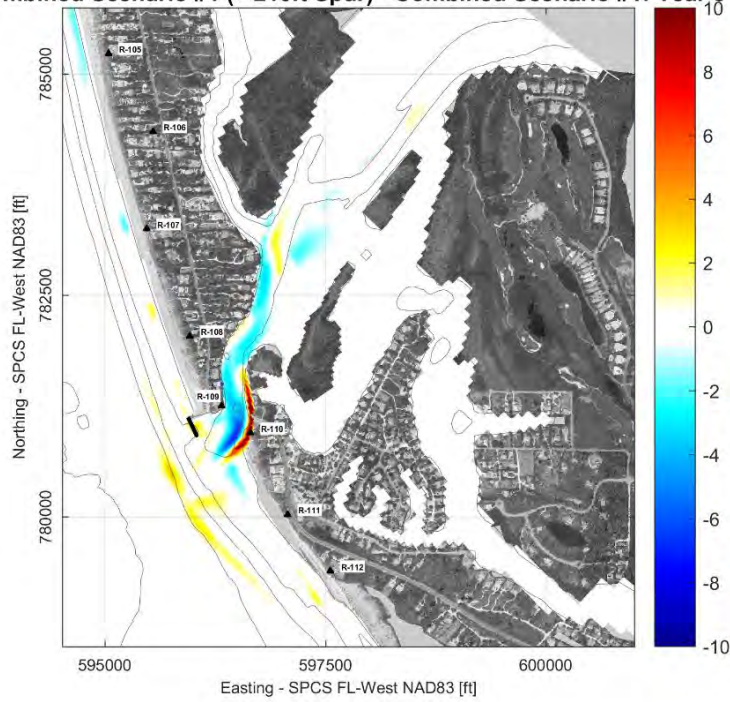
To facilitate comparisons, the length of the spurs are plotted against the average cross-sectional area benefit over the 5 years simulations. These results are shown in the enclosed plot titled "Spur sensitivity analysis," which indicates a relatively straight line suggesting a uniform, linear relationship. Therefore, the spur appears to perform better with length, which is more likely to be limited by other factors, such as construction, permitting and other practical aspects. The net effects of the tested spurs compared to the minimum cross-sectional area of the channel shown in the attached figure titled "Minimum cross-sectional area w.r.t. 'Combined Scenario #1' [sq.ft]" demonstrate the positive effects of the spurs located at the tip of the jetty compared to the relocated spur.

Except for the relocated spur, all simulations indicate negligible to slightly positive benefits for the adjacent Captiva and Sanibel beaches, which is demonstrated in the volume plot. More

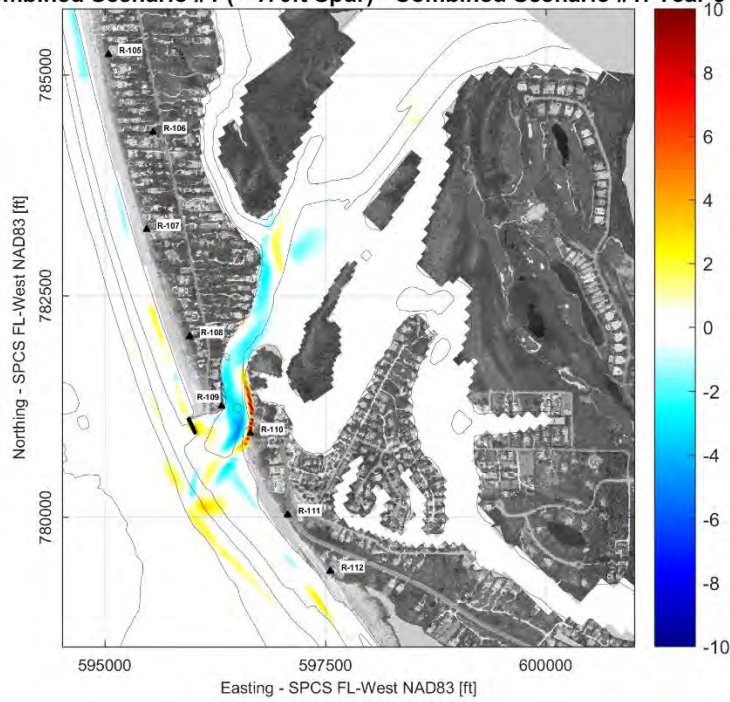
pronounced volumetric changes near the inlet are associated to relative shifts of channel location, and do not necessarily suggest shoreline retreat. The 100 ft spur was the selected option for the Combined Alternative #3 simulations.



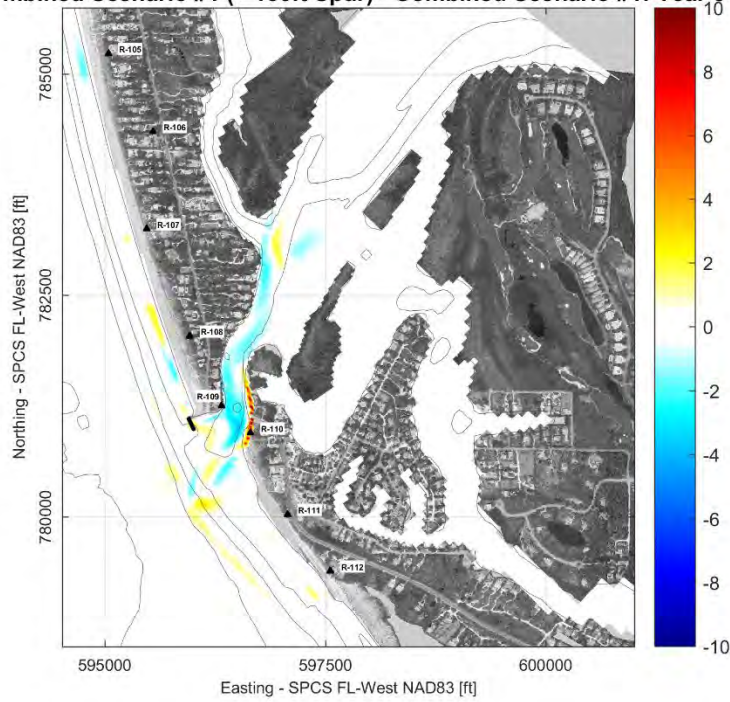
**Net changes [ft]**  
**Combined Scenario #1 (+ 210ft Spur) - Combined Scenario #1: Year 5**



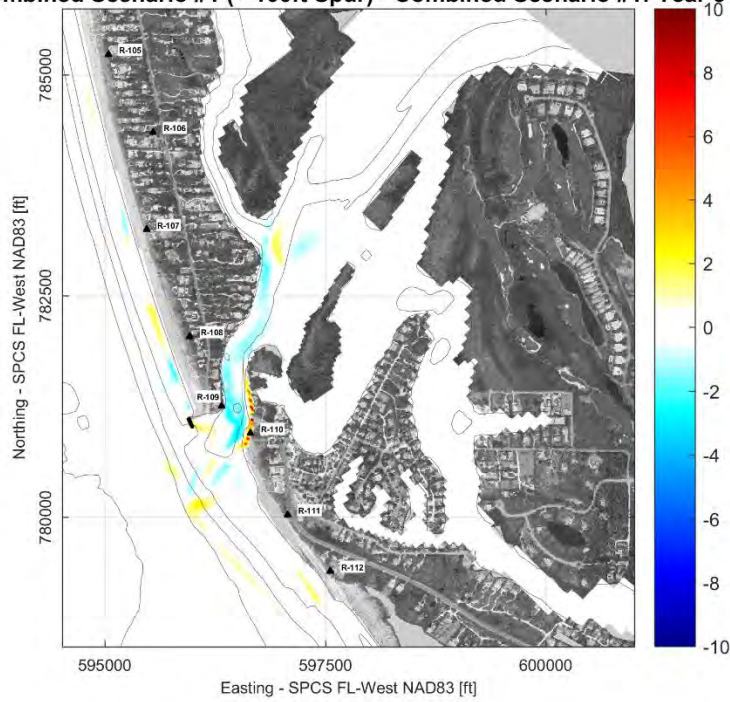
**Net changes [ft]**  
**Combined Scenario #1 (+ 170ft Spur) - Combined Scenario #1: Year 5**



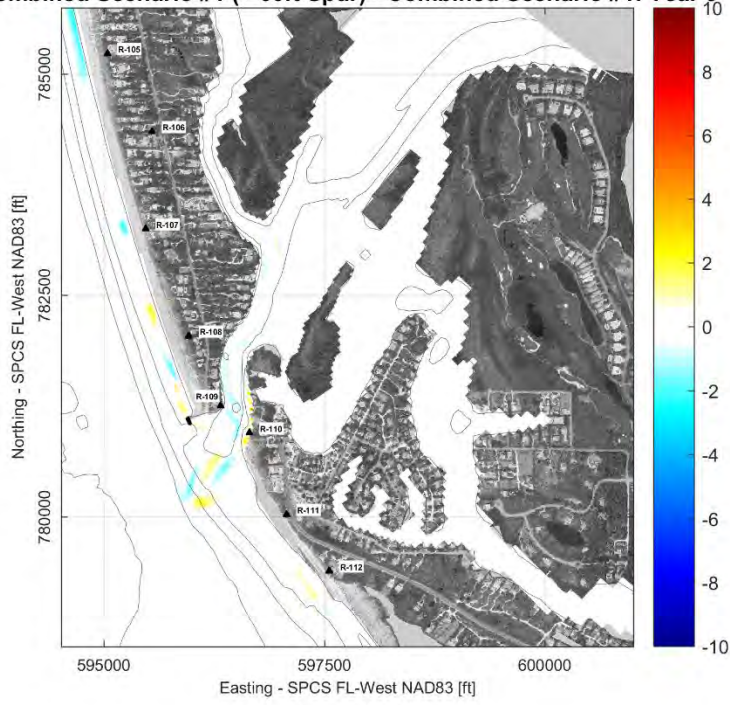
**Net changes [ft]**  
**Combined Scenario #1 (+ 130ft Spur) - Combined Scenario #1: Year 5**



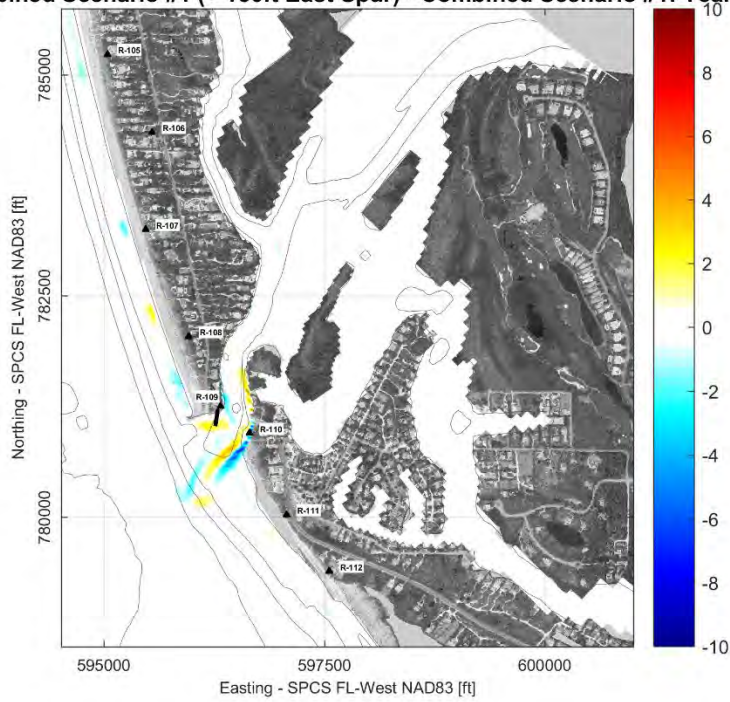
**Net changes [ft]**  
**Combined Scenario #1 (+ 100ft Spur) - Combined Scenario #1: Year 5**

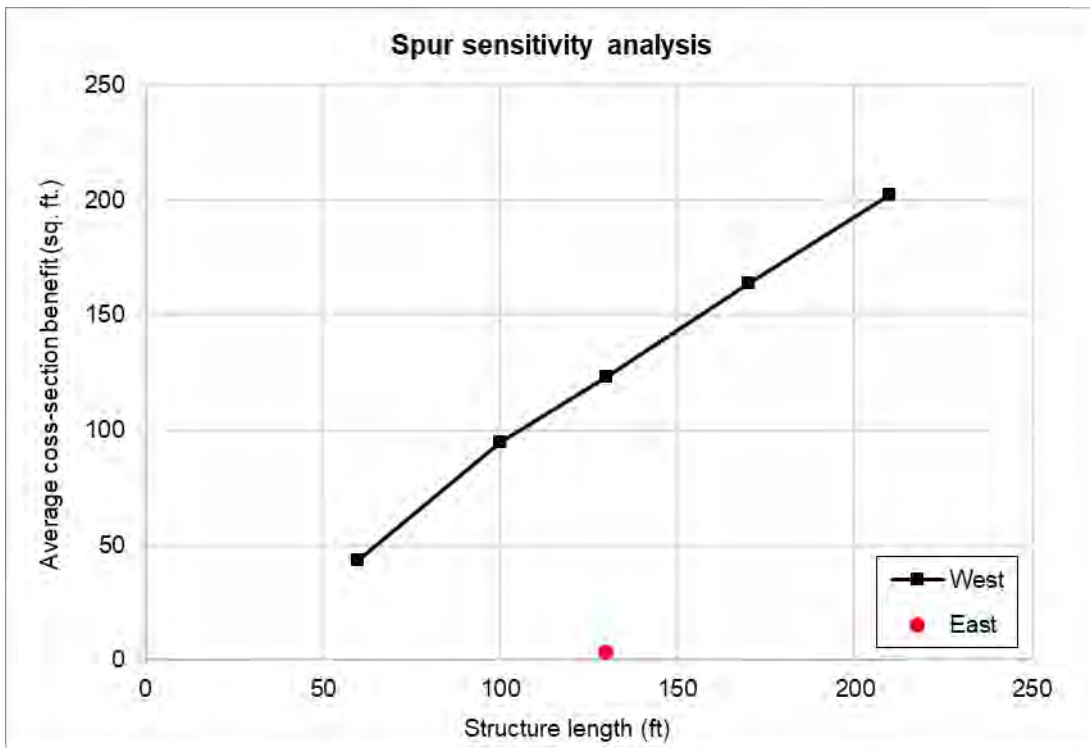
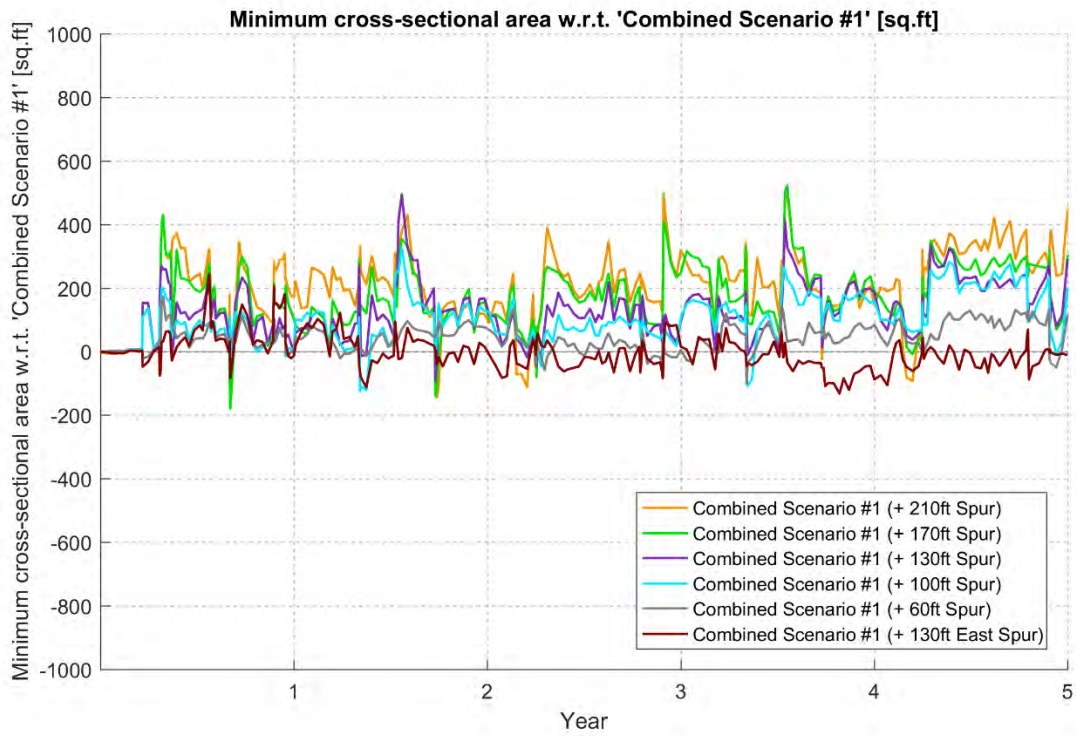


**Net changes [ft]**  
**Combined Scenario #1 (+ 60ft Spur) - Combined Scenario #1: Year 5**

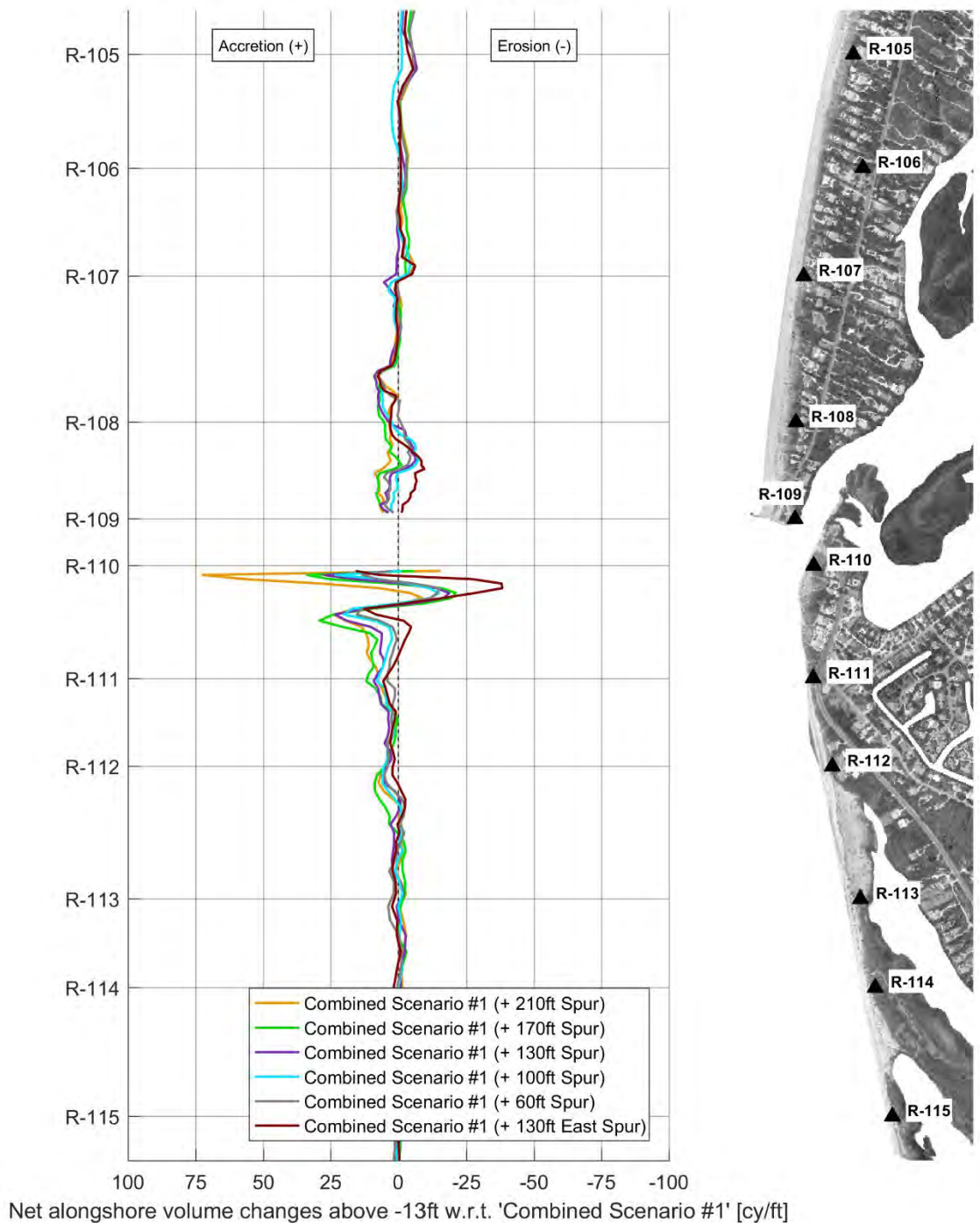


**Net changes [ft]**  
**Combined Scenario #1 (+ 130ft East Spur) - Combined Scenario #1: Year 5**





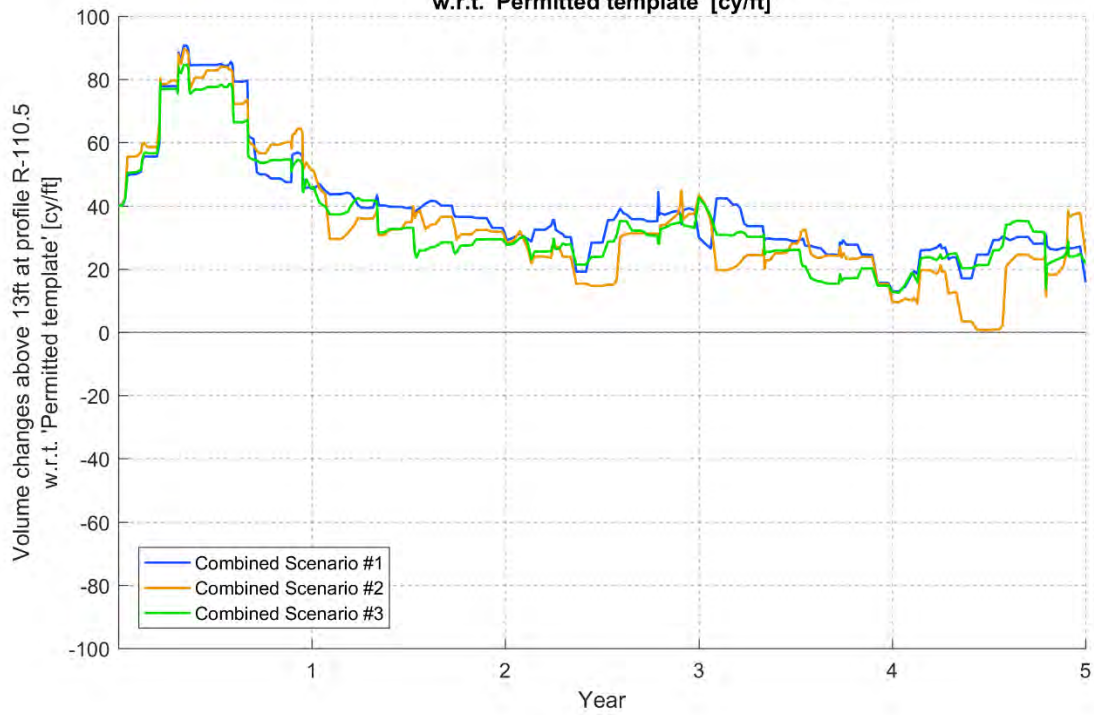
**Net alongshore volume changes above -13ft w.r.t. 'Combined Scenario #1' [cy/ft]  
Year 5**



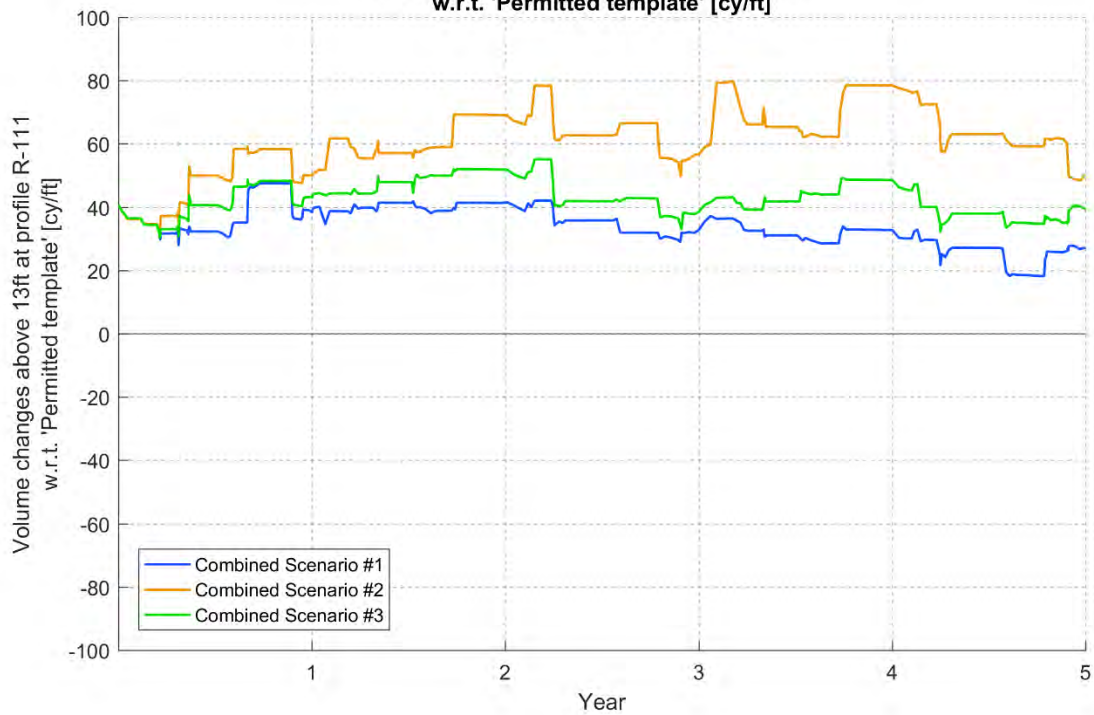
**SUB-APPENDIX A-4**

**NET VOLUME CHANGES RELATIVE TO “PERMITTED TEMPLATE” OVER THE 5  
YEAR SIMULATION PERIOD**

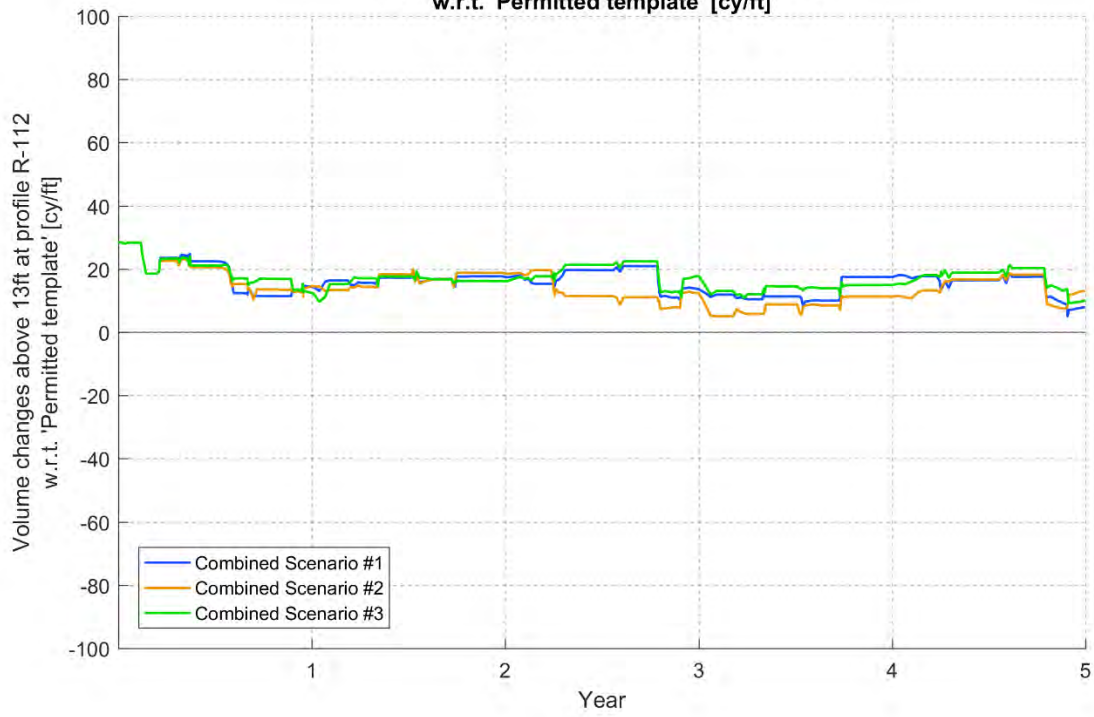
**Volume changes above 13ft at profile R-110.5  
w.r.t. 'Permitted template' [cy/ft]**



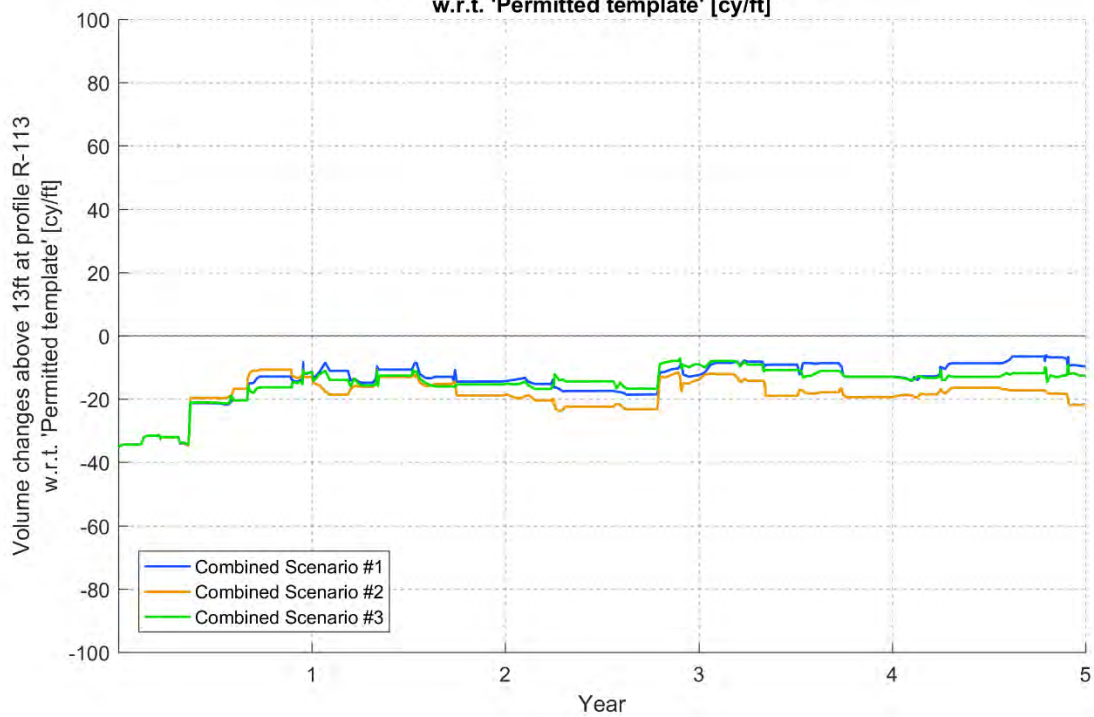
**Volume changes above 13ft at profile R-111  
w.r.t. 'Permitted template' [cy/ft]**



**Volume changes above 13ft at profile R-112  
w.r.t. 'Permitted template' [cy/ft]**



**Volume changes above 13ft at profile R-113  
w.r.t. 'Permitted template' [cy/ft]**



**SUB-APPENDIX A-5**  
**STORM SIMULATIONS FOR COMBINED SCENARIOS**

## STORM SIMULATIONS FOR COMBINED SCENARIOS

In order to evaluate potential alternatives to Blind Pass management plan, numerical models incorporating several design features were developed and evaluated under average conditions (5-year simulation). Based on this initial analysis, 3 Combined Scenarios were proposed and evaluated under average conditions (5-year simulation; main report) and under two storm conditions (described in this Sub-Appendix). The two conditions were selected to well represent winter conditions (Cold Front) and summer conditions (Hurricane Charley, 2004).

### Storm Condition – January 2016 Cold Front

During APTIM's gage deployment campaign from December 11<sup>th</sup> 2015 and January 27<sup>th</sup> 2016, three different Cold Fronts occurred. The most energetic Cold Front from that period (January 21<sup>st</sup> to 25<sup>th</sup> 2016) was selected for the production runs. The waves and wind used in the Regional Wave grid boundary are depicted in Figure 1.

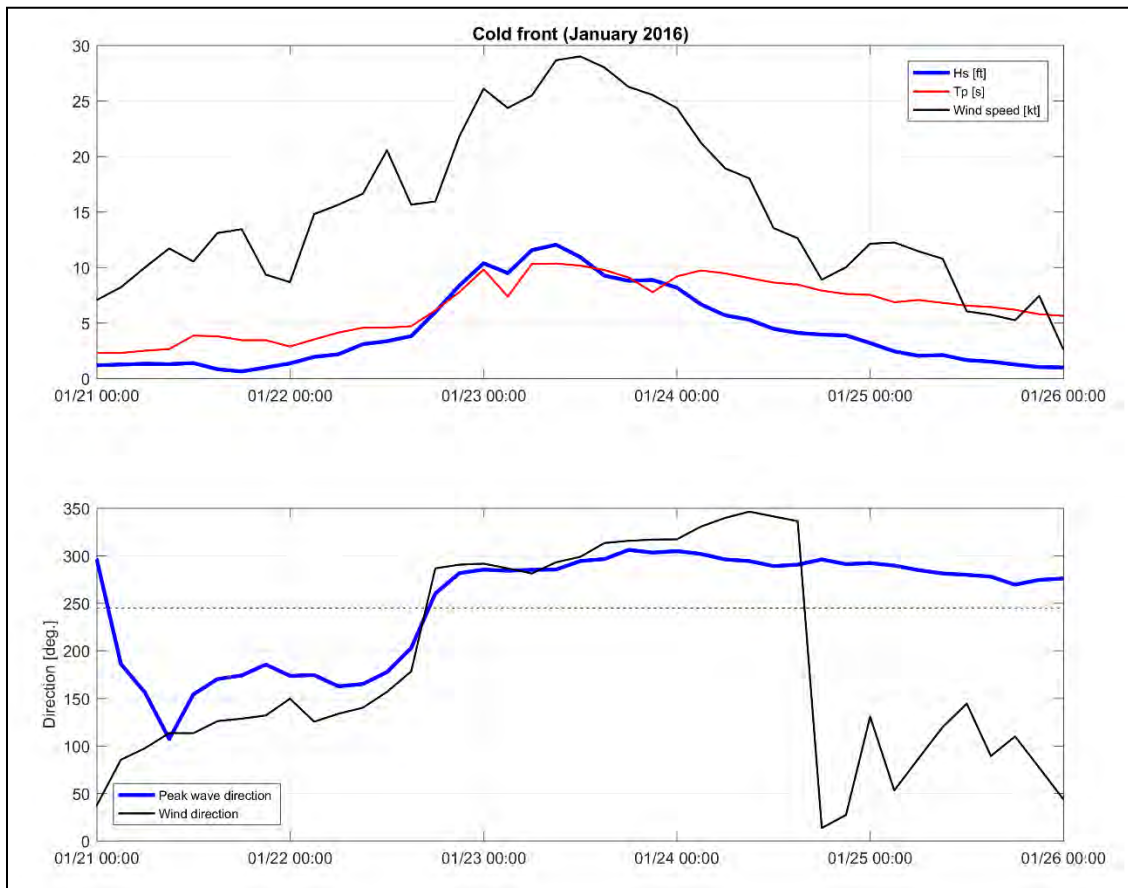


Figure 1: Waves used as boundary conditions for the Regional Wave Grid - Cold Front production runs.

## Storm Condition – Hurricane Charley (2004)

For the evaluation of a second storm event, the model was simulated using forcing conditions similar to Hurricane Charley (2004). This storm made landfall near Cayo Costa, North of Redfish Pass, as a Category 4 on the Saffir-Simpson Hurricane Scale. It was the strongest hurricane in terms of wind speed to hit the United States since Hurricane Andrew in 1992, and it was the strongest hurricane to hit southwest Florida in over 50 years. It caused catastrophic wind damage along his path, and major damage in Sanibel, Captiva and North Captiva Islands.

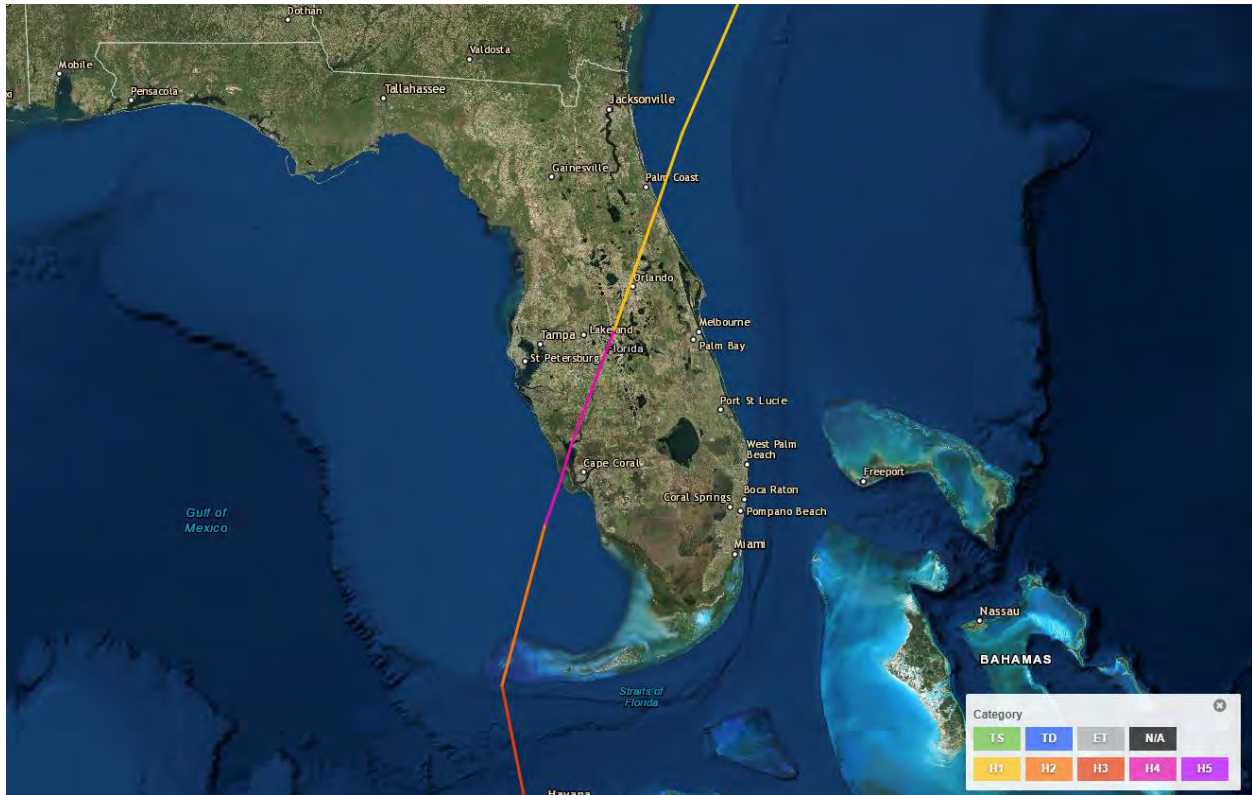


Figure 2: Hurricane Charley track (2004). Source: NOAA.

Accurate depiction of hurricane events requires the accurate computation of the storm surge, which depends on the accuracy of the wind forcing it receives. In order to well represent the storm surge generated, a large scale model grid was created, encompassing southwest Florida Gulf coast. The model grid and bathymetry (interpolated using NCEI NOAA Coastal Relief Model) is presented on Figure 3.

For this storm simulation, the Wind Enhance Scheme (WES) (Deltares, 2016) was devised to generate space varying hurricane wind fields. The program computes surface winds and pressure around the specified location of a tropical cyclone center and given a number of tropical cyclone parameters (track data: i.e. maximum wind speed, pressure drop, radius of maximum wind and positions of the tropical cyclone). This information was obtained from Pasch *et al.* (2004), and an example of the wind fields used in the model and the storm track presented in Figure 4.

The large scale Delft3D-WAVE and Delft3D-FLOW were simulated coupled using the wind fields generated with WES. These results were used as boundary conditions for the Regional Flow Grid,

which then was simulated to generate the boundary conditions for Local Flow Grid (Figure 5 and Figure 6).

Model configuration was the same as the wave and flow calibration, except for an adjustment in the wind drag coefficients (Table 1). The wind drag coefficient may be linearly dependent on the wind speed, reflecting increasing roughness of the water surface with increasing wind speed. The coefficients were based on Bryant & Akbar (2016) and Zweers *et al.* (2010).

**Table 1: Adjusted wind drag coefficients used on Hurricane Charley (2004) production runs.**

<b>Parameters</b>	<b>Delft3D-FLOW Calibration</b>	<b>Delft3D-FLOW Hurricane Charley (2004)</b>
<b>Wind Drag Coefficients</b>		
<b>0 m/s</b>	0.00063	0.001
<b>28 m/s</b>	0.00723	0.003987
<b>100 m/s</b>	0.00723	0.000456

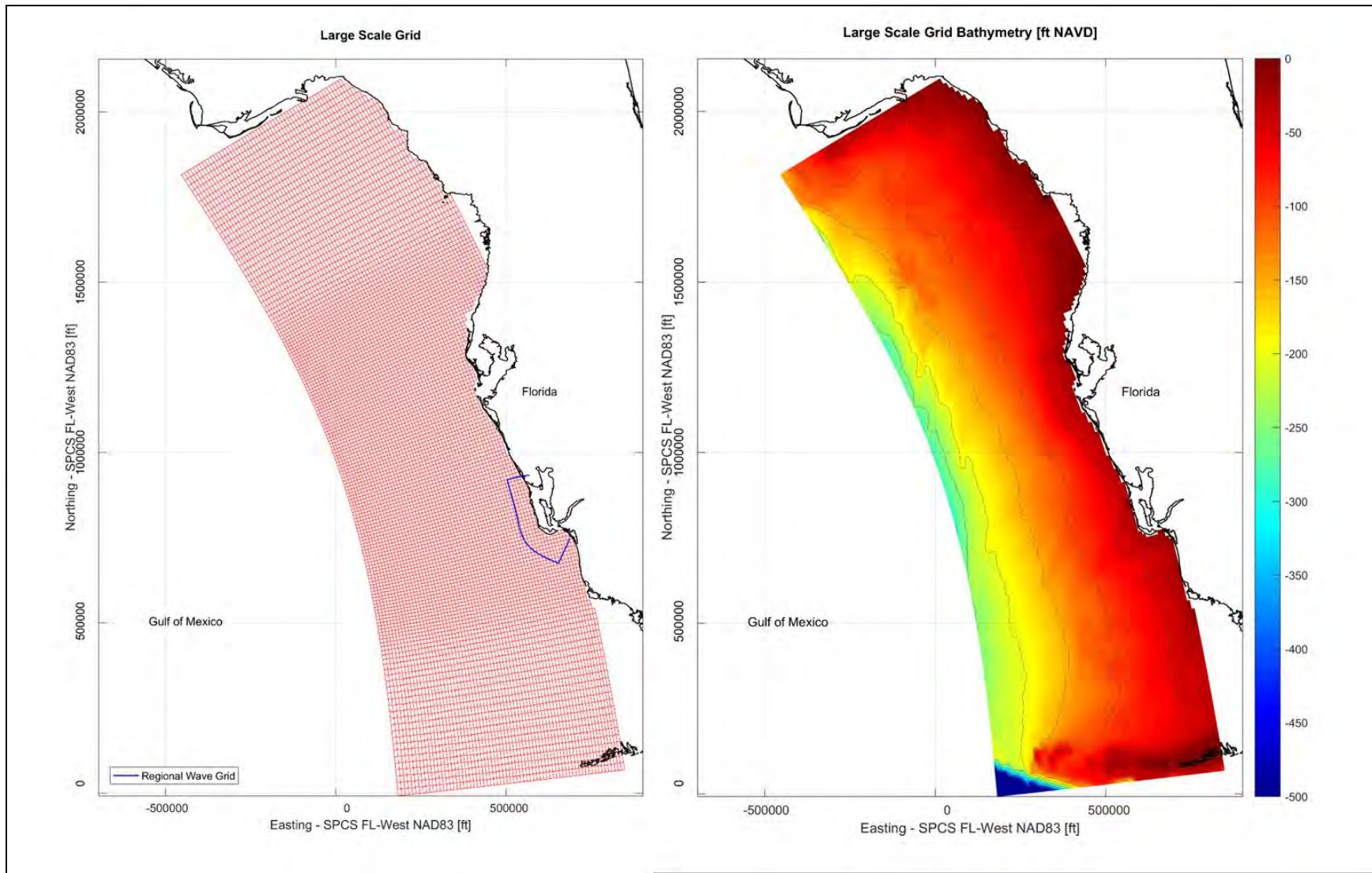
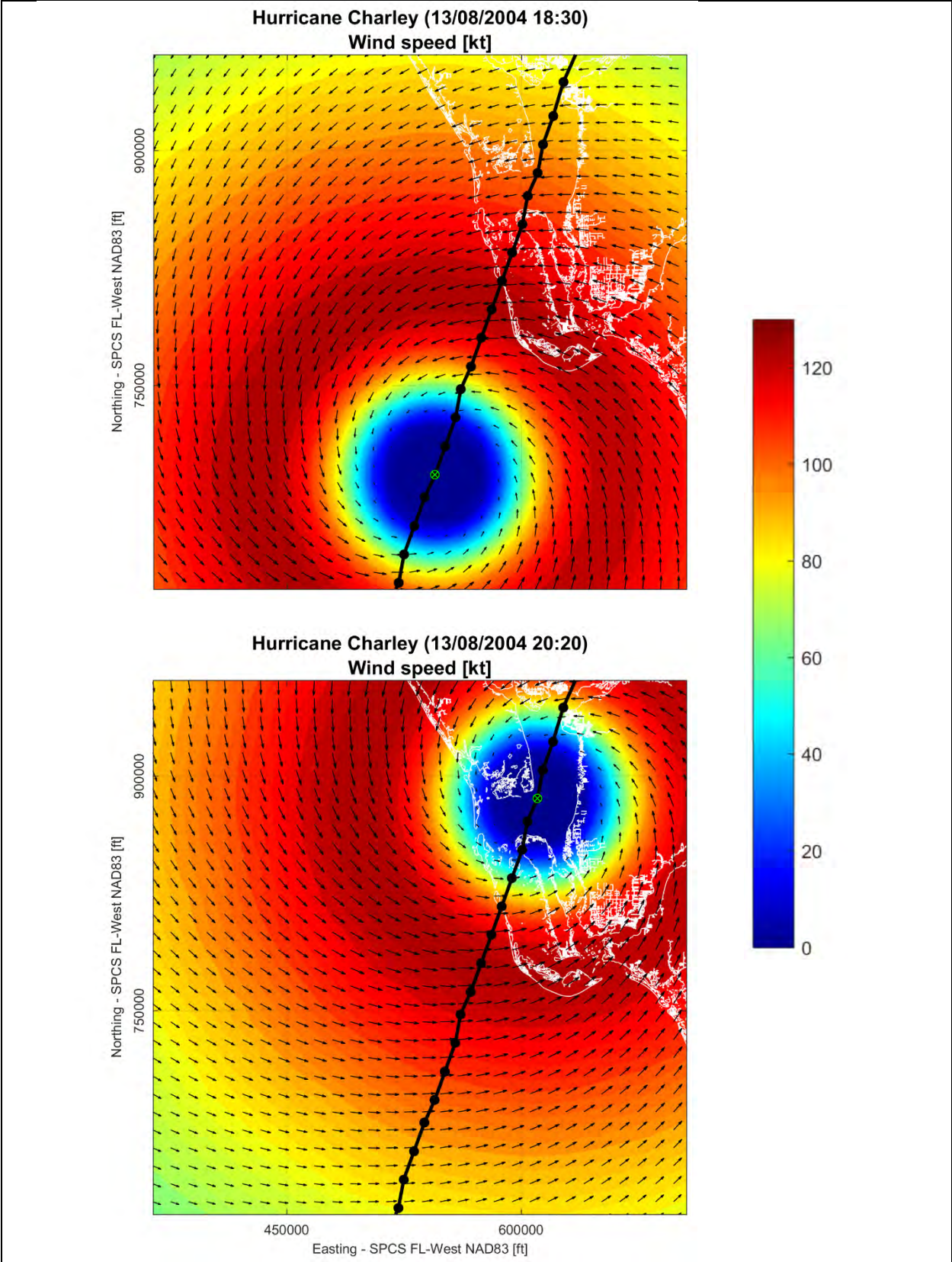
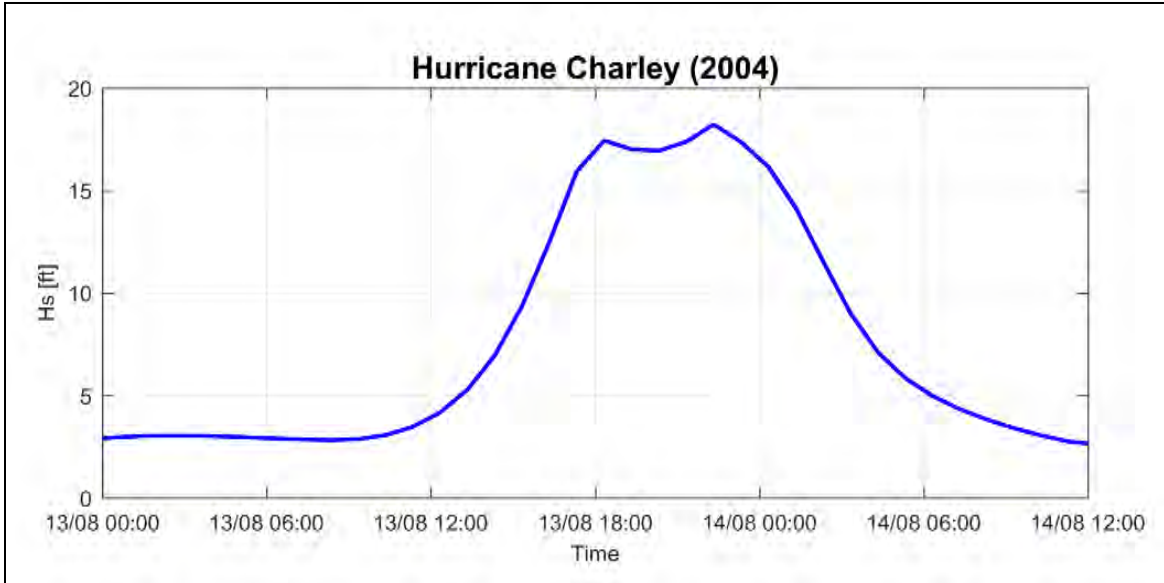


Figure 3: Large scale grid and interpolated bathymetry used to generate boundary conditions for Hurricane Charley (2004) production runs.



**Figure 4: Hurricane Charley (2004) storm track and wind fields generated with the Wind Enhancement Scheme (WES).**



**Figure 5: Waves used as boundary conditions for the Regional Wave Grid - Hurricane Charley (2004).**

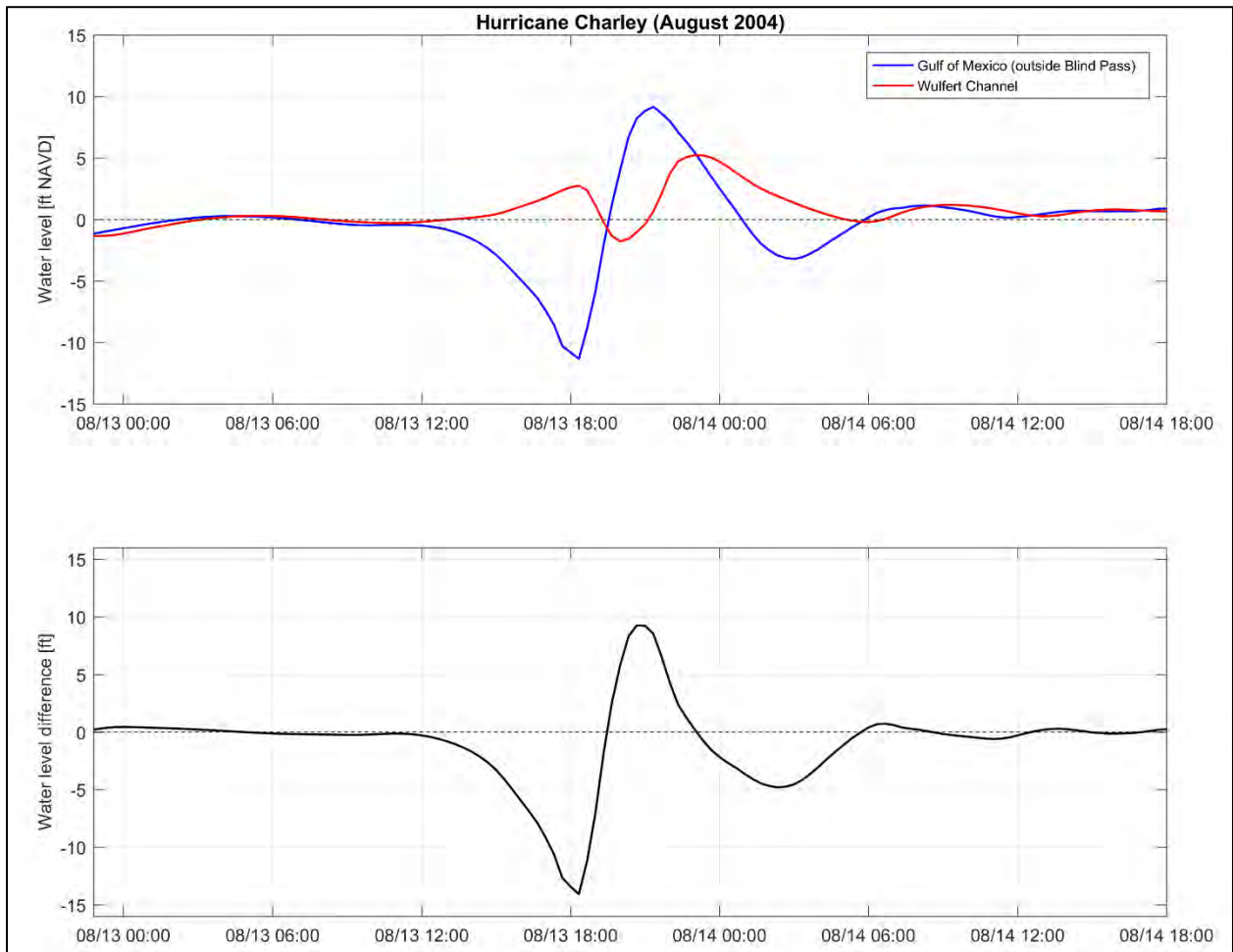


**Figure 6: Water levels calculated with the Regional Flow model and used as boundary conditions for the Local Flow model - Hurricane Charley (2004).**

## MODEL RESULTS: JANUARY 2016 COLD FRONT

### Permitted Template

The final simulated bathymetry after the cold front considering the Permitted Template is given in Figure 7.

During the peak of the cold front, waves propagate from the northwestern quadrant, driving sand transport to the south (i.e. along Captiva Island, across the tip of the Jetty, through the channel towards Sanibel Island, and along Sanibel Island). Results indicate the development of a shallow bypassing bar across the outer channel section of the dredged channel, initially dredged at -10 ft NAVD. The inner channel sections are less affected. This process is in line with the observed channel behavior after dredging projects: significant infilling rates at channel's outer section within the first few months after project completion, and gradual/slower infilling of inner channel sections. Additional details about past observations are provided introduction of the modeling study appendix, which makes reference to multiple monitoring reports.

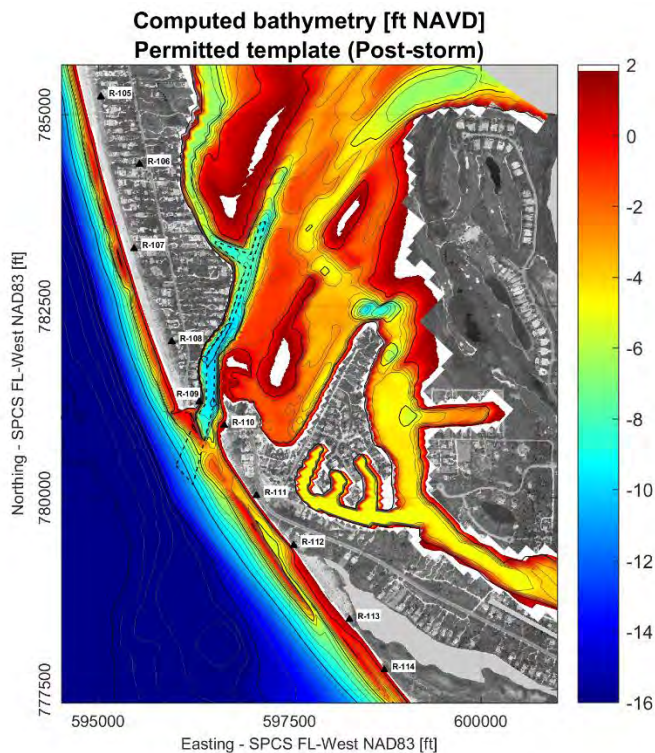


**Figure 7: Final model bathymetry of Cold Front Simulation – Permitted Template scenario. Dashed line represents dredge template boundary.**

The net bathymetry change map comparing the final simulated bathymetry for the Permitted Template and No Action scenarios is provided in Figure 8. It represents the net effects of channel dredging during the simulated Cold Front: positive changes (warm colors) indicate that the

Permitted Template is shallower than No Action; negative changes (cool colors) indicate that the Permitted Template is deeper than No Action.

These results show the bypassing bar developing across the channel (white strip crossing the channel indicating no change relative to the No Action scenario), a relatively deep inner channel – stable under the simulated time frame, an especially negative downdrift effects associated to the channel dredging. The sand accumulated in the outer section of the channel results in a debt at its downdrift side. Consequently, the channel migrates downdrift and the associated negative effects ‘diffuse’ across the adjacencies. The affected area by the end of the simulated storm is primarily north of R-112, which is not covered/compensated with beach fill placement under the current plan (beach fill is placed south of R-112).

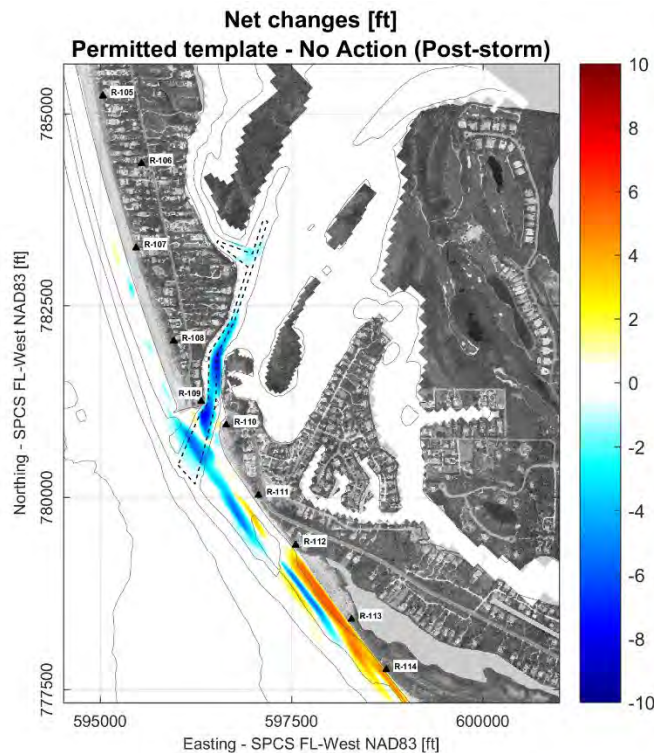


**Figure 8: Net bathymetry changes after Cold Front: Permitted Template *minus* No Action. Dashed line represents dredge template boundary.**

### **Combined Scenarios**

The net bathymetry change map comparing the final simulated bathymetry for the Combined Scenarios and the Permitted Template scenarios is provided in Figure 9 through Figure 11. These results represent the net effects of channel dredging during the simulated Cold Front: positive changes (warm colors) indicate that the Combined Scenario is shallower than Permitted Template; negative changes (cool colors) indicate that the Combined Scenario is deeper than Permitted Template.

Negative differences observed in the landward section of the channels are related to the additional dredging associated to the alternatives, and therefore are not a result of the simulated storm but of the different initial condition/dredging templates. Positive differences between R-110.5 and R-112.5 are associated to the beach fill, which was moved north of the Permitted Template and maintains most of its volume after the single simulated storm. Other differences in the seaward side of bridge relate directly to the tested design elements: improved inner channel connections and increased tidal prism, truncated channel template, relocated beach fill, and a spur on Blind Pass Jetty (Combined Scenario #3).

For all Combined Scenarios, only minimal differences are observed at the critical section of the channel near the bridge. At its seaward end, the (truncated) dredged channel remains even deeper when compared to the Permitted Template results, which is explained by the enhanced tidal prism and the spur (only in Combined Scenario #3). The outer bar seaward of the channel template is shallower, as the channel is truncated in the Combined Scenarios – but not in the Permitted Template. Finally, the additional positive benefits spread south, between R-110 and R-112, actually relates to the absence of the negative effects associated to the outer channel dredging (i.e. the benefits of the truncated template). The effects of the spur are seen in its leeward site, reducing sand migration into the outer channel section.

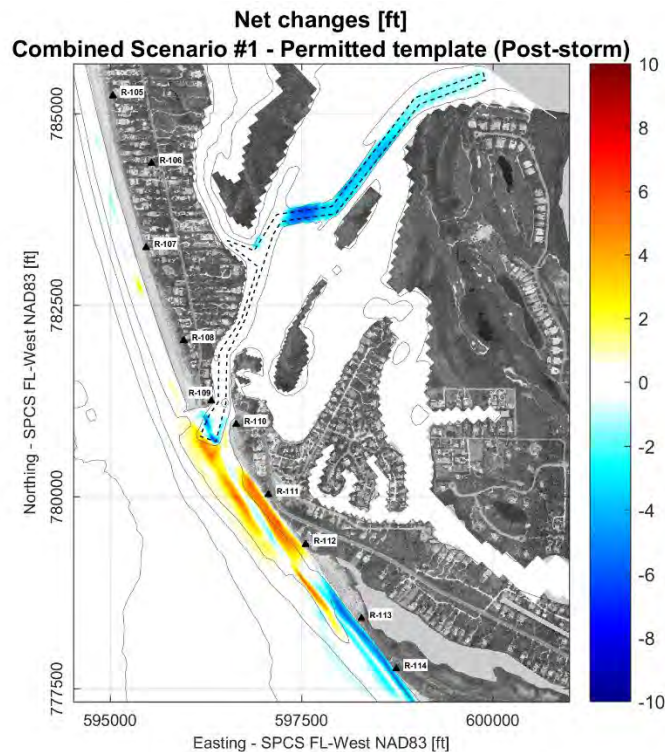


**Figure 9: Net bathymetry changes after Cold Front: Combined Scenario #1 *minus* Permitted template.**

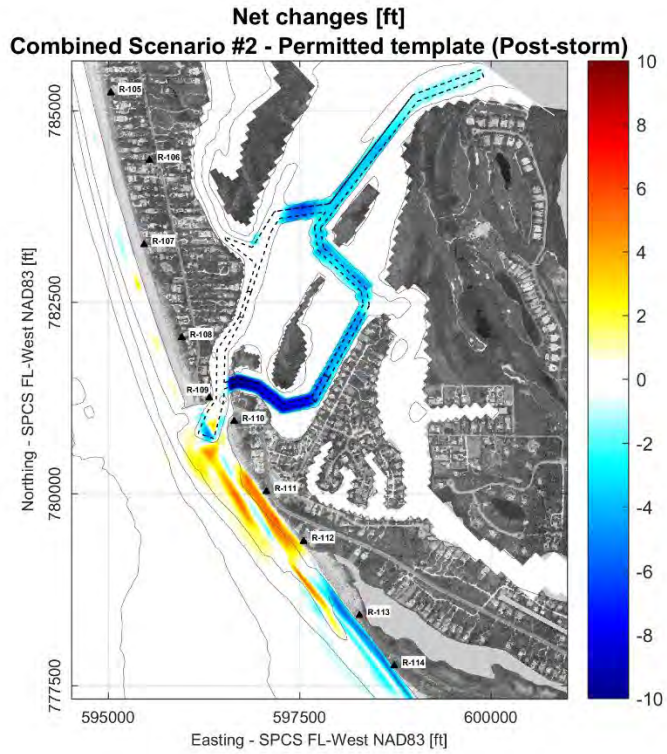


Figure 10: Net bathymetry changes after Cold Front: Combined Scenario #2 *minus* Permitted template.

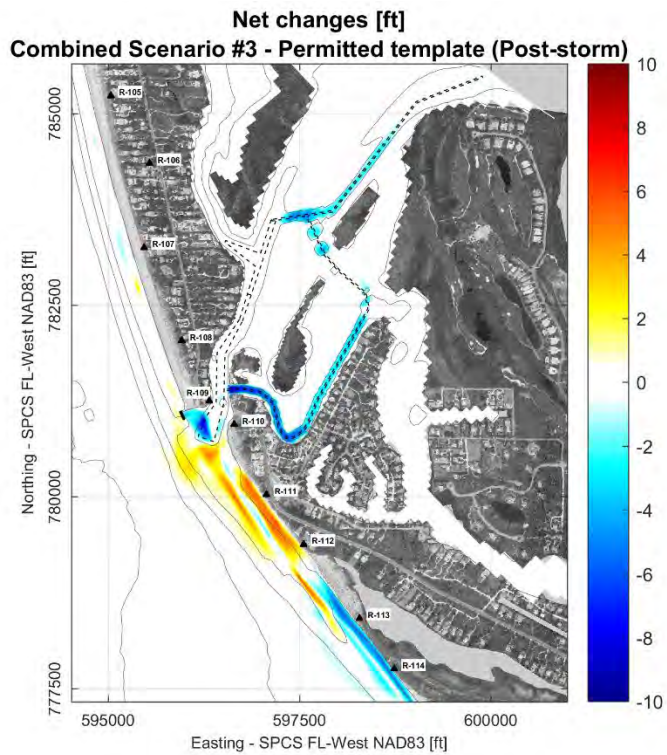
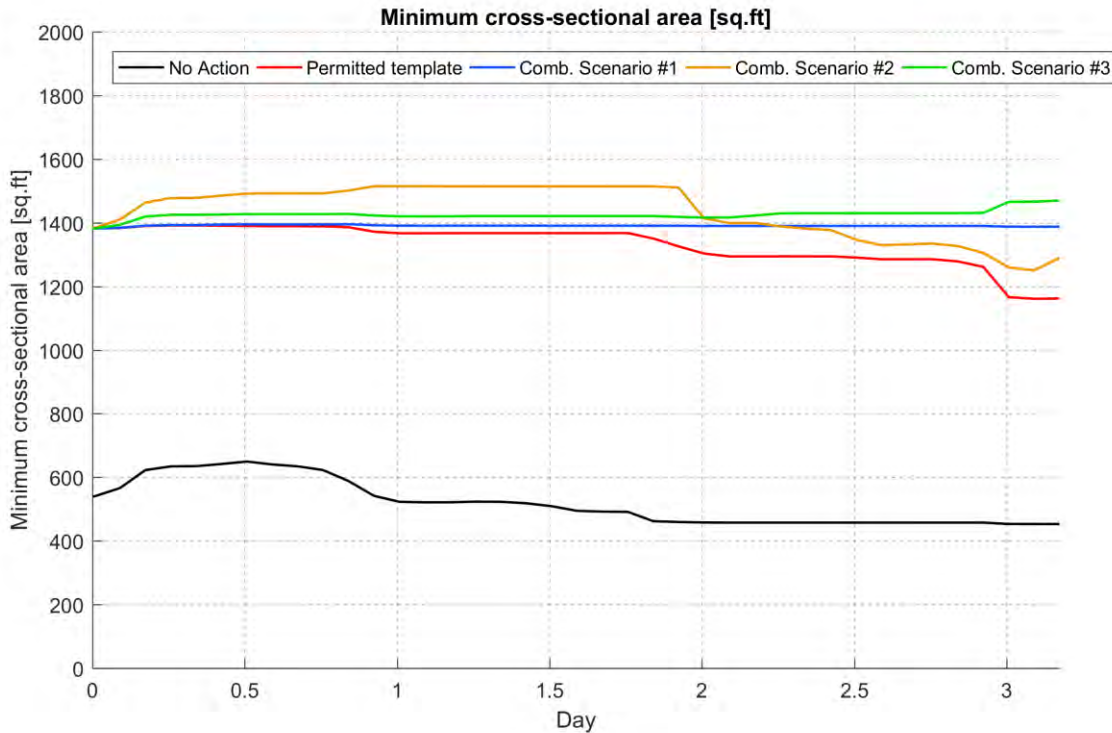


Figure 11: Net bathymetry changes after Cold Front: Combined Scenario #3 *minus* Permitted template.

The initial minimum cross-sectional area for all dredged scenarios is approximately 1400 sq. ft., while the No Action scenario is approximately 500 sq. ft. The variations over time during the Cold Front simulations are relatively small, less than 10% of its initial value. (Figure 12).



**Figure 12: Minimum cross sectional area of Blind Pass during the Cold Front simulation.**

Remarkably, the final cross-sectional area associated to the Permitted Template scenario is the minimum within the dredged alternatives. This suggests that, under the simulated conditions, the additional dredging of the outer section of the channel does not reflect in increased channel stability, but on negative effects to immediately downdrift beaches. This finding is in-line with the results of the longer term simulations (5 years) described in the main modeling study report (Appendix A).

## **MODEL RESULTS: HURRICANE CHARLEY (2004)**

### **Permitted Template**

The final bathymetry after the Hurricane Charley simulation considering the Permitted Template is given in Figure 13. Figure 14 provides the erosion/sedimentation map, showing the difference between the initial and final model bathymetry.

Model results indicate dramatic changes in the whole area due to the hurricane. These relate to the extreme wave action, the maximum storm surge and the sharp water level variation over time.

Within approximately 2 hours, category 4 hurricane winds exceeding 120 knots shifted from offshore to onshore (Figure 4).

Initially positive storm surges develop in the back bay area, as water from Pine Island Sound ‘piled up’ against the eastern shorelines of Captiva and Sanibel Islands, and a negative surge in the Gulf coast. The water level difference between the north end of Wulfert Channel and the outer section of Blind Pass (Gulf of Mexico) was approximately 14 ft, pushing water out towards the Gulf of Mexico, leading to extreme current speeds and channel scour.

After the passage of the hurricane eye over the area, winds shifted direction, positive surge built up in the Gulf side (approximately 9 ft) and slight negative surge in Pine Island Sound, resulting in a water level change in the order of 9 ft along the channel. In addition to positive storm surge, the extreme onshore winds produced significant wave height in the order of 18 ft in offshore areas adjacent to the islands. This second phase of the storm caused strong incoming currents in Blind Pass and Wulfert Channel and additional channel scour. The combination of extreme waves and storm surge along Captiva and Sanibel shoreline caused significant beach erosion and dune overtopping rolling the dunes landward.

The observed changes in Blind Pass and Wulfert channels after Hurricane Charley hit in 2004 were less severe than the model results. On that occasion the channel was completely closed and a dry beach existed between the north-end of Sanibel Island and the Blind Pass Jetty. As the peak storm surge in Wulfert Channel (~3 ft NAVD) was not enough to significantly overtop the dry beach across the channel, the out water flow during the first phase of the storm (offshore winds) was negligible. After winds shifted onshore, the peak surge in the Gulf side was higher (~ 9 ft NAVD). The beach across the channel was overtopped and sand transported landward towards inner sections. Model results and the described observations suggest that Hurricane Charley effects on Blind Pass and inner channels would had been much greater if a connection was established at that occasion.

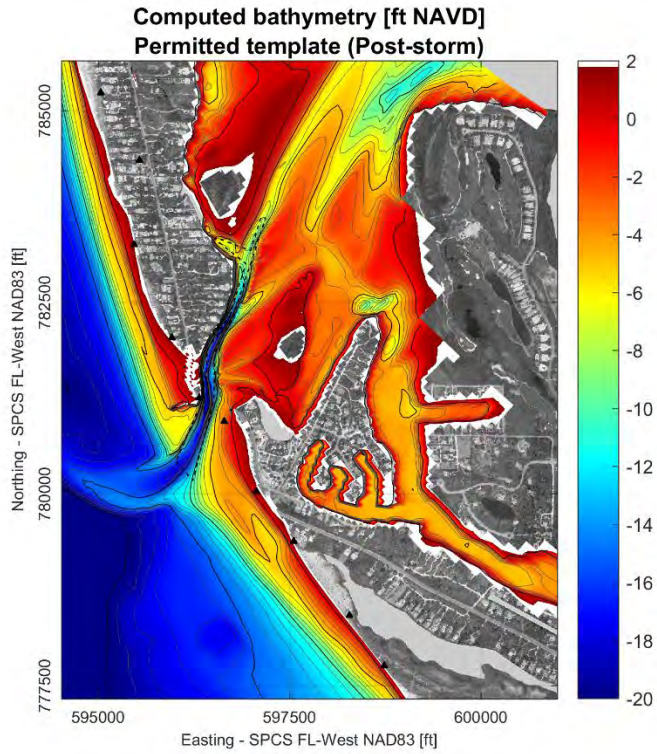


**Figure 13: Final model bathymetry of Hurricane Charley Simulation – Permitted Template scenario.**

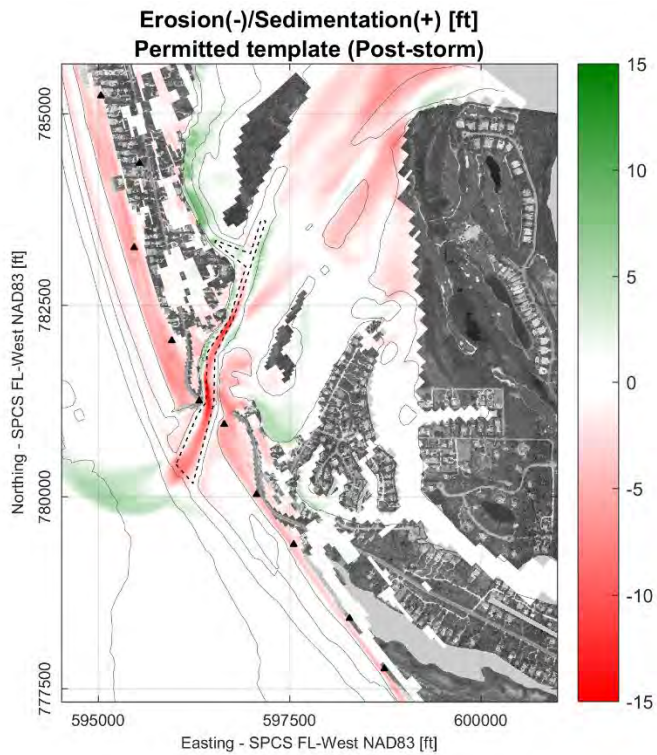


**Figure 14: Erosion/sedimentation map. Hurricane Charley simulation, Permitted Template scenario.**

## **Combined Scenarios**

The comparisons between the storm effects under the Permitted Template and the Combined Scenarios is given in Figure 15 to Figure 17. Firstly, changes are observed in the dredging and beach fill areas due to the differences in the initial bathymetries of the alternatives. The beach fill relocation north benefited the beach around profile R-111, where the Sanibel Captiva Road gets closer to the shoreline, providing protection to this critical infrastructure.

Besides the beach fill areas, minor relative changes are observed along Captiva and Sanibel shoreline and dunes, indicating that the severity of the storm along these areas is not influenced by the Alternatives – impacts are expected in either case. Significant differences occur in the inner channels and especially in the depth and location of the developed outer channel, across the bar towards deeper waters:

- Combined Scenario #1: scattered additional scour in the order of 2 ft in the channel section between Roosevelt Channel intersection and Blind Pass, due to increased flows associated to the Pine Island Sound connection. Outer channel bend north as an effect of the truncated template, maximum depth is similar.
- Combined Scenario #2: reduced channel scour in the order of 2 ft in the channel section between Roosevelt Channel intersection and Blind Pass, due to diversion and increased flows through Sunset Bay connection. Additional scour along existing flood shoal (in the order of 1 ft). Outer channel bend north as an effect of the truncated template, maximum depth increases approximately 4 ft.
- Combined Scenario #3: reduced channel scour in the order of 1 ft in the channel section between Roosevelt Channel intersection and Blind Pass, due to diversion and increased flows through Sunset Bay connection. Additional scour along existing flood shoal (in the order of 1 ft). Outer channel bend north as an effect of the truncated template, maximum depth increases approximately 3 ft.

The changes in the minimum channel cross-sectional area during Hurricane Charley simulation indicate significant cross-sectional area increase, suggesting that such extreme events have played an important role to maintain the historical existence of the pass (Figure 18). Larger cross-sectional area changes are associate to scenarios where enhanced connection to Pine Island Sound facilitate water exchanges.

It should be highlighted that the combination of multiple characteristics makes individual hurricanes unique events, as well as their effects to coastal areas. These characteristics include hurricane tracks, intensities, radius and forward speed. Therefore, the results of the Hurricane Charley simulations are a sample of the strength and potential effects of such extreme events, but should not be seen as a prognostic results of future effects.

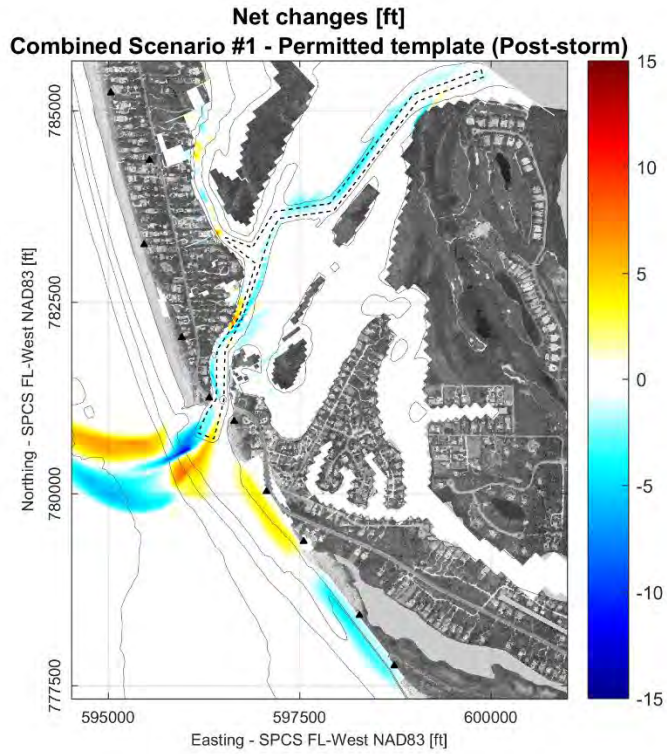


Figure 15: Net bathymetry changes after H. Charley: Combined Scenario #1 *minus* Permitted template.

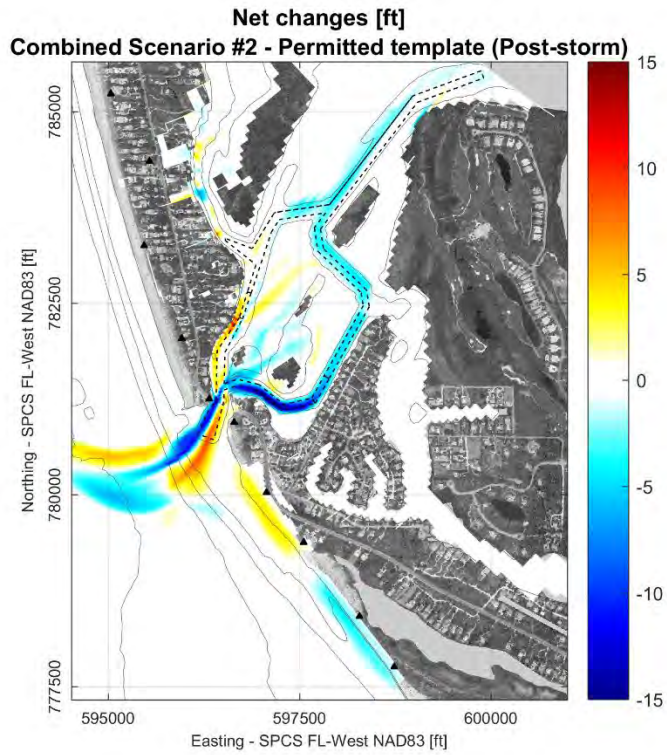


Figure 16: Net bathymetry changes after H. Charley: Combined Scenario #1 *minus* Permitted template.

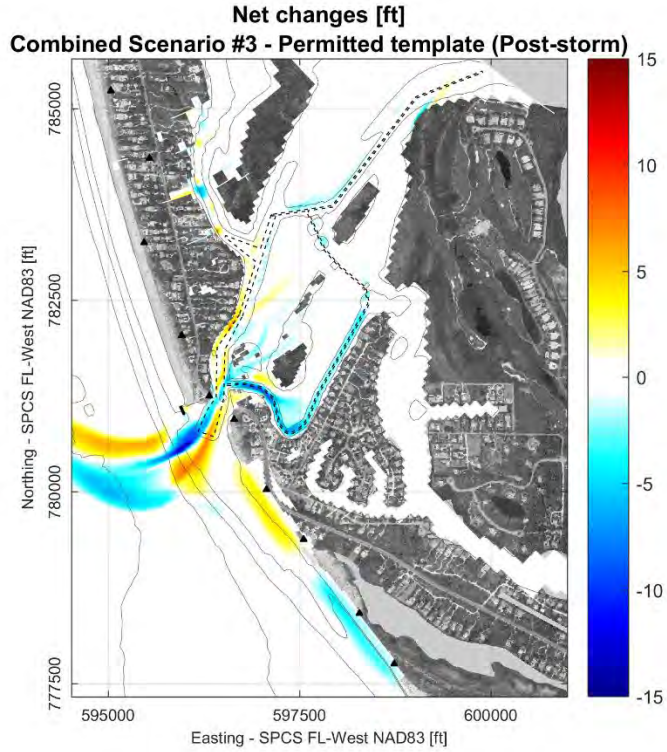


Figure 17: Net bathymetry changes after H. Charley: Combined Scenario #1 *minus* Permitted template.

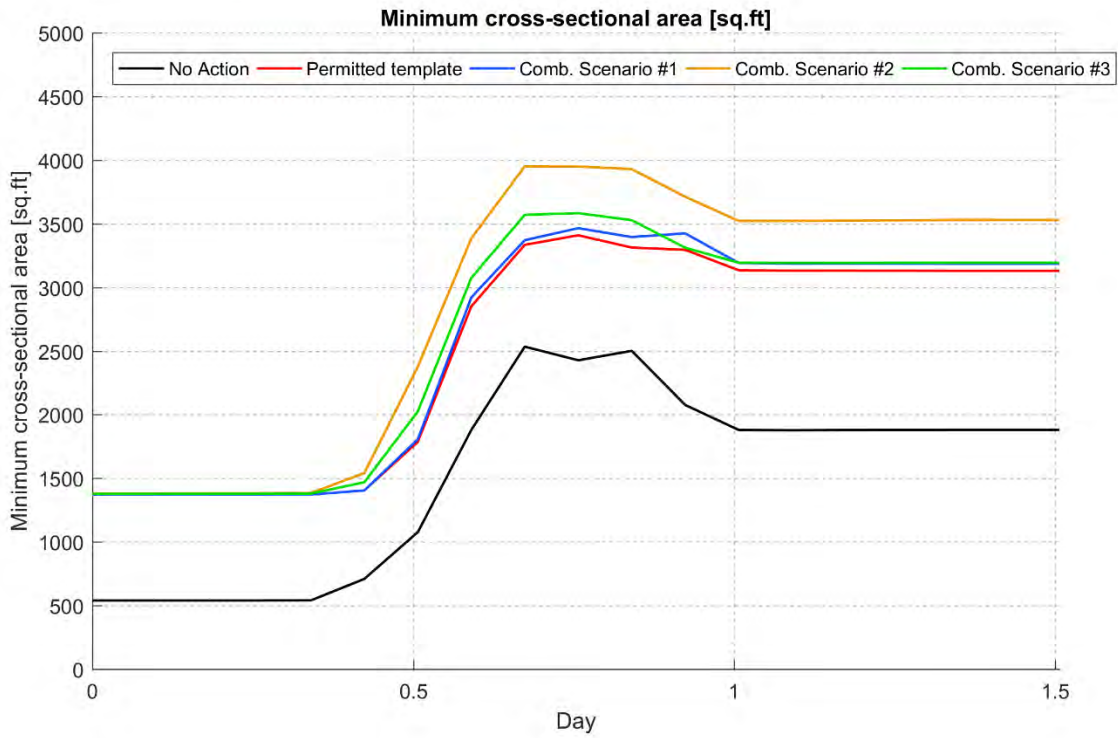


Figure 18: Minimum cross sectional area of Blind Pass during the Hurricane Charley simulation.

## REFERENCES

- Bryant, K.M., Akbar, M. 2016. An Exploration of Wind Stress Calculation Techniques in Hurricane Storm Surge Modeling. *Journal of Marine Science and Engineering*, 4(3):58.
- Deltares, 2016. Delft3D-WES, Wind Enhance Scheme for Cyclone Modeling, User Manual, Deltares, Rotterdam, Netherlands.
- Pasch, R.J., Brown, D.P., Blake, E.S. 2004. Tropical Cyclone Report, Hurricane Charley, 9-14 August 2004. National Hurricane Center. 18 October 2004 (Revised 15 September 2011).
- Zweers, N.C., Makin, V.K., de Vries, J.W., Burgers, G. 2010. A sea drag relation for hurricane wind speeds. *Geophys. Res. Lett*, 37.